University of Glasgow

Al Ghabshi, Bushra (2021) *Configurations and stability of thin films of nematic liquid crystal.* PhD thesis.

https://theses.gla.ac.uk/82720/

Copyright and moral rights for this work are retained by the author

A copy can be downloaded for personal non-commercial research or study, without prior permission or charge

This work cannot be reproduced or quoted extensively from without first obtaining permission in writing from the author

The content must not be changed in any way or sold commercially in any format or medium without the formal permission of the author

When referring to this work, full bibliographic details including the author, title, awarding institution and date of the thesis must be given

Enlighten: Theses
https://theses.gla.ac.uk/
research-enlighten@glasgow.ac.uk

Configurations and stability of thin films of nematic liquid crystal

Bushra Al Ghabshi

Submitted in fulfilment of the requirements for the
Degree of Doctor of Philosophy

School of Mathematics and Statistics
College of Science and Engineering
University of Glasgow



January 2021

Abstract

Liquid crystals are unique materials exist between the solid phase and liquid phase, and in certain ranges of temperature they show different arrangements of the molecules. Depending on the amount of order in the material, there are many different types of liquid crystal states. The nematic liquid crystals are an example of a material that has no positional order but has local orientational order, this gives rise to textures (patterns in the material) that are attractive to study. Nematic liquid crystal is an example of a material that has orientational order and no long-range positional order, this gives rise to textures (patterns in the material) that are attractive to study.

This thesis concerns liquid crystals in thin films and their configurations and stability. The aim of this thesis to to explore minimum energy configurations for thin liquid shells, coupled with surface energy and curvature effects. In particular we study a thin film of liquid crystal spanning two coaxial rings, where we use the energy derived in [66] for a thin nematic liquid crystal and study the nematic film within the Landau-de Gennes model which is described through the $\mathbf{Q}$-tensor theory.

This thesis consists of a study of two main problems. The first is the study of the equilibrium of open surfaces (with a boundary) and involves a careful derivation of natural boundary conditions associated with minimising a general surface energy. We prove a number of results about the equations and also derive a framework to study the stability of the solutions to the equilibrium by considering the incremental equations. We demonstrate this approach in some simple examples. The second main problem is a study of the equilibrium of a thin film of liquid crystal suspended between two coaxial rings. We use the results developed in the first part of the thesis to derive the equilibrium equations and boundary conditions and solve these equations numerically for a range of dimensionless parameters related to the thin film. We perform our numerical study using two different, but related, parameterisations of the order tensor. We specialise to consider axisymmetric solutions. Finally we study the stability of the isotropic distribution (state) on a fixed catenoidal geometry, we demonstrate the emergence of defects of charge $-1/2$ at the onset of nematic order. We study the nonlinear equations numerically using a nonlinear Jacobi iteration.

Contents

Abstract i

Acknowledgement ix

Declaration x

List of notation xi

1 Introduction 1

1.1 Structure of thesis . . . 1
1.2 What are liquid crystals? . . . 2
1.2.1 History of liquid crystals . . . 4
1.2.2 Classifying liquid crystals . . . 5
1.2.3 Material properties of liquid crystals . . . 9
1.2.4 Applications of Liquid Crystals . . . 11
1.3 Approaches to modelling liquid crystal . . . 13
1.4 Introduction to **Q**-tensor theory . . . 13
1.4.1 Tensor order parameter Q . . . 14
1.5 Previous works . . . 15

2 Mathematical preliminiaries 19

2.1 Tensors . . . 19
2.2 Surface calculus . . . 22
2.2.1 Surface gradient . . . 22
2.2.2 Vector fields . . . 24
2.3 Differential geometry . . . 25
2.3.1 The extrinsic curvature tensor . . . 26
2.3.2 The normal curvature . . . 26
2.3.3 Geodesic curvature . . . 27
2.3.4 Surface Divergence Theorem . . . 29
2.4 Surface increments . . . 30

2.5 Modelling liquid crystal shells . . . 33
2.6 Concluding remarks . . . 36

3 Equilibrium of open surfaces 37
3.1 The equilibrium of open surfaces . . . 37
3.1.1 Area constraint and local inextensibility . . . 38
3.1.2 Boundary conditions . . . 42
3.2 Tangential component of the equilibrium equation . . . 45
3.2.1 The case of $w\left(q, \nabla_s q\right)$ . . . 46
3.2.2 The case of $w\left(\mathbf{L}, \boldsymbol{\nu}\right)$ . . . 48
3.2.3 The case of $w\left(\mathbf{n}, \nabla_s \mathbf{n}\right)$ . . . 50
3.3 Special Examples . . . 51
3.3.1 Soap film . . . 51
3.3.2 Lipid membrane . . . 52
3.4 The normal increment of the shape equation . . . 55
3.4.1 The case of $w\left(q, \nabla_s q\right)$ . . . 56
3.4.2 Example of the case of $w(q, \nabla_s q)$ . . . 60
3.4.3 The case of $w(\mathbf{L}, \boldsymbol{\nu})$ . . . 62
3.4.4 The case of $w = \hat{w}\left(H, K\right)$ . . . 64
3.5 Examples . . . 67
3.5.1 Stability of a soap bubble . . . 67
3.5.2 Catenoid . . . 68
3.5.3 Canham-Helfrich energy . . . 78
3.6 Concluding remarks . . . 85

4 Shape and stability of a nematic film suspended between two coaxial rings 86
4.1 Introduction . . . 86
4.2 Free energy functional . . . 87
4.2.1 Parameterisations of $\mathbf{M}$ using q_0 and q_m . . . 87
4.2.2 Parameterisations of $\mathbf{M}$ using q and $\mathbf{n}$ . . . 94
4.2.3 Connection between the two parameterisations . . . 96
4.3 General equilibrium equations . . . 96
4.3.1 Boundary conditions . . . 99
4.4 Surfaces of revolution . . . 100
4.5 Dimensionless axisymmetric case using q_0 and q_m . . . 103
4.5.1 Numerical results for q_0 and q_m parameterisation . . . 106
4.6 Dimensionless axisymmetric case using q and $\mathbf{n}$ . . . 117
4.6.1 Boundary conditions . . . 118

4.6.2 Derivation of the dimensionless equilibrium equations in Hamilton form . . . 120
4.7 Stability of the isotropic distribution on the fixed geometry of the catenoid 132
4.7.1 Incremental equations of the isotropic distribution . . . 133
4.8 Weakly non-linear analysis . . . 139
4.8.1 Non-axisymmetric case . . . 141
4.8.2 Defects . . . 142
4.9 Jacobi iteration . . . 148
4.10 Application to nonlinear equation . . . 149
4.10.1 Discretisation . . . 149
4.11 Nonlinear solutions . . . 150
4.12 Concluding remarks . . . 156

5 Conclusions **157**
5.1 Future work directions . . . 158

A Details of proofs **160**

B Code used to produce results **166**
B.1 Solution of axisymmetric equations . . . 166
B.2 Solution of nonlinear equations . . . 173

List of Figures

1.1 Phase transition with temperature variation: crystaline solid, liquid crystals and isotropic liquid respectively, and the representation of molecular arrangements in each phase [21]. 4
1.2 The arrangement of molecules in the nematic phase [42]. 6
1.3 The arrangement of molecules in the cholesteric phase [42]. 8
1.4 The arrangement of molecules in the smectic phase [42]. 9
1.5 The three principle types of deformation in a nematic liquid crystal: splay, twist and bend [88]. 11

2.1 Fields defined on the surface S. 23
2.2 Tangent vectors of the surface S. 23
2.3 The vector field $\mathbf{v}$ on the surface S. 25
2.4 Curves have tangent direction in direction of $\mathbf{n}$, where $\mathbf{n}$ is a tangential unit vector field on S. 27
2.5 The surface divergence theorem relates the integral of the surface divergence of the vector field $\mathbf{f}$ on S to an integral around the boundary curve and the vector $\mathbf{k}$ is tangent to the surface and perpendicular to the boundary curve and points outwards. 29

3.1 Catenoid shape near the critical aspect ratio $\xi = 0.66$ 70
3.2 Stability curves for different modes number n, the black line refers to the minimum radius r_{min} corresponding to the critical aspect ratio (beyond which there is no solution to the equilibrium equations). For $r_{min} < r^c_{min}$ (to the left of the line) the catenoid is narrow, for $r_{min} > r^c_{min}$ (to the right of the line) the catenoid is wide. 76
3.3 The eigenvalue curves for different values of N, n against the r_{min}. 77
3.4 The minimum eigenvalue of the energy for small values of Γ. The black vertical line refers to r^c_{min} and the dashed curves refers to the normal soap curve with a corresponding n. The $\mathbf{n} = 2$ case was computed but lies outside the axes (it is off the scale). 83

3.5 The minimum eigenvalue of the energy for large values of Γ. The black vertical line refers to r^c_{min} and the dashed curves refers to the normal soap curve with a corresponding n 84

4.1 These figures shows solutions (with different y-axis scales) for q_0, q_m for different values of A, assuming the parameters κ, ξ, C have specific values. The red line corresponds to q_0 and the green one corresponds to q_m. 107

4.2 Numerical solutions for ρ for different values of the parameter A, assuming the parameters κ, ξ, C have a specific values. The blue solid line correspond to ρ, the black solid line corresponds to sphere, the dashed line corresponds to the wide catenoid and the dashed-doted line corresponds to the narrow catenoid. 109

4.3 Numerical solutions for q_0, q_m for different values of ξ, assuming the parameters κ, A, C have specific values. The red line corresponds to q_0 and the green one corresponds to q_m. 111

4.4 Numerical solutions for ρ for different values of the parameter ξ, assuming the parameters κ, A, C have a specific values. The blue solid line correspond to ρ, the black solid line corresponds to sphere, the dashed line corresponds to the wide catenoid. 112

4.5 The first plot displays the numerical solutions for q_0 for different values of the parameter κ, assuming the parameters A, ξ, C are fixed. The second plot displays the numerical solution for q_m. 113

4.6 Numerical solutions for ρ for different values of the parameter κ, assuming the parameters A, ξ, C are the same in all the sets of parameters. The blue solid line correspond to ρ, the black solid line corresponds to sphere, the dashed line corresponds to the wide catenoid. 114

4.7 Numerical solutions for q_0 and q_m, respectively for different values of the parameter C, assuming the parameters A, ξ, κ are the same in all the sets of parameters. 115

4.8 Numerical solutions for ρ for different values of the parameter C, assuming the parameters A, ξ, κ are the same in all the sets of parameters. The black solid line corresponds to sphere, the dashed line corresponds to the wide catenoid. 116

4.9 The energy as a function of A. The blue branch refers to the wide catenoid and the red brunch refers to the narrow catenoid. 117

4.10 Types of solutions for q when $\alpha = \pi/2$ where we give specific values of the parameters (ξ, C, κ) and vary the parameter A. 124

4.11 Types of solutions for ρ when $\alpha = \pi/2$ where we give specific values of the parameters (ξ, C, κ) and vary the parameter A. 125

4.12 Types of solutions for q when $\alpha = 0$ where we give specific values of the parameters (ξ, A, C) and vary the parameter κ. So here, for a fixed temperature (fixed value of A) and increasing κ we use that $q < 0$ (with $\alpha = 0$), meaning alignment along the meridians, and for the trend in q (leads to greater orders as κ increases because $|q|$ increases). 126
4.13 Types of solutions for ρ when $\alpha = 0$ where we give specific values of the parameters (ξ, A, C) and vary the parameter κ. 127
4.14 The cylindrical branches of solutions for fixed $C = 173$. The curves are two distinct branches of solution, one where $Q > 0$, $\alpha = 0$ (the black curve) and then other where $Q > 0$, $\alpha = \pi/2$ (the blue curve). 129
4.15 The first plot represents the numerical solution for q (when $q < 0$). The second plot represents the numerical solution for ρ when $\alpha = 0$, where we give specific values of the parameters (κ, A, ξ, C). 130
4.16 The first plot represents the numerical solution for q (when $q > 0$). The second plot represents the numerical solution for ρ when $\alpha = 0$, where we give specific values of the parameters (κ, A, ξ, C). 131
4.17 Plot of the critical value $\bar{a}_{c,n}$ against ρ for different mode numbers. The critical value of ρ is $\rho_c \approx 1.1996$. The wide catenoid is for $\rho < \rho_c$ and the narrow one is for for $\rho > \rho_c$. 137
4.18 Plot of $\max_n \bar{a}_{c,n}$ against the aspect ratio ξ. Critical value of $\xi = \xi_c \approx 0.6627..$ and taking in the account that $\xi = \rho/\cosh\rho$, then wide catenoid is for $\xi < \xi_c$ and the narrow one is for for $\xi > \xi_c$. The narrow catenoid is the upper branch (the green one) and the wide catenoid is the lower branch (the yellow one) and the transition between the two modes is denoted by the blue colour. 138
4.19 The first figure shows an eigenfunction for $n = 1$ and $\rho = 1.25$ and the second one shows an eigenfunction for $n = 2$ and $\rho = 2$. 146
4.20 The product of $Q\,Q'$, the first one for $n = 1$ and $\rho = 1.25$ and the second one for $n = 2$ and $\rho = 2$. 147
4.21 Plot of $|q|$ for $\rho = 0.5$ and $\bar{a} = -1$ we get an axisymmetric solution, with no defects. This agrees with the results in Figure 4.17. 151
4.22 Plot of $|q|$ for $\rho = 1.2$ and $\bar{a} = -2$ give a two defect solution with the charge of defects calculated numerically as -0.5 (which agrees our prediction based on the linear stability calculation Figure 4.17). 152
4.23 The patterns of the field-lines for 2 defects solutions 153

4.24 Plot of $|q|$ for $\rho = 2$ and $\bar{a} = -20$ make three defect solutions, all defects appears are $-1/2$, where we calculate the charge by doing a rectangular contour integral around the defect. The second part of Figure 4.24 shows the patterns of the field-lines (black curves) for 3 defects solutions. 154

4.25 The values of $\rho = 1.5$ and $\bar{a} = -2$, generate 4 defects solutions with the charge $m = -1/2$ for each defects that is calculated by doing a contour integral around the defect. In the second part of Figure 4.25 we have obtained the field-lines (black curves). This agrees with the results in Figure 4.17. 155

Acknowledgement

I gratefully acknowledge my sponsor Sultan Qaboos University for providing me the scholarship and necessary funding to complete my PhD program.

I would like to express my sincere gratitude to my supervisor Dr. Steven Roper for his endless support and encouragement, for his patience and motivation. I am truly grateful for your guidance over these years. Beside your great personality, you helped me in every way you can for completing this thesis. Thank you Steve from the depths of my heart.

A special thank you goes to my second supervisor Dr. Luigi Vergori for his continuous support and guidance, for sharing his honest opinions and insightful comments.

Thank you also to the School of Mathematics and Statistics at the University of Glasgow for providing me assistance and support all these years.

I am grateful to my lovely children Balqis, Esra and Sulaiman for always being there with me when times are good or bad. You are always believing in me and giving me strength to continue my journey in PhD. A special thanks goes to my dear husband, Mohammed for understanding, patience and always being by my side. I am also extremely grateful to my whole family for their constant love, prayers and support. Especially my brother Mohammed, my sisters Rahma and Noora. Thank you to all my friends and relatives who supported me during throughout my PhD.

Finally, I would like to say that everything I am, or ever will be, I owe it to a great women. To the soul of my mother 'Shamsaa'.

Declaration

This thesis represents work completed, between 2017 and 2021 in the School of Mathematics and Statistics at the University of Glasgow. With the exception of chapters 1 and 2 which contain introductory material and mathematical background, I declare that all the work presents in this thesis was carried out by myself under the supervision of Dr. Steven Roper. I have acknowledged all sources used and cited these in the bibliography section.

For the MatLab codes used in chapters 3 and 4, I acknowledge that my supervisor Dr. Steven Roper has given assistance in writing the code and I have modified and run them to obtain the figures and results.

The work contained in chapters 3 and 4 will be written up for publication in appropriate journals.

List of notation

$\otimes$	the tensor product
div_s	the surface divergence
∇_s	the surface gradient
Δ_s	the surface divergence of the surface gradient (surface Laplacian)
$\boldsymbol{\varepsilon}$	the Ricci alternator
δ_{ij}	The Kronecker symbol
$\mathbf{P}$	the perpendicular projection onto the tangent plane of S
$\boldsymbol{\nu}$	the normal vector to the surface
$\mathbf{I}$	second order tensor identity
$\mathbf{Q}$	second order tensor parameter
$\mathbf{M}$	second order variance tensor
q_0, q_m	two scalar order parameters
$\mathbf{e}_1$, $\mathbf{e}_2$	principle curvature directions
$\boldsymbol{\omega}$	the spin connection
ς	the apshericity
κ_i	the geodesic curvatures of the line of principle curvatures
γ	the surface tension

H	the mean curvature
K	the Gaussian curvature
$\mathbf{L}$	the extrinsic curvature tensor, a symmetric tangential second order tensor
c_1, c_2	principal curvatures
c_0	the spontaneous curvature (Canham-Helfrich energy)
$\boldsymbol{n}$	a unit vector field (the director)
$\boldsymbol{v}$	a differentiable vector field
$\mathbf{k}$	an outward unit vector to the boundary curve of the surface
$\boldsymbol{\tau}$	the conormal vector
$\boldsymbol{u}$	an arbitrary field
w	the free energy density
k	the elastic constant
$\boldsymbol{\sigma}$	the stress tensor
ψ	the normal increment
$\boldsymbol{f}$	density per unit length
$\boldsymbol{\Omega}$	an arbitrary skew tensor
$\boldsymbol{s}$	the boundary contact moment per unit length
$\kappa, \bar{\kappa}$	are bending rigidities

Chapter 1

Introduction

1.1 Structure of thesis

In this thesis we study a thin film of liquid crystal spanning two coaxial rings (rings of the same radius with parallel planes of orientation, centres along the same axis, separated by a distance) and analyse the behaviour of the liquid crystal as it interacts with the geometry of the film and also how the geometry of the film interacts with the liquid crystal. This thesis is structured as follows.

In Chapter 1, we give some historical background about the liquid crystals and review types of liquid crystals and their properties and applications. Also we give a literature review about thin films of liquid crystals. Then, we introduce approaches to modelling liquid crystals. We briefly introduce the swarm theory [78] and discuss Frank theory where the relevant paper is [16] which introduces the energy per volume in terms of the director field (its splay, twist, and bend). Also we introduce the Q-tensor theory and its parameterisation. We use [54], [69] and [76] to see this approach.

Chapter 2 contains mathematical background to modelling liquid crystals, the differential geometry of surfaces and a review of some useful results for our work. First, we introduce notation for vectors and scalars and operations involving tensors. Then, we discuss surface calculus to introduce the surface gradient, surface divergence and surface curl. Also we introduce the extrinsic curvature tensor and its invariants and relationship to the surface normal. Next, we report the surface divergence theorem as this theorem is employed in our work. Also we derive variations or increments in the different surface quantities that will be considered in Chapter 3 to study the stability of solutions to the equilibrium equations using incremental equations. At the end of this Chapter we briefly review the paper [68] that derives the surface free energy using both the Frank energy and the Q-tensor theory approach. Also we give a review of the first variation of the free energy functional and derivation of equilibrium equation using [66].

In Chapter 3, we derive the equilibrium equations for open surfaces following [66]. Our

original contribution is to extend the results of [66] to open surfaces. This gives natural boundary conditions on the boundary of the open surface. Therefore our additional parts here are terms that come from the boundary contributions. Also we discuss a range of essential boundary conditions. After we develop the equilibrium equations and boundary conditions for open surfaces, we examine the stability of their solutions via the *incremental equations* and show that this approach can give information about the stability of solutions to the equilibrium equations. Our contribution here is to develop a framework for analysing stability using the incremental problem.

In Chapter 4, we analyse the behaviour of a thin film of nematic liquid crystal spanning two coaxial rings. We derive the appropriate surface free energy involving LdG theory [42], [61] and parameterise the second order variance tensor $\mathbf{M}$. Two parameterisations of $\mathbf{M}$ are used one using the scalar order parameter q and the unit tangent vector field $\mathbf{n}$ ($|\mathbf{n}| = 1$), the other using the two scalar order parameters q_0 and q_m. We derive the equilibrium equation and boundary conditions for the catenoid using these two different parameterisations. We use the results developed in chapter 3 to derive the equilibrium equations and boundary conditions and solve the equations numerically for a range of dimensionless parameters. To do this we specialise the energy density to the axisymmetric case and derive the equilibrium equations and natural boundary conditions. Then we transform the equilibrium equation to a set of first order equations suitable for numerical work. Also we consider the stability of the isotropic distribution by fixing the geometry of the surface as catenoidal (noting that this shape does not solve the natural boundary conditions) and calculate the change to the melting temperature as a function of the geometry of the film (the aspect ratio). In the limit of vanishing elastic constant the equilibrium surfaces are expected to be catenoidal but this is singular perturbation, which means there are boundary layers near the rings where the shape deviates from that of a catenoid. Finally we consider the structure of the solution at onset of nematic order and identify defects and their locations ([1], [38], [104]).

Throughout this thesis we prove the lemmas that are necessary for the construction of our work. Also some details and proofs of our calculations are reported in the Appendix A. Appendix B gives the MatLab codes that are used to produce results and figures.

1.2 What are liquid crystals?

It was formerly assumed that matter exists in three states such as solid, liquid and gas. However, this is not entirely accurate. The degree and type of ordering of the structure or molecules are used to distinguish the states. The physical state of any material is also characterized in terms of translational and rotational motion of the molecules [42].

Liquid crystals (LCs) are a state of matter that combines properties between those of

conventional liquids and solid crystals, exhibiting the mechanical and symmetry properties of both [1]. They may flow like a liquid, but their molecules may be oriented along a common direction like in crystal. A more proper name is 'mesomorphic phases' [42].

There is a big difference between a crystal and a liquid, where the mechanical properties of these two states of matters differ. Obviously liquid flows easily whereas in crystals, the molecules are regularly stacked and the centers of mass of the different groups are situated on a three-dimensional periodic lattice [90]. In a liquid there is neither orientational or positional order and the center of mass are not ordered in this sense [42]. In liquid crystals, molecules are sensitive to the presence of physical boundaries and electric or magnetic fields. In liquid crystals weak short-range interactions can give rise to long-range orientational order. Depending on the properties of the liquid crystals, any sudden action of a field will affect orientation of the molecules to the direction of the field and this will affect the transmission of polarized light [42].

Research on liquid crystals has been involved in many fields like physics, chemistry, biology and engineering. Liquid crystals are used widely in applications of computer monitors, cell phones, calculators, watches and flat-panel televisions where the image quality of the liquid crystals displays (LCDs) has been improved and the resolution of LCDs has also become finer [64]. We will come back to the technological applications of liquid crystal in more details in section §1.2.4. Most liquid crystals are organic substances, and are called 'mesogenic' [15]. There are two distinct ways to induce the liquid crystalline phase in a mesogenic substance, either by changing its temperature or its concentration in a solvent. When the mesophase is formed by dissolving in a suitable solvent under appropriate conditions of concentration then such system is called lyotropic liquid crystal [110]. Figure 1.1 shows tendency of the molecules to point along a common direction called the director $\mathbf{n}$.

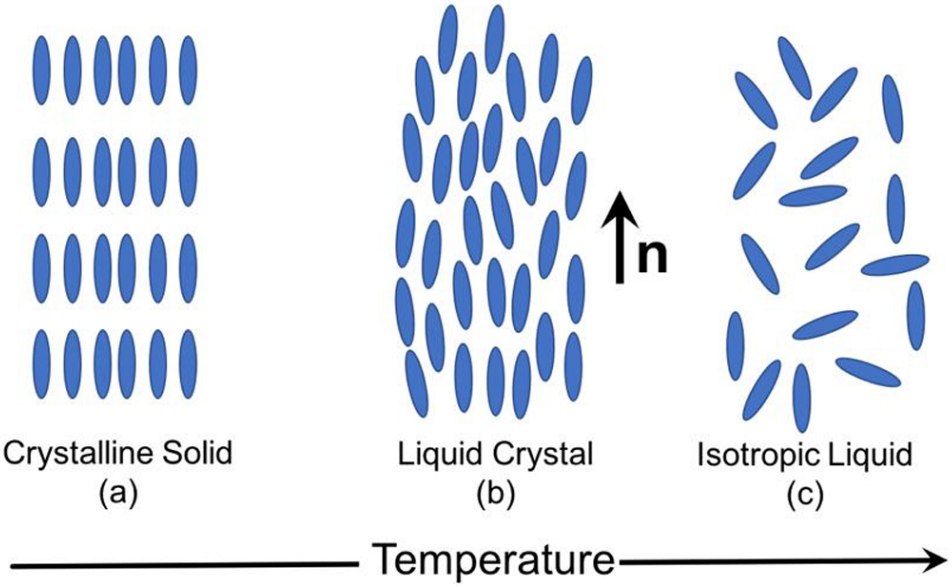


Figure 1.1: Phase transition with temperature variation: crystaline solid, liquid crystals and isotropic liquid respectively, and the representation of molecular arrangements in each phase [21].

A detailed discussion of the structure and material properties of thermotropic liquid crystals follows in section §1.2.2.

1.2.1 History of liquid crystals

This section gives some historical features of liquid crystals. The term liquid crystal appeared in the late 19th century. Liquid crystals was discovered accidentally by F. Reinitzer while he studied cholesterol benzoate of carrots. He observed two melting points when he heated this substance. He also noticed that the substance reflected polarized light and had the ability to rotate the polarization direction of the light. The cloudy substance observed by Reinitzer is called cholestric (an example of liquid crystals) [92], [110].

Reinitzer consulted Otto Lehmann, a scientist who worked on the optical description of the cloudy phase. Lehmann came to the conclusion that the cloudy liquid might rotate the polarization state of the transmitted light and showed optical birefringence. Later on, Lehmann introduced the term liquid crystals on account of the double refraction found in certain liquids [79]. In 1911, C. Mauguin performed and described the first electro-optical experiments involving a twisted nematic phase. In 1922, M. G. Friedel divided liquid crystals into three categories based on their molecular organization, which called nematic 'thread', smectic 'soapy' and cholesteric 'twisted nematic'. Friedel also understood that liquid crystals could be affected by applied electric and magnetic fields. This is an important feature for their application in display devices [110].

The modern history of liquid crystals has been dominated by the development of

electronic displays. In 1970-71, the twisted nematic cell was invented by Ferguson, Schadt and Helfrich, which plays a big role in extensive of LCDs all over the world. In the following two decades, LCDs replaced conventional display devices in many applications such as portable PCs, mobile phones and electronic devices. Today liquid crystals are used in a wide range of display applications such as high modulus fibers [22] and opto-electronic devices.

1.2.2 Classifying liquid crystals

The common experimental methods often used to classify liquid crystals are differential thermal analysis, microscopy and X-ray [15]. The molecules of liquid crystals can arrange themselves in different phases depending on the nature of the molecules, the interactions between them and the temperature. Thermotropic liquid crystals can be divided into three categories depending on the orientation and order of molecules which are: nematics, smectic and cholesteric [22].

Nematics

Nematic comes from the Greek prefix 'nemato' which means thread-like. Molecules in the nematic liquid crystal phase have an orientational order but no positional order and can flow easily. Nematic molecules tend to be parallel to a unit vector or a director called $\mathbf{n}$, where the direction of $\mathbf{n}$ varies in-time and space. So the director is a variable that is dependent on space and time, $\mathbf{n}(\mathbf{x}, t)$. The spacing between molecules in all directions is not uniform (as shown in Figure 1.2).

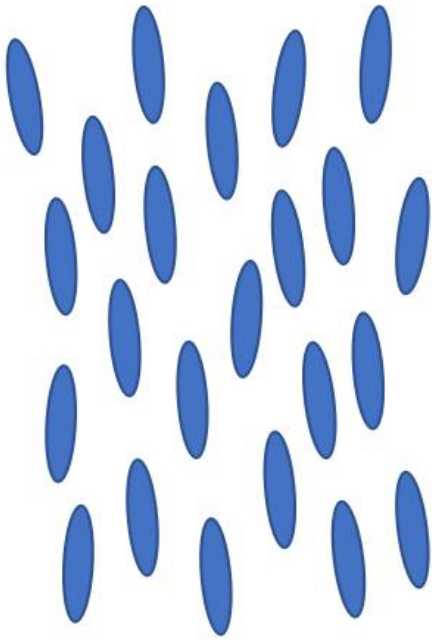


Figure 1.2: The arrangement of molecules in the nematic phase [42].

Nematics response easily to external fields like electronic, magnetic and surface fields. When nematic liquid crystal are constrained to a curved surface, the geometry changes the molecular orientation. Also depending on the shell thickness, the molecules might have an in-plane order instead of a spatial distribution [44], [103]. Depending on the basis of the structure of the constituent molecules nematics liquid crystaline phase can be categorized as calamitic nematics and discotic nematics. The calamitic nematics are formed by molecules which have rod-like structure, whereas the discotic nematics comprise disc-shaped molecules that stack up one over the other and has a high tendency to form a columnar phase [21].

Generally, nematic liquid crystals are classified into three different phases: isotropic, uniaxial and biaxial. The fundamental principle of any biaxial system is that there is no axis of complete rotational symmetry. A uniaxial system has an axis of rotational symmetry (such as the director $\mathbf{n}$ in uniaxial liquid crystal) [42].

The molecular arrangement corresponding to a biaxial system can have two shapes of the molecules either uniaxial or biaxial. For a uniaxial molecule, the shape like a cylinder or rod, where a biaxial molecule can be shaped like a plank of wood. In unaxial, there is a rotation symmetry about the axis of the molecule. Whereas in biaxial there is no rotation axis along the axis of the plank, but there are three axes of reflective symmetry (the long, intermediate and short axis of the plank) [106], [110]. The most general nematic state is the biaxial state.

Cholesterics

Cholesterics liquid crystals are similar to nematics except that they are composed of molecules which are optically active. As a consequence, the structure gains a spontaneous twist about an axis perpendicular to the director [22]. They are known as chiral nematic liquid crystals. Cholesterics molecules tend to align themselves into a helical structure (see Figure 1.3), which can be either right handed or left-handed. In the cholestric phase, the molecules are arranged in layers, each layer is rotated with respect to the one above and below it to give a spiral structure where no positional ordering within layers [40]. Also all molecules must have one and the same chirality in a pure substance. They display a privileged direction, which is the helical axis[110].

The distinction between cholesterics and nematics is based on two essential criteria. The first is that only the orientation of the axis of molecules matters in their interactions; in other words, if a molecule is turned upside-down, its interactions with its neighbours molecules are unaffected. In this sense, under exchange of head and tail, the cholestric molecules are also invariant. However this property can not be expressed in terms of mirror symmetries as reflection reverse chirality. The second feature is their natural orientation of the molecules. Assuming that no external field distorts the molecular axes, the molecules arrange themselves as if they were to minimise the free volume between the neighbouring molecules. The molecular orientation of cholesterics tend to be aligned along a preferred axis labeled by a director $\mathbf{n}$ (the unit vector indicating the preferred orientation of the long axis of liquid crystal molecules) which fails to be the same at all points in space, but varies reflecting the chirality of the molecules [110].

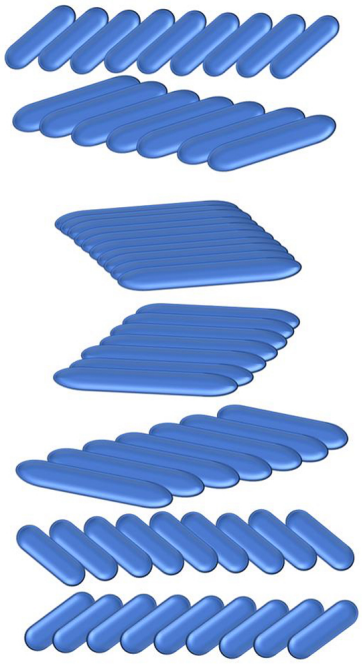


Figure 1.3: The arrangement of molecules in the cholesteric phase [42].

The z-axis is the helical axis of the system, and represent a right- handed orthonormal Cartesian coordinate system (x, y, z) points along the cholesteric axis. Then $\mathbf{n}$ can be described by the following structure

$$\mathbf{n}_x = \cos(q_0\, z + \phi), \quad \mathbf{n}_y = \sin(q_0\, z + \phi), \quad \mathbf{n}_z = 0, \tag{1.1}$$

where q_0 is a scalar, which can be either positive or negative depending on the temperature of the cholesteric liquid crystal and ϕ is an angle in the interval $[0, 2\pi[$. The angle ϕ has no intrinsic significance (as it depends only on the frame of reference employed to write (1.1)) [110]. The modulus of q_0 called the twist. Giving that $\mathbf{n}$ and $-\mathbf{n}$ are equivalent, the structure is periodic along z and the spatial period say P_s represents the distance between any two adjacent spirals:

$$P_s = \frac{2\pi}{|q_0|} \tag{1.2}$$

which is called the natural pitch. The above helix is right-handed when q_0 is positive and it is left-handed when q_0 is negative. It may happen that at some critical temperature q_0 vanishes; then the liquid crystal becomes nematic and the field described by (1.1) it therefore reduces to a constant [110].

Smectics

The third category of liquid crystal is smectics, which means soap in Greek. The name is given for certain mesophases with mechanical properties similar to soap. Thus a soap

bubble provides the most common example of a smectic liquid crystal. Smectics are different from both nematics and cholesterics. Smectics liquid crystals show a close interaction between positional and orientational ordering of molecules (see Figure 1.4). These substances are given some stiffness by such a feature, and yet they are able to flow, where the flow is allowed because it is orthogonal to the positional ordering (the layering) [110].

All smectics are layered structures with a well defined inter-layer spacing. Also smectics have further degrees of order compared to the nematic phases and usually occur at certain temperatures below the nematic domain. When smectics are heated well enough, they usually became either nematics or cholesterics before the isotropic phase [42].

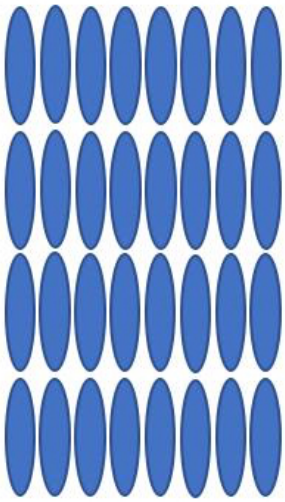


Figure 1.4: The arrangement of molecules in the smectic phase [42].

There are many numbers of smectics, however the three main types are smectics A, smectics C and hexatic smectics [42].

1.2.3 Material properties of liquid crystals

Liquid crystals have a wide range of optical properties that are important in a variety of applications. The elongated structure of the molecules causes anisotropic behaviour, which means that the physical properties of these molecules change when measured parallel or perpendicular to their length. In this section we illustrates briefly the most relevant properties.

Birefringence

The birefringence of liquid crystals phases is a result of the parallel order of molecules showing a polarizability anisotropy. The observation of birefringence is useful to recognise a liquid crystal. A mono-domain specimen of nematic medium is uniaxial and strongly birefringent. When light strikes the surface of a birefringent material, it is generally split

into two polarised components that have same frequency and different speed and at right angles to each other. The value of birefringence is determined by the structure and order of the liquid crystal phase type and the polarizability properties of the molecules, however it decreases dramatically with the increase in temperature for a given compound [22].

Viscosity

The viscosity η is an important parameter of liquid crystals. It has a practical importance in determining the on and off times of display devices [22]. Liquid crystals display anisotropic flow behaviour that give rise to six different coefficients of viscosity. One of these coefficients is the rotational viscosity, that used to describe flow that results from an axial rotation of the nematic director $\mathbf{n}$. However, the bulk viscosity is the easiest to determine among all viscosity coefficients. Generally, the viscosity decreases with the rise of temperature (all types are temperature dependent) [88].

Elastic constants

Different patterns of director deformation can be achieved because the uniaxially aligned liquid crystals can be deformed in a specific way by external mechanical force and/or magnetic fields. The continuum theory developed by Oseen [79] and Ericksen [31] explains these director deformations. The distortion free energy density F_d of nematic director $\mathbf{n}$ is derived from de Gennes [42] for the general deformation of nematic liquid crystals as [88], [91]:

$$F_d = \frac{k_1}{2}\left(\nabla \cdot \mathbf{n}\right)^2 + \frac{k_2}{2} \cdot \left(\mathbf{n} \cdot \left(\nabla \times \mathbf{n}\right)\right)^2 + \frac{k_3}{2}\left(\mathbf{n} \times \left(\nabla \times \mathbf{n}\right)\right)^2 - \frac{k_{24}}{2}\nabla \cdot \left(\mathbf{n}\left(\nabla \cdot \mathbf{n}\right) + \mathbf{n} \times \nabla \times \mathbf{n}\right). \tag{1.3}$$

where the constants k_1, k_2 and k_3 describe the elastic restoring forces in the three deformation states; namely splay, twist and bend respectively as shown in Figure 1.5 while k_{24} is called the saddle-splay modulus;

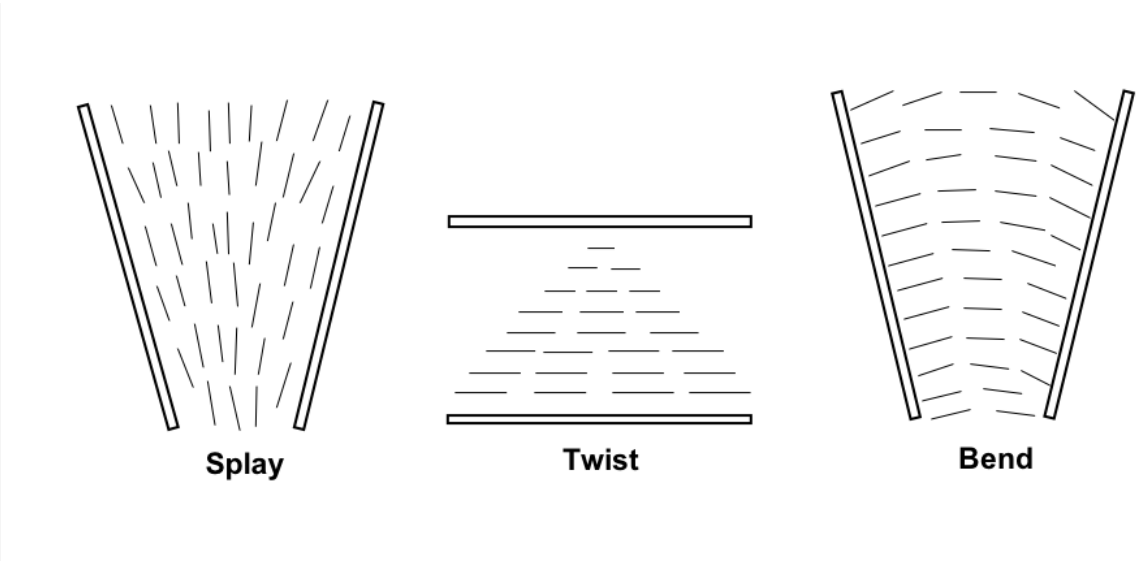


Figure 1.5: The three principle types of deformation in a nematic liquid crystal: splay, twist and bend [88].

All three elastic constants k_1, k_2 and k_3 decrease with the increase in temperature.They are essential for the the operability and efficiency of liquid crystal displays.

1.2.4 Applications of Liquid Crystals

The study of liquid crystals has opened new possibilities in the physics of condensed matter which has provided many technological branches and practical applications. Mainly applications of liquid crystals are focused on three areas including [15]:

1. The liquid crystal displays that have been used widely in digital display application (LCD).

2. The use of nematic liquid crystals in industrial laboratories and in medical clinics. There are many applications of liquid crystals in medicine and pharmacy.

3. The use of liquid crystals as solvents for chemical reactions.

The unique properties of the liquid crystaline phases and associated advantages are being widely used in the technological applications. In Section §1.2.2 we gave a brief review of molecular organization in liquid crystals and relationships between the structures and their material properties of liquid crystals that are relevant to the applications. This section will give a brief description of some examples of the applications of liquid crystals.

Liquid Crystal Displays

Liquid crystal display (LCD) is a flat panel display that operates primarily with liquid crystals. It has become the only display technology efficient of displaying the simple time

data of a digital wristwatch and the complex color images of computers and televisions. Nematic phase is the most popular type in the liquid crystal display industry because of its attractive features such as low power consumption and high contrast ratio [22].

The early 1970s was the start of researching, designing and correlating molecular structures with material properties and electro-optical effects with the aim of discovering and developing new electro-optical effects and liquid crystals that would lead to improve displays. The first commercial twisted nematic (TN) liquid crystal mixture was produced in laboratories in 1971 [89]. The mixture called Ro-TN-200 and consists of only two types of molecules with structures which are almost identical [88]. The mixture properties were sufficient to realize the first $3\frac{1}{2}$ digit, black-and-white TN-LCDs for watches, which consisted of twenty-four image components (pixels) [87].

A lot of commercial liquid crystal displays (LCDs) are based on twisted nematic (TN) or various super-twisted nematic (STN) effects, which have undergone extensive development and enhancement over the last 25 years and are still improving. Today, a lot of displays (TVs mainly) are IPS (in plane switching) or VAN (Vertical aligned nematic). Advanced liquid crystal products, that are used for realization of the thin film transistor (TFT) addressed twisted nematic (TN) displays with high information content as well as time multiplexed super twisted displays, mostly consist of more than twenty components of liquid crystal with completely different molecular structures. Modern liquid crystal materials and the advanced TFT-TN displays result in color displays of more than one million pixels [88].

The displays must be compatible with integrated electronics with lower power consumption. In addition, they should be flat and low-weight and be able to turn the electronic output signals of a multitude of electronic devices rapidly into high-quality optical images. The flexibility of liquid crystals display enables them to be used as light modulators in wide area projectors as well as direct view displays [88].

Thermography

Liquid crystals can be used for thermography like mapping surface temperature distribution. In such an application, the relevant parameters are the mean surface temperature, the mean variations and the temperature sensitivity [22]. The recent studies and researches have shown that cholesteric liquid crystals have specific physical and clinical properties where only those properties that are beneficial in medical applications for liquid crystals thermography. One of the medical applications of thermography of liquid crystals is determining the place of inflammatory injuries. Thermography of liquid crystals is also used for determining the presence and spreading of different tumours (like different types of cancer) [100].

1.3 Approaches to modelling liquid crystal

Before dealing on liquid crystals theories, I comment briefly in an earlier theory giving a short summary of the main features of this theory. It is considered as the natural precursor of Frank's theory. This theory is the swarm theory. The swarm theory was proposed by E. Bose in 1909 [78] and it applies to nematics and cholesterics only.

According to the theory, the molecules of liquid crystals group themselves in groups called swarms comprising about 100,000 molecules in each swarm and lie in the same direction. The direction of the molecules in the swarm will be different from one swarm to another. The swarm formation comes because of asymmetrical shape of the molecules and irregularly laying where their axes are distributed at random. The interactions between swarms are much weaker than those among molecules in a single swarm. Note that, without external forces such as electric or magnetic fields the orientation of the molecules in one swarm is completely independent of that in another. However external forces can orient the swarms [110].

Another theory outlined to give rise to liquid crystals is the distortion theory. The theory was proposed by H. Zocher in 1927. Later on, in 1933 Zocher applied this theory to nematics liquid crystals subject to a magnetic field. He tried to give a mathematical explanation of the distortion produced on liquid crystals by applying external fields. Zocher was successful in explaining the interactions of nematics with magnetic fields but his theory did not prevail over the swarm theory [79], [80], [110].

According to Zocher's view the orientation of the molecules changes continuously in space and it responds in an elastic manner to the external distorting actions; when these later are absent the natural orientation prevails everywhere [110].

1.4 Introduction to Q-tensor theory

This section aims to provide an introduction to the **Q**-tensor approach to model nematic liquid crystals and the appropriate free energy density. In liquid crystals we are interested in controlling the orientation so we need to introduce variable(s) to measure how spread out the molecular orientation distribution is [32]. In the 1960s de Gennes introduced the order tensor theory that allows the study of nematic isotropic phase transitions. De Gennes theory is based on the orientational probability distribution and measures the degree of orientation and biaxiality [71], [76]. This theory depends on the second order, symmetric and trace less tensor **Q** that is used as a state variable. The scalar parameter s represents the degree of orientation that vanishes at point where there is no privileged direction [61], [71], [72]. The director $\mathbf{n}$, is defined to be the average molecular orientation direction. For nematic molecules this will be the average long axis orientation. The director $\mathbf{n}$ depends on both space and time coordinates, $\mathbf{n}(x,t)$. Let θ_m denotes the angle between a molecule

and the director. To measure the amount of orientational order of the molecules will use the scalar order parameter which is denoted by s. This is a weighted average of the molecular orientation angles θ_m between the molecular axes and the director.Therefore the scalar s is interpreted as the degree of orientation [32], [110]

$$s = \frac{1}{2}\langle 3\cos^2\theta_m - 1\rangle \tag{1.4}$$

where $\langle\,\rangle$ denotes the statistical average and equation (1.4) is the second order Legendre polynomial. The scalar order parameter lies within the interval $-\frac{1}{2} \leq s \leq 1$ [32], [68], [110].

1.4.1 Tensor order parameter Q

The $\mathbf{Q}$ tensor theory is based on the average molecular orientation measured by the second order variance tensor field $\mathbf{M}$ given by

$$\mathbf{M} = \langle \mathbf{n} \otimes \mathbf{n}\rangle = \int_{S^2} \rho(\mathbf{n};\mathbf{x})\mathbf{n}\otimes\mathbf{n}\, dS \tag{1.5}$$

where ρ is a probability density defined on the surface of the unit sphere and tells us the probability of finding a molecule with orientation $\mathbf{n}$. Obviously,

$$\int_{S^2} \rho(\mathbf{n};\mathbf{x})\, dS = 1 \tag{1.6}$$

and since nematics have a molecular mirror symmetry (the head and tail of the molecule can be changed without any physical change) then the probability measure is even where $\rho(\mathbf{n}) = \rho(-\mathbf{n})$. This probability varies as we move around the material and so $\mathbf{M}$ depends on position in the material. Note that $\mathbf{M}$ is symmetric and it has unit trace

$$\operatorname{tr}\mathbf{M} = \int_{S^2} \rho\mathbf{n}\cdot\mathbf{n}\, dS = \int_{S^2} \rho\, dS = 1. \tag{1.7}$$

We define $\mathbf{Q}$ to be the traceless part of $\mathbf{M}$ so

$$\mathbf{Q} = \mathbf{M} - \frac{1}{3}\mathbf{I}. \tag{1.8}$$

The $\mathbf{Q}$-tensor is traceless and symmetric. When $\mathbf{Q} = \mathbf{0}$ the distribution is called isotropic and there are no preferred directions for the molecules. The liquid crystal is in its melted state when $\mathbf{Q} = \mathbf{0}$. If $\mathbf{Q}$ is non-zero then, as it is symmetric it can be written with respect

to a basis of orthonormal eigenvectors $\mathbf{n}$, $\mathbf{e}_+$ and $\mathbf{e}_-$

$$\mathbf{Q} = s\left(\mathbf{n}\otimes\mathbf{n} - \frac{1}{3}\mathbf{I}\right) + \lambda\left(\mathbf{e}_+\otimes\mathbf{e}_+ - \mathbf{e}_-\otimes\mathbf{e}_-\right) \tag{1.9}$$

the eigenvectors have corresponding eigenvalues $2s/3$, $\lambda - s/3$ and $-\lambda - s/3$. Since $\mathbf{M}$ is positive definite we must have that $|\lambda| < (1-s)/3$ and $-1/2 \leq s \leq 1$. If $s = 1$ then $\lambda = 0$ and we have perfect alignment along the direction $\mathbf{n}$. If $s = -1/2$ and $\lambda = 0$ then we have isotropic distribution in the plane perpendicular to $\mathbf{n}$.

1.5 Previous works

In this section we provide a summary of the main works where this thesis is based on. We outline the contributions are made by the relevant papers ([16], [54], [66], [67] [68], [70]) and how they are related to our work. These papers are used to perform the new calculations for the catenoid problem.

The classical continuum theory is based on works of Oseen ([79], [80]), Zocher [114] and Frank [16] (OZF) and it is considered as the first steps towards the present understanding of the elastic properties of liquid crystals [56].

The work of [68] establishes how to derive an effective surface free energy from a bulk free energy, by using a 'thickened surface' of thickness h and passes to an effective surface energy in the limit as $h \to 0$. It does this in two cases, one using the Frank energy (see[16]) (using the director) and another using the $\mathbf{Q}$-tensor theory. In the one constant approximation (where all the elastic moduli corresponding to the splay, twist and bend contributions are equal) the effective total energies are

$$W_{OZF} = \int_S \frac{1}{2}k|\nabla_s\mathbf{n}|^2\,dS \tag{1.10}$$

and

$$W = \int_S \frac{1}{2}k|\nabla_s\mathbf{M}|^2\,dS \tag{1.11}$$

where $\mathbf{M}$ is the second-order variance tensor that measures the distribution of the molecules (see §1.4.1). The work of [68] establishes the model we will use when studying the shape and stability of a nematic film suspended between two coaxial rings. In comparison to earlier models, the surface energies calculated by [68] have extra terms to describe the elasticity of the shell. These terms are considered to be the link of the extrinsic curvature of the shell and the nematic order parameters. The results presented in this paper serve as a basis for further studies towards curved nematics liquid crystal configurations. Throughout our thesis we make use of the general theory covered in [68], we use the expression for the energy density, find the shape equation and two equilibrium equations (corresponding

to q_0 and q_m) and the boundary terms when considering the first variation of (1.11) within the framework of Landau-de Gennes theory for nematic liquid crystal film (w_{LdG}). To the liquid crystal energy (the elastic and Landau-de Gennes terms w_{LdG}) we also add a surface tension, a constant energy per unit area of the surface.

The paper [113] gives some backgrounds for general expressions for the first and second variation of the shape equation and equilibrium equations. This paper expresses these variations for arbitrary shapes. This paper has details of how to derive the general equilibrium equations and the shape equation by making use of parameterisations of the surface to calculate the first variation and calculate the stability using the second variation. This formalism can be applied to analyse the stability of the catenoid, however [66] has different way to perform this type of calculation.

The work of [66] explains how to derive the equilibrium equations for a very general surface energy for closed surfaces (without a boundary). The paper illustrates the approach on a number of examples, including the soap film, lipid bi-layers (Canham-Helfrich energy) and other surfaces with structure (such as liquid crystals). The authors consider the first variation and derive an effective stress and couple tensor that has some mechanical interpretation. The main results of the paper are the derivation of a shape equation and equations for the order parameters (which might be scalar, vector or tensor). We will use these results when deriving both the equivalent expressions for open surfaces in Chapter 3 and the equilibrium equations in Chapter 4 and derive the natural boundary conditions. In order to derive these equations we consider the variations of free energy density w, that is to calculate δw as the other quantities were done in [66].

The work of [54] studies the appearance of defects on a ellipsoid shell of liquid crystal. They show that the position of the defects depends on the curvature of the surface and use a relaxation method to solve the non-linear equations numerically. The calculations in this paper demonstrate the calculation of $\nabla_s \mathbf{Q}$ using the q_0 and q_m parameterisation and find the geometric quantities (curvatures) on the surface. Using [54] we have learned the details of how to specialise the equilibrium problem to the catenoid problem and look for axisymmetric solution. Specialising to axisymmetric surfaces allows us to explicitly calculate the mean (H) and Gauss curvatures (K) and other geometric quantities involving the geodesic curvature of lines of principal curvature on the surface. Our fields become $q_0(z), q_m(z)$ and for the shape $R(z)$ and so we get an equilibrium equation for each of these that we can examine for solutions.

The work of [70] is closest to the problem that we study in Chapter 4. In this work the authors consider a thin film of liquid crystal suspended between two co-axial rings and model the surface energy using the Frank theory. They show that depending on the dimensionless bending energy and the orientation of $\mathbf{n}$ (the director) there are a number of branches of solutions, including cylindrical shapes, spherical shapes and catenoidal-shapes,

with the distribution of the director uniform in many cases, but also proving that there are some parameter regimes where the director field must be non-uniform.

The paper [67] studies the extrinsic curvature effects on nematic shells through the Frank theory to surface director fields. It considers an example of nematics on a cylindrical shell to demonstrate this effects and used the Frank elastic moduli to control the influence of the curvature. The study done in this paper shows that, the alignment of the molecules on the cylindrical surface have a stable configurations that depend on the twist and bend elastic moduli.

The work of [69] is considered to be an extension of the work done in [67] and [68]. It used the surface energy proposed in [68] to study the effect of the extrinsic curvature on the alignment of the nematic liquid crystals on a cylindrical surface. This study shows that the alignment of the nematic molecules is in the direction of the principle direction of smallest curvature (alignment along the cylinder axis).

Experimental work on thin films of liquid crystal has included the work of [58]. In this paper the authors try to control the interaction of colloidal particles by coating them with a thin film of liquid crystal, they vary the thickness of the film in order to control the number and type of defects that appear. In this way they aim to control the nature of the interactions of the particles. They observe the predicted tetrahedral arrangement of defects but also a large range of other types, depending on the film thickness.

Another experimental work on nematic films of liquid crystals has been done in [33]. The authors study the behaviour of spherical shells of liquid crystals by varying their thickness around the sphere and investigate the defects structures of these spherical shells. They observe the defect structure eventually merges with a bulk nematic liquid crystal drop at the limit of very thick shells.

The work of [112] develops a theoretical explanation of the geometric structure of ellipsoidal vesicles and cylindrical vesicles. In this paper the authors present a simple model free energy (as a function of the membrane geometry and the in-plane nematic order) and analyse (analytically and numerically) the low free energy in various parameter regimes.

The work of [39] is a study of defect structure for a two-dimensional liquid crystal (but the molecules can be directed out-of-plane, this is different to when the molecules are constrained to lie in-plane. The authors examine the structure of defects with different charges, which are imposed via a choice of boundary condition.

The paper [71] do a comparison between ferromagnetic and nematic shells. Both ferromagnetic and nematic shells have local interaction and anchoring potential. They also have similar curvature-induced effects. However they have different order parameters, a vector in ferromagnetic and a tensor in nematic shells. The investigation done on the spherical shells yields that ferromagnetic shells have integer topological charge vortices

while the texture of nematic shells admit half-integer charge vortices. The paper [72] provides supplementary information and derives the surface Frank-Rapini-Papoular energy density as a result of a perturbation analysis of the 3D energy functional assuming that the region of nematics is very thin.

The paper [76] considers one-constant approximation and explore the 3D Landau-de Gennes and $\mathbf{Q}$ tensor model as a generic surface model (a thin film limit) and modify the derived energy by adding a penalty term to enforce uniaxiality weakly . The model is applied to the curved surface to discuss the impact of curvature on the ordering of the liquid crystal.

Our work makes use of the main results of the papers above and extends to obtain new contributions where we perform a numerical exploration of the solution for the catenoid problem, identify defects and find charge of defects at the onset of nematic order.

Chapter 2

Mathematical preliminiaries

This chapter collects the mathematical background needed in the rest of the thesis. In particular, since we will be concerned with thin films (shells) of liquid crystal in different geometries we will need a number of results concerning the calculus of scalar, vector, tensor fields on surfaces and operations involving tensor that are used throughout this thesis.

The structure of the chapter is as follows. We introduce the mathematical terminology and notation used for scalar, vector and tensor fields. After this we discuss how to compute directional derivatives on surfaces and introduce the surface gradient operator [54], [66], [67] and [68]. We review the required differential geometry, including introducing the extrinsic curvature tensor, principal curvatures and principal directions and the apshericity on a surface [5], [30]. Since we will be concerned with the behaviour of liquid crystal films and shells we review useful results and theories from [54], [66], [67] and [68] and how these results and theories are used to derive surface free energies.

2.1 Tensors

For our purposes a tensor is a linear map between the vector spaces $\mathcal{V}$ and $\mathcal{W}$ such that $\mathbf{S} : \mathcal{V} \to \mathcal{W}$. Most often $\mathcal{V}$ will be $\mathbb{R}^3$ or the tangent space at a point on a surface and $\mathcal{W}$ will be $\mathbb{R}^3$. In particular we will be interested in tensor fields defined on surfaces. We write $\mathbf{S}$ as a tensor and $\mathbf{Sv}$ to mean $\mathbf{S}(\mathbf{v})$, and linearity means

$$\mathbf{S}(\mathbf{u}+\mathbf{v}) = \mathbf{S}(\mathbf{u}) + \mathbf{S}(\mathbf{v}) = \mathbf{Su} + \mathbf{Sv}.$$

The zero tensor is defined by

$$\mathbf{0v} = \mathbf{0}, \forall\, \mathbf{v} \in \mathcal{V}. \tag{2.1}$$

We have a multiplication of tensors via composition (provided the co-domain of $\mathbf{T}$ and domain of $\mathbf{S}$ are compatible), so given $\mathbf{S}$ and $\mathbf{T}$ are tensors, $\mathbf{ST}$ is such that

$$(\mathbf{ST})(\mathbf{v}) = \mathbf{S}(\mathbf{T}(\mathbf{v})) = \mathbf{ST}\,\mathbf{v}. \tag{2.2}$$

Let $\mathcal{L}(\mathcal{V}, \mathcal{W})$ be the space of linear maps between $\mathcal{V}$ and $\mathcal{W}$. Given that $\mathbf{A}$ and $\mathbf{B}$ are elements of $\mathcal{L}(\mathcal{V}, \mathcal{V})$, then the sum of them is defined as [110]

$$(\mathbf{A} + \mathbf{B})\,\mathbf{v} = \mathbf{A}\mathbf{v} + \mathbf{B}\mathbf{v}, \text{ for all } \mathbf{v} \in \mathcal{V},$$

and the multiplication of a tensor $\mathbf{A}$ by a scalar $\lambda \in \mathbb{R}$ via,

$$(\lambda\mathbf{A})\,\mathbf{v} = \lambda \cdot \mathbf{A}(\mathbf{v}) \text{ for all } \mathbf{v} \in \mathcal{V}.$$

If $\mathcal{W} = \mathcal{V}$ the identity of $\mathcal{L}(\mathcal{V}, \mathcal{V})$ is the tensor $\mathbf{I}$ defined by

$$\mathbf{I}\,\mathbf{v} = \mathbf{v}, \quad \text{for all } \mathbf{v}.$$

Let $\mathbf{a}$ and $\mathbf{b}$ be two vectors of $\mathcal{V}$, we can construct a linear map called the tensor product of $\mathbf{a}$ and $\mathbf{b}$ as the tensor $\mathbf{a} \otimes \mathbf{b} \in \mathcal{L}(\mathcal{V})$ such that

$$(\mathbf{a} \otimes \mathbf{b})\,\mathbf{v} = (\mathbf{b} \cdot \mathbf{v})\,\mathbf{a} = \mathbf{a}\,(\mathbf{b} \cdot \mathbf{v}) \quad \text{for all } \mathbf{v} \in \mathcal{V}, \tag{2.3}$$

and we have

$$\mathbf{a} \cdot (\mathbf{b} \otimes \mathbf{v}) = (\mathbf{a} \cdot \mathbf{b})\,\mathbf{v} \tag{2.4}$$

$$(\mathbf{a} \otimes \mathbf{b})(\mathbf{v} + \mathbf{u}) = (\mathbf{a} \otimes \mathbf{b})\,\mathbf{v} + (\mathbf{a} \otimes \mathbf{b})\,\mathbf{u} \tag{2.5}$$

$$(\mathbf{a} \otimes \mathbf{b})(\lambda\mathbf{v}) = \lambda\,(\mathbf{a} \otimes \mathbf{b})\,\mathbf{v} \tag{2.6}$$

$$\mathbf{v} \cdot (\mathbf{a} \times \mathbf{b}) = \mathbf{a} \cdot (\mathbf{b} \times \mathbf{v}) = \mathbf{b} \cdot (\mathbf{v} \times \mathbf{a}) \tag{2.7}$$

$$(\mathbf{a} \otimes \mathbf{b})(\mathbf{u} \otimes \mathbf{v}) = (\mathbf{b} \cdot \mathbf{u})\,\mathbf{a} \otimes \mathbf{v}. \tag{2.8}$$

Also, given a tensor $\mathbf{A}$ and the tensor product $\mathbf{a} \otimes \mathbf{b}$,

$$\mathbf{A}\,(\mathbf{a} \otimes \mathbf{b}) = (\mathbf{A}\,\mathbf{a}) \otimes \mathbf{b}. \tag{2.9}$$

Given a basis for the n-dimensional vector space $\mathcal{V}$ (in particular one which is orthonormal with respect to some inner product on $\mathcal{V}$, we will use the scalar product on $\mathbb{R}^n$), we can form a basis for our space of tensors

$$\mathbf{e}_i \otimes \mathbf{e}_j \quad i, j = 1, \ldots, n.$$

(these n^2 tensors form a basis for tensors).

Using that a tensor is linear we define the components with respect this basis such that

$$[\mathbf{S}]_{ij} = \mathbf{e}_i \cdot (\mathbf{S}\,\mathbf{e}_j)\,, \qquad \mathbf{S} = \sum_{i=1}^{n}\sum_{j=1}^{n} [\mathbf{S}]_{ij}\,\mathbf{e}_i \otimes \mathbf{e}_j$$

where

$$(\mathbf{e}_i \otimes \mathbf{e}_j)\,\mathbf{e}_q = (\mathbf{e}_q \cdot \mathbf{e}_j)\,\mathbf{e}_i = \delta_{jq}\mathbf{e}_i \tag{2.10}$$

and δ_{jq} is the Kronecker symbol:

$$\delta_{jq} = \begin{cases} 1 & \text{if} \quad j = q \\ 0 & \text{if} \quad j \neq q. \end{cases} \tag{2.11}$$

So a tensor can be represented by its components in a matrix.

Let $\mathbf{u}$ and $\mathbf{v}$ be three dimensional vectors then the scalar, vector and tensor products of $\mathbf{u}$ and $\mathbf{v}$ are denoted by $\mathbf{u}\cdot\mathbf{v}, \mathbf{u}\times\mathbf{v}$ and $\mathbf{u}\otimes\mathbf{v}$ respectively. In Cartesian components, we have $\mathbf{u}\cdot\mathbf{v} = u_i\,v_i$, $(\mathbf{u}\times\mathbf{v})_i = \varepsilon_{ijk}\,u_j\,v_k$ and $(\mathbf{u}\otimes\mathbf{v})_{ij} = u_i\,v_j$, where ε is the Ricci alternator (a third order tensor). We denote vectors here by lowercase boldface letters, where tensors are denoted by capital boldface letters. Denoting by superscript T the tensor $\mathbf{A}^T$ is called the transpose of $\mathbf{A}$. The transpose of a tensor is the unique tensor that satisfies

$$\left(\mathbf{A}^T\mathbf{u}\right)\cdot\mathbf{v} = \mathbf{u}\cdot(\mathbf{A}\,\mathbf{v}) \quad \text{for all}\,\mathbf{u},\mathbf{v}, \tag{2.12}$$

where the components of $\mathbf{A}^T$ are the transpose of the components of $\mathbf{A}$, $\left[\mathbf{A}^T\right]_{ij} = [\mathbf{A}]_{ji}$.

The symmetric and skew-symmetric tensors are respectively defined as

$$\text{symmetric}\ \mathbf{A} = \mathbf{A}^T, \quad \text{skew-symmetric}\ \mathbf{A} = -\mathbf{A}^T. \tag{2.13}$$

The set of all symmetric second-order tensors and the set of all skew second-order tensors are linear subspaces of $\mathcal{L}(\mathcal{V})$.

Any tensor $\mathbf{C}$ which is neither symmetric nor skew can be written as the sum of two tensors, one symmetric and the other skew:

$$\mathbf{C} = \mathbf{S} + \mathbf{W}, \quad \mathbf{S} = \frac{1}{2}\left(\mathbf{C} + \mathbf{C}^T\right) \quad \text{and} \quad \mathbf{W} = \frac{1}{2}\left(\mathbf{C} - \mathbf{C}^T\right) \tag{2.14}$$

where $\mathbf{S}$ is symmetric and $\mathbf{W}$ is skew: they are called the symmetric part and the skew-symmetric part of $\mathbf{C}$. Given two vectors $\mathbf{a}$ and $\mathbf{b}$ and two tensors $\mathbf{A}$ and $\mathbf{B}$, we can have the following properties:

$$(\mathbf{a}\otimes\mathbf{b})^T = \mathbf{b}\otimes\mathbf{a} \quad \text{for all}\,\mathbf{a},\mathbf{b}\in\mathcal{V}. \tag{2.15}$$

Also

$$\left(\mathbf{A}^T\right)^T = \mathbf{A}, \quad (\mathbf{A}+\mathbf{B})^T = \mathbf{A}^T + \mathbf{B}^T, \quad (\mathbf{A}\,\mathbf{B})^T = \mathbf{B}^T\,\mathbf{A}^T, \tag{2.16}$$

and

$$[\mathbf{A}\,(\mathbf{a}\otimes\mathbf{b})]^T = \mathbf{b}\otimes\mathbf{A}\mathbf{a}, \quad \mathbf{A}\,(\mathbf{a}\otimes\mathbf{b}) = [\mathbf{b}\otimes\mathbf{A}\mathbf{a}]^T = (\mathbf{A}\mathbf{a})\otimes\mathbf{b}, \quad (\mathbf{a}\otimes\mathbf{b})\,\mathbf{A} = \mathbf{a}\otimes\mathbf{A}^T\mathbf{b}. \tag{2.17}$$

The trace is a linear mapping operator from $L(\mathcal{V})$ to $\mathbb{R}$. The trace of a tensor is defined as the sum of its diagonal components, where $\operatorname{tr}\mathbf{A} = \sum_i A_{ii}$. Using both trace and transpose we can define a scalar product on tensors as $\mathbf{A}\cdot\mathbf{B} = \operatorname{tr}\left(\mathbf{A}^T\mathbf{B}\right)$, in components $\mathbf{A}\cdot\mathbf{B} = A_{ij}\,B_{ij}$. The trace possesses the following properties:

$$\operatorname{tr}\mathbf{A}^T = \operatorname{tr}\mathbf{A} \quad \text{for all } \mathbf{A}\in L(\mathcal{V}), \tag{2.18}$$

$$\operatorname{tr}\mathbf{I} = n, \tag{2.19}$$

where $\mathbf{I}$ is the identity tensor and n is the dimension of the vector space,

$$\operatorname{tr}\mathbf{W} = 0 \quad \text{whenever } \mathbf{W} \text{ is skew.} \tag{2.20}$$

2.2 Surface calculus

We will be concerned with fields defined on surfaces and how to calculate these fields in a given coordinate system. In particular surface energy densities that will depend on scalar fields, director fields (vector fields) and tensor order parameters (tensor fields) as these ingredients will be used to model the behaviour of a shell of liquid crystal. The most common differential operators acting on our fields can be expressed in terms of surface gradient (∇_s). We introduce the operators ∇_s and div_s, which stands for surface gradient and surface divergence, respectively. Also we need to introduce the surface Laplacian operator Δ_s that is defined as the surface divergence of the surface gradient where $\Delta_s\phi = \operatorname{div}_s(\nabla_s\phi)$.

2.2.1 Surface gradient

Let ϕ be a differentiable scalar field on the surface S, where $\phi : S\to\mathbb{R}$. We let $p\in S$ and T_p be the tangent plane of S at p and $Y(t)$ be a curve in S such that $Y : I\to S$ and $I\subseteq\mathbb{R}$, passing through p, with tangent $\mathbf{t}$ at p as shown in Figure 2.1,

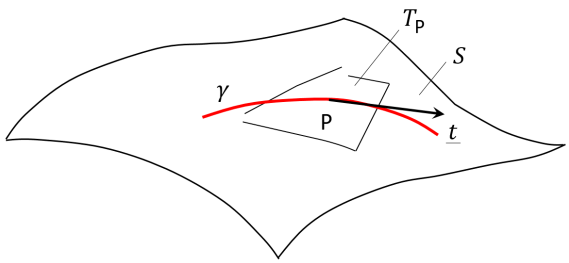


Figure 2.1: Fields defined on the surface S.

so $Y(0) = p \in S, Y'(0) = \mathbf{t} \in T_pS$, and define

$$\phi\big(Y(t)\big) =: \Phi(t), \tag{2.21}$$

and

$$\left.\frac{d\Phi}{dt}\right|_{t=0} = Y'(t) \cdot \nabla_s\phi = \mathbf{t} \cdot \nabla_s\phi|_p \tag{2.22}$$

where $\nabla_s\phi$ is called the surface gradient and gives information about directional derivatives on S. Officially $\nabla_s\phi \in (T_pS)^*$ (the dual of tangent space). So we can only take scalar products of $\nabla_s\phi$ with elements of T_pS. This is why sometimes we write $\nabla\phi$ and then we have $\nabla_s\phi = \mathbf{P}\nabla\phi$ where $\mathbf{P}$ takes any vector and maps to T_pS (projector). So $\nabla_s\phi$ can now take any vector.

In order to calculate $\nabla_s\phi$ in practice requires a parameterisation of S, say $\mathbf{r}(u^1, u^2)$ then $\partial\mathbf{r}/\partial u^1$ and $\partial\mathbf{r}/\partial u^2$ are tangent vectors. Let $\mathbf{g}_1 = \partial\mathbf{r}/\partial u^1$ and $\mathbf{g}_2 = \partial\mathbf{r}/\partial u^2$. Then let $\boldsymbol{\nu}$ be perpendicular to S with $\mathbf{g}_1, \mathbf{g}_2, \boldsymbol{\nu}$ a right-handed triple as shown in Figure 2.2

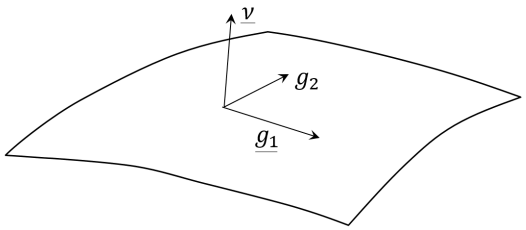


Figure 2.2: Tangent vectors of the surface S.

The normal satisfies

$$\mathbf{g}_1 \cdot \boldsymbol{\nu} = 0, \quad \mathbf{g}_2 \cdot \boldsymbol{\nu} = 0, \tag{2.23}$$

but $\mathbf{g}_1$ is not necessarily perpendicular to $\mathbf{g}_2$. Let $\mathbf{g}^1, \mathbf{g}^2, \boldsymbol{\nu}$ be the *reciprocal basis* to $\mathbf{g}_1, \mathbf{g}_2, \boldsymbol{\nu}$. This means

$$\boldsymbol{\nu} \cdot \mathbf{g}^i = 0, \tag{2.24}$$

and

$$\mathbf{g}^i \cdot \mathbf{g}_j = \delta^i_j = \begin{cases} 1 & \text{if} \quad i = j \\ 0 & \text{if} \quad i \neq j. \end{cases} \tag{2.25}$$

Then the surface gradient in coordinates u^1, u^2 has expression

$$\nabla_s \phi = \mathbf{g}^1 \frac{\partial \Phi}{\partial u^1} + \mathbf{g}^2 \frac{\partial \Phi}{\partial u^2}, \tag{2.26}$$

where $\Phi\left(u^1, u^2\right) = \phi\big(\mathbf{r}\left(u^1, u^2\right)\big)$. In order to calculate $\mathbf{g}^1$ and $\mathbf{g}^2$, we can use the first fundamental form. Let

$$E = \mathbf{g}_1 \cdot \mathbf{g}_1, \quad G = \mathbf{g}_2 \cdot \mathbf{g}_2, \quad F = \mathbf{g}_1 \cdot \mathbf{g}_2.$$

so that

$$[g_{ij}] = \begin{bmatrix} E & F \\ F & G \end{bmatrix} \tag{2.27}$$

and

$$\left(g^{-1}\right)_{ij} = \begin{bmatrix} G & -F \\ -F & E \end{bmatrix} \frac{1}{EG - F^2} \tag{2.28}$$

then

$$\mathbf{g}^1 = \frac{G\mathbf{g}_1 - F\mathbf{g}_2}{EG - F^2}, \quad \mathbf{g}^2 = \frac{E\mathbf{g}_2 - F\mathbf{g}_1}{EG - F^2}. \tag{2.29}$$

It is easy to check that

$$\mathbf{g}^1 \cdot \mathbf{g}_1 = \frac{G\left(\mathbf{g}_1 \cdot \mathbf{g}_1\right) - F\left(\mathbf{g}_2 \cdot \mathbf{g}_1\right)}{EG - F^2} = 1$$

and

$$\mathbf{g}^1 \cdot \mathbf{g}_2 = \frac{G\left(\mathbf{g}_1 \cdot \mathbf{g}_2\right) - F\left(\mathbf{g}_2 \cdot \mathbf{g}_2\right)}{EG - F^2} = 0,$$

so

$$\nabla_s \phi = \frac{(G\mathbf{g}_1 - F\mathbf{g}_2)}{EG - F^2} \frac{\partial \Phi}{\partial u^1} + \frac{(E\mathbf{g}_2 - F\mathbf{g}_1)}{EG - F^2} \frac{\partial \Phi}{\partial u^2}. \tag{2.30}$$

Expression (2.30) allows us to calculate the surface gradient for a particular parameterisation of the surface.

2.2.2 Vector fields

The tensor field $\mathbf{P}$ as introduced in §2.2.1 is the perpendicular projection onto the tangent space at a point p,

$$\mathbf{P} = \mathbf{I} - \boldsymbol{\nu} \otimes \boldsymbol{\nu}. \tag{2.31}$$

with $\mathbf{I}$ is the identity tensor, is then a differentiable tensor field provided the normal is smooth. A vector field $\mathbf{v}$ on the surface S is said to be tangential if $\mathbf{v}(p) \in T_p$ for all $p \in S$ where T_p is the tangent plane at p. A tensor field $\mathbf{A}$ on S is tangential if at each point $p \in S$, $\mathbf{A}(p)\mathbf{w} \in T_p$ for all $\mathbf{w} \in \mathcal{V}$ and $\mathbf{A}(p)\boldsymbol{\nu}(p) = 0$.

In general, vector fields have a normal component and a tangential component, $\mathbf{v} \cdot \boldsymbol{\nu}$ is the normal component and $\mathbf{v} - (\mathbf{v} \cdot \boldsymbol{\nu})\boldsymbol{\nu} = \mathbf{P}\mathbf{v}$ is the tangential component. See Figure 2.3

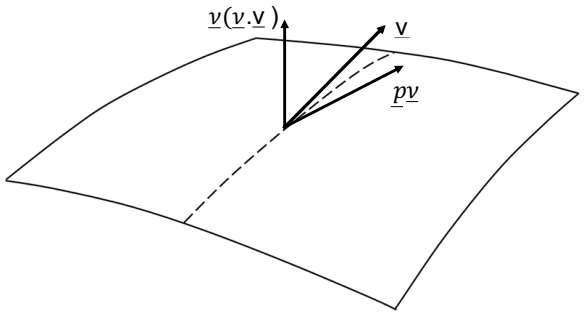


Figure 2.3: The vector field $\mathbf{v}$ on the surface S.

To calculate the surface gradient of a vector field $\mathbf{v}$,

$$\mathbf{V} = \mathbf{v}\big(\mathbf{r}\left(u^1, u^2\right)\big) \tag{2.32}$$

so

$$\nabla_s \mathbf{v} = \frac{\partial \mathbf{V}}{\partial u^1} \otimes \mathbf{g}^1 + \frac{\partial \mathbf{V}}{\partial u^2} \otimes \mathbf{g}^2 \tag{2.33}$$

The trace of the surface gradient of $\mathbf{v}$ defines the surface divergence of $\mathbf{v}$ where

$$\operatorname{div}_s \mathbf{v} = \operatorname{tr}\left(\nabla_s \mathbf{v}\right) = \nabla_s \mathbf{v} \cdot \mathbf{P}, \tag{2.34}$$

$$\operatorname{div}_s \mathbf{v} = \mathbf{g}^1 \cdot \frac{\partial \mathbf{V}}{\partial u^1} + \mathbf{g}^2 \cdot \frac{\partial \mathbf{V}}{\partial u^2}. \tag{2.35}$$

which is a scalar field on the surface S. The surface curl of a vector field $\mathbf{v}$ is defined as $\operatorname{curl}_s \mathbf{v} = -\epsilon \nabla_s \mathbf{v}$, where ϵ is the Ricci alternator [66].

2.3 Differential geometry

A curvature is the central notion of the differential geometry of surfaces. It tells us the geometry of the surface. For curves on surfaces there are two parts, the normal curvature (curved because it lies on surface and the surface is curved) and the geodesic curvature measures curvature within a surface [5].

2.3.1 The extrinsic curvature tensor

We need to introduce the extrinsic curvature tensor and its invariants and relationship to the normal vector $\boldsymbol{\nu}$. Extrinsic curvature of the nematic liquid crystal film has been shown to affect the ordering of the molecules [67], [68]. The tensor field $\mathbf{L} = -\nabla_s \boldsymbol{\nu}$ represents the extrinsic curvature tensor at a point of a surface S. The tensor $\mathbf{L}$ is symmetric and tangential (because $\boldsymbol{\nu}$ is unit vector) where at each point $p \in S$, $\mathbf{L}(p)\,\mathbf{v} \in$ the tangent plane T_p in S for all $\mathbf{v} \in \mathcal{V}$ and $\mathbf{L}(p)\,\boldsymbol{\nu}(p) = 0$. We consider $\mathbf{L}$ as a linear map from T_p to the tangent plane at p itself whose eigenvalues are c_1, c_2 called the principal curvatures. The eigenvalues correspond to the eigenvectors $\mathbf{e}_1$ and $\mathbf{e}_2$ which represent the principal curvatures and principal directions at p. Note that $\mathbf{e}_1$ and $\mathbf{e}_2$ are orthonormal,

$$\mathbf{L} = c_1\,\mathbf{e}_1 \otimes \mathbf{e}_1 + c_2\,\mathbf{e}_2 \otimes \mathbf{e}_2, \tag{2.36}$$

Two scalar invariant fields associated with the tensor $\mathbf{L}$ can be defined on S. Thus, the trace of $\mathbf{L}$ gives twice the mean curvature H, where

$$H = \frac{c_1 + c_2}{2} = \frac{1}{2}\operatorname{tr}\mathbf{L}, \tag{2.37}$$

and

$$\operatorname{tr}(\mathbf{L}) = \mathbf{L}\cdot\mathbf{P} = -\operatorname{div}_s \boldsymbol{\nu} = c_1 + c_2 = 2H \tag{2.38}$$

The second invariant is the Gaussian curvature K, the product of the principal curvatures

$$K = \frac{1}{2}\left[(\operatorname{tr}\mathbf{L})^2 - \operatorname{tr}\mathbf{L}^2\right] = c_1\,c_2. \tag{2.39}$$

Also we can calculate the apshericity, a quantity that measures the difference in the two principal curvatures,

$$\varsigma = \frac{c_1 - c_2}{2}. \tag{2.40}$$

Note that $\varsigma = 0$ when $c_1 = c_2$ and for a sphere $\varsigma = 0$ everywhere. According to the Cayley-Hamilton theorem that implies [70],

$$\mathbf{L}^2 - 2H\mathbf{L} + K\mathbf{P} = \mathbf{0}, \tag{2.41}$$

which can be useful when simplifying expressions involving $\mathbf{L}$.

2.3.2 The normal curvature

The curves in Figure 2.4 have tangent direction in the direction of $\mathbf{n}$, where $\mathbf{n}$ is a tangential unit vector field. We need to find what is the normal curvature of such curves parametrised by arc-length.

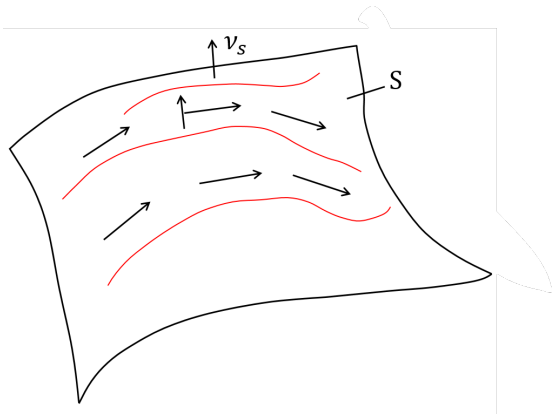


Figure 2.4: Curves have tangent direction in direction of $\mathbf{n}$, where $\mathbf{n}$ is a tangential unit vector field on S.

Given a tangential unit vector field $\mathbf{n}$ on a surface S, defined a curve $\mathbf{X}(t)$ such that $\mathbf{X} : \mathbb{R} \to S$ where S is a surface with smooth unit normal field $\boldsymbol{\nu}$ and $\dot{\mathbf{X}}$ is everywhere parallel to $\mathbf{n}$. Then $|\dot{\mathbf{X}}| = 1$ (arc-length parameterisation) and $\dot{\mathbf{X}}(t) = \mathbf{n}(\mathbf{X}(t))$. By chain rule $\ddot{\mathbf{X}} = (\nabla_s \mathbf{n})\dot{\mathbf{X}} = (\nabla_s \mathbf{n})\mathbf{n}$. This curve has at a point 0 curvature $\kappa(0)$, which in the case $\kappa(0) \neq 0$ is given by [5]. We aim to find the normal curvature for this curve, then using

$$\ddot{\mathbf{X}} = (\nabla_s \mathbf{n})\mathbf{n}, \tag{2.42}$$

and the definition of normal curvature,

$$k_n = \boldsymbol{\nu} \cdot \ddot{\mathbf{X}} = \boldsymbol{\nu} \cdot (\nabla_s \mathbf{n})\mathbf{n},$$

we can write k_n as

$$k_n = \mathbf{n} \cdot \nabla_s (\mathbf{n} \cdot \boldsymbol{\nu}) - (\mathbf{n} \cdot \nabla_s \boldsymbol{\nu})\mathbf{n},$$

and since $\mathbf{n} \cdot \boldsymbol{\nu} = 0$ everywhere on the surface, then

$$k_n = \mathbf{n} \cdot \mathbf{L}\mathbf{n}. \tag{2.43}$$

So for every curve with tangent $\mathbf{n}$ in the surface the normal curvature is $\mathbf{n} \cdot \mathbf{L}\mathbf{n}$

2.3.3 Geodesic curvature

The function k_g is called the geodesic curvature of the curve in the surface and measures how far the curve is from being a geodesic (the shortest distance between two points on surface). If the geodesic curvature is zero then the curvature of $\mathbf{X}$ is identical to the normal curvature [46]. Consider a surface S with smooth unit normal field $\boldsymbol{\nu}$, a point p on S and a curve $\mathbf{X}$ on S passing through p and parallel to $\mathbf{n}$. The geodesic curvature k_g is equal

to the curvature of the projection of $\mathbf{X}$ onto the tangent plane to S,

$$k_g = \ddot{\mathbf{X}}(t) \cdot \left(\boldsymbol{\nu} \times \dot{\mathbf{X}}(t)\right) \tag{2.44}$$

so

$$k_g = (\nabla_s \mathbf{n})\,\mathbf{n} \cdot (\boldsymbol{\nu} \times \mathbf{n})$$

so with the definition $\mathbf{t} = \boldsymbol{\nu} \times \mathbf{n}$,

$$k_g = \mathbf{t} \cdot (\nabla_s \mathbf{n})\,\mathbf{n} = \mathbf{n} \cdot (-\nabla_s \mathbf{t})\,\mathbf{n}$$

which can be written as

$$k_g = -\mathbf{n} \cdot (\nabla_s \mathbf{t})\,\mathbf{n}. \tag{2.45}$$

Example

As an example we consider curves on an axisymmetric surface. We use cylindrical polar coordinates (r, θ, z) and an orthonormal basis $\mathbf{e}_r$, $\mathbf{e}_\theta$ and $\mathbf{e}_z$. Let the axis of revolution of the surface be in the $\mathbf{e}_z$ direction. Suppose the shape of the surface is specified by a function $R(z)$ so that points on the surface are

$$\mathbf{x}(z, \theta) = R(z)\mathbf{e}_r(\theta) + z\mathbf{e}_z.$$

A curve on the surface can be specified by two functions $\Theta(t)$ and $Z(t)$ and is given by

$$\boldsymbol{\alpha}(t) = R(Z(t))\mathbf{e}_r(\Theta(t)) + Z(t)\mathbf{e}_z.$$

We can calculate the geodesic curvature of the parallels (curves with constant z) by setting $\Theta(t) = t$ and $Z(t) = Z_0$, a constant. Then

$$\begin{aligned}\boldsymbol{\alpha}' &= Z'(t)\left(R'(z)\mathbf{e}_r\left(\Theta(t)\right) + \mathbf{e}_z\right) + R(Z(t))\Theta'(t)\mathbf{e}_\theta(\Theta(t)) \\ &= R(Z_0)\mathbf{e}_\theta(t).\end{aligned}$$

For example, in order to define the geodesic curvature for curves that circle an axisymmetric surface, we let $\boldsymbol{\alpha}$ be a curve on a surface S parameterised by t and the scalar $k_g(t)$ be the geodesic curvature of $\boldsymbol{\alpha}$ at the point $p = \boldsymbol{\alpha}(t_0)$ so that $k_g = \frac{\boldsymbol{\alpha}'' \cdot (\mathbf{n} \times \boldsymbol{\alpha}')}{|\boldsymbol{\alpha}'|^3}$. If $\boldsymbol{\alpha}(t) = R(z)\,\mathbf{e}_r(t)$ then $\boldsymbol{\alpha}' = R\mathbf{e}_\theta$, $|\boldsymbol{\alpha}'| = R$ and $\boldsymbol{\alpha}'' = -R\mathbf{e}_r$. Recall that $\boldsymbol{\nu} = \frac{\mathbf{e}_r - R'\mathbf{e}_z}{\sqrt{1+(R')^2}}$, then $\boldsymbol{\nu} \times \boldsymbol{\alpha}' = \frac{R\mathbf{e}_r + R\,r'\mathbf{e}_z}{\sqrt{1+(R')^2}}$ and k_g becomes

$$k_g = -\frac{R'}{R\sqrt{1 + (R')^2}}. \tag{2.46}$$

2.3.4 Surface Divergence Theorem

The surface divergence theorem allows us to calculate the integral of the surface divergence of a vector field $\mathbf{v}$ over a patch of the surface S, to an integral of the vector field along the boundary of the patch ∂S.

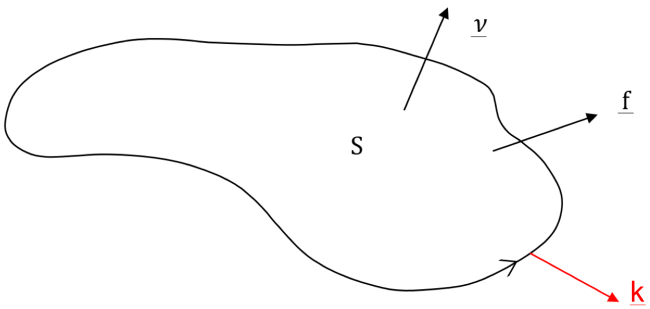


Figure 2.5: The surface divergence theorem relates the integral of the surface divergence of the vector field $\mathbf{f}$ on S to an integral around the boundary curve and the vector $\mathbf{k}$ is tangent to the surface and perpendicular to the boundary curve and points outwards.

Let $\mathbf{v}$ be a differentiable vector field on a surface S with normal $\boldsymbol{\nu}$, such that

$$\mathbf{v} = \mathbf{v}_s + \mathbf{v}_{\boldsymbol{\nu}}, \tag{2.47}$$

where $\mathbf{v}_s = \mathbf{P}\mathbf{v}$ is its projection on the tangent space and $\mathbf{v}_{\boldsymbol{\nu}} = (\mathbf{v}\cdot\boldsymbol{\nu})\,\boldsymbol{\nu}$ is the projection of $\mathbf{v}$ along the normal $\boldsymbol{\nu}$. Then, one obtains

$$\begin{aligned} \operatorname{div}_s(\mathbf{v}_s + \mathbf{v}_{\boldsymbol{\nu}}) &= \operatorname{div}_s(\mathbf{P}\mathbf{v}) + \operatorname{div}_s\big(\boldsymbol{\nu}\,(\mathbf{v}\cdot\boldsymbol{\nu})\big) \\ &= \operatorname{div}_s(\mathbf{P}\mathbf{v}) + (\operatorname{div}_s\boldsymbol{\nu})\;\mathbf{v}\cdot\boldsymbol{\nu} + \boldsymbol{\nu}\cdot\nabla_s(\mathbf{v}\cdot\boldsymbol{\nu}), \text{ but } \boldsymbol{\nu}\cdot\nabla_s(\mathbf{v}\cdot\boldsymbol{\nu}) = 0 \end{aligned}$$

so

$$\int_S \operatorname{div}_s \mathbf{v}\, dS = \int_S \operatorname{div}_s(\mathbf{P}\,\mathbf{v})\, dS - \int_S 2H\,(\mathbf{v}\cdot\boldsymbol{\nu})\, dS, \tag{2.48}$$

as $\operatorname{div}_s\boldsymbol{\nu} = -2H$. Let $\mathbf{k}$ be a vector that tangent to the surface and perpendicular to the boundary curve and points outwards. For any tangential vector field $\mathbf{t}$, the divergence theorem states [66]

$$\int_{\partial S} \mathbf{t}\cdot\mathbf{k}\, dl = \int_S \operatorname{div}_s \mathbf{t}\, dS, \tag{2.49}$$

so

$$\int_S \operatorname{div}_s \mathbf{v}\, dS = \int_{\partial S} \mathbf{k}\cdot(\mathbf{P}\,\mathbf{v})\, dl - \int_S 2H\,\mathbf{v}\cdot\boldsymbol{\nu}\, dS, \tag{2.50}$$

but $\mathbf{k}\cdot\mathbf{P}\mathbf{v} = \mathbf{v}\cdot\left(\mathbf{P}^T\mathbf{k}\right) = \mathbf{v}\cdot\mathbf{k}$, so for a general vector field

$$\int_S \operatorname{div}_s \mathbf{v}\, dS = \int_{\partial S} \mathbf{v}\cdot\mathbf{k}\, dl - \int_S 2H\,\mathbf{v}\cdot\boldsymbol{\nu}\, dS. \tag{2.51}$$

The surface divergence of a tensor field $\mathbf{S}$ on S is a mapping $\operatorname{div}_s \mathbf{S} : S \to \mathbb{R}^n$ that assigns at each point p of S a vector field on S defined by

$$\mathbf{u}\cdot\operatorname{div}_s \mathbf{S} = \operatorname{div}_s\left(\mathbf{S}^T\mathbf{u}\right) \qquad \forall\,\mathbf{u}\in\mathbb{R}^n. \tag{2.52}$$

For any scalar field ϕ, vector field $\mathbf{v}$ and tensorial field $\mathbf{S}$, we have the following identities:

$$\operatorname{div}_s(\phi\mathbf{v}) = \phi\operatorname{div}_s\mathbf{v} + \nabla_s\phi\cdot\mathbf{v} \tag{2.53}$$

$$\operatorname{div}_s(\phi\mathbf{S}) = \phi\operatorname{div}_s\mathbf{S} + \mathbf{S}\nabla_s\phi \tag{2.54}$$

$$\operatorname{div}_s\left(\mathbf{S}^T\mathbf{v}\right) = (\operatorname{div}_s\mathbf{S})\cdot\mathbf{v} + \mathbf{S}\cdot\nabla_s\mathbf{v}. \tag{2.55}$$

Given a tensor $\mathbf{S}$ and a constant vector $\mathbf{u}$,

$$\begin{aligned}\int_{\partial S}\mathbf{u}\cdot(\mathbf{S}\mathbf{k})\, dl &= \int_{\partial S}\left(\mathbf{S}^T\mathbf{u}\right)\cdot\mathbf{k}\, dl = \int_S \operatorname{div}_s\left(\mathbf{S}^T\mathbf{u}\right) + 2H\left(\mathbf{S}^T\mathbf{u}\right)\cdot\boldsymbol{\nu}\, dS\\ &= \int_S \mathbf{u}\cdot(\operatorname{div}_s\mathbf{S}) + 2H\,(\mathbf{S}\boldsymbol{\nu})\cdot\mathbf{u}\, dS = \mathbf{u}\cdot\int_S(\operatorname{div}_s\mathbf{S} + 2H\mathbf{S}\boldsymbol{\nu})\, dS,\end{aligned}$$

therefore, we end up with

$$\int_{\partial S}\mathbf{S}\,\mathbf{k}\, dl = \int_S(\operatorname{div}_s\mathbf{S} + 2H\mathbf{S}\boldsymbol{\nu})\, dS. \tag{2.56}$$

2.4 Surface increments

In this section we introduce the idea of an increment of the equilibrium equations. We consider an incremental change to the surface shape and the fields defined on the surface (for example q, $\mathbf{n}$ or any other fields that the energy density w depends on). We increment all fields and the surface shape (which means we write $q = q_0 + t\delta q$, $\mathbf{r} + t\mathbf{u}$) and calculate the t-derivative evaluated at $t = 0$. The fact that we are perturbing the interface shape means that the surface differential are operators also affected by the increment. The resulting linear equations for the incremental quantities have coefficients that depend on the solution to the equilibrium equations. In general the incremental equations will have only trivial solutions, except perhaps at certain solutions of the equilibrium equations.

When we take increments the surface can deform as well as the field defined on the surface so that in general there will be two parts to an increment, one due to the surface changes and the other due to the field changes. In this section we focus on normal incre-

ments this will help us later to compute the first variation of the free energy density δw and also to derive the incremental equations. We compute the first variation of quantities whose variation depends on the perturbations of the surface S which is the case with $\boldsymbol{\nu}$ and $\nabla_s \boldsymbol{\nu}$. We will be concerned with finding variations of functionals defined on surfaces.

Following [66], the variation of $\boldsymbol{\nu}$ is given as

$$\delta \boldsymbol{\nu} = -\left(\nabla_s \mathbf{u}\right)^T \boldsymbol{\nu}. \tag{2.57}$$

where the points on the surface S are displaced by the vector field $\mathbf{u}$. In order to compute the first variation, we assume that the surface is deformed and $\mathbf{u}$ is considered as an arbitrary field. To compute the first variation of the surface gradient of $\boldsymbol{\nu}$, keep in mind that the operators δ and ∇_s do not commute and both the first variation of $\boldsymbol{\nu}$ and its surface gradient depend on the geometry of the surface [66].

The first variation operator δ follows the product rule. Given tensors $\mathbf{A}$, and $\mathbf{B} \in L(\mathcal{V})$

$$\delta(\mathbf{AB}) = (\delta \mathbf{A})\,\mathbf{B} + \mathbf{A}\,(\delta \mathbf{B}).$$

The surface gradient of $\boldsymbol{\nu}$ is defined by $\nabla_s \boldsymbol{\nu} = (\nabla \boldsymbol{\nu})\,\mathbf{P}$. The first variation operator δ obeys the product rule $\delta(\nabla \boldsymbol{\nu}\,\mathbf{P}) = (\delta(\nabla \boldsymbol{\nu}))\,\mathbf{P} + \nabla \boldsymbol{\nu}\,(\delta \mathbf{P})$. We calculate the first variation of $\nabla \boldsymbol{\nu}$ taking into account (2.57),

$$\delta(\nabla \boldsymbol{\nu}) = -\nabla\left[\left(\nabla_s \mathbf{u}\right)^T \boldsymbol{\nu}\right] - (\nabla \boldsymbol{\nu})\,(\nabla \mathbf{u}), \tag{2.58}$$

and for $\mathbf{P} = \mathbf{I} - \boldsymbol{\nu} \otimes \boldsymbol{\nu}$, we have

$$\delta \mathbf{P} = -\delta \boldsymbol{\nu} \otimes \boldsymbol{\nu} - \boldsymbol{\nu} \otimes \delta \boldsymbol{\nu} \tag{2.59}$$

$$= \left(\nabla_s \mathbf{u}^T\right) \boldsymbol{\nu} \otimes \boldsymbol{\nu} + \boldsymbol{\nu} \otimes \left(\nabla_s \mathbf{u}^T\right) \boldsymbol{\nu}, \tag{2.60}$$

that, combined through the product rule and by taking into account the definition of $\mathbf{L}$, one can obtain

$$\delta \mathbf{L} = \mathbf{L}\left(\nabla_s \mathbf{u}\right)^T \boldsymbol{\nu} \otimes \boldsymbol{\nu} + \nabla_s\left[\left(\nabla_s \mathbf{u}\right)^T \boldsymbol{\nu}\right] - \mathbf{L}\left(\nabla_s \mathbf{u}\right). \tag{2.61}$$

One of the ways to study the stability is to consider the incremental equations. In Chapter 3, we derive and consider the stability of solutions to the equilibrium equations, so we need to consider variations or increments in the different surface quantities. We introduce the normal increments where

$$\mathbf{u} = \psi\, \boldsymbol{\nu} \tag{2.62}$$

so that

$$\nabla_s \mathbf{u} = \boldsymbol{\nu} \otimes \nabla_s \psi - \mathbf{L}\psi \,. \tag{2.63}$$

and

$$(\nabla_s \mathbf{u})^T \boldsymbol{\nu} = \nabla_s \psi, \tag{2.64}$$

$$\mathrm{div}_s \left((\nabla_s \mathbf{u})^T \boldsymbol{\nu} \right) = \Delta_s \psi. \tag{2.65}$$

This allows us to obtain the variations $\delta\boldsymbol{\nu}$, $\delta\mathbf{P}$ and $\delta\mathbf{L}$ in terms of the *normal increment* ψ,

$$\delta (\mathbf{L} \cdot \mathbf{P}) = (\delta \mathbf{L}) \cdot \mathbf{P} + (\delta \mathbf{P}) \cdot \mathbf{L} \tag{2.66}$$

but $\delta\boldsymbol{\nu} = -(\nabla_s \mathbf{u})^T \boldsymbol{\nu} = -\nabla_s \psi$, then (2.60) becomes

$$\delta \mathbf{P} = \nabla_s \psi \otimes \boldsymbol{\nu} + \boldsymbol{\nu} \otimes \nabla_s \psi. \tag{2.67}$$

by using (2.63) and (2.64), $\delta\mathbf{L}$ can be given as

$$\delta \mathbf{L} = \mathbf{L} \nabla_s \psi \otimes \boldsymbol{\nu} + \nabla_s (\nabla_s \psi) - \mathbf{L} (\boldsymbol{\nu} \otimes \nabla_s \psi - \mathbf{L}\psi) \,. \tag{2.68}$$

where $\mathbf{L}(\boldsymbol{\nu} \otimes \nabla_s \psi) = 0$ since $\mathbf{L}\boldsymbol{\nu} = 0$. Then

$$\delta \mathbf{L} \cdot \mathbf{P} = \mathrm{div}_s \left(\nabla_s \mathbf{u}^T \boldsymbol{\nu} \right) - (\mathbf{L} \nabla_s \mathbf{u}) \cdot \mathbf{P}, \tag{2.69}$$

$$\mathbf{L} \cdot \delta \mathbf{P} = \mathbf{L} \cdot [\nabla_s \psi \otimes \boldsymbol{\nu} + \boldsymbol{\nu} \otimes \nabla_s \psi] = 0, \quad (\text{since } \mathbf{L}\boldsymbol{\nu} = 0) \tag{2.70}$$

from (2.69) and (2.70), we write (2.66) as

$$\delta (\mathbf{L} \cdot \mathbf{P}) = \mathrm{div}_s \left(\nabla_s \mathbf{u}^T \boldsymbol{\nu} \right) - \mathbf{L} \cdot \nabla_s \mathbf{u} \tag{2.71}$$

$$= \Delta_s \psi + (\mathbf{L} \cdot \mathbf{L}) \psi = 2\delta H, \tag{2.72}$$

since $H = \frac{1}{2} \mathrm{tr} (\mathbf{L}\mathbf{P}) = \frac{1}{2} \mathbf{L} \cdot \mathbf{P}$.

With $\delta\mathbf{P}$ given in (2.67),

$$\delta (\nabla_s \phi) = \nabla_s (\delta \phi) + \left(\left(\nabla_s \mathbf{u}^T \boldsymbol{\nu} \right) \cdot \nabla_s \phi \right) \boldsymbol{\nu} - \nabla_s \mathbf{u}^T \nabla_s \phi. \tag{2.73}$$

Applying this result for the scalar field q, the first variation of its surface gradient is

$$\delta (\nabla_s q) = \nabla_s (\delta q) + \left[\left((\nabla_s \mathbf{u})^T \boldsymbol{\nu} \right) \cdot \nabla_s q \right] \boldsymbol{\nu} - (\nabla_s \mathbf{u})^T \nabla_s q \tag{2.74}$$

$$= \nabla_s (\delta q) + (\nabla_s \psi \cdot \nabla_s q) \boldsymbol{\nu} + \psi \, \mathbf{L} \nabla_s q. \tag{2.75}$$

For increment of surface gradients of vector fields, we use the result for scalar fields in (2.73). Let $\mathbf{a}$ be a vector field defined on S. Then for $\mathbf{a}$, we take scalar product with a

constant vector $\mathbf{c}$ such that $\mathbf{c}\cdot\mathbf{a}$ is scalar field and $\mathbf{c}\cdot\delta\left(\nabla_s\mathbf{a}\right)=\delta\left(\nabla_s\left(\mathbf{c}\cdot\mathbf{a}\right)\right)$. Now we use (2.73) and then

$$\mathbf{c}\cdot\delta\left(\nabla_s\mathbf{a}\right)=\mathbf{c}\cdot\left[\nabla_s\left(\delta\mathbf{a}\right)+\left(\left(\nabla_s\mathbf{u}^T\boldsymbol{\nu}\right)\cdot\nabla_s\mathbf{a}\right)\boldsymbol{\nu}-\nabla_s\mathbf{u}^T\nabla_s\mathbf{a}\right]. \tag{2.76}$$

Also we find

$$\delta\left(\mathrm{div}_s\,\mathbf{a}\right)=\mathrm{div}_s\left(\delta\mathbf{a}\right)+\psi\left(\mathbf{L}\cdot\nabla_s\mathbf{a}\right). \tag{2.77}$$

Let $\mathbf{n}$ be a unit vector field. We need to obtain the variations of the surface gradient of the unit vector field $\mathbf{n}$. First we know that the surface is deformed and then $\mathbf{n}$ may change because S changes and the modulus of $\mathbf{n}$ is constant, so we can write $\mathbf{n}'=\mathbf{n}+\epsilon\delta\mathbf{n}$, with $\delta\mathbf{n}\cdot\mathbf{n}=0$. Since $\mathbf{n}'$ lies in the tangent space of the deformed surface then $\mathbf{n}'\cdot\boldsymbol{\nu}'=0$ where $\delta\mathbf{n}\cdot\boldsymbol{\nu}=\mathbf{n}\cdot\left(\nabla_s\mathbf{u}\right)^T\boldsymbol{\nu}$. The vector field $\mathbf{n}$ can freely rotate around the normal vector $\boldsymbol{\nu}$ by an angle $\delta\theta=\delta\mathbf{n}\cdot\left(\boldsymbol{\nu}\times\mathbf{n}\right)$ where $\delta\theta$ is an independent scalar variation without affecting the shape of the surface. Therefore we get,(from [66])

$$\delta\mathbf{n}=\boldsymbol{\tau}\delta\theta+\left[\boldsymbol{\nu}\cdot\left(\nabla_s\mathbf{u}\right)\mathbf{n}\right]\boldsymbol{\nu}, \tag{2.78}$$

where $\boldsymbol{\tau}=\boldsymbol{\nu}\times\mathbf{n}$. Now we can compute the variation of $\nabla\mathbf{n}$:

$$\delta\nabla\mathbf{n}=\nabla\left(\boldsymbol{\tau}\delta\theta\right)+\nabla\left[\left(\boldsymbol{\nu}\otimes\boldsymbol{\nu}\right)\left(\nabla\mathbf{u}\right)\mathbf{n}\right]-\left(\nabla\mathbf{n}\right)\left(\nabla\mathbf{u}\right) \tag{2.79}$$

and with the aid of equation (2.60), yields

$$\delta\left(\nabla_s\mathbf{n}\right)=\nabla_s\mathbf{n}\left[\left(\nabla_s\mathbf{u}\right)^T\boldsymbol{\nu}\otimes\boldsymbol{\nu}-\nabla_s\mathbf{u}\right]+\nabla_s\left(\boldsymbol{\tau}\delta\theta\right)+\nabla_s\left[\left(\boldsymbol{\nu}\otimes\boldsymbol{\nu}\right)\left(\nabla_s\mathbf{u}\right)\mathbf{n}\right]. \tag{2.80}$$

By end of this section we have derived the variations or increments in the different surface quantities that will be needed to consider the stability of solutions to the equilibrium equations in chapter 3.

2.5 Modelling liquid crystal shells

This section explains the main approach of modelling liquid crystals in shells using the Q-tensor theory. The main assumption is that to assume that the molecules are all aligned in the tangent directions when confined to a thin shell or film.

For closed shells whose topology is not that of a torus, the director field $\mathbf{n}$ shows singular points or defects (regions where the local orientational order of the system is undefined). As a result, topological defects are often present in shells [9], [14], [37].

We can avoid the mathematical singularities of using the director theory by introducing a tensorial order parameter $\mathbf{M}$, that describes defects as melting points where the nematics

melt into a liquid phase (isotropic states) [32]. See §1.4.1 for introduction to the use of $\mathbf{M}$ in modelling.

In the work of [68] the molecule directions are assumed to lie in the tangent plane to the surface and so the orientation is represented by a unit vector $\mathbf{m}$ lying on the tangent plane of the shell, such that $f_p(\mathbf{m})$ is the probability that a molecule placed in p is oriented along $\mathbf{m}$ and $f_p : S_2 \to \mathbb{R}^+$, where S_2 is the unit sphere. The probability measure is even where $f_p(\mathbf{m}) = f_p(-\mathbf{m})$ and the first moment of the distribution $f_p(\boldsymbol{\nu}) = 0$. Recall that the second moment of the distribution of $\mathbf{m}$ is the variance tensor $\mathbf{M} = \langle \mathbf{m} \otimes \mathbf{m} \rangle$ so that

$$\mathbf{M} = \langle \mathbf{m} \otimes \mathbf{m} \rangle = \int_{\mathbb{S}} \mathbf{m} \otimes \mathbf{m}\, f_p(\mathbf{m})\, d\Omega. \tag{2.81}$$

where Ω is the area measure on S_2. By definition, $\mathbf{M}$ has unit trace, is symmetric, positive and semidefinite

$$\operatorname{tr}(\mathbf{M}) = \int_S \mathbf{m} \cdot \mathbf{m}\, f_p(\mathbf{m})\, d\Omega = \int_S f_p(\mathbf{m})\, d\Omega = 1. \tag{2.82}$$

If all the molecules are forced to be oriented in the tangent plane of the surface with normal vector $\boldsymbol{\nu}$, then

$$\mathbf{M}\boldsymbol{\nu} = \int_{\mathbb{S}} \mathbf{m}(\mathbf{m} \cdot \boldsymbol{\nu})\, f_p(\mathbf{m})\, d\Omega = \mathbf{0}, \tag{2.83}$$

either $\mathbf{m} \cdot \boldsymbol{\nu} = 0$ or because there is no chance to find $\mathbf{m}$ in direction $\boldsymbol{\nu}$ we have $\mathbf{m} \cdot \boldsymbol{\nu} \neq 0$ but $f_p(\mathbf{m}) = 0$. Then $\boldsymbol{\nu}$ is an eigenvector of $\mathbf{M}$ with zero eigenvalue. Other eigenvectors of $\mathbf{M}$ are $\mathbf{n}$ and $\mathbf{t}$, $\mathbf{n}$ with larger eigenvalue (λ_n) and $\mathbf{t}$ with the smaller eigenvalue (λ_t) where $\mathbf{n} \cdot \boldsymbol{\nu} = 0$ and $\mathbf{t} \cdot \boldsymbol{\nu} = 0$. We define $\mathbf{n}$ and $\mathbf{t}$ to be the eigenvectors of the variance tensor $\mathbf{M}$ and orthogonal to $\boldsymbol{\nu}$ so that $\mathbf{M}$ an be written as

$$\mathbf{M} = 0 \cdot \boldsymbol{\nu} \otimes \boldsymbol{\nu} + \lambda_n \mathbf{n} \otimes \mathbf{n} + \lambda_t \mathbf{t} \otimes \mathbf{t},$$

also $\operatorname{tr}(\mathbf{M}) = 1$ so $\lambda_n + \lambda_t = 1$. We can write the eigenvalues λ_n and λ_t in terms of λ as $\lambda = \lambda_n - \frac{1}{2}$ and $\lambda_t - \frac{1}{2} = -\lambda$. Also we have $\mathbf{P} = \mathbf{I} - \boldsymbol{\nu} \otimes \boldsymbol{\nu} = \mathbf{n} \otimes \mathbf{n} + \mathbf{t} \otimes \mathbf{t}$. Thus the variance tensor $\mathbf{M}$ is given in the form

$$\mathbf{M} = \frac{1}{2}(\mathbf{I} - \boldsymbol{\nu} \otimes \boldsymbol{\nu}) + \lambda(\mathbf{n} \otimes \mathbf{n} - \mathbf{t} \otimes \mathbf{t}), \tag{2.84}$$

where it is considered as the most general form [54].

The sign of λ is not essential because the order tensors associated with negative values of λ and director $\mathbf{n}$ agree with the order tensors associated with the positive degree of order of $-\lambda$ and director $\mathbf{t}$. Considering (2.84), if $\lambda = 0$ then the normal vector $\boldsymbol{\nu}$ is the optical axes and the molecules are randomly distributed orthogonally to $\boldsymbol{\nu}$. In case of $\lambda = \pm\frac{1}{2}$ the molecules are perfectly ordered along $\mathbf{n}$ or $\mathbf{t}$.

The Landau-de Gennes potential is a temperature-dependent thermodynamic contribution to the total free energy that takes into account the material tendency to spontaneously arrange in ordered or disordered states [69]. It is widely used to describe the thermo-mechanical response of liquid crystals. The Landau-de Gennes potential uses a symmetric traceless second order tensor $\mathbf{Q}$ to describe the distribution of the molecules. The form of Landau-de Gennes energy density is denoted by w_{LdG} and given by [54]

$$w_{LdG} = \frac{a}{2}\operatorname{tr}(\mathbf{Q}^2) + \frac{c}{4}\operatorname{tr}(\mathbf{Q}^2)^2, \tag{2.85}$$

where $\mathbf{Q}$ is the traceless part of $\mathbf{M}$. On a surface this means $\mathbf{Q} = \mathbf{M} - \frac{1}{2}\mathbf{P} = q\left(\mathbf{n}\otimes\mathbf{n} - \frac{1}{2}\mathbf{P}\right)$, where $\mathbf{P} = \mathbf{I} - \boldsymbol{\nu}\otimes\boldsymbol{\nu}$ is the projection to the tangent plane to the surface and $q = 2\lambda \in [-1, 1]$. This accounts for the temperature dependence of the degree of orientation, where a depends on temperature and c is a positive material constant. Thus whenever a is positive we get the minimum potential at $q = 0$, whereas for negative a we get it at $q = \pm\sqrt{\frac{-a}{c}}$. According to the expression $a = a_0\frac{(T - T_c^*)}{T_c}$ the parameter a depends on the temperature T [68].

An alternative and equivalent parameterisation of the variance tensor $\mathbf{M}$ (given in (2.84)) is in terms of a two-dimensional degree of order q and a director $\mathbf{n}$. If $q = 0$ then the distribution is isotropic on the surface, if $q = 1$ then the distribution is perfect alignment along $\mathbf{n}$, if $q = -1$ then the distribution is perfect alignment along the direction $\mathbf{t} = \boldsymbol{\nu}\times\mathbf{n}$ (in other words perpendicular to the direction $\mathbf{n}$). Following [9], We write

$$\mathbf{M} = q\,\mathbf{n}\otimes\mathbf{n} + \frac{1}{2}(1-q)\,\mathbf{P}, \tag{2.86}$$

where $|q| \le 1$. It is easy to see that $|q| \le 1$ by considering that the tensor $\mathbf{M}$ is a positive definite tensor and for any $\mathbf{x}$, $\mathbf{x}\cdot(\mathbf{M}\,\mathbf{x}) \ge 0$. The variance tensor $\mathbf{M}$ has eigenvectors $\mathbf{n}, \mathbf{t}$ and $\boldsymbol{\nu}$, where $\mathbf{t} = \boldsymbol{\nu}\times\mathbf{n}$. We have $\mathbf{M}\mathbf{n} = \frac{1}{2}(1+q)\,\mathbf{n}, \mathbf{M}\mathbf{t} = \frac{1}{2}(1-q)\,\mathbf{t}$ and $\mathbf{M}\boldsymbol{\nu} = 0$. This means, since $\mathbf{M}$ is positive semi-definite, $\mathbf{x}\cdot(\mathbf{M}\mathbf{x}) > 0$ for $\mathbf{x} \ne 0$ so that $1 + q \ge 0$ or $1 - q \ge 0$ which gives $|q| \le 1$. In this parameterisation $\mathbf{Q} = q\,(\mathbf{n}\otimes\mathbf{n} - \mathbf{t}\otimes\mathbf{t})/2$ and $\mathbf{Q}^2 = q^2\mathbf{P}/4$ and so $\operatorname{tr}(\mathbf{Q}^2) = q^2/2$. Therefore in this parameterisation we have

$$w_{LdG} = \frac{a}{4}q^2 + \frac{c}{8}q^4. \tag{2.87}$$

We will need the results of this section in chapter 4 when we parameterise the tensor $\mathbf{Q}$ in order to perform calculations of the equilibrium configurations and the stability for a thin film in the shape of a catenoid.

For more computational convenience we use two different parameterisations of $\mathbf{M}$. One parameterisation is in terms of the scalar order parameter q and the unit tangent vector

field $\mathbf{n}$ and the other parameterisation is in terms of two scalar order parameters q_0 and q_m. When $q = 0$, we face a problem when using the first parameterisation, since $\mathbf{n}$ is undefined and so is α (α is the angle between $\mathbf{n}$ and some tangent direction to the surface). Thus numerical work becomes easier when we consider q_0 and q_m since we do not have to worry about $\mathbf{n}$. However, for physical interpretations we can understand what is happening when we consider the parameterisation using q and $\mathbf{n}$. We can also use the two parameterisations as a cross-check of our calculations.

2.6 Concluding remarks

By the end of this chapter, we have introduced different objects and notations that will appear in this work and how to do calculus on surfaces. These objects will be used to define the surface energy density we will consider in later chapters. We also have included the surface divergence theorem and other useful identities.

Chapter 3

Equilibrium of open surfaces

In this chapter, we extend previous published work [66] on the equilibrium of closed surfaces to the equilibrium and stability of open surfaces with a boundary. Given a general surface energy we derive the natural boundary conditions and equilibrium equations.

For an open surface with a fixed boundary the relevant papers are [67],[68], [72], [76] and [113] which derive the surface free energy and give some background to this type of calculation for *closed* fluid membranes. In particular we re-derive the results of [66] in the context of *open* surfaces and present the derivation of the equilibrium equations and identify the natural boundary conditions for the problem. We illustrate the natural boundary conditions for a number of examples of the energies found in [66].

In order to study the stability of solutions, we prove that the tangential component of the shape equation is always satisfied whenever the other equilibrium equations are satisfied. This allows us to consider only the normal increments to the normal component of the shape equation when considering the incremental problem. We derive the incremental equations for some specific examples. We also derive the incremental boundary conditions for a surface with constant surface energy density $w = \gamma$ and Canham-Helfrich energies. A Canham-Helfrich-like term appears when we later consider the equilibrium of a thin film of liquid crystal, arising due to the curvature of the surface.

In our work we show that as the energy depends on a number of fields (scalar, vector, tensors), there will be an equilibrium equation for each field and a shape equation for the shape.

3.1 The equilibrium of open surfaces

Our calculations in this section extend the results of [66] to the equilibrium of open surfaces. We derive the equilibrium equations and the corresponding boundary conditions. Our new contribution is the derivation of the terms that come from the boundary contri-

butions. In our case (for an open surface) the functional to be minimised is the

$$W(S) = \int_S w\, dA + \lambda \left(\int_S dA - A_0 \right) \tag{3.1}$$

which consists of the surface free energy plus an additional term to allow us to enforce a constraint of fixed surface area A_0. Notice that, unlike for a closed surface, we cannot impose a constraint of fixed volume enclosed by the surface (since this is not defined for an open surface). where S is considered to be an open surface describing the shape perhaps spanning some fixed boundary, w is the free-energy density (per area) and the Lagrange multiplier λ is used to enforce a constraint of a constant surface area (in some applications we will set $\lambda = 0$ and not constrain the area).

3.1.1 Area constraint and local inextensibility

In this section we interpret the total energy. We consider an orientable open surface S, provided at each point with a unit normal $\boldsymbol{\nu}$. We recall the extrinsic curvature tensor field $\mathbf{L} = -\nabla_s \boldsymbol{\nu}$ (see §2.3.1). Also the energy depends on q and $\mathbf{n}$, a scalar and vector order parameter. Then equilibrium configurations are the extremal points of the functional defined on S,

$$W = \int_S w\left(\boldsymbol{\nu}, \mathbf{L}, \mathbf{n}, \nabla_s \mathbf{n}, q, \nabla_s q\right) dS, \tag{3.2}$$

where w is the free energy density. Note that W depends on the extrinsic curvature tensor $\mathbf{L}$ which has invariants H and K that denote the mean and the Gaussian curvature on S respectively.

To demand that the overall area of the surface is fixed we can add a constraint to the energy in the form of a Lagrange multiplier λ and will replace (3.2) with the effective energy $W_{\mathit{eff}} = W + \lambda\left(\int_S dS - A_0\right)$. Variation of this effective energy gives,

$$\delta W_{\mathit{eff}} = \delta W + \lambda \int_S \mathrm{div}_s\, \mathbf{u}\, dS, \tag{3.3}$$

where $\mathbf{u}$ is an arbitrary field, representing the incremental deformation of the surface.

The total area of the surface can be fixed without local inextensibility (we can stretch some parts of the surface and compress others). If we want to impose *local* inextensibility we must introduce a constraint at every point on the surface via a scalar field λ defined on the surface. Variations of the energy then give,

$$\delta W_{\mathit{eff}} = \delta W + \int_S \lambda\ \mathrm{div}_s\, \mathbf{u}\, dS, \tag{3.4}$$

where λ is a scalar field on S. In our progress we consider λ = constant (global area

constraint), where [66] provides that the inextensibility constraint λ is not necessarily constant, with the physical meaning of a surface tension.

Now, for the total effective energy given in the form:

$$W = \int_S w\left(\boldsymbol{\nu}, \mathbf{L}, \mathbf{n}, \nabla_s \mathbf{n}, q, \nabla_s q\right) dS + \lambda\left(\int_S dS - A_0\right), \tag{3.5}$$

as a consequence of the Reynolds transport theorem, the functional variation can be written in the form:

$$\delta W_{\mathit{eff}} = \int_S \delta w \, dS + \int_S w \, \mathrm{div}_s \, \mathbf{u} \, dS + \int_S \lambda \, \mathrm{div}_s \, \mathbf{u} \, dS. \tag{3.6}$$

Therefore

$$\delta W_{\mathit{eff}} = \int_S (\lambda + w) \, \mathrm{div}_s \, \mathbf{u} \, dS + \int_S \delta w \, dS. \tag{3.7}$$

We will deal with each term in δw separately.

By using the surface divergence theorem §2.3.4, where $\mathbf{k}$ is normal to the boundary curve ∂S, and tangent to S, the first integral of (3.7) can be expressed as

$$\int_{\partial S} (\lambda + w) \, \mathbf{u} \cdot \mathbf{k} \, dS - \int_S 2 \, (\lambda + w) \, H \, \mathbf{u} \cdot \boldsymbol{\nu} \, + \mathbf{u} \cdot \nabla_s w \, dS. \tag{3.8}$$

Note that,

$$\mathrm{div}_s\Big((\lambda + w) \, \mathbf{P}\mathbf{u}\Big) = \left[\mathrm{div}_s \, (\lambda + w) \, \mathbf{P}\right] \cdot \mathbf{u} \, + \, (\lambda + w) \, \mathbf{P} \cdot (\nabla_s \mathbf{u})$$

$$(\lambda + w) \, \mathrm{div}_s \, \mathbf{u} = \mathrm{div}_s\Big((\lambda + w) \, \mathbf{P}\mathbf{u}\Big) \, - \mathrm{div}_s\Big((\lambda + w) \, \mathbf{P}\Big) \cdot \mathbf{u}.$$

We show that the term $\int_S (\lambda + w) \, \mathrm{div}_s \, \mathbf{u} \, dS$ can be written and incorporated into a stress $\boldsymbol{\sigma}$,

$$\int_S (\lambda + w) \, \mathrm{div}_s \, \mathbf{u} \, dS = \int_S \mathrm{div}_s\Big((\lambda + w) \, \mathbf{P}\mathbf{u}\Big) \, dS \, - \int_S \mathrm{div}_s\Big((\lambda + w) \, \mathbf{P}\Big) \cdot \mathbf{u} \, dS$$

$$= \int_{\partial S} (\lambda + w) \, (\mathbf{P}\mathbf{u}) \cdot \mathbf{k} \, dS - \int_S 2 \, (\lambda + w) \, H \, \, (\mathbf{P}\mathbf{u}) \cdot \boldsymbol{\nu} \, dS - \int_S \mathrm{div}_s\Big((\lambda + w) \, \mathbf{P}\Big) \cdot \mathbf{u} \, dS.$$

But the integral $\int_S 2 \, (\lambda + w) \, H \, \, (\mathbf{P}\mathbf{u}) \cdot \boldsymbol{\nu} \, dS = 0$ because $\mathbf{P}\mathbf{u}$ is tangential. Thus

$$\int_S (\lambda + w) \, \mathrm{div}_s \, \mathbf{u} \, dS \, = \int_{\partial S} (\lambda + w) \, \mathbf{u} \cdot \mathbf{k} \, dS - \int_S \mathrm{div}_s \, (\boldsymbol{\sigma}) \cdot \mathbf{u} \, dS, \tag{3.9}$$

where the stress tensor $\boldsymbol{\sigma} = (\lambda + w) \, \mathbf{P}$. Now we consider the second term of (3.7). The

first variation of free-energy density can be written as

$$\delta w = \frac{\partial w}{\partial \boldsymbol{\nu}} \cdot \delta \boldsymbol{\nu} + \frac{\partial w}{\partial \mathbf{L}} \cdot \delta \mathbf{L} + \frac{\partial w}{\partial \mathbf{n}} \cdot \delta \mathbf{n} + \frac{\partial w}{\partial \nabla_s \mathbf{n}} \cdot \delta \left(\nabla_s \mathbf{n} \right) + \frac{\partial w}{\partial q} \cdot \delta q + \frac{\partial w}{\partial \nabla_s q} \cdot \delta \nabla_s q. \quad (3.10)$$

We introduce the following notation (following [67])

$$\boldsymbol{\beta} = \frac{\partial w}{\partial \boldsymbol{\nu}}, \quad \boldsymbol{\Lambda} = \frac{\partial w}{\partial \mathbf{L}}, \quad \mathbf{g} = \frac{\partial w}{\partial \mathbf{n}}, \quad \mathbf{G} = \frac{\partial w}{\partial \nabla_s \mathbf{n}} \quad f = \frac{\partial w}{\partial q}, \quad \mathbf{b} = \frac{\partial w}{\partial \nabla_s q}. \quad (3.11)$$

We also define $\mathbf{b}_s = \mathbf{P}\mathbf{b}$, $\mathbf{g}_s = \mathbf{P}\mathbf{g}$, $\mathbf{G}_s = \mathbf{G}\mathbf{P}$, $\boldsymbol{\Lambda}_s = \boldsymbol{\Lambda}\mathbf{P}$. The variations of $\boldsymbol{\nu}$ and $\nabla_s \boldsymbol{\nu}$ depends on the perturbation to the shape of S and so on $\boldsymbol{\nu}$. In the case of other variables describing the microstructure, the variations vary independently of the surface.

By using the variations of $\delta\boldsymbol{\nu}, \delta\mathbf{L}, \delta\mathbf{n}, \delta\left(\nabla_s \mathbf{n}\right)$ and $\delta\left(\nabla_s q\right)$ given in §2.4(see also [66]), equation (3.10) becomes

$$\begin{aligned} \delta w = \operatorname{div}_s \Big\{ \left[\left(\nabla_s \mathbf{u} \right) \boldsymbol{\Lambda}_s \right]^T \boldsymbol{\nu} + \left[\left(\boldsymbol{\nu} \otimes \mathbf{n} \right) \cdot \nabla_s \mathbf{u} \right] \mathbf{G}_s^T \boldsymbol{\nu} + \mathbf{G}_s^T \boldsymbol{\tau} \delta\theta + \mathbf{b}_s \, \delta \, q \Big\} \\ + \boldsymbol{\sigma}_E \cdot \nabla_s \mathbf{u} + \left(\mathbf{g} - \operatorname{div}_s \mathbf{G}_s \right) \cdot \boldsymbol{\tau} \delta\theta + \left(f - \operatorname{div}_s \mathbf{b}_s \right) \delta q. \end{aligned} \quad (3.12)$$

Recall that $\boldsymbol{\Lambda}_s = \boldsymbol{\Lambda}\mathbf{P}$, $\mathbf{G}_s = \mathbf{G}\mathbf{P}$, $\mathbf{b}_s = \mathbf{P}\mathbf{b}$, and we define $\boldsymbol{\sigma}_E$ to be

$$\begin{aligned} \boldsymbol{\sigma}_E = & -\mathbf{L}\boldsymbol{\Lambda}_s - \left(\nabla_s \mathbf{n} \right)^T \mathbf{G}_s - \nabla_s q \otimes \mathbf{b}_s \\ & - \boldsymbol{\nu} \otimes \Big\{ \mathbf{P} \left(\boldsymbol{\beta} + \operatorname{div}_s \boldsymbol{\Lambda} \right) - \mathbf{L}\boldsymbol{\Lambda}\boldsymbol{\nu} + \left[\boldsymbol{\nu} \cdot \left(\operatorname{div}_s \mathbf{G}_s - \mathbf{g} \right) \right] \mathbf{n} - \left(\nabla_s \mathbf{n} \right)^T \mathbf{G}\boldsymbol{\nu} - \left(\mathbf{b} \cdot \boldsymbol{\nu} \right) \nabla_s q \Big\}, \end{aligned} \quad (3.13)$$

the second integral of (3.7) becomes

$$\begin{aligned} \int_S \delta w \, dS = \int_S \operatorname{div}_s \Big\{ \left[\left(\nabla_s \mathbf{u} \right) \boldsymbol{\Lambda}_s \right]^T \boldsymbol{\nu} + \left[\left(\boldsymbol{\nu} \otimes \mathbf{n} \right) \cdot \nabla_s \mathbf{u} \right] \mathbf{G}_s^T \boldsymbol{\nu} + \mathbf{G}_s^T \boldsymbol{\tau} \delta\theta + \mathbf{b}_s \delta q \Big\} \, dS \\ + \int_S \boldsymbol{\sigma}_E \cdot \nabla_s \mathbf{u} + \left(\mathbf{g} - \operatorname{div}_s \mathbf{G}_s \right) \cdot \boldsymbol{\tau} \delta\theta + \left(f - \operatorname{div}_s \mathbf{b}_s \right) \delta q \, dS. \end{aligned} \quad (3.14)$$

We set $\mathbf{F} = \left[\left(\nabla_s \mathbf{u} \right) \Lambda_s \right]^T \boldsymbol{\nu} + \left[\left(\boldsymbol{\nu} \otimes \mathbf{n} \right) \cdot \nabla_s \mathbf{u} \right] \mathbf{G}_s^T \boldsymbol{\nu} + \mathbf{G}_s^T \boldsymbol{\tau} \delta\theta + \mathbf{b}_s \delta q$. In order to apply the surface divergence theorem we show that $\mathbf{F}$ is tangential. Taking each part in term:

$$\begin{gathered} \left[\left(\nabla_s \mathbf{u} \, \boldsymbol{\Lambda}_s \right)^T \boldsymbol{\nu} \right] \cdot \boldsymbol{\nu} = \left(\nabla_s \mathbf{u} \, \boldsymbol{\Lambda}\mathbf{P}\boldsymbol{\nu} \right) \cdot \boldsymbol{\nu} = 0, \\ \left(\left(\boldsymbol{\nu} \otimes \mathbf{n} \right) \cdot \nabla_s \mathbf{u} \right) \mathbf{G}_s^T \boldsymbol{\nu} \cdot \boldsymbol{\nu} = \left(\left(\boldsymbol{\nu} \otimes \mathbf{n} \right) \cdot \nabla_s \mathbf{u} \right) \mathbf{G}\mathbf{P}\boldsymbol{\nu} \cdot \boldsymbol{\nu} = 0, \\ \left(\mathbf{G}_s^T \boldsymbol{\tau} \delta\theta \right) \cdot \boldsymbol{\nu} = \left(\left(\mathbf{G}\mathbf{P} \right)^T \boldsymbol{\tau} \delta\theta \right) \cdot \boldsymbol{\nu} = \left(\mathbf{G}\mathbf{P}\boldsymbol{\nu} \delta\theta \right) \cdot \boldsymbol{\tau} = 0, \\ \left(\mathbf{b}_s \delta q \right) \cdot \boldsymbol{\nu} = \left(\mathbf{P}\mathbf{b} \delta q \right) \cdot \boldsymbol{\nu} = \delta q \left(\mathbf{P}\mathbf{b} \right) \cdot \boldsymbol{\nu} = \delta q \mathbf{b} \cdot \left(\mathbf{P}^T \boldsymbol{\nu} \right) = \delta q \mathbf{b} \cdot \left(\mathbf{P}\boldsymbol{\nu} \right) = 0. \end{gathered}$$

So since $\mathbf{F}$ is tangential and applying the surface divergence theorem from §2.3.4 we arrive

at

$$\int_S \delta w\, dS = \int_{\partial S} \left[\left[(\nabla_s \mathbf{u})\, \mathbf{\Lambda}_s \right]^T \boldsymbol{\nu} + \left[(\boldsymbol{\nu} \otimes \mathbf{n}) \cdot \nabla_s \mathbf{u} \right] \mathbf{G}_s^T \boldsymbol{\nu} + \mathbf{G}_s^T \boldsymbol{\tau} \delta\theta + \mathbf{b}_s \delta q \right] \cdot \mathbf{k}\, dl + \int_S \boldsymbol{\sigma}_E \cdot \nabla_s \mathbf{u}\, dS + \int_S (\mathbf{g} - \operatorname{div}_s \mathbf{G}_s) \cdot \boldsymbol{\tau} \delta\theta\, dS + \int_S (f - \operatorname{div}_s \mathbf{b}_s)\, \delta q\, dS. \quad (3.15)$$

The term $\int_S \boldsymbol{\sigma}_E \cdot \nabla_s \mathbf{u}\, dS$ in (3.15) can be written as

$$\int_S \boldsymbol{\sigma}_E \cdot \nabla_s \mathbf{u}\, dS = \int_S \operatorname{div}_s \left(\boldsymbol{\sigma}_E^T \mathbf{u} \right) - (\operatorname{div}_s \boldsymbol{\sigma}_E) \cdot \mathbf{u}\, dS.$$

By using the identity $\operatorname{div}_s \left(\boldsymbol{\sigma}_E^T \mathbf{u} \right) = (\operatorname{div}_s \boldsymbol{\sigma}_E) \cdot \mathbf{u} + \boldsymbol{\sigma}_E \cdot \nabla_s \mathbf{u}$ and applying the divergence theorem, we obtain the following

$$\begin{aligned} \int_S \operatorname{div}_s \left(\boldsymbol{\sigma}_E^T \mathbf{u} \right)\, dS &= \int_{\partial S} \left(\boldsymbol{\sigma}_E^T \mathbf{u} \right) \cdot \mathbf{k}\, dl - \int_S 2H \left(\boldsymbol{\sigma}_E^T \mathbf{u} \right) \cdot \boldsymbol{\nu} + (\operatorname{div}_s \boldsymbol{\sigma}_E) \cdot \mathbf{u}\, dS \\ &= \int_{\partial S} (\boldsymbol{\sigma}_E \mathbf{k}) \cdot \mathbf{u}\, dl - \int_S 2H\, (\boldsymbol{\sigma}_E \boldsymbol{\nu}) \cdot \mathbf{u} + (\operatorname{div}_s \boldsymbol{\sigma}_E) \cdot \mathbf{u}\, dS, \end{aligned}$$

note that $\boldsymbol{\sigma}_E \boldsymbol{\nu} = \mathbf{0}$. As a result of this, we have

$$\int_S \delta w\, dS = \int_{\partial S} \left[\left[(\nabla_s \mathbf{u})\, \mathbf{\Lambda}_s \right]^T \boldsymbol{\nu} + \left[(\boldsymbol{\nu} \otimes \mathbf{n}) \cdot \nabla_s \mathbf{u} \right] \mathbf{G}_s^T \boldsymbol{\nu} + \mathbf{G}_s^T \boldsymbol{\tau} \delta\theta + \mathbf{b}_s \delta q \right] \cdot \mathbf{k}\, dl + \int_{\partial S} (\boldsymbol{\sigma}_E \mathbf{k}) \cdot \mathbf{u}\, dl + \int_S (\mathbf{g} - \operatorname{div}_s \mathbf{G}_s) \cdot \boldsymbol{\tau} \delta\theta\, dS + \int_S (f - \operatorname{div}_s \mathbf{b}_s)\, \delta q\, dS - \int_S (\operatorname{div}_s \boldsymbol{\sigma}_E) \cdot \mathbf{u}\, dS, \quad (3.16)$$

and with $\boldsymbol{\sigma} = (\lambda + w)\, \mathbf{P} + \boldsymbol{\sigma}_E$, finally we find that the variation of the energy in equation (3.7) is given by

$$\begin{aligned} \delta W = &\int_{\partial S} (\boldsymbol{\sigma} \mathbf{k}) \cdot \mathbf{u}\, dl - \int_S \operatorname{div}_s (\boldsymbol{\sigma}) \cdot \mathbf{u}\, dS \\ &+ \int_{\partial S} \left[\left[(\nabla_s \mathbf{u})\, \mathbf{\Lambda}_s \right]^T \boldsymbol{\nu} + \left[(\boldsymbol{\nu} \otimes \mathbf{n}) \cdot \nabla_s \mathbf{u} \right] \mathbf{G}_s^T \boldsymbol{\nu} + \mathbf{G}_s^T \boldsymbol{\tau} \delta\theta + \mathbf{b}_s \delta q \right] \cdot \mathbf{k}\, dl \\ &+ \int_S \left[\mathbf{g} - \operatorname{div}_s \mathbf{G}_s \right] \cdot \boldsymbol{\tau} \delta\theta\, dS + \int_S \left[f - \operatorname{div}_s \mathbf{b}_s \right] \delta q\, dS, \quad (3.17) \end{aligned}$$

where the terms

$$- \int_S \operatorname{div}_s (\boldsymbol{\sigma}) \cdot \mathbf{u}\, dS, \qquad \int_S \left[\mathbf{g} - \operatorname{div}_s \mathbf{G}_s \right] \cdot \boldsymbol{\tau} \delta\theta\, dS, \qquad \int_S \left[f - \operatorname{div}_s \mathbf{b}_s \right] \delta q\, dS,$$

allow us to find the the equilibrium equations of the corresponding variation. Since at

equilibrium $\delta W = 0$ for any $\mathbf{u}$, $\delta\theta$ and δq, the equilibrium equations becomes

$$\operatorname{div}_s \boldsymbol{\sigma} = \mathbf{0}, \tag{3.18}$$

$$(\operatorname{div}_s \mathbf{G}_s - \mathbf{g}) \cdot \boldsymbol{\tau} = 0, \tag{3.19}$$

$$\operatorname{div}_s \mathbf{b} - f = 0, \tag{3.20}$$

(where $\boldsymbol{\tau} = \boldsymbol{\nu} \times \mathbf{n}$).

The system of the equations (3.18)-(3.20) is completed by including the area constraint

$$\int_S dA = A_0. \tag{3.21}$$

The requirement that

$$\int_{\partial S} (\boldsymbol{\sigma}\mathbf{k}) \cdot \mathbf{u}\, dS + \int_{\partial S} (\boldsymbol{\sigma}_E \mathbf{k}) \cdot \mathbf{u}\, dS + \int_{\partial S} \left[\left[(\nabla_s \mathbf{u})\, \boldsymbol{\Lambda}_s \right]^T \boldsymbol{\nu} + \left[(\boldsymbol{\nu} \otimes \mathbf{n}) \cdot \nabla_s \mathbf{u} \right] \mathbf{G}_s^T \boldsymbol{\nu} + \mathbf{G}_s^T \boldsymbol{\tau} \delta\theta + \mathbf{b}_s \delta q \right] \cdot \mathbf{k}\, dS = 0, \tag{3.22}$$

gives us the relevant boundary conditions are for the variations we consider.

The shape equation is found by taking the scalar product of $\boldsymbol{\nu}$ with (3.18). As we shall see the tangential component of $\operatorname{div}_s \boldsymbol{\sigma} = \mathbf{0}$ is automatically satisfied, whenever the other equilibrium equations are satisfied, leaving us only to consider the normal component $\boldsymbol{\nu} \cdot \operatorname{div}_s \boldsymbol{\sigma} = 0$.

We write the normal component of (3.18) as

$$\boldsymbol{\nu} \cdot (\operatorname{div}_s \boldsymbol{\sigma}) = 0,$$
$$\operatorname{div}_s \left(\boldsymbol{\sigma}^T \boldsymbol{\nu} \right) - \boldsymbol{\sigma} \cdot \nabla_s \boldsymbol{\nu} = 0.$$

with $\mathbf{L} = -\nabla_s \boldsymbol{\nu}$, we obtain the *shape equation*

$$\operatorname{div}_s \left(\boldsymbol{\sigma}^T \boldsymbol{\nu} \right) + \boldsymbol{\sigma} \cdot \mathbf{L} = 0. \tag{3.23}$$

3.1.2 Boundary conditions

For open surfaces the equilibrium equations for the different scalar, vector and tensor fields and the shape equation, must be supplemented by appropriate boundary conditions. We find the relevant boundary conditions by examining (3.22). We will be concerned with boundaries that are fixed, which means that in (3.22), on the boundary of S, we must have

$$\mathbf{u} \cdot \mathbf{k} = 0 \tag{3.24}$$

and

$$\mathbf{u}\cdot\boldsymbol{\nu}=0. \tag{3.25}$$

But in general we can allow $\mathbf{u}\cdot\mathbf{l}=0$ where $\mathbf{l}$ is tangent to the boundary curve, since a variation in this direction does not affect the shape of the boundary curve (so the boundary can still be described as fixed). We will see that this freedom enters in a particular way to the form of the boundary conditions we will derive. We observe from (3.17) that there are several boundary terms which we collect into the expression (3.26),

$$\int_{\partial S}(\boldsymbol{\sigma}\mathbf{k})\cdot\mathbf{u}+\left[\left(\nabla_s\mathbf{u}\boldsymbol{\Lambda}\right)^T\boldsymbol{\nu}+\left[(\boldsymbol{\nu}\otimes\mathbf{n})\cdot\nabla_s\mathbf{u}\right]\mathbf{G}_s^T\boldsymbol{\nu}+\mathbf{G}_s^T\boldsymbol{\tau}\delta\theta+\mathbf{b}_s\delta q\right]\cdot\mathbf{k}\,dl. \tag{3.26}$$

We note that we can decompose $\mathbf{u}$ in terms of components

$$\mathbf{u}=(\mathbf{u}\cdot\mathbf{k})\,\mathbf{k}+(\mathbf{u}\cdot\mathbf{l})\,\mathbf{l}+(\mathbf{u}\cdot\boldsymbol{\nu})\,\boldsymbol{\nu} \tag{3.27}$$

and so the term involving $\boldsymbol{\sigma}$ can be written, at the boundary

$$(\boldsymbol{\sigma}\mathbf{k})\cdot\mathbf{u}=\left[(\boldsymbol{\sigma}\mathbf{k})\cdot\mathbf{l}\right](\mathbf{u}\cdot\mathbf{l}), \tag{3.28}$$

(since $\mathbf{u}\cdot\boldsymbol{\nu}=\mathbf{u}\cdot\mathbf{k}=0$). In this expression we evaluate using the expression for $\boldsymbol{\sigma}$,

$$(\boldsymbol{\sigma}\mathbf{k})\cdot\mathbf{l}=-\mathbf{l}\cdot\mathbf{L}\boldsymbol{\Lambda}_s\mathbf{k}-\mathbf{l}\cdot\left(\nabla_s\mathbf{n}\right)^T\mathbf{G}_s\mathbf{k}-\mathbf{l}\cdot(\nabla_s q\otimes\mathbf{b}_s)\,\mathbf{k}. \tag{3.29}$$

In this expression we expand $\mathbf{G}_s\mathbf{k}$ using the orthonormal basis $\{\mathbf{n},\boldsymbol{\tau},\boldsymbol{\nu}\}$, where $\boldsymbol{\tau}=\boldsymbol{\nu}\times\mathbf{n}$. In doing so we note that, since $\mathbf{n}$ is a unit vector, $\left(\nabla_s\mathbf{n}\right)^T\mathbf{n}=\mathbf{0}$, then

$$\begin{aligned}\mathbf{l}\cdot\nabla_s\mathbf{n}^T\mathbf{G}_s\mathbf{k}&=\mathbf{l}\cdot\left(\nabla_s\mathbf{n}^T\mathbf{n}\right)(\mathbf{n}\cdot\mathbf{G}_s\mathbf{k})+\mathbf{l}\cdot\left(\nabla_s\mathbf{n}^T\boldsymbol{\tau}\right)(\boldsymbol{\tau}\cdot\mathbf{G}_s\mathbf{k})+\mathbf{l}\cdot\left(\nabla_s\mathbf{n}^T\boldsymbol{\nu}\right)(\boldsymbol{\nu}\cdot\mathbf{G}_s\mathbf{k})\\&=\mathbf{l}\cdot\left(\nabla_s\mathbf{n}^T\boldsymbol{\tau}\right)(\boldsymbol{\tau}\cdot\mathbf{G}_s\mathbf{k})+\mathbf{l}\cdot\left(\nabla_s\mathbf{n}^T\boldsymbol{\nu}\right)(\boldsymbol{\nu}\cdot\mathbf{G}_s\mathbf{k}) &(3.30)\\&=\mathbf{l}\cdot\left(\nabla_s\mathbf{n}^T\boldsymbol{\tau}\right)\left(\mathbf{k}\cdot\mathbf{G}_s^T\boldsymbol{\tau}\right)+(\mathbf{l}\cdot\mathbf{L}\mathbf{n})\left(\mathbf{k}\cdot\mathbf{G}_s^T\boldsymbol{\nu}\right) &(3.31)\end{aligned}$$

which allows us to rewrite the boundary terms in (3.26) as

$$\begin{aligned}\int_{\partial S}\Big(&\mathbf{b}_s\cdot\mathbf{k}\left[\delta q-(\mathbf{l}\cdot\nabla_s q)\,(\mathbf{u}\cdot\mathbf{l})\right]+\mathbf{k}\cdot\left(\mathbf{G}_s^T\boldsymbol{\tau}\right)\left[\delta\theta-\mathbf{l}\cdot\left(\nabla_s\mathbf{n}\right)^T\boldsymbol{\tau}\,(\mathbf{u}\cdot\mathbf{l})\right]+\\&\nabla_s\,(\mathbf{u}\cdot\boldsymbol{\nu})\cdot\left[\mathbf{n}\left(\mathbf{G}_s^T\boldsymbol{\nu}\right)\cdot\mathbf{k}+\boldsymbol{\Lambda}_s\mathbf{k}\right]\Big)\,dl.\end{aligned} \tag{3.32}$$

We note that if the boundary is fixed then $\mathbf{l}\cdot\nabla_s(\mathbf{u}\cdot\boldsymbol{\nu})=0$, leaving only the $\mathbf{k}$-component of $\nabla_s(\mathbf{u}\cdot\boldsymbol{\nu})$ as non-zero, therefore the boundary terms can be written

$$\int_{\partial S}\Big(\mathbf{b}_s\cdot\mathbf{k}\left[\delta q-(\mathbf{l}\cdot\nabla_s q)(\mathbf{u}\cdot\mathbf{l})\right]+\mathbf{k}\cdot\left(\mathbf{G}_s^T\boldsymbol{\tau}\right)\left[\delta\theta-\mathbf{l}\cdot(\nabla_s\mathbf{n})^T\boldsymbol{\tau}(\mathbf{u}\cdot\mathbf{l})\right]+ (\mathbf{k}\cdot\nabla_s(\mathbf{u}\cdot\boldsymbol{\nu}))\,\mathbf{k}\cdot\left[\mathbf{n}\left(\mathbf{G}_s^T\boldsymbol{\nu}\right)\cdot\mathbf{k}+\boldsymbol{\Lambda}_s\mathbf{k}\right]\Big)\,dl. \tag{3.33}$$

At this stage we are now ready to consider the relevant boundary conditions for our equilibrium equations. We must first note that if the value of q or the direction of $\mathbf{n}$ is fixed on the boundary then the variations δq, $\delta\theta$ and $\mathbf{u}$ are not independent on the boundary curve. This means, if q is fixed then $\delta q=\nabla_s q\cdot\mathbf{u}$ and since the only component of $\mathbf{u}$ that is non-zero is the $\mathbf{l}$-component and so we have

$$\delta q-(\mathbf{l}\cdot\nabla_s q)(\mathbf{u}\cdot\mathbf{l})=0. \tag{3.34}$$

This expression is the one that appears in the boundary terms. So if q is fixed on the boundary (an essential boundary condition) then the boundary term is zero. If q is not fixed then we can guarantee the boundary term is zero by setting the *natural boundary condition*

$$\mathbf{b}_s\cdot\mathbf{k}=0. \tag{3.35}$$

Similarly, using that $\delta\mathbf{n}=\boldsymbol{\tau}\delta\theta+\mathbf{n}(\nabla_s\mathbf{u})^T\boldsymbol{\nu}$ and also that if $\mathbf{n}$ is fixed (strong anchoring) then $\delta\mathbf{n}=(\nabla_s\mathbf{n})\,\mathbf{l}(\mathbf{u}\cdot\mathbf{l})$ and we arrive at the

$$\delta\theta-\boldsymbol{\tau}\cdot(\nabla_s\mathbf{n})\,\mathbf{l}(\mathbf{u}\cdot\mathbf{l}) \tag{3.36}$$

again this is the term that appears in the boundary terms and so if we have strong anchoring the boundary term is zero. If $\mathbf{n}$ is free to rotate then the *natural boundary condition* is

$$\left(\mathbf{G}_s^T\boldsymbol{\tau}\right)\cdot\mathbf{k}=0. \tag{3.37}$$

Finally, although the boundary is fixed, the shape could be free to rotate around the boundary curve. If the slope of the boundary is fixed then, at the boundary we have $\delta\boldsymbol{\nu}=\nabla_s\boldsymbol{\nu}\mathbf{u}=-\mathbf{L}\mathbf{u}$, but we also have $\delta\boldsymbol{\nu}=-\nabla_s\mathbf{u}^T\boldsymbol{\nu}=-\nabla_s(\mathbf{u}\cdot\boldsymbol{\nu})-\mathbf{L}\mathbf{u}$ which means that if the slope is fixed $\mathbf{k}\cdot\nabla_s(\mathbf{u}\cdot\boldsymbol{\nu})=0$. This is the term that appears in the boundary term. If the slope is not fixed then the natural boundary condition is

$$\mathbf{k}\cdot\left[\mathbf{n}\left(\mathbf{G}_s^T\boldsymbol{\nu}\right)\cdot\mathbf{k}+\boldsymbol{\Lambda}_s\mathbf{k}\right]=0. \tag{3.38}$$

This is equivalent to the *torque* (as defined in [66]) being zero. So if the boundary is free to rotate then it is torque-free. In summary we have the following *natural boundary*

conditions corresponding to a scalar order parameter, a tangential vector order parameter and the surface being free to rotate around the boundary curves,

$$\mathbf{b}_s \cdot \mathbf{k} = 0, \quad \left(\mathbf{G}_s^T \boldsymbol{\tau}\right) \cdot \mathbf{k} = 0, \quad \mathbf{k} \cdot \left[\mathbf{n}\left(\mathbf{G}_s^T \boldsymbol{\nu}\right) \cdot \mathbf{k} + \boldsymbol{\Lambda}_s \mathbf{k}\right] = 0.$$

Now, we can use these *boundary conditions* to solve for equilibrium configurations of surfaces.

3.2 Tangential component of the equilibrium equation

In order to develop a framework for studying the stability of solutions, we prove that the tangential component of the shape equation is always satisfied whenever the other equilibrium equations are satisfied. This allows us to just consider the normal component of the shape equation and then we only need to consider normal increments of the normal component of the shape equation. To obtain the tangential part of the equilibrium equation $\operatorname{div}_s \boldsymbol{\sigma} = 0$, we consider $\mathbf{P} \operatorname{div}_s \boldsymbol{\sigma} = \mathbf{0}$ where $\mathbf{P}$ destroys the normal component. Since

$$\left(\mathbf{P} \operatorname{div}_s \boldsymbol{\sigma}\right)_i = P_{ij}\sigma_{jk;k} = \left(P_{ij}\sigma_{jk}\right)_{;k} - P_{ij;k}\sigma_{jk}$$

and with

$$P_{ij;k} = \left(\delta_{ij} - \nu_i\nu_j\right)_{;k} = -\nu_{i;k}\nu_j - \nu_i\nu_{j;k} = L_{ik}\nu_j + L_{jk}\nu_i,$$

it is easy to find

$$\begin{aligned} P_{ij;k}\sigma_{jk} &= L_{ik}\nu_j\sigma_{jk} + L_{jk}\nu_i\sigma_{jk} \\ &= \mathbf{L}\boldsymbol{\sigma}^T\boldsymbol{\nu} + \left(\mathbf{L} \cdot \boldsymbol{\sigma}\right)\boldsymbol{\nu}. \end{aligned}$$

Therefore,

$$\mathbf{P} \operatorname{div}_s \boldsymbol{\sigma} = \operatorname{div}_s \left(\mathbf{P}\boldsymbol{\sigma}\right) - \mathbf{L}\boldsymbol{\sigma}^T\boldsymbol{\nu} - \left(\mathbf{L} \cdot \boldsymbol{\sigma}\right)\boldsymbol{\nu}. \tag{3.39}$$

Recall that the free energy density is $w\left(\boldsymbol{\nu}, \mathbf{L}, \mathbf{n}, \nabla_s\mathbf{n}, q, \nabla_s q\right)$ and $\boldsymbol{\sigma} = \left(\lambda + w\right)\mathbf{P} + \boldsymbol{\sigma}_E$ where

$$\begin{aligned} \boldsymbol{\sigma}_E = &-\mathbf{L}\boldsymbol{\Lambda}_s - \left(\nabla_s\mathbf{n}\right)^T \mathbf{G}_s - \nabla_s q \otimes \mathbf{b}_s \\ &- \boldsymbol{\nu} \otimes \left\{\mathbf{P}\left(\boldsymbol{\beta} + \operatorname{div}_s \boldsymbol{\Lambda}_s\right) - \mathbf{L}\boldsymbol{\Lambda}\boldsymbol{\nu} + \left[\boldsymbol{\nu} \cdot \left(\operatorname{div}_s \mathbf{G}_s - \mathbf{g}\right)\right]\mathbf{n} - \left(\nabla_s\mathbf{n}\right)^T \mathbf{G}\boldsymbol{\nu} - \left(\mathbf{b} \cdot \boldsymbol{\nu}\right)\nabla_s q\right\} \end{aligned} \tag{3.40}$$

In order to organise the calculation we consider w and its dependence on different fields. We can put these results together to prove a more general case. So we consider different dependence of w on $q, \nabla_s q$ and other variables.

3.2.1 The case of $w\left(q, \nabla_s q\right)$

In this case, $\mathbf{G}=0, \mathbf{g}=0, \mathbf{\Lambda}=0, \boldsymbol{\beta}=0,\ f$ and $\mathbf{b}$ are not necessarily zero.

$$\boldsymbol{\sigma}_E = -\nabla_s q \otimes \mathbf{b}_s + \left[\boldsymbol{\nu} \otimes \nabla_s q\right](\mathbf{b}\cdot\boldsymbol{\nu}) \tag{3.41}$$

and

$$\boldsymbol{\sigma} = (\lambda + w)\,\mathbf{P} - \nabla_s q \otimes \mathbf{b}_s + \left[\boldsymbol{\nu} \otimes \nabla_s q\right](\mathbf{b}\cdot\boldsymbol{\nu}) \tag{3.42}$$

so

$$\mathbf{P}\boldsymbol{\sigma} = (\lambda + w)\,\mathbf{P} - (\nabla_s q) \otimes \mathbf{b}_s\,, \qquad (\mathbf{P}\nabla_s q = \nabla_s q)$$

$$\operatorname{div}_s(\mathbf{P}\boldsymbol{\sigma}) = (\lambda + w)\,\mathbf{P}\cdot\mathbf{L}\boldsymbol{\nu} + \nabla_s\lambda + \nabla_s w - \operatorname{div}_s(\nabla_s q \otimes \mathbf{b}_s)\,. \tag{3.43}$$

Also

$$\mathbf{L}\cdot\boldsymbol{\sigma} = (\lambda + w)\,\mathbf{P}\cdot\mathbf{L} - \left(\mathbf{L}^T\nabla_s q\right)\cdot\mathbf{b}_s\,, \quad \left(\text{using}\,\mathbf{L}^T = \mathbf{L}\right)$$

$$(\mathbf{L}\cdot\boldsymbol{\sigma})\,\boldsymbol{\nu} = (\lambda + w)\,(\mathbf{P}\cdot\mathbf{L})\,\boldsymbol{\nu} - \left[\mathbf{L}^T(\nabla_s q)\cdot\mathbf{b}_s\right]\boldsymbol{\nu} \tag{3.44}$$

and

$$\boldsymbol{\sigma}^T\boldsymbol{\nu} = \nabla_s q\,(\mathbf{b}\cdot\boldsymbol{\nu})$$

$$\mathbf{L}\boldsymbol{\sigma}^T\boldsymbol{\nu} = \mathbf{L}\nabla_s q\,(\mathbf{b}\cdot\boldsymbol{\nu})\,. \tag{3.45}$$

Using (3.43),(3.44) and (3.45) gives

$$\mathbf{P}\operatorname{div}_s(\boldsymbol{\sigma}) = \nabla_s\lambda + \nabla_s w - \operatorname{div}_s(\nabla_s q \otimes \mathbf{b}_s) + \left[\mathbf{L}^T(\nabla_s q)\cdot\mathbf{b}_s\right]\boldsymbol{\nu} - \mathbf{L}\nabla_s q\,(\mathbf{b}\cdot\boldsymbol{\nu})\,. \tag{3.46}$$

Now

$$\begin{aligned}\nabla_s w = \left[w\left(q, \nabla_s q\right)\right]_{,j} P_{ji} &= q_{,j}P_{ji}\frac{\partial w}{\partial q} + \frac{\partial w}{\partial \nabla_s q_k}\frac{\partial \nabla_s q_k}{\partial \nabla_s q_j}P_{ij} \\ &= f\nabla_s q + \mathbf{b}\cdot\nabla_s\left(\nabla_s q\right).\end{aligned}$$

Lemma 3.2.1. *Let* $\mathbf{b} = (\mathbf{b}\cdot\boldsymbol{\nu})\,\boldsymbol{\nu} + \mathbf{b}_s$ *and* $\mathbf{c} = (\mathbf{c}\cdot\boldsymbol{\nu})\,\boldsymbol{\nu} + \mathbf{c}_s$. *The surface divergence for* $\mathbf{c}\otimes\mathbf{b}$ *for vectorial fields* $\mathbf{b}$ *and* $\mathbf{c}$ *is given by,*

$$\operatorname{div}_s(\mathbf{c}\otimes\mathbf{b}) = \mathbf{c}_s\operatorname{div}_s\mathbf{b} + (\nabla_s\mathbf{c})\,\mathbf{b}. \tag{3.47}$$

Proof.

$$\nabla_s \mathbf{b} = (\mathbf{b}\cdot\boldsymbol{\nu})\,\nabla_s\boldsymbol{\nu} + \boldsymbol{\nu}\otimes\nabla_s\,(\mathbf{b}\cdot\boldsymbol{\nu}) + \nabla_s\mathbf{b}_s$$
$$\nabla_s \mathbf{c} = (\mathbf{c}\cdot\boldsymbol{\nu})\,\nabla_s\boldsymbol{\nu} + \boldsymbol{\nu}\otimes\nabla_s\,(\mathbf{c}\cdot\boldsymbol{\nu}) + \nabla_s\mathbf{c}_s$$
$$\operatorname{div}_s \mathbf{b} = (\nabla_s\mathbf{b})\cdot\mathbf{P} = -\,(\mathbf{b}\cdot\boldsymbol{\nu})\,\mathbf{L}\cdot\mathbf{P} + \operatorname{div}_s\mathbf{b}_s$$

$$\operatorname{div}_s(\mathbf{c}\otimes\mathbf{b}) = -\,(\mathbf{c}\cdot\boldsymbol{\nu})\,\mathbf{L}\,\mathbf{b} + \boldsymbol{\nu}\,\mathbf{b}\cdot\nabla_s\,(\mathbf{c}\cdot\boldsymbol{\nu}) + (\nabla_s\mathbf{c}_s)\,\mathbf{b} + \mathbf{c}\,(-\,(\mathbf{b}\cdot\boldsymbol{\nu})\,\mathbf{L}\cdot\mathbf{P} + \operatorname{div}_s\mathbf{b}_s)$$

$$= -\,(\mathbf{c}\cdot\boldsymbol{\nu})\,\mathbf{L}\,\mathbf{b}_s + \boldsymbol{\nu}\,\mathbf{b}_s\cdot\nabla_s\,(\mathbf{c}\cdot\boldsymbol{\nu}) + (\nabla_s\mathbf{c}_s)\,\mathbf{b}_s - \mathbf{c}_s\,(\mathbf{b}\cdot\boldsymbol{\nu})\,\mathbf{L}\cdot\mathbf{P} + (\mathbf{c}\cdot\boldsymbol{\nu})\,\boldsymbol{\nu}\operatorname{div}_s\mathbf{c}_s + \mathbf{c}_s\operatorname{div}_s\mathbf{b}_s,$$

If $\mathbf{c}\cdot\boldsymbol{\nu} = 0$ so $\mathbf{c} = \mathbf{c}_s$ and $\mathbf{b}\cdot\boldsymbol{\nu} = 0$, then

$$\operatorname{div}_s(\mathbf{c}\otimes\mathbf{b}) = \operatorname{div}_s(\mathbf{c}_s\otimes\mathbf{b}_s) = (\nabla_s\mathbf{c})\,\mathbf{b} + \mathbf{c}\operatorname{div}_s\mathbf{b}. \tag{3.48}$$

□

From Lemma (3.2.1), we deduce that,

$$\operatorname{div}_s(\nabla_s q\otimes\mathbf{b}_s) = (\nabla_s\nabla_s q)\,\mathbf{b}_s + \nabla_s q\operatorname{div}_s\mathbf{b}_s. \tag{3.49}$$

Then equation (3.46) becomes,

$$\mathbf{P}\operatorname{div}_s(\boldsymbol{\sigma}) = \nabla_s\lambda + \nabla_s q\,(f - \operatorname{div}_s\mathbf{b}_s) \tag{3.50}$$
$$+\big[\mathbf{b}\,\nabla_s\nabla_s q - \nabla_s\nabla_s q\,\mathbf{b}_s - \mathbf{b}\cdot\boldsymbol{\nu}\,\mathbf{L}\,\nabla_s q + [\mathbf{b}_s\cdot(\mathbf{L}\,\nabla_s q)]\,\boldsymbol{\nu}\big].$$

Let ϕ be a scalar field defined on the surface S. Surface derivatives do not commute so $\nabla_s\nabla_s\phi$ is not symmetric (for more details see [54]),

$$\nabla_s\nabla_s\phi - (\nabla_s\nabla_s\phi)^T = \boldsymbol{\nu}\otimes\mathbf{L}\nabla_s\phi - \mathbf{L}\nabla_s\phi\otimes\boldsymbol{\nu}. \tag{3.51}$$

We need to apply (3.51) to simplify (3.50), however In our case we have a vectorial field, say $\mathbf{a}$ instead of the scalar field ϕ. So we need to modify (3.51) by using a constant vector, say $\mathbf{d}$ as following:

$$\Big[\nabla_s\nabla_s\mathbf{a} - \nabla_s\,(\nabla_s\mathbf{a})^T\Big]_{ijk}\,d_i = d_i\,(a_{i:jk} - a_{i:kj}) = (d_i\,a_i)_{:jk} - (d_i\,a_i)_{:kj}$$
$$= \nu_i\,L_{jk}\,(d_l\,a_l)_{:k} - \nu_j\,L_{ik}\,(d_l\,a_l)_{:k} = d_l\,[\nu_i\,L_{jk}\,a_{l:k} - \nu_j\,L_{ik}\,a_{l:k}]\,.$$

Therefore,

$$\nabla_s\nabla_s\mathbf{a} - (\nabla_s\nabla_s\mathbf{a})^T = \boldsymbol{\nu}\otimes\mathbf{L}\,(\nabla_s\mathbf{a})^T - \mathbf{L}\,(\nabla_s\mathbf{a})^T\otimes\boldsymbol{\nu}. \tag{3.52}$$

Depending on the result obtained in (3.52), we have the following lemma:

Lemma 3.2.2. *For the scalar field q and vectorial field $\mathbf{b}$, we have*

$$\mathbf{b}\nabla_s\nabla_s q - \nabla_s\nabla_s q\mathbf{b}_s = \mathbf{b}\cdot\boldsymbol{\nu}\mathbf{L}\nabla_s q - [\mathbf{b}_s\cdot(\mathbf{L}\nabla_s q)]\,\boldsymbol{\nu}. \tag{3.53}$$

Proof.

$$\begin{aligned}\mathbf{b}\nabla_s\nabla_s q - \nabla_s\nabla_s q\mathbf{b}_s &= \mathbf{b}\left((\nabla_s\nabla_s q)^T + \boldsymbol{\nu}\otimes\mathbf{L}_s\nabla_s q - \mathbf{L}\nabla_s q - \mathbf{L}\nabla_s q\otimes\boldsymbol{\nu}\right) - (\nabla_s\nabla_s q)\,\mathbf{b}_s,\\ &= [(\mathbf{b}\cdot\boldsymbol{\nu})\,\boldsymbol{\nu} + \mathbf{b}_s]\left[(\nabla_s\nabla_s q)^T + \boldsymbol{\nu}\otimes\mathbf{L}_s\nabla_s q - \mathbf{L}\nabla_s q\otimes\boldsymbol{\nu}\right] - (\nabla_s\nabla_s q)\,\mathbf{b}_s,\end{aligned}$$

then

$$\mathbf{b}\nabla_s\nabla_s q - \nabla_s\nabla_s q\mathbf{b}_s = \mathbf{b}\cdot\boldsymbol{\nu}\mathbf{L}\nabla_s q - [\mathbf{b}_s\cdot(\mathbf{L}\nabla_s q)]\,\boldsymbol{\nu}.$$

□

Therefore,

$$\mathbf{P}\,\mathrm{div}_s(\boldsymbol{\sigma}) = \nabla_s\lambda + \nabla_s q\,(f - \mathrm{div}_s\,\mathbf{b}_s). \tag{3.54}$$

If λ is constant or in particular $\lambda = 0$ and if $f - \mathrm{div}_s\,\mathbf{b}_s = 0$ is satisfied then $\mathbf{P}\,\mathrm{div}_s(\boldsymbol{\sigma})$ is automatically zero, so the tangential part of $\mathrm{div}_s\,\boldsymbol{\sigma} = 0$ is automatically satisfied when the other equilibrium equations are.

3.2.2 The case of $w(\mathbf{L},\boldsymbol{\nu})$

Considering this case, we get the stress

$$\boldsymbol{\sigma} = (\lambda + w)\,\mathbf{P} - \mathbf{L}\boldsymbol{\Lambda}_s - \boldsymbol{\nu}\otimes(\mathbf{P}\boldsymbol{\beta} + \mathbf{P}\,\mathrm{div}_s\,\boldsymbol{\Lambda}_s) + \boldsymbol{\nu}\otimes(\mathbf{L}\boldsymbol{\Lambda}\boldsymbol{\nu}), \tag{3.55}$$

and so

$$\mathbf{P}\boldsymbol{\sigma} = (\lambda + w)\,\mathbf{P} - \mathbf{L}\boldsymbol{\Lambda}_s$$

and

$$\mathrm{div}_s(\mathbf{P}\boldsymbol{\sigma}) = \nabla_s\lambda + \nabla_s w - \mathrm{div}_s(\mathbf{L}\boldsymbol{\Lambda}_s) + (\lambda + w)\,\mathbf{P}\cdot\mathbf{L}\,\boldsymbol{\nu}. \tag{3.56}$$

To proceed note that

$$\mathrm{div}_s(\mathbf{L}\boldsymbol{\Lambda}_s) = \left[L_{ij}\left(\Lambda_s\right)_{jk}\right]_{:k} = L_{ij:k}\left(\Lambda_s\right)_{jk} + L_{ij}\left(\Lambda_s\right)_{jk:k} = [\nabla_s\mathbf{L}] : \boldsymbol{\Lambda}_s + \mathbf{L}\,\mathrm{div}_s\,\boldsymbol{\Lambda}_s.$$

$$\mathbf{L}\left(\boldsymbol{\sigma}^T\boldsymbol{\nu}\right) = -\mathbf{L}\left(\boldsymbol{\beta} + \mathrm{div}_s\,\boldsymbol{\Lambda}_s\right) + \mathbf{L}^2\boldsymbol{\Lambda}\boldsymbol{\nu} \tag{3.57}$$

$$(\mathbf{L}\cdot\boldsymbol{\sigma})\,\boldsymbol{\nu} = -\left(\mathbf{L}^2\cdot\boldsymbol{\Lambda}_s\right)\boldsymbol{\nu} + (\lambda + w)\,\mathbf{P}\cdot\mathbf{L}\,\boldsymbol{\nu}, \tag{3.58}$$

with

$$\begin{aligned}\nabla_s w &= \nu_{i:j}\frac{\partial w}{\partial \nu_i} + \frac{\partial w}{\partial L_{ij}} L_{ij;k} \\ &= -\mathbf{L}\boldsymbol{\beta} + \boldsymbol{\Lambda} : \nabla_s \mathbf{L}\end{aligned}$$

From (3.56),(3.57)and (3.58), one can obtain

$$\begin{aligned}\mathbf{P}\,\mathrm{div}_s\,\boldsymbol{\sigma} &= \left[\nabla_s\lambda + \nabla_s w - \mathrm{div}_s\left(\mathbf{L}\boldsymbol{\Lambda}_s\right)\right] + \mathbf{L}\left(\boldsymbol{\beta} + \mathrm{div}_s\,\boldsymbol{\Lambda}_s\right) - \mathbf{L}^2\boldsymbol{\Lambda}\boldsymbol{\nu} + \left(\mathbf{L}^2\cdot\boldsymbol{\Lambda}_s\right)\boldsymbol{\nu}, \\ &= \nabla_s\lambda - \mathbf{L}\boldsymbol{\beta} + \boldsymbol{\Lambda} : \nabla_s\mathbf{L} + \mathbf{L}\boldsymbol{\beta} + \mathbf{L}\,\mathrm{div}_s\,\boldsymbol{\Lambda}_s - \mathrm{div}_s\left(\mathbf{L}\boldsymbol{\Lambda}_s\right) - \mathbf{L}^2\boldsymbol{\Lambda}\boldsymbol{\nu} + \left(\mathbf{L}^2\cdot\boldsymbol{\Lambda}_s\right)\boldsymbol{\nu}, \\ &= \nabla_s\lambda + \boldsymbol{\Lambda} : \nabla_s\mathbf{L} + \mathbf{L}\,\mathrm{div}_s\,\boldsymbol{\Lambda}_s - \left(\nabla_s\mathbf{L} : \boldsymbol{\Lambda}_s + \mathbf{L}\,\mathrm{div}_s\,\boldsymbol{\Lambda}_s\right) - \mathbf{L}^2\boldsymbol{\Lambda}\boldsymbol{\nu} + \left(\mathbf{L}^2\cdot\boldsymbol{\Lambda}_s\right)\boldsymbol{\nu},\end{aligned}$$

so

$$\begin{aligned}\mathbf{P}\,\mathrm{div}_s\,\boldsymbol{\sigma} &= \nabla_s\lambda + \boldsymbol{\Lambda} : \nabla_s\mathbf{L} - \nabla_s\mathbf{L} : \boldsymbol{\Lambda}_s - \mathbf{L}^2\boldsymbol{\Lambda}\boldsymbol{\nu} + \left(\mathbf{L}^2\cdot\boldsymbol{\Lambda}_s\right)\boldsymbol{\nu}, \\ &= \nabla_s\lambda - \boldsymbol{\Lambda} : \nabla_s\nabla_s\boldsymbol{\nu} + \nabla_s\nabla_s\boldsymbol{\nu} : \boldsymbol{\Lambda}_s - \mathbf{L}^2\boldsymbol{\Lambda}\boldsymbol{\nu} + \left(\mathbf{L}^2\cdot\boldsymbol{\Lambda}_s\right)\boldsymbol{\nu}.\end{aligned}$$

Lemma 3.2.3. *For the tensorial field* $\mathbf{A}$ *and vectorial field* $\mathbf{a}$*, where* $\mathbf{A}$ *can be defined as* $\mathbf{A} = \mathbf{A}_s + \mathbf{A}\boldsymbol{\nu}\otimes\boldsymbol{\nu}$*, we have*

$$\mathbf{A} : \nabla_s\nabla_s\mathbf{a} - \nabla_s\left(\nabla_s\mathbf{a}\right)^T : \mathbf{A}_s = \mathbf{L}\left(\nabla_s\mathbf{a}\right)^T\mathbf{A}\,\boldsymbol{\nu} - \left[\mathbf{L}\cdot\left(\nabla_s\mathbf{a}\right)^T\mathbf{A}_s\right]\boldsymbol{\nu}. \tag{3.59}$$

Proof.

$$\begin{aligned}\mathbf{A} : \nabla_s\nabla_s\mathbf{a} - \nabla_s\left(\nabla_s\mathbf{a}\right)^T : \mathbf{A}_s &= \left[\mathbf{A}_s + \mathbf{A}\boldsymbol{\nu}\otimes\boldsymbol{\nu}\right] : \nabla_s\nabla_s\mathbf{a} - \nabla_s\left(\nabla_s\mathbf{a}\right)^T : \mathbf{A}_s \\ &= \left(A_s\right)_{jk}\,a_{j:ki} - a_{j:ik}\left(A_s\right)_{jk} + \left[a_{i:jk}\right]\left(A\nu\right)_i\,\nu_j\end{aligned}$$

but $\left[a_{i:jk}\right]\left(A\nu\right)_i\,\nu_j = \left(A\nu\right)_i\left(\left(a_{i:j}\nu_j\right)_{:k} - a_{i:j}\nu_{j:k}\right) = \left(\mathbf{A}\boldsymbol{\nu}\right)\nabla_s\mathbf{a}\,\mathbf{L} = \mathbf{L}\left(\nabla_s\mathbf{a}\right)^T\mathbf{A}\boldsymbol{\nu}$. Now,

$$\begin{aligned}\mathbf{A} : \nabla_s\nabla_s\mathbf{a} - \nabla_s\left(\nabla_s\mathbf{a}\right)^T : \mathbf{A}_s &= \left(A_s\right)_{jk}\left(a_{j:ik} - \nu_i\,L_{km}\,a_{j:m} + L_{im}\,a_{j:m}\nu_k\right) \\ &\quad - a_{j:ik}\left(A_s\right)_{jk} + \mathbf{L}\left(\nabla_s\mathbf{a}\right)^T\mathbf{A}\boldsymbol{\nu} \\ &= \mathbf{L}\left(\nabla_s\mathbf{a}\right)^T\mathbf{A}\boldsymbol{\nu} - \boldsymbol{\nu}\left[\left(\mathbf{A}_s\,\mathbf{L}\right)\cdot\nabla_s\mathbf{a}\right] = \mathbf{L}\left(\nabla_s\mathbf{a}\right)^T\mathbf{A}\boldsymbol{\nu} - \left[\mathbf{L}\cdot\left(\nabla_s\mathbf{a}\right)\mathbf{A}_s\right]\boldsymbol{\nu}.\end{aligned}$$

□

Using Lemma (3.2.3) with $\mathbf{a} = -\boldsymbol{\nu}$, we obtain

$$\boldsymbol{\Lambda} : \nabla_s\mathbf{L} - \nabla_s\mathbf{L} : \boldsymbol{\Lambda}_s = \mathbf{L}^2\boldsymbol{\Lambda}\boldsymbol{\nu} - \left(\mathbf{L}^2\cdot\boldsymbol{\Lambda}_s\right)\boldsymbol{\nu}, \tag{3.60}$$

so

$$\mathbf{P}\,\mathrm{div}_s\,\boldsymbol{\sigma} = \nabla_s\lambda. \tag{3.61}$$

Again if λ is constant (or equal to zero), $\mathbf{P}\,\mathrm{div}_s\,\boldsymbol{\sigma} = \mathbf{0}$, automatically.

3.2.3 The case of $w(\mathbf{n}, \nabla_s\mathbf{n})$

Recall that $\mathbf{n}$ is a unit vector and tangential. In this case we have,

$$\boldsymbol{\sigma} = (\lambda + w)\,\mathbf{P} - (\nabla_s\mathbf{n})^T\,\mathbf{G}_s - \boldsymbol{\nu}\otimes\mathbf{n}\,[\boldsymbol{\nu}\cdot(\mathrm{div}_s\,\mathbf{G}_s - \mathbf{g})] + \boldsymbol{\nu}\otimes\left((\nabla_s\mathbf{n})^T\,\mathbf{G}\boldsymbol{\nu}\right) \tag{3.62}$$

$$\mathbf{P}\boldsymbol{\sigma} = (\lambda + w)\,\mathbf{P} - (\nabla_s\mathbf{n})^T\,\mathbf{G}_s$$

$$\mathrm{div}_s\,(\mathbf{P}\boldsymbol{\sigma}) = \nabla_s\lambda + \nabla_s w - \mathrm{div}_s\left((\nabla_s\mathbf{n})^T\,\mathbf{G}_s\right), \tag{3.63}$$

$$\mathbf{L}\boldsymbol{\sigma}^T\boldsymbol{\nu} = -\mathbf{L}\mathbf{n}\boldsymbol{\nu}\cdot(\mathrm{div}_s\,\mathbf{G}_s - \mathbf{g}) + \mathbf{L}\,(\nabla_s\mathbf{n})^T\,\mathbf{G}\boldsymbol{\nu}, \tag{3.64}$$

$$(\mathbf{L}\cdot\boldsymbol{\sigma})\,\boldsymbol{\nu} = -\left[\mathbf{L}\cdot\left((\nabla_s\mathbf{n})^T\,\mathbf{G}_s\right)\right]\boldsymbol{\nu}. \tag{3.65}$$

Then

$$\mathbf{P}\,\mathrm{div}_s\,\boldsymbol{\sigma} = \nabla_s\lambda + \nabla_s w - \mathrm{div}_s\left((\nabla_s\mathbf{n})^T\,\mathbf{G}_s\right) + \mathbf{L}\mathbf{n}\boldsymbol{\nu}\cdot(\mathrm{div}_s\,\mathbf{G}_s - \mathbf{g})$$
$$-\mathbf{L}\,(\nabla_s\mathbf{n})^T\,\mathbf{G}\boldsymbol{\nu} + \left[\mathbf{L}\cdot\nabla_s\mathbf{n}^T\mathbf{G}_s\right]\boldsymbol{\nu},$$

with

$$\nabla_s w = (\nabla_s n)_{ij}\,\frac{\partial w}{\partial n_j} + [\nabla_s\,(\nabla_s n)]_{ijk}\left(\frac{\partial w}{\partial\nabla_s n}\right)_{jk} = \mathbf{g}\cdot\nabla_s\mathbf{n} + \mathbf{G} : \nabla_s\nabla_s\mathbf{n}$$

$$\mathbf{P}\,\mathrm{div}_s\,\boldsymbol{\sigma} = \nabla_s\lambda + \mathbf{G} : \nabla_s\nabla_s\mathbf{n} + \left(\nabla_s\mathbf{n}^T - \mathbf{L}\mathbf{n}\otimes\boldsymbol{\nu}\right)\mathbf{g} - \mathbf{L}\,(\nabla_s\mathbf{n})^T\,\mathbf{G}\boldsymbol{\nu} + \left[\mathbf{L}\cdot\nabla_s\mathbf{n}^T\mathbf{G}_s\right]\boldsymbol{\nu}$$
$$-\mathrm{div}_s\left((\nabla_s\mathbf{n})^T\,\mathbf{G}_s\right) + \mathbf{L}\mathbf{n}\boldsymbol{\nu}\cdot\mathrm{div}_s\,\mathbf{G}_s \tag{3.66}$$

with

$$\mathrm{div}_s\left(\nabla_s\mathbf{n}^T\mathbf{G}_s\right) = \left[(\nabla_s\mathbf{n})^T_{ik}\,(\mathbf{G}_s)_{kj}\right]_{:j} = \left[(\nabla_s\mathbf{n})_{ki}\,(\mathbf{G}_s)_{kj}\right]_{:j}$$
$$= (\nabla_s\mathbf{n})_{ki}\,\mathrm{div}_s\,(\mathbf{G}_s) + (\nabla_s\mathbf{n})_{ki:j}\,(\mathbf{G}_s)_{kj} = (\nabla_s\mathbf{n})^T\,\mathrm{div}_s\,(\mathbf{G}_s) + n_{k:ij}\,(\mathbf{G}_s)_{kj}$$

$$\mathbf{P}\,\mathrm{div}_s\,\boldsymbol{\sigma} = \nabla_s\lambda + \left[\nabla_s\mathbf{n}^T - \mathbf{L}\mathbf{n}\otimes\boldsymbol{\nu}\right]\cdot(\mathbf{g} - \mathrm{div}_s\,\mathbf{G}_s)$$
$$+\,\mathbf{G} : \nabla_s\nabla_s\mathbf{n} - \nabla_s\,(\nabla_s\mathbf{n})^T : \mathbf{G}_s - \mathbf{L}\,(\nabla_s\mathbf{n})^T\,\mathbf{G}\boldsymbol{\nu} + \left[\mathbf{L}\cdot\nabla_s\mathbf{n}^T\mathbf{G}_s\right]\boldsymbol{\nu}. \tag{3.67}$$

Applying Lemma (3.2.3) for $\mathbf{G} : \nabla_s \nabla_s \mathbf{n} - \nabla_s \left(\nabla_s \mathbf{n}\right)^T : \mathbf{G}_s$, gives

$$\mathbf{G} : \nabla_s \nabla_s \mathbf{n} - \nabla_s \left(\nabla_s \mathbf{n}\right)^T : \mathbf{G}_s = \mathbf{L} \left(\nabla_s \mathbf{n}\right)^T \mathbf{G}\boldsymbol{\nu} - \left[\mathbf{L} \cdot \nabla_s \mathbf{n}^T \mathbf{G}_s\right] \boldsymbol{\nu}. \tag{3.68}$$

Finally we get

$$\mathbf{P} \operatorname{div}_s \boldsymbol{\sigma} = \nabla_s \lambda + \left[\nabla_s \mathbf{n}^T - \mathbf{L}\mathbf{n} \otimes \boldsymbol{\nu}\right] \cdot \left(\mathbf{g} - \operatorname{div}_s \mathbf{G}_s\right). \tag{3.69}$$

Recall that $\boldsymbol{\tau} = \boldsymbol{\nu} \times \mathbf{n}$ and consider the part $\left[\nabla_s \mathbf{n}^T - \mathbf{L}\mathbf{n} \otimes \boldsymbol{\nu}\right]$, for

$$\left[\nabla_s \mathbf{n}^T - \mathbf{L}\mathbf{n} \otimes \boldsymbol{\nu}\right] \cdot \boldsymbol{\nu} = \boldsymbol{\nu} \cdot \nabla_s \mathbf{n} - \mathbf{L}\mathbf{n} = -\mathbf{n} \cdot \left(\nabla_s \boldsymbol{\nu}\right) - \mathbf{L}\mathbf{n} = \mathbf{L}\mathbf{n} - \mathbf{L}\mathbf{n} = 0$$

and for

$$\left[\nabla_s \mathbf{n}^T - \mathbf{L}\mathbf{n} \otimes \boldsymbol{\nu}\right] \cdot \mathbf{n} = \mathbf{n} \cdot \nabla_s \mathbf{n} = \frac{1}{2} \nabla_s \left(\mathbf{n} \cdot \mathbf{n}\right) = 0.$$

In this case we have $\left[\nabla_s \mathbf{n}^T - \mathbf{L}\mathbf{n} \otimes \boldsymbol{\nu}\right] = \mathbf{f} \otimes \boldsymbol{\tau}$ for some $\mathbf{f}$ where $\boldsymbol{\nu} \cdot \boldsymbol{\tau} = 0$, $\mathbf{n} \cdot \boldsymbol{\tau} = 0$ and $\mathbf{f} = \left(\nabla_s \mathbf{n}\right)^T \boldsymbol{\tau} = -\left(\nabla_s \boldsymbol{\tau}\right)^T \mathbf{n}$.

Now, we can write,

$$\mathbf{P} \operatorname{div}_s \boldsymbol{\sigma} = \nabla_s \lambda + \mathbf{f} \left[\boldsymbol{\tau} \cdot \left(\mathbf{g}_s - \operatorname{div}_s \mathbf{G}_s\right)\right]. \tag{3.70}$$

In this case we see that once again, if λ is a constant or equal to zero and if $\boldsymbol{\tau} \cdot \left(\mathbf{g}_s - \operatorname{div}_s \mathbf{G}_s\right) = 0$ is satisfied then $\mathbf{P} \operatorname{div}_s \left(\boldsymbol{\sigma}\right) = 0$.

We can combine these results to show that in general the tangential component of (3.18) is satisfied automatically whenever the other equilibrium equations are satisfied.

3.3 Special Examples

A soap film and lipid membrane are two examples of soft thin structures which will be considered to illustrate the application of the formalism given in the previous work of this chapter. We consider these examples to illustrate the derivation of appropriate equilibrium boundary conditions.

3.3.1 Soap film

A soap film (a film between rings) is an example of a surface dominated by surface tension, where the energy functional is given by:

$$W_{\mathit{eff}} = \int_S \gamma \, dA \tag{3.71}$$

where γ is considered to be the surface tension and in general depends on the orientation of $\boldsymbol{\nu}$ though here we take it as a constant. There is no surface area constraint so $\lambda = 0$ where the surface is considered to be extensible. Thus the free-energy density is $w = \gamma$ and $\boldsymbol{\sigma} = \gamma\,\mathbf{P}$, whereas $\boldsymbol{\sigma}_E = 0$. Using the shape equation (3.23), $\boldsymbol{\sigma} \cdot \mathbf{L} = 0$ because $\boldsymbol{\sigma}^T\boldsymbol{\nu} = 0$, then we deduce the shape equation is $2H\gamma = 0$, so equilibrium surfaces are minimal surfaces.

Using (3.17) we get,

$$\delta W_{\mathit{eff}}[S] = \int_{\partial S} w\,\mathbf{u}\cdot\mathbf{k}\,dA - \int_S \operatorname{div}_s(\boldsymbol{\sigma})\cdot\mathbf{u}\,dA \tag{3.72}$$

and from the divergence theorem, we have

$$\operatorname{div}_s \boldsymbol{\sigma} = \gamma \operatorname{div}_s \mathbf{P}. \tag{3.73}$$

The surface divergence of the tangential tensor field $\mathbf{P}$ is $\operatorname{div}_s \mathbf{P} = 2H\boldsymbol{\nu}$. Thus (3.73) becomes

$$\operatorname{div}_s \boldsymbol{\sigma} = 2H\,\gamma\,\boldsymbol{\nu},$$

so

$$\operatorname{div}_s(\gamma\,\mathbf{P})\cdot\mathbf{u} = 2H\,\gamma\,\mathbf{u}\cdot\boldsymbol{\nu}. \tag{3.74}$$

As a result of this

$$\delta W_{\mathit{eff}}[S] = \int_{\partial S} w\,\mathbf{u}\cdot\mathbf{k}\,dA - \int_S 2H\boldsymbol{\nu}\,\gamma\cdot\mathbf{u}\,dA. \tag{3.75}$$

The shape equation is $H = 0$. A soap film attached to two coaxial parallel rings takes the shape of a catenoid. The boundary term gave $\mathbf{u}\cdot\mathbf{k} = 0$ on ∂S. The term $\mathbf{u}\cdot\mathbf{k} = 0$ will be our essential boundary condition of the incremental problem.

3.3.2 Lipid membrane

A lipid bilayer is a thin polar membrane made of two layers of lipid molecules. A well-known model to describe their equilibrium configuration is the Canham-Helfrich model [18]. We consider the energy in the case of the lipid membrane to derive the appropriate equilibrium equations and boundary conditions. The energy density is

$$w = \gamma + \frac{\kappa}{2}(2H + c_0)^2 + \bar{\kappa}\,K \tag{3.76}$$

where κ and $\bar{\kappa}$ are the bending rigidity constants and c_0 is the spontaneous curvature.

For the tangential component of $\operatorname{div}_s \mathbf{L}$ we can use the representation of $\mathbf{L}$ in terms of principle curvatures and principle tangent vectors. We need the following lemmas to have

the result

$$\operatorname{div}_s \mathbf{L} = 2\left[\nabla_s H + \left(2H^2 - K\right)\boldsymbol{\nu}\right]$$

that is needed to find $\operatorname{div}_s \boldsymbol{\Lambda}$, leads to the expression of $\mathbf{P}\operatorname{div}_s \boldsymbol{\Lambda}$ and so we can easily calculate $\boldsymbol{\sigma}_E$ and $\boldsymbol{\sigma}$.

Lemma 3.3.1. *The surface divergence of the tangential tensor field* $\mathbf{P}$ *is*

$$\operatorname{div}_s \mathbf{P} = 2H\boldsymbol{\nu}, \tag{3.77}$$

where H *is the mean curvature.*

Lemma 3.3.2. *The surface divergence of the curvature tensor field* $\mathbf{L}$ *is*

$$\operatorname{div}_s \mathbf{L} = 2\left[\nabla_s H + \left(2H^2 - K\right)\boldsymbol{\nu}\right], \tag{3.78}$$

where H *is the mean curvature and* K *is the Gauss curvature.*

The question arose about how the energy w is defined with respect to the curvature tensor $\mathbf{L}$. In the definition of the energy we use the trace of the extrinsic curvature tensor, which is a tangential tensor field. We show here that we can use the trace either on the full space of 3-dimensional rank-2 tensors or a trace that is restricted to tangential tensor fields on S. The calculations show that the end result for the stress is the same whichever we use. We explored this question as part of understanding the literature on this type of energy.

Now, we take H as a scalar valued function of a tensor argument in the following two ways

$$H_1 = \operatorname{tr}(\mathbf{A}), \qquad H_2 = \operatorname{tr}(\mathbf{AP})$$

when evaluated at $\mathbf{L}$ ($\mathbf{L} = -\nabla_s \boldsymbol{\nu}$) then H_1 and H_2 are twice the mean curvature of the surface. However the two functions have different derivatives when viewed as scalar functions of a tensor argument,

$$\frac{\partial H_1}{\partial \mathbf{A}} = \mathbf{I}, \qquad \frac{\partial H_2}{\partial \mathbf{A}} = \mathbf{P}.$$

The quantity $\boldsymbol{\Lambda}$ is defined in [66] as a derivative of the free energy density with respect to the tensor argument $\mathbf{L}$. The question is whether the use of H_1 and H_2 both give the same expression for stress $\boldsymbol{\sigma}$. The relevant expressions are

$$\boldsymbol{\sigma} = (\lambda + w)\,\mathbf{P} + \boldsymbol{\sigma}_E$$

and

$$\boldsymbol{\sigma}_E = -\mathbf{L}\boldsymbol{\Lambda}_s - \boldsymbol{\nu} \otimes \left[\mathbf{P}\operatorname{div}_s \boldsymbol{\Lambda} - \mathbf{L}\boldsymbol{\Lambda}\boldsymbol{\nu}\right],$$

where $\boldsymbol{\Lambda}_s = \boldsymbol{\Lambda}\,\mathbf{P}$.

Now consider the energy of the lipid membrane in (3.76) where

$$\boldsymbol{\beta} = \mathbf{0}\,, \quad \mathbf{g} = \mathbf{0}\,, \quad \mathbf{G} = \mathbf{0}\,, \quad f = 0\,, \quad \mathbf{b} = \mathbf{0}.$$

We may use H_1 and H_2 for H and similarly for the Gauss curvature K where

$$K_1 = \frac{1}{2}\left[\mathrm{tr}_1\left(\mathbf{L}\right)^2 - \mathrm{tr}_1\left(\mathbf{L}^2\right)\right] = \frac{1}{2}\left[\left(\mathbf{L}\cdot\mathbf{I}\right)^2 - \mathbf{L}^2\cdot\mathbf{I}\right],$$

and

$$\frac{\partial K_1}{\partial \mathbf{L}} = \frac{1}{2}\left[2\left(\mathbf{L}\cdot\mathbf{I}\right)\mathbf{I} - 2\mathbf{L}\right] = H_1\mathbf{I} - \mathbf{L},$$

so that

$$\mathbf{P}\,\frac{\partial K_1}{\partial \mathbf{L}} = H_1\mathbf{P} - \mathbf{L}. \tag{3.79}$$

In the case of K_2 we have

$$K_2 = \frac{1}{2}\left[\mathrm{tr}_2\left(\mathbf{L}\right)^2 - \mathrm{tr}_2\left(\mathbf{L}^2\right)\right] = \frac{1}{2}\left[\left(\mathbf{L}\cdot\mathbf{P}\right)^2 - \mathbf{L}^2\cdot\mathbf{P}\right],$$

and

$$\frac{\partial K_2}{\partial \mathbf{L}} = \frac{1}{2}\left[2\left(\mathbf{L}\cdot\mathbf{P}\right)\mathbf{P} - 2\mathbf{L}\right] = H_2\mathbf{P} - \mathbf{L}. \tag{3.80}$$

The quantity $\boldsymbol{\Lambda}$ in the case of using H_1 and K_1 is

$$\boldsymbol{\Lambda} = \kappa\left(2H + c_0\right)\mathbf{I} + \bar{\kappa}\left(2H\mathbf{I} - \mathbf{L}\right), \tag{3.81}$$

and in the case of using H_2 and K_2 is

$$\boldsymbol{\Lambda} = \kappa\left(2H + c_0\right)\mathbf{P} + \bar{\kappa}\left(2H\mathbf{P} - \mathbf{L}\mathbf{P}\right). \tag{3.82}$$

Note that in both cases $\boldsymbol{\Lambda}_s$ is the same. Let us consider the remaining term in the expression for $\boldsymbol{\sigma}_E$

$$\boldsymbol{\nu}\otimes\mathbf{L}\,\boldsymbol{\Lambda}\,\boldsymbol{\nu},$$

in the first case (using H_1 and K_1)we have that $\boldsymbol{\Lambda}\,\boldsymbol{\nu} = \kappa\left(2H + c_0\right)\boldsymbol{\nu} + 2\bar{\kappa}H\,\boldsymbol{\nu}$ and so $\mathbf{L}\boldsymbol{\Lambda}\boldsymbol{\nu} = 0$, in the second case (using H_2 and K_2) we have that $\boldsymbol{\Lambda}\boldsymbol{\nu} = 0$ so in both cases this term in $\boldsymbol{\sigma}_E$ is zero. Now consider

$$-\boldsymbol{\nu}\otimes\left(\mathbf{P}\,\mathrm{div}_s\,\boldsymbol{\Lambda}\right).$$

In the first case (using H_1 and K_1)we have

$$\begin{aligned}\operatorname{div}_s \boldsymbol{\Lambda} &= 2\left(\kappa+\bar{\kappa}\right)\nabla_s H - \bar{\kappa}\operatorname{div}_s \mathbf{L} \\ &= 2\left(\kappa+\bar{\kappa}\right)\nabla_s H - \bar{\kappa}\left(2\nabla_s H + 2\left(2H-K\right)^2\boldsymbol{\nu}\right),\end{aligned}$$

$$\mathbf{P}\operatorname{div}_s \boldsymbol{\Lambda} = 2\kappa\nabla_s H,$$

and in the second case (using H_2 and K_2) we have

$$\operatorname{div}_s \boldsymbol{\Lambda} = 2\left(\kappa+\bar{\kappa}\right)\nabla_s H + 2H\boldsymbol{\nu}\left[\kappa\left(2H+c_0\right)+\bar{\kappa}\right] - \bar{\kappa}\operatorname{div}_s\left(\mathbf{LP}\right), \tag{3.83}$$

which leads to the same expression for $\mathbf{P}\operatorname{div}_s \boldsymbol{\Lambda}$.

In both cases each of the terms involving $\boldsymbol{\Lambda}$ and its derivatives leads to the same result for $\boldsymbol{\sigma}_E$.

$$\boldsymbol{\sigma}_E = -\mathbf{L}\boldsymbol{\Lambda}_s - \boldsymbol{\nu}\otimes 2\kappa\nabla_s H. \tag{3.84}$$

Therefore

$$\boldsymbol{\sigma} = \left(\lambda+\gamma+\frac{\kappa}{2}\left(2H+c_0\right)^2+\bar{\kappa}K\right)\mathbf{P} - \mathbf{L}\boldsymbol{\Lambda}_s - \boldsymbol{\nu}\otimes 2\kappa\nabla_s H. \tag{3.85}$$

The shape equation is $\operatorname{div}_s\left(\boldsymbol{\sigma}^T\boldsymbol{\nu}\right) + \boldsymbol{\sigma}\cdot\mathbf{L} = 0$ which gives

$$\Delta_s H + \left(2H+c_0\right)\left(2H^2-K\right) - \frac{1}{2}\left(2H+c_0\right)^2 H - \frac{H\gamma}{\kappa} = 0,$$

so the equilibrium equation is

$$\Delta_s H + \left(2H+c_0\right)\left(H^2 - K - \frac{1}{2}Hc_0\right) - \frac{H\gamma}{\kappa} = 0. \tag{3.86}$$

The boundary terms on ∂S (see the earlier discussion in section §3.1.2) give $\mathbf{u}\cdot\mathbf{k} = 0$ is the *essential boundary* condition. Using (3.38) given in §3.1.2, $\mathbf{k}\cdot\boldsymbol{\Lambda}_s\mathbf{k} = 0$ on ∂S is the *natural boundary* condition and $\boldsymbol{\Lambda}_s$ is given in (3.82).

3.4 The normal increment of the shape equation

Now that we have obtained the equilibrium equations and boundary conditions, we need to examine the stability of their solutions. One way is look at the second variations and consider its positive definiteness. Sometimes the stability may depend on one or more material or geometrical parameters. Another way to investigate the static stability of the equilibrium equations is the incremental equations. The incremental equations are the increments of the equilibrium equations that give operators that appear in the second variation and boundary terms. In this section, we demonstrate the derivation of the

incremental equations and incremental boundary conditions for some specific cases. We work to find the normal increment of the shape equation given in (3.23). An increment of the shape equation gives

$$\delta\big(\mathrm{div}_s\left(\boldsymbol{\sigma}^T\boldsymbol{\nu}\right)\big)+\delta\left(\mathbf{L}\cdot\boldsymbol{\sigma}\right)=0. \tag{3.87}$$

We have $\delta\left(\mathrm{div}_s\,\mathbf{a}\right)=\mathrm{div}_s\left(\delta\mathbf{a}\right)+\psi\left(\mathbf{L}\cdot\nabla_s\mathbf{a}\right)$,

$$\mathrm{div}_s\big(\delta\left(\boldsymbol{\sigma}^T\boldsymbol{\nu}\right)\big)+\psi\mathbf{L}\cdot\nabla_s\left(\boldsymbol{\sigma}^T\boldsymbol{\nu}\right)+\delta\mathbf{L}\cdot\boldsymbol{\sigma}+\mathbf{L}\cdot\delta\boldsymbol{\sigma}=0,$$

$$\mathrm{div}_s\big(\left(\delta\boldsymbol{\sigma}\right)^T\boldsymbol{\nu}+\boldsymbol{\sigma}^T\delta\boldsymbol{\nu}\big)+\psi\mathbf{L}\cdot\nabla_s\left(\boldsymbol{\sigma}^T\boldsymbol{\nu}\right)+\delta\mathbf{L}\cdot\boldsymbol{\sigma}+\mathbf{L}\cdot\delta\boldsymbol{\sigma}=0.$$

Recall that $\delta\boldsymbol{\nu}=-\nabla_s\psi$,

$$\mathrm{div}_s\left(\delta\boldsymbol{\sigma}^T\boldsymbol{\nu}-\boldsymbol{\sigma}^T\nabla_s\psi\right)+\psi\mathbf{L}\cdot\nabla_s\left(\boldsymbol{\sigma}^T\boldsymbol{\nu}\right)+\delta\mathbf{L}\cdot\boldsymbol{\sigma}+\mathbf{L}\cdot\delta\boldsymbol{\sigma}=0. \tag{3.88}$$

We have $\delta\mathbf{L}=\mathbf{L}\nabla_s\psi\otimes\boldsymbol{\nu}+\nabla_s\left(\nabla_s\psi\right)+\mathbf{L}^2\psi$,

$$\mathrm{div}_s\left(\delta\boldsymbol{\sigma}^T\boldsymbol{\nu}-\boldsymbol{\sigma}^T\nabla_s\psi\right)+\psi\mathbf{L}\cdot\nabla_s\left(\boldsymbol{\sigma}^T\boldsymbol{\nu}\right)+\mathbf{L}\cdot\delta\boldsymbol{\sigma}+\nabla_s\psi\cdot\left(\mathbf{L}\boldsymbol{\sigma}\boldsymbol{\nu}\right)+\boldsymbol{\sigma}\cdot\mathbf{L}^2\psi+\boldsymbol{\sigma}\cdot\left(\nabla_s\nabla_s\psi\right)=0. \tag{3.89}$$

Note that the equilibrium equation $\mathrm{div}_s\,\boldsymbol{\sigma}=0$ and $\left(\mathrm{div}_s\,\boldsymbol{\sigma}\right)\cdot\mathbf{a}=\mathrm{div}_s\left(\boldsymbol{\sigma}^T\mathbf{a}\right)-\boldsymbol{\sigma}\cdot\nabla_s\mathbf{a}$ then

$$\mathrm{div}_s\left(\boldsymbol{\sigma}^T\nabla_s\psi\right)=\mathrm{div}_s\,\boldsymbol{\sigma}\cdot\nabla_s\psi+\boldsymbol{\sigma}\cdot\nabla_s\left(\nabla_s\psi\right)=0, \tag{3.90}$$

so

$$\mathrm{div}_s\left(\delta\boldsymbol{\sigma}^T\boldsymbol{\nu}\right)+\psi\mathbf{L}\cdot\nabla_s\left(\boldsymbol{\sigma}^T\boldsymbol{\nu}\right)+\mathbf{L}\cdot\delta\boldsymbol{\sigma}+\nabla_s\psi\cdot\left(\mathbf{L}\boldsymbol{\sigma}\boldsymbol{\nu}\right)+\boldsymbol{\sigma}\cdot\mathbf{L}^2\psi=0, \tag{3.91}$$

that can be written as

$$\mathrm{div}_s\left(\delta\boldsymbol{\sigma}^T\boldsymbol{\nu}\right)+\psi\mathbf{L}\cdot\nabla_s\left(\boldsymbol{\sigma}^T\boldsymbol{\nu}\right)+\mathbf{L}\cdot\delta\boldsymbol{\sigma}+\boldsymbol{\sigma}\cdot\left[\mathbf{L}\nabla_s\psi\otimes\boldsymbol{\nu}-\mathbf{L}^2\psi\right]=0. \tag{3.92}$$

This is the general form of the incremental shape equation, where we can apply this to particular cases of $\delta\boldsymbol{\sigma}$.

3.4.1 The case of $w\left(q,\nabla_s q\right)$

We show in this case when the function w has a very simple form, the stability of the shape and of q decouple. First, we find the incremental equations for the equilibrium equation

(3.20). We have

$$\delta w = \frac{\partial w}{\partial q}\cdot\delta q + \frac{\partial w}{\partial \nabla_s q}\cdot\delta\left(\nabla_s q\right) = f\cdot\delta q + \mathbf{b}\cdot\delta\left(\nabla_s q\right), \tag{3.93}$$

$$\delta f = \delta\left(\frac{\partial w}{\partial q}\right) = \frac{\partial^2 w}{\partial q^2}\delta q + \left[\frac{\partial^2 w}{\partial q\,\partial\nabla_s q}\right]\cdot\delta\left(\nabla_s q\right) = c\,\delta q + \mathbf{d}\cdot\delta\left(\nabla_s q\right), \tag{3.94}$$

$$\delta\mathbf{b} = \delta\left(\frac{\partial w}{\partial \nabla_s q}\right) = \left(\frac{\partial^2 w}{\partial q\,\partial\nabla_s q}\right)\delta q + \left(\frac{\partial^2 w}{\partial\nabla_s q\,\partial\nabla_s q}\right)\delta\left(\nabla_s q\right) = \mathbf{d}\,\delta q + \mathbf{h}\,\delta\left(\nabla_s q\right), \tag{3.95}$$

where $c = \partial^2 w/\partial q^2$, $\mathbf{d} = (\partial^2 w/\partial q\,\partial\nabla_s q)$ and $\mathbf{h} = (\partial^2 w/\partial\nabla_s q\,\partial\nabla_s q)$.

To calculate δf given in (3.94) we recall (2.75), then

$$\delta f = c\,\delta q + \mathbf{d}\cdot\left[\nabla_s\left(\delta q\right) + \left(\nabla_s\psi\cdot\nabla_s q\right)\boldsymbol{\nu} + \psi\,\mathbf{L}\nabla_s q\right]. \tag{3.96}$$

To obtain $\delta\left(\mathrm{div}_s\,\mathbf{b}_s\right)$ for the tangential field $\mathbf{b}$ where $\mathbf{b}_s = \mathbf{P}\mathbf{b}$ and $\delta\left(\mathbf{P}\mathbf{b}\right) = \left(\delta\mathbf{P}\right)\mathbf{b} + \mathbf{P}\delta\mathbf{b}$, the normal increments:

$$\delta\left(\mathbf{b}_s\right) = \left(\delta\mathbf{b}\right)_s + \left(\mathbf{b}\cdot\boldsymbol{\nu}\right)\nabla_s\psi + \boldsymbol{\nu}\left(\mathbf{b}_s\cdot\nabla_s\psi\right), \tag{3.97}$$

and from (2.77) we obtain

$$\delta\left(\mathrm{div}_s\,\mathbf{b}_s\right) = \mathrm{div}_s\left(\delta\mathbf{b}_s\right) + \psi\left(\mathbf{L}\cdot\nabla_s\mathbf{b}_s\right). \tag{3.98}$$

By combining equations (3.96) and (3.98) we arrive at

$$\delta\left(f - \mathrm{div}_s\,\mathbf{b}_s\right) = c\,\delta q + \mathbf{d}\cdot\left[\nabla_s\left(\delta q\right) + \left(\nabla_s\psi\cdot\nabla_s q\right)\boldsymbol{\nu} + \psi\,\mathbf{L}\nabla_s q\right] - \mathrm{div}_s\left(\delta\mathbf{b}_s\right) - \psi\left(\mathbf{L}\cdot\nabla_s\mathbf{b}_s\right), \tag{3.99}$$

where

$$\mathrm{div}_s\left(\delta\mathbf{b}_s\right) = \mathrm{div}_s\left(\mathbf{P}\delta\mathbf{b}\right) + \nabla_s\left(\mathbf{b}\cdot\boldsymbol{\nu}\right)\cdot\nabla_s\psi + \left(\mathbf{b}\cdot\boldsymbol{\nu}\right)\Delta_s\psi - \left(\mathbf{P}\cdot\mathbf{L}\right)\left(\mathbf{b}_s\cdot\nabla_s\psi\right). \tag{3.100}$$

This yields,

$$\begin{aligned}\delta\left(f - \mathrm{div}_s\,\mathbf{b}_s\right) &= c\,\delta q + \mathbf{d}\cdot\left[\nabla_s\left(\delta q\right) + \left(\nabla_s\psi\cdot\nabla_s q\right)\boldsymbol{\nu} + \psi\,\mathbf{L}\nabla_s q\right]\\ &\quad - \mathrm{div}_s\left(\mathbf{P}\delta\mathbf{b}\right) - \nabla_s\left(\mathbf{b}\cdot\boldsymbol{\nu}\right)\cdot\nabla_s\psi - \left(\mathbf{b}\cdot\boldsymbol{\nu}\right)\Delta_s\psi + \left(\mathbf{P}\cdot\mathbf{L}\right)\left(\mathbf{b}_s\cdot\nabla_s\psi\right) - \psi\left(\mathbf{L}\cdot\nabla_s\mathbf{b}_s\right),\end{aligned} \tag{3.101}$$

$$\begin{aligned}&= c\,\delta q + \mathbf{d}\cdot\left[\nabla_s\left(\delta q\right) + \left(\nabla_s\psi\cdot\nabla_s q\right)\boldsymbol{\nu} + \psi\,\mathbf{L}\nabla_s q\right]\\ &\quad - \mathrm{div}_s\left[\mathbf{P}\big(\mathbf{d}\delta q + \mathbf{h}\cdot\left[\nabla_s\left(\delta q\right) + \left(\nabla_s\psi\cdot\nabla_s q\right)\boldsymbol{\nu} + \psi\,\mathbf{L}\nabla_s q\right]\big)\right] - \nabla_s\left(\mathbf{b}\cdot\boldsymbol{\nu}\right)\cdot\nabla_s\psi\\ &\qquad - \left(\mathbf{b}\cdot\boldsymbol{\nu}\right)\Delta_s\psi + \left(\mathbf{P}\cdot\mathbf{L}\right)\left(\mathbf{b}_s\cdot\nabla_s\psi\right) - \psi\left(\mathbf{L}\cdot\nabla_s\mathbf{b}_s\right).\end{aligned} \tag{3.102}$$

To obtain the shape equation for this case, we find

$$\boldsymbol{\sigma} = (\lambda + w)\,\mathbf{P} - \nabla_s q \otimes \mathbf{b}_s + [\boldsymbol{\nu} \otimes \nabla_s q]\,(\mathbf{b}\cdot\boldsymbol{\nu})\,, \tag{3.103}$$

$$\boldsymbol{\sigma}^T\boldsymbol{\nu} = \nabla_s q\,(\mathbf{b}\cdot\boldsymbol{\nu})\,, \tag{3.104}$$

$$\boldsymbol{\sigma}\cdot\mathbf{L} = (\lambda + w)\,\mathbf{P}\cdot\mathbf{L} - \mathbf{b}_s\,(\mathbf{L}\nabla_s q)\,. \tag{3.105}$$

Then, equation (3.23) becomes

$$\mathrm{div}_s\big(\nabla_s q\,(\mathbf{b}\cdot\boldsymbol{\nu})\big) + (\lambda + w)\,\mathbf{P}\cdot\mathbf{L} - \mathbf{b}_s\cdot(\mathbf{L}\nabla_s q) = 0\,. \tag{3.106}$$

We aim to find the incremental equation related to equation (3.106), so will consider each term of (3.106) separately as follow:

first, note that

$$\delta\big(\mathrm{div}_s\,[\nabla_s q\,(\mathbf{b}\cdot\boldsymbol{\nu})]\big) = \mathrm{div}_s\big[\delta\,[\nabla_s q\,(\mathbf{b}\cdot\boldsymbol{\nu})]\big] + \psi\big[\mathbf{L}\cdot\nabla_s\,[\nabla_s q\,(\mathbf{b}\cdot\boldsymbol{\nu})]\big], \tag{3.107}$$

where

$$\delta\,[\nabla_s q\,(\mathbf{b}\cdot\boldsymbol{\nu})] = \delta\,(\nabla_s q)\,(\mathbf{b}\cdot\boldsymbol{\nu}) + \nabla_s q\delta\,(\mathbf{b}\cdot\boldsymbol{\nu})\,,$$

$$\begin{aligned}
&= \big[\nabla_s\,(\delta q) + (\nabla_s\psi\cdot\nabla_s q)\,\boldsymbol{\nu} + \psi\mathbf{L}\nabla_s q\big]\,(\mathbf{b}\cdot\boldsymbol{\nu}) + \nabla_s q\big[(\mathbf{d}\delta q)\cdot\boldsymbol{\nu} + [\mathbf{h}\cdot\delta\,(\nabla_s q)]\cdot\boldsymbol{\nu}\big]\\
&\qquad -\nabla_s q\,(\mathbf{b}\cdot\nabla_s\psi)\,,\\
&= \nabla_s\,(\delta q)\,(\mathbf{b}\cdot\boldsymbol{\nu}) + \nabla_s\psi\cdot\nabla_s q\,\boldsymbol{\nu}\,(\mathbf{b}\cdot\boldsymbol{\nu}) + \psi\,\mathbf{L}\nabla_s q\,(\mathbf{b}\cdot\boldsymbol{\nu}) + \nabla_s q\big[(\mathbf{d}\delta q)\cdot\boldsymbol{\nu} + [\mathbf{h}\cdot\delta\,(\nabla_s q)]\cdot\boldsymbol{\nu}\big]\\
&\qquad -\nabla_s q\,(\mathbf{b}\cdot\nabla_s\psi)\,,
\end{aligned}$$

so

$$\begin{aligned}
\mathrm{div}_s\big[\delta\,(\nabla_s q\,(\mathbf{b}\cdot\boldsymbol{\nu}))\big] &= \mathrm{div}_s\big(\nabla_s\,(\delta q)\,(\mathbf{b}\cdot\boldsymbol{\nu})\big) + \mathrm{div}_s\big(\nabla_s\psi\cdot\nabla_s q\,\boldsymbol{\nu}\,(\mathbf{b}\cdot\boldsymbol{\nu})\big) + \mathrm{div}_s\big(\psi\,\mathbf{L}\nabla_s q\,(\mathbf{b}\cdot\boldsymbol{\nu})\big)\\
&\quad + \mathrm{div}_s\big[\nabla_s q\big((\mathbf{d}\delta q)\cdot\boldsymbol{\nu} + [\mathbf{h}\cdot\delta\,(\nabla_s q)]\cdot\boldsymbol{\nu}\big)\big] - \mathrm{div}_s\big((\mathbf{b}\cdot\nabla_s\psi)\,\nabla_s q\big),
\end{aligned}$$

but $\mathrm{div}_s\big(\nabla_s\psi\cdot\nabla_s q\,\boldsymbol{\nu}\,(\mathbf{b}\cdot\boldsymbol{\nu})\big) = -\big(\nabla_s\psi\cdot\nabla_s q\;(\mathbf{b}\cdot\boldsymbol{\nu})\big)\,(\mathbf{L}\cdot\mathbf{P})$, so

$$\begin{aligned}
\delta\big(\mathrm{div}_s\,[\nabla_s q\,(\mathbf{b}\cdot\boldsymbol{\nu})]\big) &= \mathrm{div}_s\big(\nabla_s\,(\delta q)\,(\mathbf{b}\cdot\boldsymbol{\nu})\big) - \big(\nabla_s\psi\cdot\nabla_s q\;(\mathbf{b}\cdot\boldsymbol{\nu})\big)\,(\mathbf{L}\cdot\mathbf{P}) + \mathrm{div}_s\big(\psi\,\mathbf{L}\nabla_s q\,(\mathbf{b}\cdot\boldsymbol{\nu})\big)\\
&+ \mathrm{div}_s\big[\nabla_s q\big((\mathbf{d}\delta q)\cdot\boldsymbol{\nu} + [\mathbf{h}\cdot(\nabla_s\,(\delta q) + (\nabla_s\psi\cdot\nabla_s q)\,\boldsymbol{\nu} + \psi\,\mathbf{L}\nabla_s q)]\cdot\boldsymbol{\nu}\big)\big] - \mathrm{div}_s\big((\mathbf{b}\cdot\nabla_s\psi)\,\nabla_s q\big)\\
&\quad + \psi\big[\mathbf{L}\cdot\nabla_s\,[\nabla_s q\,(\mathbf{b}\cdot\boldsymbol{\nu})]\big]. \qquad (3.108)
\end{aligned}$$

For $\delta\big((\lambda+w)\,\mathbf{P}\cdot\mathbf{L}\big)$, we can write

$$\begin{aligned}
\delta\big((\lambda+w)\,\mathbf{P}\cdot\mathbf{L}\big) &= \delta\,(\lambda+w)\,(\mathbf{P}\cdot\mathbf{L}) + (\lambda+w)\,\delta\,(\mathbf{P}\cdot\mathbf{L})\,,\\
&= \delta w\,(\mathbf{P}\cdot\mathbf{L}) + (\lambda+w)\,[\Delta_s\psi + (\mathbf{L}\cdot\mathbf{L})\,\psi]\,,\\
&= [f\cdot\delta q + \mathbf{b}\cdot\delta\,(\nabla_s q)]\,(\mathbf{P}\cdot\mathbf{L}) + (\lambda+w)\,[\Delta_s\psi + (\mathbf{L}\cdot\mathbf{L})\,\psi]\,,\\
&= (f\cdot\delta q)\,(\mathbf{P}\cdot\mathbf{L}) + \mathbf{b}\cdot[\nabla_s\,(\delta q) + (\nabla_s\psi\cdot\nabla_s q)\,\boldsymbol{\nu} + \psi\,\mathbf{L}\nabla_s q]\,(\mathbf{P}\cdot\mathbf{L})\\
&\quad + (\lambda+w)\,[\Delta_s\psi + (\mathbf{L}\cdot\mathbf{L})\,\psi]\,,
\end{aligned}$$

$$\begin{aligned}
&= (f\cdot\delta q)\,(\mathbf{P}\cdot\mathbf{L}) + \mathbf{b}\cdot\nabla_s\,(\delta q)\,(\mathbf{P}\cdot\mathbf{L}) + (\mathbf{b}\cdot\boldsymbol{\nu})\,(\nabla_s\psi\cdot\nabla_s q)\,(\mathbf{P}\cdot\mathbf{L})\\
&\quad + (\mathbf{b}\cdot\mathbf{L}\nabla_s q)\,\psi\,(\mathbf{P}\cdot\mathbf{L}) + (\lambda+w)\,\Delta_s\psi + (\lambda+w)\,(\mathbf{L}\cdot\mathbf{L})\,\psi. \qquad (3.109)
\end{aligned}$$

Now, we need to find $\delta\,[(\mathbf{L}\nabla_s q)\cdot\mathbf{b}_s]$, which can be given as follow:

$$\begin{aligned}
\delta\,[(\mathbf{L}\nabla_s q)\cdot\mathbf{b}_s] &= \delta\,(\mathbf{L}\nabla_s q)\cdot\mathbf{b}_s + (\mathbf{L}\nabla_s q)\cdot\delta\,(\mathbf{b}_s)\,,\\
&= \mathbf{b}_s\cdot[\delta\mathbf{L}\,\nabla_s q + \mathbf{L}\,\delta\,(\nabla_s q)] + (\mathbf{L}\nabla_s q)\cdot\delta\,(\mathbf{b}_s)\,,\\
&= \big[\big(\mathbf{L}\,\nabla_s\psi\otimes\boldsymbol{\nu} + \nabla_s\,(\nabla_s\psi) - \mathbf{L}\,(\boldsymbol{\nu}\otimes\nabla_s\psi - \mathbf{L}\psi)\big)\nabla_s q\big]\cdot\mathbf{b}_s + \mathbf{b}_s\cdot\mathbf{L}\,\delta\,(\nabla_s q)\\
&\quad + \mathbf{L}\nabla_s q\cdot\big[(\delta\mathbf{b})_s + (\mathbf{b}\cdot\boldsymbol{\nu})\,\nabla_s\psi + \boldsymbol{\nu}\,(\mathbf{b}_s\cdot\nabla_s\psi)\big],
\end{aligned}$$

finally

$$\begin{aligned}
\delta\,[(\mathbf{L}\nabla_s q)\cdot\mathbf{b}_s] &= [\nabla_s\,(\nabla_s\psi)\,\nabla_s q]\cdot\mathbf{b}_s + \big(\mathbf{L}^2\,\psi\,\nabla_s q\big)\cdot\mathbf{b}_s + \mathbf{L}\,\nabla_s q\cdot(\delta\mathbf{b})_s + (\mathbf{b}\cdot\boldsymbol{\nu})\,\nabla_s\psi\cdot(\mathbf{L}\nabla_s q)\\
&\quad + \mathbf{b}_s\cdot\mathbf{L}\nabla_s\,(\delta q) + \mathbf{b}_s\cdot\mathbf{L}^2\psi\nabla_s q. \qquad (3.110)
\end{aligned}$$

As a result of equation (3.108), (3.109) and (3.110), we conclude that the incremental equation related to the shape equation is given by:

$$\begin{aligned}
&\mathrm{div}_s\big(\nabla_s\,(\delta q)\,(\mathbf{b}\cdot\boldsymbol{\nu})\big) - \big(\nabla_s\psi\cdot\nabla_s q\;(\mathbf{b}\cdot\boldsymbol{\nu})\big)\,(\mathbf{L}\cdot\mathbf{P}) + \mathrm{div}_s\big(\psi\,\mathbf{L}\nabla_s q\,(\mathbf{b}\cdot\boldsymbol{\nu})\big)\\
&+\mathrm{div}_s\big[\nabla_s q\big((\mathbf{d}\,\delta q)\cdot\boldsymbol{\nu} + [\mathbf{h}\cdot(\nabla_s\,(\delta q) + (\nabla_s\psi\cdot\nabla_s q)\,\boldsymbol{\nu} + \psi\,\mathbf{L}\nabla_s q)]\cdot\boldsymbol{\nu}\big)\big] - \mathrm{div}_s\big((\mathbf{b}\cdot\nabla_s\psi)\,\nabla_s q\big)\\
&+\psi\big[\mathbf{L}\cdot\nabla_s\,[\nabla_s q\,(\mathbf{b}\cdot\boldsymbol{\nu})]\big] + (f\,\delta q)\,(\mathbf{P}\cdot\mathbf{L}) + \mathbf{b}\cdot\nabla_s\,(\delta q)\,(\mathbf{P}\cdot\mathbf{L}) + (\mathbf{b}\cdot\boldsymbol{\nu})\,(\nabla_s\psi\cdot\nabla_s q)\,(\mathbf{P}\cdot\mathbf{L})\\
&\quad + (\mathbf{b}\cdot\mathbf{L}\nabla_s q)\,\psi\,(\mathbf{P}\cdot\mathbf{L}) + (\lambda+w)\,\Delta_s\psi + (\lambda+w)\,(\mathbf{L}\cdot\mathbf{L})\,\psi - [\nabla_s\,(\nabla_s\psi)\,\nabla_s q]\cdot\mathbf{b}_s\\
&-\big(\mathbf{L}^2\,\psi\,\nabla_s q\big)\cdot\mathbf{b}_s - \mathbf{L}\,\nabla_s q\cdot(\delta\mathbf{b})_s - (\mathbf{b}\cdot\boldsymbol{\nu})\,\nabla_s\psi\cdot(\mathbf{L}\nabla_s q) - \mathbf{b}_s\cdot\mathbf{L}\nabla_s\,(\delta q) - \mathbf{b}_s\cdot\mathbf{L}^2\psi\nabla_s q = 0.
\end{aligned} \qquad (3.111)$$

In general, (3.111) above is very complicated. It can be simplified for some cases depends on the given details.

Incremental Boundary conditions

We need to derive appropriate essential and natural incremental boundary conditions to solve the incremental equations related to equilibrium equation. We consider open surfaces but where the boundary is fixed. The essential boundary conditions for q is q is fixed on the boundary then we know

$$\delta q = \mathbf{u} \cdot \nabla_s q, \tag{3.112}$$

and since we are dealing with normal increments, $\mathbf{u} = \psi \boldsymbol{\nu}$ so

$$\delta q = \psi \boldsymbol{\nu} \cdot \nabla_s q, \tag{3.113}$$

$$\delta q = 0. \tag{3.114}$$

If we have the natural boundary condition $\mathbf{b}_s \cdot \mathbf{k} = 0$ then the incremental boundary condition is

$$(\delta \mathbf{b}_s) \cdot \mathbf{k} + \mathbf{b}_s \cdot \delta \mathbf{k} = 0 \tag{3.115}$$

where $\mathbf{k}$ is tangent to surface and to normal to the boundary and $\mathbf{k} = \boldsymbol{\nu} \times \mathbf{l}$ where $\mathbf{l}$ is tangent (anticlockwise) fixed as this is shape of boundary. Note that since $\mathbf{l}$ is fixed, $\delta \mathbf{k} = \delta \boldsymbol{\nu} \times \mathbf{l}$ and $\delta \boldsymbol{\nu} = -\nabla_s \mathbf{u}^T \boldsymbol{\nu} = -\nabla_s \psi$, then

$$\delta \mathbf{k} = \nabla_s \psi \times \mathbf{l}. \tag{3.116}$$

So

$$\delta \left(\mathbf{b}_s \right) \cdot \mathbf{k} + \mathbf{b}_s \cdot (\nabla_s \psi \times \mathbf{l}) = 0, \tag{3.117}$$

and since $\nabla_s \psi \times \mathbf{l}$ must lie in the normal direction then $\mathbf{b}_s \cdot (\nabla_s \psi \times \mathbf{l}) = 0$. Thus

$$\mathbf{k} \cdot \delta \left(\mathbf{b}_s \right) = 0 \tag{3.118}$$

is the incremental boundary condition. We can simplify (3.118) by using (3.97).

3.4.2 Example of the case of $w(q, \nabla_s q)$

To illustrate the application of the formalism obtained previously, we study the catenoid problem (the problem of a film with given surface energy suspended between two coaxial rings) with

$$w(q, \nabla_s q) = \gamma + W_0 \left(\hat{w}(q) + \frac{1}{2} \epsilon^2 |\nabla_s q|^2 \right)$$

where W_0 is an energy per area and ϵ is a length scale.

$$\mathbf{b} = \mathbf{b}_s = \frac{\partial w}{\partial \nabla_s q} = \epsilon^2 W_0 \nabla_s q, \qquad c = \frac{\partial^2 w}{\partial q^2} = W_0 \hat{w}''(q),$$
$$\mathbf{d} = \frac{\partial^2 w}{\partial q \, \partial \nabla_s q} = 0, \qquad \mathbf{h} = \frac{\partial^2 w}{\partial \nabla_s q \, \partial \nabla_s q} = \epsilon^2 W_0 \mathbf{I},$$

then, from equation (3.102), we have

$$\begin{aligned}\delta\left(f - \operatorname{div}_s \mathbf{b}_s\right) &= \hat{w}''(q)\,\delta q - \epsilon^2 \operatorname{div}_s\big(\mathbf{P}\left[\nabla_s \delta q + (\nabla_s \psi \cdot \nabla_s q)\,\boldsymbol{\nu} + \psi \mathbf{L} \nabla_s q\right]\big) \\ &\quad + \epsilon^2 (\mathbf{P}\cdot\mathbf{L})(\nabla_s q \cdot \nabla_s \psi) - \epsilon^2 \psi (\mathbf{L}\cdot\nabla_s \nabla_s q), \\ &= \hat{w}''(q)\,\delta q - \epsilon^2\left[(\mathbf{P}\cdot\mathbf{L})(\nabla_s q \cdot \nabla_s \psi) - \psi(\mathbf{L}\cdot\nabla_s\nabla_s q) - \operatorname{div}_s\left[\mathbf{P}\nabla_s(\delta q)\right]\right]\end{aligned}$$

$$= \hat{w}''(q)\,\delta q - \epsilon^2\left[(\mathbf{P}\cdot\mathbf{L})(\nabla_s q \cdot \nabla_s \psi) - \psi(\mathbf{L}\cdot\nabla_s\nabla_s q) - \Delta_s(\delta q)\right] \tag{3.119}$$

and from (3.111), we obtain the incremental equation related to the shape equation of this case

$$\begin{aligned}&w'(q)\;\delta q\,(\mathbf{P}\cdot\mathbf{L}) + \epsilon^2 \nabla_s q \cdot \nabla_s(\delta q)\,(\mathbf{P}\cdot\mathbf{L}) + \epsilon^2\big(\nabla_s q \cdot (\mathbf{L}\nabla_s q)\big)(\mathbf{P}\cdot\mathbf{L})\,\psi + (\lambda + w)\,\Delta_s \psi \\ &+(\lambda + w)(\mathbf{L}\cdot\mathbf{L})\,\psi - \epsilon^2 \nabla_s q\cdot[\nabla_s(\nabla_s\psi)\,\nabla_s q] - 2\epsilon^2 \nabla_s q\cdot\big(\mathbf{L}\nabla_s(\delta q)\big) - 3\epsilon^2 \nabla_s q\cdot\big(\mathbf{L}^2\psi\nabla_s q\big) = 0.\end{aligned} \tag{3.120}$$

If the geometry is fixed $(\psi = 0)$, then the incremental equation is

$$\hat{w}''(q)\;\delta q - \epsilon^2 \Delta_s \delta q = 0. \tag{3.121}$$

Applying the essential boundary condition $q =$ constant to our equilibrium equation

$$\epsilon^2 \Delta_s q - \hat{w}'(q) = 0 \tag{3.122}$$

and $\hat{w}'(q) = 0$ (since $\Delta_s q = 0$ when q is constant) and natural boundary condition is $\mathbf{k}\cdot\nabla_s q = 0$.

If the geometry is not fixed, then we get incremental equations related to the shape equations as follows.

From $f - \operatorname{div}_s \mathbf{b}_s = 0$ we have

$$D_1[\delta q] + D_2[\psi] = 0,$$

where

$$D_1\left[\delta q\right] = \hat{w}''\left(q\right)\,\delta q - \epsilon^2\Delta_s\delta q, \tag{3.123}$$

$$D_2\left[\psi\right] = \epsilon^2\mathbf{L}\cdot\left(\nabla_s\nabla_s q\right)\psi + \left(\mathbf{P}\cdot\mathbf{L}\right)\epsilon^2\nabla_s q\cdot\nabla_s\psi, \tag{3.124}$$

and from incremental shape equation in (3.120), we have

$$D_3\left[\delta q\right] + D_4\left[\psi\right] = 0,$$

and the shape equation is

$$\left(\gamma + \hat{w} + \frac{1}{2}\epsilon^2\left|\nabla_s q\right|^2\right)\,\mathbf{P}\cdot\mathbf{L} = 0, \tag{3.125}$$

where

$$D_3\left[\delta q\right] = w'\left(q\right)\,\delta q\left(\mathbf{P}\cdot\mathbf{L}\right) + \epsilon^2\nabla_s q\cdot\nabla_s\left(\delta q\right)\left(\mathbf{P}\cdot\mathbf{L}\right) - 2\epsilon^2\nabla_s q\cdot\left(\mathbf{L}\nabla_s\left(\delta q\right)\right), \tag{3.126}$$

$$\begin{aligned} D_4\left[\psi\right] = {} & \epsilon^2\left(\nabla_s q\cdot\left(\mathbf{L}\nabla_s q\right)\right)\left(\mathbf{P}\cdot\mathbf{L}\right)\psi + \left(\lambda + w\right)\Delta_s\psi + \left(\lambda + w\right)\left(\mathbf{L}\cdot\mathbf{L}\right)\psi \\ & - \epsilon^2\nabla_s q\cdot\left[\nabla_s\left(\nabla_s\psi\right)\nabla_s q\right] - 3\epsilon^2\nabla_s q\cdot\left(\mathbf{L}^2\psi\nabla_s q\right). \end{aligned} \tag{3.127}$$

If q is constant, then $\mathbf{P}\cdot\mathbf{L} = 0$. Recall that the equilibrium equation is given in (3.122) and the natural boundary condition is $\mathbf{k}\cdot\nabla_s q = 0$, clearly $q = q_0 =$ constant such that $w'\left(q_0\right) = 0$ is a solution then the shape equation is $H = 0$. Then the incremental equations is

$$\Delta_s\psi + \mathbf{L}\cdot\mathbf{L}\psi = 0, \tag{3.128}$$

$$-\epsilon^2\Delta_s\left(\delta q\right) + \hat{w}''\left(q\right)\delta q = 0. \tag{3.129}$$

In this case the equation for ψ and δq are decoupled. The incremental boundary conditions are $\mathbf{k}\cdot\delta\left(\nabla_s q\right) = 0$ and $\psi = 0$.

3.4.3 The case of $w(\mathbf{L}, \boldsymbol{\nu})$

In this section also we need to find the incremental equations where the free-energy density depends on the symmetric tangential tensor $\mathbf{L}$ and the normal vector to the surface $\boldsymbol{\nu}$ and

$$\delta w = \frac{\partial w}{\partial\boldsymbol{\nu}}\cdot\delta\boldsymbol{\nu} + \frac{\partial w}{\partial\mathbf{L}}\cdot\delta\mathbf{L} = \boldsymbol{\beta}\cdot\delta\boldsymbol{\nu} + \boldsymbol{\Lambda}\cdot\delta\mathbf{L},$$

$$= \boldsymbol{\beta}\cdot\left(-\nabla_s\mathbf{u}^T\boldsymbol{\nu}\right) + \boldsymbol{\Lambda}\cdot\left[\mathbf{L}\left(\nabla_s\mathbf{u}\right)^T\boldsymbol{\nu}\otimes\boldsymbol{\nu} + \nabla_s\left[\left(\nabla_s\mathbf{u}\right)^T\boldsymbol{\nu}\right] - \mathbf{L}\left(\nabla_s\mathbf{u}\right)\right],$$

$$= -\boldsymbol{\beta}\cdot\nabla_s\psi + \boldsymbol{\Lambda}\cdot\left[\mathbf{L}\,\nabla_s\psi\otimes\boldsymbol{\nu} + \nabla_s\left(\nabla_s\psi\right) - \mathbf{L}\left(\boldsymbol{\nu}\otimes\nabla_s\psi - \mathbf{L}\psi\right)\right] \tag{3.130}$$

where $\boldsymbol{\beta} = \frac{\partial w}{\partial \boldsymbol{\nu}}$ and $\boldsymbol{\Lambda} = \frac{\partial w}{\partial \mathbf{L}}$. The stress tensor in this case is given by

$$\boldsymbol{\sigma} = (\lambda + w)\,\mathbf{P} - \mathbf{L}\boldsymbol{\Lambda}_s - \boldsymbol{\nu}\otimes\left(\mathbf{P}\boldsymbol{\beta} + \mathbf{P}\,\mathrm{div}_s\,\boldsymbol{\Lambda}_s\right) + \boldsymbol{\nu}\otimes\left(\mathbf{L}\boldsymbol{\Lambda}\boldsymbol{\nu}\right) \tag{3.131}$$

and the shape equation associated with (3.23) is

$$\mathrm{div}_s\left[\mathbf{L}\boldsymbol{\Lambda}\boldsymbol{\nu} - \left(\boldsymbol{\beta} + \mathrm{div}_s\,\boldsymbol{\Lambda}_s\right)\right] + (\lambda + w)\,\mathbf{P}\cdot\mathbf{L} - \mathbf{L}^2\cdot\boldsymbol{\Lambda}_s = 0. \tag{3.132}$$

To obtain the incremental equation to the shape equation first we need to know how to find $\delta\left(\mathrm{div}_s\,\mathbf{T}\right)$, where $\mathbf{T}$ could be any tensor filed defined on the surface S.

Lemma 3.4.1. *If* $\mathbf{T}$ *is a tensor field defined on* S*, then*

$$\delta\left(\mathrm{div}_s\,\mathbf{T}\right) = \mathrm{div}_s\left(\delta\mathbf{T}\right) + \psi\left[\mathrm{div}_s\left(\mathbf{T}\mathbf{L}\right) - \mathbf{T}\,\mathrm{div}_s\left(\mathbf{L}\right)\right]. \tag{3.133}$$

Proof. Take a constant vector $\mathbf{k}$ defined on the surface S, then

$$\mathbf{k}\cdot\left(\delta\left(\mathrm{div}_s\,\mathbf{T}\right)\right) = \delta\left(\mathbf{k}\cdot\mathrm{div}_s\,\mathbf{T}\right) = \delta\big(\mathrm{div}_s\left(\mathbf{T}^T\,\mathbf{k}\right)\big),$$

From (2.77),we deduce that

$$\delta\big(\mathrm{div}_s\left(\mathbf{T}^T\,\mathbf{k}\right)\big) = \mathrm{div}_s\left(\delta\mathbf{T}\right)\cdot\mathbf{k} + \psi\,\mathbf{L}\cdot\left[\nabla_s\left(\mathbf{T}^T\mathbf{k}\right)\right]$$

however $\left[\nabla_s\left(\mathbf{T}^T\,\mathbf{k}\right)\right]_{ij} = \left[\left(\mathbf{T}^T\right)_{ip}\,k_p\right]_{:j} = \left[T_{pi}\,k_p\right]_{:j} = k_p\left[T_{pi:j}\right] = \mathbf{k}\cdot\left[\nabla_s\mathbf{T}\right]$. Thus, we can write

$$\mathbf{k}\cdot\left(\delta\left(\mathrm{div}_s\,\mathbf{T}\right)\right) = \left[\mathrm{div}_s\left(\delta T\right) + \psi\,\mathbf{L}\cdot\left(\nabla_s\mathbf{T}\right)\right]\cdot\mathbf{k} = \left[\mathrm{div}_s\left(\delta T\right) + \psi\,\left(\nabla_s\mathbf{T}\right):\mathbf{L}\right]\cdot\mathbf{k},$$

and since

$$\begin{aligned}\left(\nabla_s\mathbf{T}\right):\mathbf{L} = T_{pi:j}\,L_{ij} &= \left[T_{pi}\,L_{ij}\right]_{:j} - T_{pi}\,L_{ij:j}\\ &= \mathrm{div}_s\left(\mathbf{T}\,\mathbf{L}\right) - \mathbf{T}\,\mathrm{div}_s\left(\mathbf{L}\right).\end{aligned}$$

Then we arrive at

$$\delta\left(\mathrm{div}_s\,\mathbf{T}\right) = \mathrm{div}_s\left(\delta\mathbf{T}\right) + \psi\left[\mathrm{div}_s\left(\mathbf{T}\mathbf{L}\right) - \mathbf{T}\,\mathrm{div}_s\left(\mathbf{L}\right)\right].$$

□

3.4.4 The case of $w = \hat{w}(H, K)$

Now we consider a simpler case which includes the Canham-Helfrich energy discussed previously in §3.5.3. In order to derive the incremental equation of this case we note

$$\delta w = \frac{\partial \hat{w}}{\partial H}\,\delta H + \frac{\partial \hat{w}}{\partial K}\,\delta K.$$

So first, we calculate δH and δK

$$\delta H = \frac{1}{2}\left(\delta \mathbf{L} \cdot \mathbf{P}\right) = \frac{1}{2}\left(\Delta_s \psi + \mathbf{L}^2 \cdot \mathbf{P}\psi\right),$$

$$= \frac{1}{2}\left(\Delta_s \psi + 2\left(2H^2 - K\right)\psi\right). \tag{3.134}$$

Taking into account that $2K = \left(\mathrm{tr}\left(\mathbf{L}\right)\right)^2 - \mathrm{tr}\left(\mathbf{L}^2\right)$ and $\mathrm{tr}\left(\mathbf{L}\right) = 2H$, we get $\mathrm{tr}\left(\mathbf{L}^2\right) = 4H^2 - 2K$, so

$$\delta K = \left(2H\mathbf{P} - \mathbf{L}\right) \cdot \delta \mathbf{L},$$

in this case $\mathbf{L}\boldsymbol{\nu} = 0$, then

$$\delta \mathbf{L} = \mathbf{L}\nabla_s \psi \otimes \boldsymbol{\nu} + \nabla_s \nabla_s \psi + \mathbf{L}^2 \psi,$$

and so

$$\delta K = \left(2H\mathbf{P} - \mathbf{L}\right) \cdot \left(\mathbf{L}\nabla_s \psi \otimes \boldsymbol{\nu} + \nabla_s \nabla_s \psi + \mathbf{L}^2 \psi\right). \tag{3.135}$$

For

$$\boldsymbol{\Lambda} = \frac{\partial \hat{w}}{\partial H}\frac{\partial H}{\partial \mathbf{L}} + \frac{\partial \hat{w}}{\partial K}\frac{\partial K}{\partial \mathbf{L}} = \frac{\partial \hat{w}}{\partial H}\frac{1}{2}\mathbf{P} + \frac{\partial \hat{w}}{\partial K}\left(2H\mathbf{P} - \mathbf{L}\right), \tag{3.136}$$

we have

$$\boldsymbol{\sigma} = \hat{w}\mathbf{P} - \mathbf{L}\boldsymbol{\Lambda}_s - \boldsymbol{\nu} \otimes \left[\mathbf{P}\,\mathrm{div}_s\,\boldsymbol{\Lambda}_s\right] + \boldsymbol{\nu} \otimes \mathbf{L}\boldsymbol{\Lambda}\boldsymbol{\nu}, \tag{3.137}$$

so we can calculate both $\boldsymbol{\sigma}^T\boldsymbol{\nu}$ and $\boldsymbol{\sigma} \cdot \mathbf{L}$ and get the shape equation. With $\mathbf{L}\boldsymbol{\Lambda}\boldsymbol{\nu} = 0$

$$\boldsymbol{\sigma}^T\boldsymbol{\nu} = \mathbf{L}\boldsymbol{\Lambda}\boldsymbol{\nu} - \mathbf{P}\,\mathrm{div}_s\,\boldsymbol{\Lambda}_s = -\mathbf{P}\,\mathrm{div}_s\,\boldsymbol{\Lambda}_s, \tag{3.138}$$

and

$$\boldsymbol{\sigma} \cdot \mathbf{L} = \hat{w}\left(\mathbf{P} \cdot \mathbf{L}\right) - \mathbf{L} \cdot \left(\mathbf{L}\boldsymbol{\Lambda}_s\right), \tag{3.139}$$

where $\mathbf{L}\boldsymbol{\Lambda}_s = \mathbf{L} \cdot \left[\frac{\partial \hat{w}}{\partial H}\frac{1}{2}\mathbf{P} + \frac{\partial \hat{w}}{\partial K}\left(2H\mathbf{P} - \mathbf{L}\right)\right]$ and by using $\mathbf{L}^2 - 2H\mathbf{L} + K\mathbf{P} = 0$ so that $2H\mathbf{L} - \mathbf{L}^2 = K\mathbf{P}$, given $K = -\frac{1}{2}\left[\left(\mathbf{L} \cdot \mathbf{L}\right) - \left(\mathbf{L} \cdot \mathbf{P}\right)^2\right]$, we get

$$\mathbf{L}\boldsymbol{\Lambda}_s = \frac{\partial \hat{w}}{\partial H}\frac{1}{2}\mathbf{L} + \frac{\partial \hat{w}}{\partial K}\left(2H\mathbf{L} - \mathbf{L}^2\right), \tag{3.140}$$

so that

$$\mathbf{L}\cdot(\mathbf{L}\boldsymbol{\Lambda}_s)=\mathbf{L}^2\cdot\left[\frac{\partial\hat{w}}{\partial H}\frac{1}{2}\mathbf{P}+\frac{\partial\hat{w}}{\partial K}(2H\mathbf{P}-\mathbf{L})\right]$$
$$=\frac{\partial\hat{w}}{\partial H}\frac{1}{2}\left(\mathbf{L}^2\cdot\mathbf{P}\right)+\frac{\partial\hat{w}}{\partial K}(2H\mathbf{P}-\mathbf{L})\cdot\mathbf{L}^2=\frac{1}{2}\frac{\partial\hat{w}}{\partial H}(\mathbf{L}\cdot\mathbf{L})+\frac{\partial\hat{w}}{\partial K}K(\mathbf{P}\cdot\mathbf{L})$$

that reduces to

$$\mathbf{L}\cdot(\mathbf{L}\boldsymbol{\Lambda}_s)=\left(2H^2-K\right)\frac{\partial\hat{w}}{\partial H}+2HK\frac{\partial\hat{w}}{\partial K}. \tag{3.141}$$

Thus, (3.139) becomes

$$\boldsymbol{\sigma}\cdot\mathbf{L}=2H\hat{w}-2H\,K\,\frac{\partial\hat{w}}{\partial K}-\left(2H^2-K\right)\frac{\partial\hat{w}}{\partial H}. \tag{3.142}$$

Our shape equation becomes

$$-\operatorname{div}_s(\operatorname{div}_s\boldsymbol{\Lambda}_s)+\left(2H\hat{w}-2H\,K\,\frac{\partial\hat{w}}{\partial K}-\left(2H^2-K\right)\frac{\partial\hat{w}}{\partial H}\right)=0 \tag{3.143}$$

where

$$\boldsymbol{\Lambda}_s=\frac{1}{2}\mathbf{P}\frac{\partial\hat{w}}{\partial H}+(2H\mathbf{P}-\mathbf{L})\frac{\partial\hat{w}}{\partial K} \tag{3.144}$$

and with $\operatorname{div}_s\mathbf{P}=2H\boldsymbol{\nu}$, we get

$$\operatorname{div}_s\boldsymbol{\Lambda}_s=H\frac{\partial\hat{w}}{\partial H}\boldsymbol{\nu}+\frac{1}{2}\nabla_s\frac{\partial\hat{w}}{\partial H}+(2H\mathbf{P}-\mathbf{L})\nabla_s\left(\frac{\partial\hat{w}}{\partial K}\right)+\operatorname{div}_s(2H\mathbf{P}-\mathbf{L})\frac{\partial\hat{w}}{\partial K}, \tag{3.145}$$

we have

$$\operatorname{div}_s(2H\mathbf{P})=2H\operatorname{div}_s\mathbf{P}+\mathbf{P}\nabla_s(2H)=2\nabla_sH+2H\operatorname{div}_s\mathbf{P}$$
$$=2\nabla_sH+2H(2H\boldsymbol{\nu})=2\nabla_sH+4H^2\boldsymbol{\nu}$$

and

$$\operatorname{div}_s\mathbf{L}=2\left[\nabla_sH+\left(2H^2-K\right)\boldsymbol{\nu}\right]$$

this gives,

$$\operatorname{div}_s(2H\mathbf{P}-\mathbf{L})=2\nabla_sH+4H^2\boldsymbol{\nu}-\left(2\nabla_sH+4H^2\boldsymbol{\nu}-2K\boldsymbol{\nu}\right)=2K\boldsymbol{\nu}. \tag{3.146}$$

In this case, our equation in (3.145) can be written as

$$\operatorname{div}_s\boldsymbol{\Lambda}_s=H\frac{\partial\hat{w}}{\partial H}\boldsymbol{\nu}+\frac{1}{2}\nabla_s\frac{\partial\hat{w}}{\partial H}+(2H\mathbf{P}-\mathbf{L})\nabla_s\frac{\partial\hat{w}}{\partial K}+2K\boldsymbol{\nu}\frac{\partial\hat{w}}{\partial K}, \tag{3.147}$$

and

$$\mathbf{P}\,\mathrm{div}_s\,\mathbf{\Lambda}_s = \frac{1}{2}\nabla_s\frac{\partial\hat{w}}{\partial H} + (2H\mathbf{P}-\mathbf{L})\,\nabla_s\frac{\partial\hat{w}}{\partial K}. \tag{3.148}$$

The shape equation in (3.149) becomes

$$\mathrm{div}_s\left(-\frac{1}{2}\nabla_s\frac{\partial\hat{w}}{\partial H}-(2H\mathbf{P}-\mathbf{L})\,\nabla_s\frac{\partial\hat{w}}{\partial K}\right)+2H\hat{w}-2HK\frac{\partial\hat{w}}{\partial K}-\left(2H^2-K\right)\frac{\partial\hat{w}}{\partial H}=0, \tag{3.149}$$

which can be simplified more as

$$-\frac{1}{2}\Delta_s\frac{\partial\hat{w}}{\partial H}-\mathrm{div}_s\,(2H\mathbf{P}-\mathbf{L})\cdot\nabla_s\frac{\partial\hat{w}}{\partial K}-(2H\mathbf{P}-\mathbf{L})\cdot\left(\nabla_s\nabla_s\frac{\partial\hat{w}}{\partial K}\right)$$
$$+2H\hat{w}-2HK\frac{\partial\hat{w}}{\partial K}-\left(2H^2-K\right)\frac{\partial\hat{w}}{\partial H}=0.$$

Using (3.146), the second term $\mathrm{div}_s\,(2H\mathbf{P}-\mathbf{L})\cdot\nabla_s\,(\partial\hat{w}/\partial K)=0$. Then we get

$$\frac{1}{2}\Delta_s\frac{\partial\hat{w}}{\partial H}+(2H\mathbf{P}-\mathbf{L})\cdot\left(\nabla_s\nabla_s\frac{\partial\hat{w}}{\partial K}\right)-2H\hat{w}+2HK\frac{\partial\hat{w}}{\partial K}+\left(2H^2-K\right)\frac{\partial\hat{w}}{\partial H}=0 \tag{3.150}$$

is the 4th order shape equation.

Boundary conditions

Referring back to §3.1.2, The essential boundary condition is $\mathbf{k}\cdot\nabla_s\,(\mathbf{u}\cdot\boldsymbol{\nu})=0$, where the slope is fixed. For the natural boundary condition, with the aid of (3.38) (where $\mathbf{G}_s=0$) we obtain $\mathbf{k}\cdot(\mathbf{\Lambda}_s\mathbf{k})=0$ as the natural boundary condition. Since $\mathbf{\Lambda}_s=\frac{1}{2}\mathbf{P}\,(\partial\hat{w}/\partial H)+(2H\mathbf{P}-\mathbf{L})\,(\partial\hat{w}/\partial K)$ then $\mathbf{k}\cdot(\mathbf{\Lambda}_s\mathbf{k})=\frac{1}{2}\,(\partial\hat{w}/\partial H)+(2H-\mathbf{k}\cdot\mathbf{L}\mathbf{k})\,(\partial\hat{w}/\partial K)$. Note that $2H=\mathrm{tr}\,(\mathbf{L})=\mathbf{k}\cdot\mathbf{L}\mathbf{k}+\mathbf{l}\cdot\mathbf{L}\mathbf{l}$, ($\mathbf{l}$ is the tangent direction to the boundary) then we have

$$\frac{1}{2}\frac{\partial\hat{w}}{\partial H}+\mathbf{l}\cdot\mathbf{L}\mathbf{l}\frac{\partial\hat{w}}{\partial K}=0 \tag{3.151}$$

is the natural boundary condition.

For the incremental boundary condition, we take the increment of the boundary condition $\mathbf{k}\cdot(\mathbf{\Lambda}_s\mathbf{k})=0$ so that

$$\delta\mathbf{k}\cdot(\mathbf{\Lambda}_s\mathbf{k})+\mathbf{k}\cdot\delta\,(\mathbf{\Lambda}_s\mathbf{k})\,, \tag{3.152}$$

with $\delta\mathbf{k}$ given in (3.116) our incremental boundary condition is given as

$$\mathbf{k}\cdot(\delta\mathbf{\Lambda}_s\,\mathbf{k})=0. \tag{3.153}$$

3.5 Examples

In this section we illustrate the use of the incremental equations and the incremental boundary conditions we developed in the previous sections on some simple examples: the soap film in two different geometries (soap bubble and catenoid) and also the Calham-Helfrich energy in the catenoid geometry. We will see in chapter 4 that this has some relevance to the stability of a nematic film.

3.5.1 Stability of a soap bubble

To illustrate the stability of a bubble, we consider a thin film with constant surface energy enclosing a fixed volume. In this case the constraint of a fixed volume $\mathrm{Vol}(V) = V_0$, must be included where V is the region enclosed by S (otherwise minimising the surface energy would be achieved by shrinking the surface to nothing). The volume constraint is [66]

$$\int_V 1 dV = V_0. \tag{3.154}$$

Written in terms of a surface integral (by applying the surface divergence theorem §2.3.4), we have

$$\int_S \frac{1}{3} (\mathbf{r} \cdot \boldsymbol{\nu}) \, dS = V_0. \tag{3.155}$$

Furthermore, with $\boldsymbol{\sigma} = \gamma \mathbf{P}$, the shape equation $(\mathrm{div}_s \boldsymbol{\sigma}) \cdot \boldsymbol{\nu} = \mu$ reduces to the equilibrium equation $2H\gamma = \mu$ (Young-Laplace law) where μ is the Lagrange multiplier for the volume constraint. For the incremental equation

$$2\gamma \cdot \left[\Delta_s \psi + 2 \left(2H^2 - K \right) \psi \right] = \delta\mu,$$

so

$$\Delta_s \psi + 2 \left(2H^2 - K \right) \psi = \frac{\delta\mu}{2\gamma}. \tag{3.156}$$

Now to determine $\delta\mu$ we need to think about the volume constraint in (3.155),

$$\int_S \mathbf{u} \cdot \boldsymbol{\nu} + \mathbf{r} \cdot \delta\boldsymbol{\nu} + (\mathbf{r} \cdot \boldsymbol{\nu}) \, \mathrm{div}_s \, \mathbf{u} \, dS = 0$$

so

$$\int_S \mathbf{u} \cdot \boldsymbol{\nu} + \mathbf{r} \cdot \boldsymbol{\nu} \, \mathrm{div}_s \, \mathbf{u} - \mathbf{r} \cdot \left[\nabla_s \mathbf{u}^T \boldsymbol{\nu} \right] \, dS = 0$$

Now

$$\mathbf{r} \cdot \boldsymbol{\nu} \, \mathrm{div}_s \, \mathbf{u} - \mathbf{r} \cdot \nabla_s \mathbf{u}^T \boldsymbol{\nu} = \mathrm{div}_s \left(\mathbf{r} \cdot \boldsymbol{\nu} \, \mathbf{u} - \mathbf{u} \cdot \boldsymbol{\nu} \, \mathbf{r} \right) + 2\mathbf{u} \cdot \boldsymbol{\nu},$$

the term $(\mathbf{r} \cdot \boldsymbol{\nu} \, \mathbf{u} - \mathbf{u} \cdot \boldsymbol{\nu} \, \mathbf{r})$ is tangential as $[\mathbf{r} \cdot \boldsymbol{\nu} \, \mathbf{u} - \mathbf{u} \cdot \boldsymbol{\nu} \, \mathbf{r}] \cdot \boldsymbol{\nu} = (\mathbf{r} \cdot \boldsymbol{\nu}) (\mathbf{u} \cdot \boldsymbol{\nu}) - (\mathbf{u} \cdot \boldsymbol{\nu}) (\mathbf{r} \cdot \boldsymbol{\nu}) = 0$, so $\int_S \mathrm{div}_s \left(\mathbf{r} \cdot \boldsymbol{\nu} \, \mathbf{u} - \mathbf{u} \cdot \boldsymbol{\nu} \, \mathbf{r} \right) \, dS = 0$ if $\mathbf{r} \cdot \boldsymbol{\nu} \, \mathbf{u} - \mathbf{u} \cdot \boldsymbol{\nu} \, \mathbf{r}$ is tangential and S is closed. There-

fore, $\int_S 3\mathbf{u}\cdot\boldsymbol{\nu}\,dS = 0$ and with $\mathbf{u} = \psi\boldsymbol{\nu}$, we get

$$\int_S \psi\,dS = 0, \tag{3.157}$$

so overall the volume is not changed.

On the sphere we have $H = -1/R, K = 1/R^2$ and $\mu = -\frac{2\gamma}{R}$ is the radius that is determined by volume constraint where $V_0 = \frac{4}{3}\pi R^3$. We are interested in the stability, so we look to the incremental equations. Using spherical polar coordinates,

$$\psi = \hat{\psi}\Gamma^l_m(\theta,\phi), \tag{3.158}$$

where Γ^l_m is a spherical harmonic, which has the property that it is the eigen function of the surface Laplacian,

$$\Delta_s\Gamma^l_m = -\frac{l(l+1)}{R^2}\Gamma^l_m, \tag{3.159}$$

where l and m are integers and $0 \le m \le l$ that represents different types of perturbations of a sphere. Another property that can be used that integral over the surface is zero,

$$\int_S \Gamma^l_m\,dS = 0. \tag{3.160}$$

In terms of $\hat{\psi}$ the incremental equations become

$$\hat{\psi}\,\Gamma^l_m\left(-\frac{l(l+1)}{R^2}\right) + 2\left(\frac{2}{R^2} - \frac{1}{R^2}\right)\hat{\psi}\Gamma^l_m = \delta\mu, \tag{3.161}$$

by integrating Γ^l_m over the surface, we deduce $\delta\mu = 0$ and so point-wise we have

$$\left[\frac{2 - l(l+1)}{R^2}\right]\hat{\psi}\,\Gamma^l_m = 0. \tag{3.162}$$

In this case, we can have $\hat{\psi} = 0$, where Γ^l_m can not be zero since it depends on θ and ϕ. Or we can have non-trivial solutions only when $l(l+1) = 2$ so $l = 1$, but this is just a translation of original shape and and so the shape is stable. The conclusion is that a soap bubble is a stable surface.

3.5.2 Catenoid

A catenoid is a surface that spans two coaxial rings. The classical configuration has the radii of the two rings equal and the rings separated by some fixed distance. The energy density is again $w = \gamma$, a constant, and so the shape equation with no volume constraint tells us that the catenoid is a minimal surface with $H = 0$. We take coordinates such that

the z-axis is parallel to the axis of the two rings and the rings are located at $z = \pm h$ and the axisymmetric surface is described in cylindrical polar coordinates by $r(z)$.

To find solutions we use the expression for the mean curvature of an axisymmetric surface from Chapter 2, that is

$$2H = \frac{r''}{(1+r'^2)^{3/2}} - \frac{1}{r\,(1+r'^2)^{1/2}}. \tag{3.163}$$

To help the analysis we scale r with the radius of the rings r_0 and the coordinate z with the distance h, so $r(z) = r_0 R(\zeta)$ where $\zeta = z/h$. We also introduce the ratio $\xi = h/r_0$ which measures the aspect ratio of the system. In these coordinates we have

$$2H = \frac{\xi}{r_0}\left[\frac{R''}{(\xi^2+R'^2)^{3/2}} - \frac{1}{R\,(\xi^2+R'^2)^{1/2}}\right] \tag{3.164}$$

and so the equation for the shape of the minimal surface (the catenoid) is, from $H = 0$,

$$R'' = \frac{1}{R}\left(\xi^2 + R'^2\right) \tag{3.165}$$

with the boundary conditions that $R = 1$ at $\zeta = \pm 1$. It is straightforward to solve this equation and the solution is

$$R = \frac{\xi}{a}\cosh\left(a\zeta\right) \tag{3.166}$$

where, from the boundary conditions, a satisfies the nonlinear equation

$$\frac{\xi}{a}\cosh a = 1. \tag{3.167}$$

This equation has two solutions provided ξ is not too large and no solutions beyond a critical value of $\xi = \xi_c \approx 0.6627...$

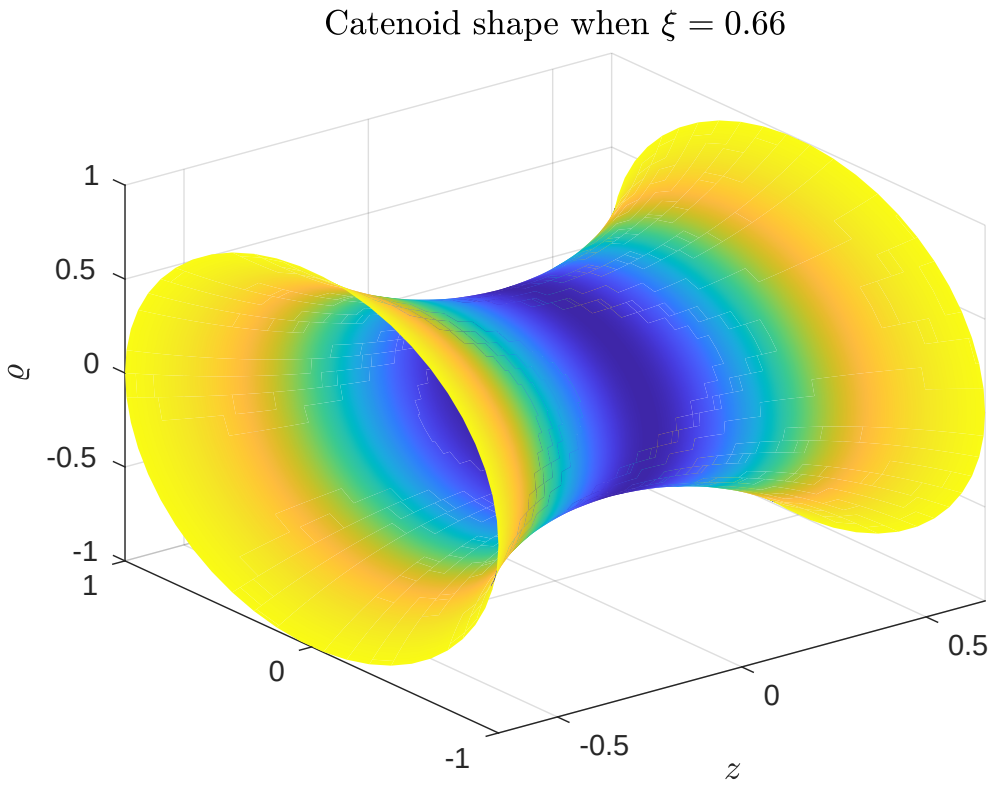


Figure 3.1: Catenoid shape near the critical aspect ratio $\xi = 0.66$

This means a minimal surface does not exist if the rings are too far apart, and also provided the rings are not too far apart there are two solutions for each ξ. We call these solutions the 'wide' and 'narrow' catenoid shapes as in one case the minimum radius ξ/a is near 1 (the wide catenoid) and in the other case the minimum radius ξ/a is nearer 0 (the narrow catenoid). This establishes that there are two equilibrium solutions, but it does not establish the stability of the shapes, which in general requires us to examine the second variation of the energy. We will consider the incremental equations and their connection with the second variation to study the stability.

The incremental equation $\delta H = 0$ gives, using normal increments,

$$\nabla_s \psi + 2\left(2H^2 - K\right)\psi = 0 \tag{3.168}$$

and since the equilibrium solutions are always $H = 0$ this reduces to

$$\nabla_s \psi - 2K\psi = L\left[\psi\right] = 0. \tag{3.169}$$

The spectrum of the linear operator L tells us about the stability of the shape. If L has

all eigenvalues positive then the shape is stable but if at least one eigenvalue is negative then the shape is unstable. Since the boundaries are fixed we have that $\psi = 0$ at the boundaries as our incremental boundary conditions.

Second variation and the incremental equations

To motivate the use of the incremental equations we consider a one-dimensional problem, which is to minimise the following

$$J[y] = \int_0^1 w(x, y, y')\, dx \tag{3.170}$$

We note that the first variation

$$J_1[y](\eta) = \frac{\partial}{\partial s} J[y + s\eta]\big|_{s=0} = \int_0^1 \left[\frac{\partial w}{\partial y} - \frac{d}{dx}\left(\frac{\partial w}{\partial y'}\right)\right] \eta\, dx + \left[\eta \frac{\partial w}{\partial y'}\right]_0^1. \tag{3.171}$$

Define

$$L[y] = \frac{\partial w}{\partial y} - \frac{d}{dx}\left(\frac{\partial w}{\partial y'}\right). \tag{3.172}$$

The second variation is related to

$$J_2[y](\eta, \delta) = \frac{\partial}{\partial t} J_1[y + t\delta](\eta)\big|_{t=0}. \tag{3.173}$$

The second variation is in fact $J_2[y](\eta, \eta)$. But J_2 can be written

$$J_2[y](\eta, \delta) = \int_0^1 etalim_{t\to 0}\left(\frac{L[y + t\delta] - L[y]}{t}\right) dx + \left[\eta \frac{\partial^2 w}{\partial y \partial y'}\delta + \eta \frac{\partial^2 w}{\partial y'^2}\delta'\right]_0^1. \tag{3.174}$$

We call the linear operator on δ given by

$$I[y, \delta] = \lim_{t\to 0}\left(\frac{L[y + t\delta] - L[y]}{t}\right) \tag{3.175}$$

the incremental equation. If y is specified at the boundaries $x = 0$ and $x = 1$ then $\eta = \delta = 0$ at the boundaries, if not then the natural boundary conditions for (3.172) are $\partial w/\partial y' = 0$ and the incremental boundary conditions are

$$\frac{\partial^2 w}{\partial y \partial y'}\delta + \frac{\partial^2 w}{\partial y'^2}\delta' = 0 \tag{3.176}$$

at $x = 0$ and $x = 1$.

If we have a solution, say Y, to (3.172) that satisfies either the natural or the essential boundary conditions as appropriate then if we can find a solution to the eigenvalue

problem, with incremental boundary conditions,

$$I[Y, \delta] = \lambda\delta \tag{3.177}$$

say δ^* with corresponding $\lambda^* < 0$, then Y is not a minimiser of J, since

$$J_2[Y](\delta^*, \delta^*) = \int_0^1 \delta^* I[Y, \delta^*]\, dx = \lambda^* \int_0^1 (\delta^*)^2\, dx < 0. \tag{3.178}$$

In this way the eigenvalue problem constructed from the incremental equations can give us some information about the stability of solutions to the Euler-Lagrange equations (3.172).

This idea can be extended to higher-order problems in more dimensions and with variable domain (the surface) [13], [41], [77].

Eigenvalue problems

We are interested in finding the eigenvalues of a problem of the form

$$\mathcal{L}[q] = \lambda q, \tag{3.179}$$

where q is a general variable and $\mathcal{L}$ is a linear operator and some homogeneous boundary conditions at $z = a$ and $z = b$. This means that $\alpha_a q(a) + \beta_a q'(a) = 0$ and $\alpha_b q(b) + \beta_b q'(b) = 0$ for some constants α_a, α_b, β_a and β_b. For example

$$\mathcal{L}[q] = -q'' \tag{3.180}$$

for $z \in (-1, 1)$ and $q(-1) = 0$ and $q(1) = 0$. In this case the problem can be solved analytically, but in general not. How do we approximate the eigenvalues? There are two approaches we can take, one is called the *shooting method* or the *compound matrix method*, another is to discretise the problem and convert it into a problem to find the eigenvalues of a banded diagonal matrix. We will focus on the discretisation method here. Take $z_k = -1 + hk$ where $h = 2/N$ and $k = 0, 1, \ldots, N$ and approximate the ODE at the point z_k by using finite difference approximations of the derivative. For example, for the second derivative

$$q''(z_k) \approx \frac{q_{k+1} + q_{k-1} - 2q_k}{h^2} \tag{3.181}$$

for $k = 1, \ldots, N - 1$. The example problem above then becomes

$$q_0 = q_N = 0, \qquad -\frac{q_{k+1} + q_{k-1} - 2q_k}{h^2} = \lambda q_k \tag{3.182}$$

which can be written as the following matrix problem, let $\mathbf{q} = (q_1, \ldots, q_{N-1})$ and $\mathbf{M}$ be an $(N-1) \times (N-1)$ matrix,

$$\mathbf{M} = \frac{1}{h^2} \begin{pmatrix} 2 & -1 & 0 & \ldots & 0 & 0 \\ -1 & 2 & 1 & \ldots & 0 & 0 \\ 0 & -1 & 2 & \ldots & 0 & 0 \\ \vdots & \vdots & \vdots & \ddots & \vdots & \vdots \\ 0 & \ldots & \ldots & \ldots & 2 & -1 \\ 0 & \ldots & \ldots & \ldots & -1 & 2 \end{pmatrix}. \tag{3.183}$$

Then the eigenvalue problem is reduced to one of finding the eigenvalues of the matrix $\mathbf{M}$,

$$\mathbf{Mq} = \lambda \mathbf{q}. \tag{3.184}$$

There are ways to estimate the largest and the smallest eigenvalues. The Matlab command `eig` gives approximations.

Derivative boundary conditions

If we replace the boundary conditions in the above example with $q'(-1) = 0$ and $q'(1) = 0$ then we have to deal with a derivative boundary condition. We do this by introducing a *fictitious node*. This is a point outside the domain $[-1, 1]$ that we use to express the derivative boundary condition. The fictitious nodes give rise to values q_{-1} and q_{N+1}. An approximation to the derivative, using centred finite differences, is

$$q'(z_k) \approx \frac{q_{k+1} - q_{k-1}}{2h}. \tag{3.185}$$

Using the centred difference approximation we have $q'(\pm 1) = 0$ leading to

$$q_1 - q_{-1} = 0, \qquad q_{N+1} - q_{N-1} = 0 \tag{3.186}$$

so $q_{-1} = q_1$ and $q_{N+1} = q_{N-1}$. These values of the fictitious nodes can now be used in the differential equation at $z = \pm 1$, so

$$-\frac{q_{-1} + q_1 - 2q_0}{h^2} = \lambda q_0, \qquad -\frac{q_{N-1} + q_{N+1} - 2q_N}{h^2} = \lambda q_N \tag{3.187}$$

leading to

$$-\frac{2q_1 - 2q_0}{h^2} = \lambda q_0, \qquad -\frac{2q_{N-1} - 2q_N}{h^2} = \lambda q_N. \tag{3.188}$$

For this problem we let $\mathbf{q} = (q_0, q_1, \ldots, q_N)$ and $\mathbf{M}$ is an $(N+1) \times (N+1)$ matrix

$$\mathbf{M} = \frac{1}{h^2} \begin{pmatrix} 2 & -2 & 0 & \ldots & 0 & 0 \\ -1 & 2 & 1 & \ldots & 0 & 0 \\ 0 & -1 & 2 & \ldots & 0 & 0 \\ \vdots & \vdots & \vdots & \ddots & \vdots & \vdots \\ 0 & \ldots & \ldots & \ldots & 2 & -1 \\ 0 & \ldots & \ldots & \ldots & -2 & 2 \end{pmatrix} \tag{3.189}$$

and we find the eigenvalues $\mathbf{Mq} = \lambda \mathbf{q}$.

Other useful central differences expressions

Often the eigenvalue problem is related to a Sturm-Liouville problem

$$\mathcal{L}[q] = \frac{1}{w(z)} \left[\frac{d}{dz} \left(p(z) \frac{dq}{dz} \right) + r(z) q(z) \right] \tag{3.190}$$

with p and r given functions. This linear operator is self-adjoint and so the eigenvalues are real and eigenfunctions are orthogonal with respect to the inner product defined by

$$\langle f, g \rangle = \int_a^b \overline{f(z)} g(z) w(z)\, dz \tag{3.191}$$

where $\bar{\cdot}$ denotes complex conjugation. We see in this expression that there is the derivative

$$\frac{1}{w(z)} \frac{d}{dz} \left(p(z) \frac{dq}{dz} \right) \tag{3.192}$$

and a centred difference approximation to this is obtained by recognising that, providing p has sufficient smoothness, the derivative can be written

$$\frac{1}{2w(z)} \left((pq)'' + pq'' - p''q \right) \tag{3.193}$$

and the standard centred difference formula used on each term.

We studied this example to introduce the reader to using the incremental equations to study the stability of a simple problem. Even though the energy is as simple as can be the example highlights that when studying the stability we need an equilibrium solution and also, in general to solve a eigenvalue problem. To show stability of different modes of catenoid, we calculate incremental equations derived from the equilibrium equation. Then we calculate the numerical spectrum of the linear operator $L[\psi] = \lambda \psi$ and decide on stability based on eigenvalues λ.

Given $r(z)$ (or $R(\zeta)$) the surface Laplacian is

$$\begin{aligned}\Delta_s\phi &= \frac{1}{r\left(1+r'^2\right)^{\frac{1}{2}}}\frac{\partial}{\partial z}\left[\frac{r}{\left(1+r'^2\right)^{\frac{1}{2}}}\frac{\partial\phi}{\partial z}\right]+\frac{1}{r^2}\frac{\partial^2\phi}{\partial\theta^2}\\ &= \frac{1}{r_0^2}\left[\frac{1}{R^2}\frac{\partial^2\phi}{\partial\theta^2}+\frac{1}{R\left(\xi^2+R'^2\right)^{\frac{1}{2}}}\frac{\partial}{\partial\zeta}\left(\frac{R}{\left(\xi^2+R'^2\right)^{\frac{1}{2}}}\frac{\partial\phi}{\partial\zeta}\right)\right].\end{aligned}$$

So the incremental equation is

$$\frac{1}{r_0^2}\left[\frac{1}{R^2}\frac{\partial^2\psi}{\partial\theta^2}+\frac{1}{R\left(\xi^2+R'^2\right)^{\frac{1}{2}}}\frac{\partial}{\partial\zeta}\left(R\left(\xi^2+R'^2\right)^{-\frac{1}{2}}\frac{\partial\psi}{\partial\zeta}\right)\right]+\frac{h^2}{r_0^4}\frac{R''}{R\left(\xi^2+R'^2\right)^2}\psi=0. \quad (3.194)$$

Scale K with r_0^{-2} and H with r_0^{-1} then

$$2\hat{H}=\xi\left[\frac{R''}{\left(\xi^2+R'^2\right)^{\frac{3}{2}}}-\frac{1}{R\left(\xi^2+R'^2\right)^{\frac{1}{2}}}\right],\quad \hat{K}=-\xi^2\frac{R''}{R\left(\xi^2+R'^2\right)^2} \quad (3.195)$$

and discretise to calculate the stability. Let $\psi=\hat{\psi}(\zeta)\,e^{in\theta}$, where n gives different perturbations, then

$$\frac{1}{R^2}\frac{\partial^2\psi}{\partial\theta^2}=-\frac{1}{R^2}\hat{\psi}\,n^2\,e^{in\theta}. \quad (3.196)$$

On minimal surface, $R''=\frac{\left(\xi^2+R'^2\right)}{R}$ so

$$K=-\xi^2\frac{1}{R^2\left(\xi^2+R'^2\right)}$$

with aid of incremental equation in (3.194), discretise

$$\frac{1}{2R\left(\xi^2+R'^2\right)^{\frac{1}{2}}}\left[\frac{R}{\left(\xi^2+R'^2\right)^{\frac{1}{2}}}\hat{\psi}'\right]'+\left[\frac{\xi^2}{R^2\left(\xi^2+R'^2\right)}-\frac{n^2}{2R^2}\right]\hat{\psi}=\lambda\hat{\psi}. \quad (3.197)$$

Recall that R is given in (3.166) then $R'=\xi\sinh(a\xi)$ and so $\left(\xi^2+R'^2\right)^{1/2}=\xi\cosh(a\xi)$. So using these informations, (3.197) becomes

$$\frac{1}{2\left(\xi^2/a\right)\cosh^2\xi a}\frac{1}{a}\hat{\psi}''+\left[\frac{\xi^2}{\left(\xi^2/a^2\right)\cosh^2\xi a}\cdot\frac{1}{\xi^2\cosh^2\xi a}-\frac{n^2}{2\left(\xi^2/a^2\right)\cosh^2\xi a}\right]=\lambda\hat{\psi},$$

that can be simplified to be

$$\frac{1}{2\cosh^2\xi a}\left[\hat{\psi}''+\frac{2}{\cosh^2\xi a}\hat{\psi}-n^2\hat{\psi}\right]\frac{a^2}{\xi^2}=\lambda\hat{\psi}. \quad (3.198)$$

Now we have our new eigenvalue problem (3.198) (that depends on the aspect ratio) with

two boundary conditions $\hat{\psi} = 0$ at $\zeta = \pm 1$. To solve such problem we need to estimate the minimum eigenvalue numerically. One way to do this is to discretise the problem by solving an equivalent matrix equation.

Let $\hat{\psi}_i$ be the approximation to $\hat{\psi}(\zeta_i)$ where $\zeta_i = -1 + \Delta(i-1), i = 1, \ldots, N+1$ and $\Delta = 2/N$. When $i = 0, \zeta$ corresponds to $\zeta = -1$ and for $i = N+1$, $\zeta_{N+1} = 1$. For $\hat{\psi}''$ at $\zeta = \zeta_i$

$$\hat{\psi}'' = \frac{\hat{\psi}_{i+1} + \hat{\psi}_{i-1} - 2\hat{\psi}_i}{\Delta^2}. \tag{3.199}$$

Thus, we approximate the eigenvalue problem in (3.198),

$$\frac{1}{2\cosh^2 \xi_i a}\left[\frac{\hat{\psi}_{i+1} + \hat{\psi}_{i-1} - 2\hat{\psi}_i}{\Delta^2} + \frac{2}{\cosh^2 \xi_i a}\hat{\psi}_i - n^2\hat{\psi}_i\right]\frac{a^2}{\xi^2} = \lambda\hat{\psi}_i, \tag{3.200}$$

with $\hat{\psi}_1 = 0$ and $\hat{\psi}_{N+1} = 0$ as boundary conditions.

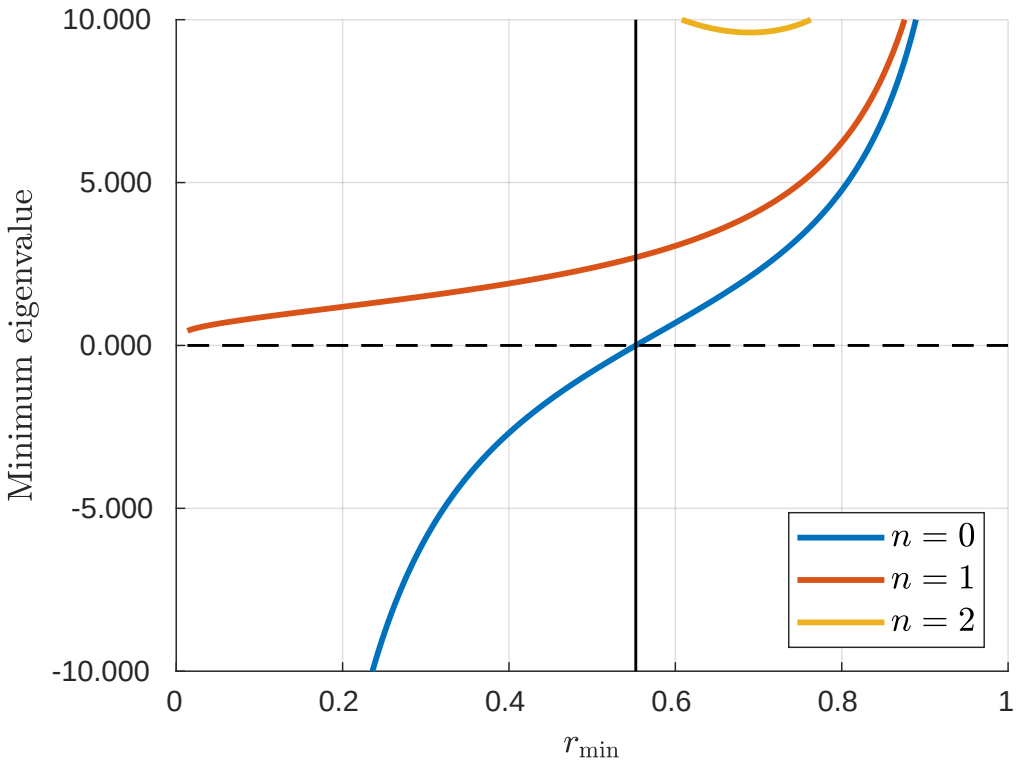


Figure 3.2: Stability curves for different modes number n, the black line refers to the minimum radius r_{min} corresponding to the critical aspect ratio (beyond which there is no solution to the equilibrium equations). For $r_{min} < r^c_{min}$ (to the left of the line) the catenoid is narrow, for $r_{min} > r^c_{min}$ (to the right of the line) the catenoid is wide.

Figure 3.2 tells us that for $n = 1, 2$ the minimum eigenvalue is always positive (there are no zeros) so there is no change in the stability for those modes (stable). For the axisymmetric perturbation (the blue line) there is a change in the stability where the thin (narrow) catenoid (to the left of r^c_{min}) is unstable and the thick (wide) catenoid (to the right of r^c_{min}) is stable.

We should note that, with the numerical approach we are only approximating the eigenvalues of interest and we need to understand how good the approximation is. In order to this, we produce the following figure that contains the eigenvalue curves for different values of N, n against the r_{min}. The values of N used are $10, 20, 50, 100, 200$. Figure 3.3 shows that how curves change (and converge) with increasing N. We can see the curves change in the zoomed in figure that the error is decreasing like $1/N^2$ since in the list of N we gave there is a doubling of N from one value to another and the error (measured from the final curve to any other) decreases by factor $1/4$ for each doubling of N.

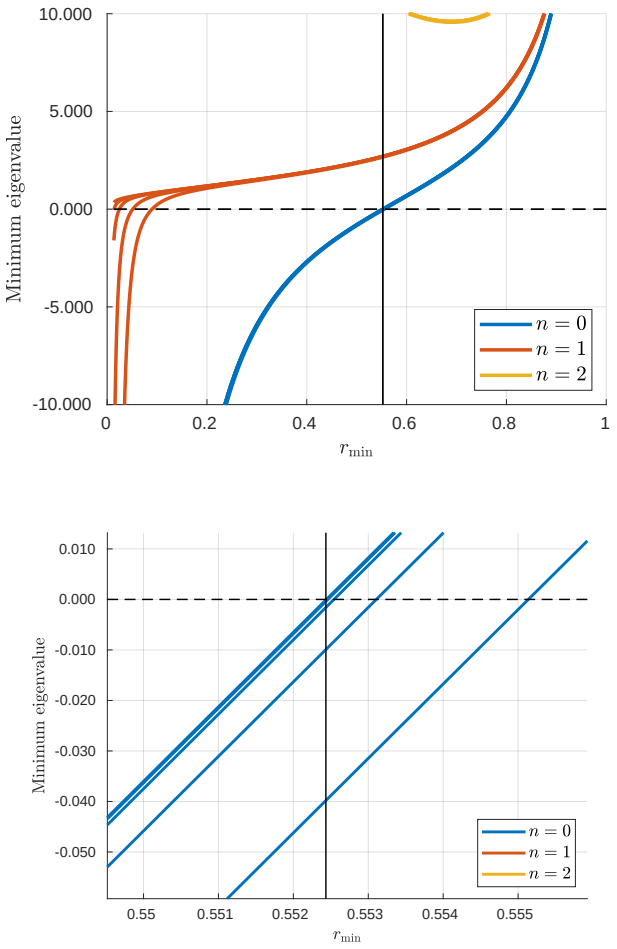


Figure 3.3: The eigenvalue curves for different values of N, n against the r_{min}.

3.5.3 Canham-Helfrich energy

The next level of complexity is to consider $\hat{w}(H,K)$. One example is the Canham-Helfrich energy

$$\hat{w} = \gamma + \frac{1}{2}k_1\left(2H + c_0\right)^2 + \bar{k}K. \tag{3.201}$$

We need to find the corresponding equilibrium equation and incremental equations for this example, (in particular, the stability of Calham-Helfrich problem when $\bar{k} = 0$ and $c_0 = 0$). Indeed we consider this example because in Chapter 4, as we shall see, there is a term of the form $H^2 - \beta K$ that appears in the surface energy when considering a thin film of liquid crystal so we study it here to gain some insight into the stability of surfaces with this type of energy. For this calculation we need

$$\frac{\partial \hat{w}}{\partial H} = 2k_1\left(2H - c_0\right), \qquad \frac{\partial \hat{w}}{\partial K} = \bar{k},$$
$$\frac{\partial^2 \hat{w}}{\partial H^2} = 4k_1, \qquad \frac{\partial^2 \hat{w}}{\partial K^2} = 0, \qquad \frac{\partial^2 \hat{w}}{\partial H \partial K} = 0.$$

From the general form given in (3.150), we obtain the equilibrium equation (no volume constraint as we consider the same geometry as the catenoid example),

$$\frac{1}{2}\Delta_s\left[2k_1\left(2H + c_0\right)\right] - 2H\left(\frac{1}{2}k_1\left(2H - c_0\right)^2 + \bar{k}K\right) + \left(2H^2 - K\right)2k_1\left(2H - c_0\right)$$
$$+2H\bar{k}K - \frac{H\gamma}{k_1} = 0,$$

which can be simplified to be

$$\Delta_s H + \left(2H + c_0\right)\left(H^2 - K - \frac{H\,c_0}{2}\right) - \frac{H\gamma}{k_1} = 0. \tag{3.202}$$

In order to find the incremental equation of the given $\hat{w}$ where $\delta\hat{w} = \delta H\frac{\partial \hat{w}}{\partial H} + \delta K\frac{\partial \hat{w}}{\partial K}$, first we need to obtain $\delta\left(\Delta_s H\right)$.

In general, for any scalar field ϕ defined on the surface S, we have

$$\delta\left[\Delta_s\phi\right] = \delta\big(\mathrm{div}_s\left(\nabla_s\phi\right)\big). \tag{3.203}$$

Applying (2.75) and (2.77) two of our results that already worked with in order to calculate equation (3.203) gives

$$\delta\left(\Delta_s\phi\right) = \mathrm{div}_s\big(\delta\left(\nabla_s\phi\right)\big) + \psi\mathbf{L}\cdot\left(\nabla_s\nabla_s\phi\right)$$
$$= \mathrm{div}_s\big(\nabla_s\left(\delta\phi\right) + \nabla_s\psi\cdot\nabla_s\phi\,\boldsymbol{\nu} + \psi\mathbf{L}\nabla_s\phi\big) + \psi\mathbf{L}\cdot\left(\nabla_s\nabla_s\phi\right)$$

$$= \Delta_s\left(\delta\phi\right) - 2H\left(\nabla_s\psi\cdot\nabla_s\phi\right) + \nabla_s\psi\cdot\left(\mathbf{L}\nabla_s\phi\right) + \psi\mathbf{L}\cdot\nabla_s\nabla_s\phi + \psi\left(\mathrm{div}_s\,\mathbf{L}\right)\cdot\nabla_s\phi + \psi\,\mathbf{L}\cdot\nabla_s\nabla_s\phi,$$

and by substituting $\operatorname{div}_s \mathbf{L} = 2\big(\nabla_s H + (2H^2 - K)\,\boldsymbol{\nu}\big)$ in the above equation, we get

$$\delta\left(\Delta_s \phi\right) = \Delta_s\left(\delta\phi\right) + 2\nabla_s H \cdot \nabla_s \phi\,\psi - 2H\left(\nabla_s \psi \cdot \nabla_s \phi\right) + \nabla_s \psi \cdot \left(\mathbf{L}\nabla_s \phi\right) + 2\psi\,\mathbf{L} : \nabla_s \nabla_s \phi. \tag{3.204}$$

If $\phi = H$, then

$$\delta\left(\Delta_s H\right) = \Delta_s\left(\delta H\right) + 2\nabla_s H \cdot \nabla_s H\,\psi - 2H\left(\nabla_s \psi \cdot \nabla_s H\right) + \nabla_s \psi \cdot \left(\mathbf{L}\,\nabla_s H\right) + 2\psi\,\mathbf{L} \cdot \nabla_s \nabla_s H. \tag{3.205}$$

Now, we need to deal with the second part of (3.202) to find $\delta\left[(2H - c_0)\left(H^2 - K + \frac{1}{2}Hc_0\right)\right]$. Suppose that $\hat{f}\left(H, K\right) = (2H - c_0)\left(H^2 - K + \frac{1}{2}Hc_0\right)$, then we have $\delta\hat{f} = \delta H\left(\partial\hat{f}/\partial H\right) + \delta K\left(\partial\hat{f}/\partial K\right)$. Recall that (given in section §3.4.4) $\delta H = \frac{1}{2}\Delta_s\psi + (2H^2 - K)\,\psi$ and $\delta K = (2H\mathbf{P} - \mathbf{L}) \cdot (\mathbf{L}\nabla_s\psi \otimes \boldsymbol{\nu} + \nabla_s\nabla_s\psi + \mathbf{L}^2\psi)$ then we obtain

$$\begin{aligned}\delta\left[(2H - c_0)\left(H^2 - K + \frac{1}{2}Hc_0\right)\right] &= \frac{1}{2}\left[\Delta_s\psi + 2\left(2H^2 - K\right)\psi\right]\left(6H^2 - \frac{1}{2}c_0^2 - 2K\right) \\ &\quad - (2H - c_0)\left[2HK\psi + (2HP - \mathbf{L}) \cdot \nabla_s\nabla_s\psi\right].\end{aligned} \tag{3.206}$$

Hence our incremental shape equation is given by

$$\begin{aligned}&\Delta_s\left(\delta H\right) + 2\nabla_s H \cdot \nabla_s H\,\psi - 2H\left(\nabla_s\psi \cdot \nabla_s H\right) + \nabla_s\psi \cdot \left(\mathbf{L}\,\nabla_s H\right) \\ &\qquad + 2\psi\,\mathbf{L} \cdot \nabla_s\nabla_s H + \frac{1}{2}\left[\Delta_s\psi + 2\left(2H^2 - K\right)\psi\right]\left(6H^2 - \frac{1}{2}c_0^2 - 2K\right) \\ &\qquad - (2H - c_0)\left[2HK\psi + (2HP - \mathbf{L}) \cdot \nabla_s\nabla_s\psi\right] = 0.\end{aligned} \tag{3.207}$$

Incremental Boundary conditions

For fixed boundaries, the normal increment $\psi = 0$ on the boundaries. The natural boundary condition which is sufficient for solving the incremental shape equation in (3.207) is $\frac{1}{2}\frac{\partial\hat{w}}{\partial H} + (\mathbf{l} \cdot \mathbf{L}\mathbf{l})\,\frac{\partial\hat{w}}{\partial K} = 0$. In case of $\hat{w} = \frac{1}{2}k_1\left(2H - c_0\right)^2 + \bar{k}K$, the natural boundary condition becomes

$$k_1\left(2H - c_0\right) + \bar{k}\left(\mathbf{l} \cdot \mathbf{L}\mathbf{l}\right) = 0, \tag{3.208}$$

where $\mathbf{l}$ is in the tangent direction to the boundary curve and there is no increment of $\mathbf{l}$ so $\delta\mathbf{l} = 0$ since the boundary is fixed. To get the incremental boundary condition, we have

$$\begin{aligned}\delta\big(k_1\left(2H - c_0\right) + \bar{k}\left(\mathbf{l} \cdot \mathbf{L}\mathbf{l}\right)\big) &= 2k_1\delta H + \bar{k}\delta\left(\mathbf{l} \cdot \mathbf{L}\mathbf{l}\right) \\ &= 2k_1\delta H + \bar{k}\left[\delta\mathbf{l} \cdot \left(\mathbf{L}\mathbf{l}\right) + \mathbf{l} \cdot \delta\left(\mathbf{L}\mathbf{l}\right)\right] \\ &= 2k_1\delta H + \bar{k}\left[\mathbf{l} \cdot \left(\delta\mathbf{L}\,\mathbf{l} + \mathbf{L}\delta\,\mathbf{l}\right)\right] = 2k_1\delta H + \bar{k}\left[\mathbf{l} \cdot \left(\delta\mathbf{L}\,\mathbf{l}\right)\right] \\ &= 2k_1\delta H + \bar{k}\left[\mathbf{l} \cdot \left(\mathbf{L}\,\nabla_s\psi \otimes \boldsymbol{\nu} + \nabla_s\left(\nabla_s\psi\right) - \mathbf{L}\left(\boldsymbol{\nu} \otimes \nabla_s\psi - \mathbf{L}\psi\right)\,\mathbf{l}\right)\right].\end{aligned}$$

Then our incremental boundary condition is

$$2k_1\delta H + \bar{k}\,\mathbf{l}\cdot\left(\nabla_s\nabla_s\psi + \mathbf{L}^2\psi\right)\mathbf{l} = 0, \tag{3.209}$$

and with $\delta H = \frac{1}{2}\left(\Delta_s\psi + 2\left(2H^2 - K\right)\psi\right)$, equation (3.209) can be written as,

$$k_1\left(\Delta_s\psi + 2\left(2H^2 - K\right)\psi\right) + \bar{k}\,\mathbf{l}\cdot\left(\nabla_s\nabla_s\psi + \mathbf{L}^2\psi\right)\mathbf{l} = 0. \tag{3.210}$$

If we take $c_0 = 0$ and $\bar{k} = 0$, then our energy function becomes

$$w = \gamma + 2k_1H^2, \tag{3.211}$$

and the equilibrium equation simplifies to

$$\Delta_s H + 2H\left(H^2 - K\right) - \frac{\gamma\, H}{k_1} = 0. \tag{3.212}$$

Note that, the quantity $H^2 - K$ is just the squared asphericity. By scaling $r_1/r_0 = \rho$, $r = r_0\, R$, $z = h\,\zeta$ and $\xi = h/r_0$ then

$$\tilde{\Delta}_s\tilde{H} + 2\tilde{H}\left(\tilde{H}^2 - \tilde{K}\right) - \frac{\gamma\, r_0^2}{k_1}\tilde{H} = 0. \tag{3.213}$$

We scale $\Delta_s = \frac{1}{r_0^2}\tilde{\Delta}_s$, $H = \frac{1}{r_0}\tilde{H}$ and $K = \frac{1}{r_0^2}\tilde{K}$. Let $\Gamma = \left(\gamma\, r_0^2\right)/k_1$ be the dimensionless surface tension, so the dimensionless equilibrium equation becomes (we have dropped $\tilde{}$ variables)

$$\Delta_s H + 2H\left(H^2 - K\right) - \Gamma\, H = 0. \tag{3.214}$$

The boundary conditions are

$$R = 1 \text{ at } \zeta = 1, \quad R = \rho = r_1/r_0 \quad \text{at } \zeta = -1. \tag{3.215}$$

Also, we have

$$\frac{1}{2}w_H + \mathbf{l}\cdot\mathbf{L}\,\mathbf{l}\,w_K = 0. \tag{3.216}$$

At the boundary $H = 0$, therefore $H = 0$ is a solution of equilibrium equation and the boundary conditions, where $H = 0$ is $\xi\left[R''/\left(\xi^2 + R'^2\right)^{\frac{3}{2}} - 1/R\left(\xi^2 + R'^2\right)^{\frac{1}{2}}\right] = 0$. If $\rho = 1$ then $R = (\xi/a)\cosh(a\,\xi)$ and applying $R(1) = 1$, we have the aspect ratio $\xi = a/\cosh a$ that is independent of $\Gamma = \left(\gamma\, r_0^2\right)/k_1$. Thus we show that for the equilibrium equation $\Delta_s H + 2H\left(H^2 - K\right) - \Gamma\, H = 0$, $H = 0$ is a solution for all Γ.

Note that $H = 0$ so some terms in the incremental equation (3.207) are zeros (terms

involving $H, \nabla_s H)$. So we find that the incremental equation can be written

$$\Delta_s \Psi - 2K\Psi - \Gamma\Psi = 0, \tag{3.217}$$

where $\Psi = \delta H = \frac{1}{2}(\Delta_s \psi - 2K\psi)$, $\psi = 0$ at $\zeta = \pm 1$ (as the boundary is fixed). Remember that $H = 0$ at $\zeta = \pm 1$. Therefore the incremental boundary conditions are $\Psi = 0$ at $\zeta = \pm 1$, $\delta H = 0$ at $\zeta = \pm 1$. We can write the incremental equation as

$$(\Delta_s - 2K - \Gamma)\Psi = 0, \tag{3.218}$$

and $\Psi = \frac{1}{2}(\Delta_s \psi - 2K\psi)$ with the incremental boundary condition $\psi = 0$ and $\Psi = 0$ at $\zeta = \pm 1$.

The stability of solutions of the energy $w = \gamma + 2k_1 H^2$

Consider the energy given in (3.201), we take $c_0 = 0$ and $\bar{k} = 0$ then the energy becomes

$$w = \gamma + 2k_1 H^2. \tag{3.219}$$

To study the stability of minimisers of the energy given in (3.219) we study the linear operator derived from the incremental equations. The incremental equations are

$$\Delta_s \Psi - 2K\Psi - \Gamma\Psi = 0, \qquad \Psi = \frac{1}{2}(\Delta_s \psi - 2K\psi) \tag{3.220}$$

with incremental boundary conditions $\psi = 0$ and $\Psi = 0$. We use the incremental equations to identify the following eigenvalue problem

$$\Delta_s \Psi - 2K\Psi - \Gamma\Psi = L_1[\Psi] = \lambda\psi, \qquad \Psi = \frac{1}{2}(\Delta_s \psi - 2K\psi) = L_2[\psi] \tag{3.221}$$

with $\psi = 0$ and $\Psi = 0$ at $\zeta = \pm 1$ as boundary conditions. We need to discretise the eigenvalue problem given in (3.221). We can use the information from our study of the soap film catenoid problem. Given an eigenfunction of L_2 with eigenvalue λ then we also have an eigenfunction of $L_1 L_2$ with eigenvalue $\lambda(\lambda + \Gamma)$. We have stability if all the eigenvalues are positive and instability when at least one of the eigenvalues is negative.

The following figures show the minimum eigenvalue of the energy for different Γ. Note that for Large Γ that corresponds to the surface tension case, so when we rescale the eigenvalue with Γ the result is quite close to the soap film problem as you see in Figure 3.5 (as $\Gamma \to \infty$ the result is the soap film). For large Γ, the term H^2 is negligible comparing to the constant term. The H^2 contribution to the energy appears to maintain the narrow catenoid, as the minimum eigenvalue returns to being positive for small r_{min}. If Γ is large

we may expect to have a big film or very strong surface tension. Strong surface tension means that $\gamma \gg r_0^2/k_1$. A big film means that the radius $r_0 \gg \sqrt{k_1/\gamma}$ which is like an elastocapillary length.

The point made is that the stability returns to stable for the narrow catenoid in the regime of Γ large. The narrow catenoid is stabilised when $r_{min} \approx \sqrt{k_1/\gamma}$. When you're in the narrow case. When the neck is thin, making the catenoid narrower will reduce the surface area but increase the bending energy by a greater amount and this leads to a stabilisation of the film.

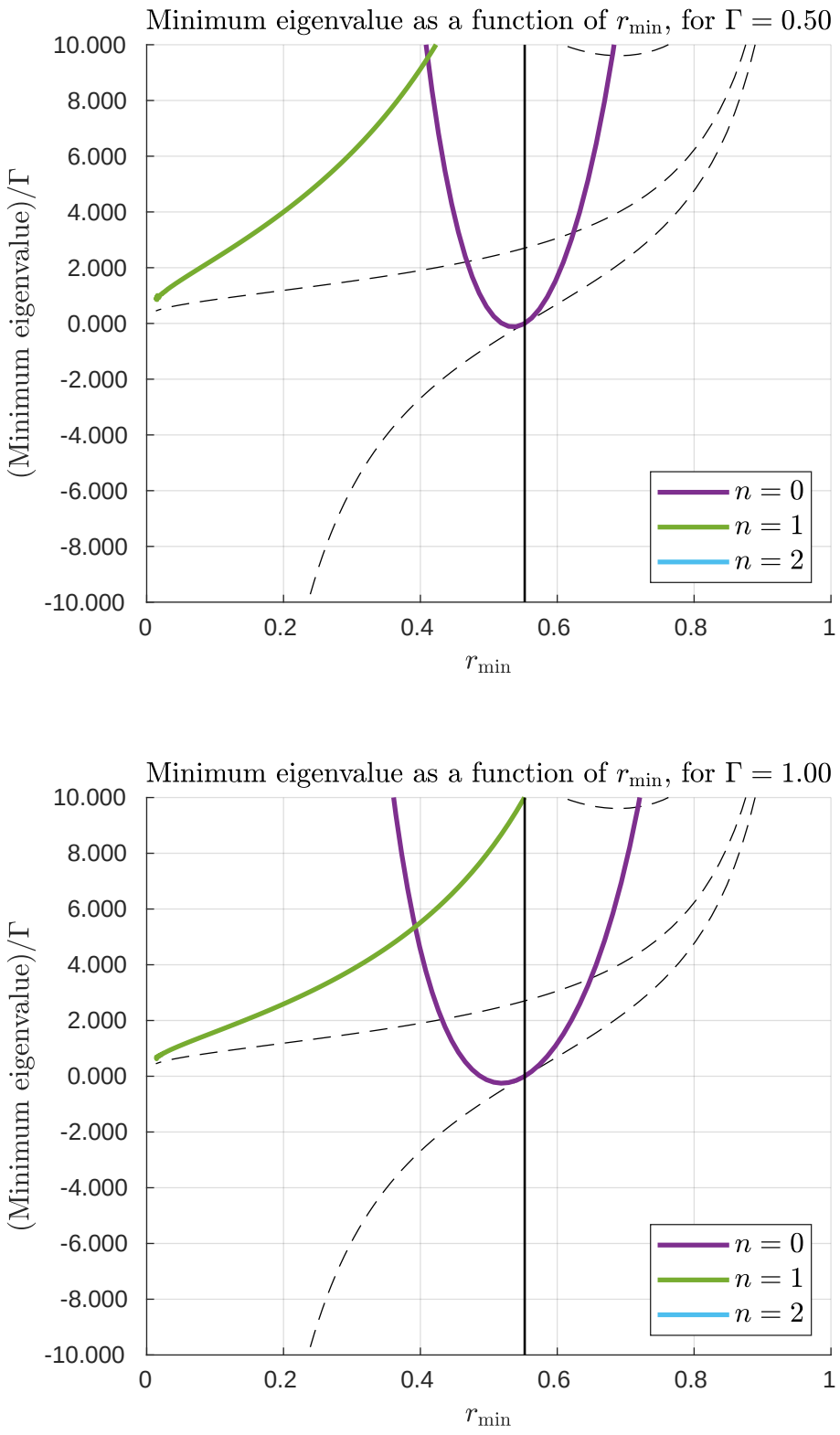


Figure 3.4: The minimum eigenvalue of the energy for small values of Γ. The black vertical line refers to r^c_{min} and the dashed curves refers to the normal soap curve with a corresponding n. The $\mathbf{n} = 2$ case was computed but lies outside the axes (it is off the scale).

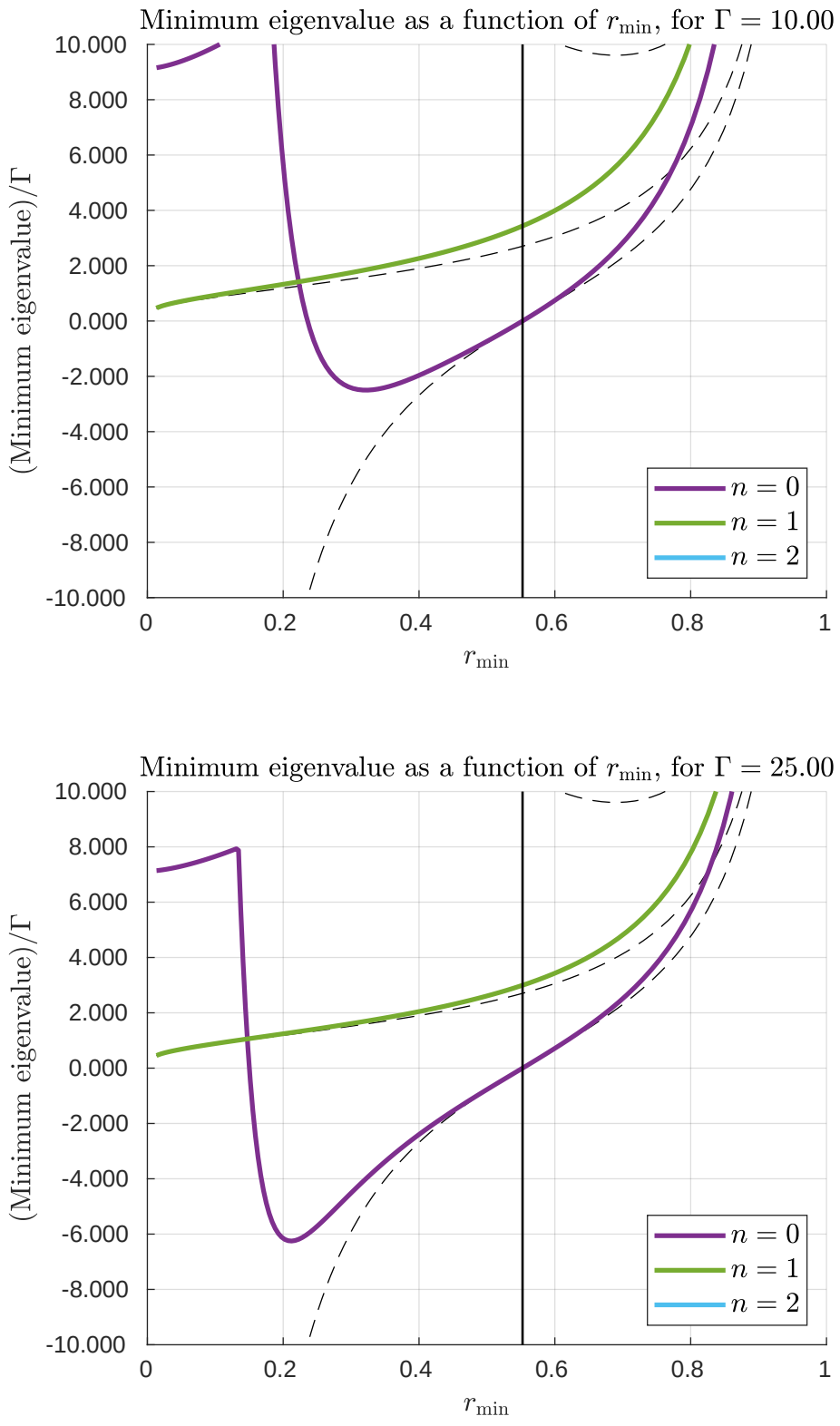


Figure 3.5: The minimum eigenvalue of the energy for large values of Γ. The black vertical line refers to r^c_{min} and the dashed curves refers to the normal soap curve with a corresponding n

3.6 Concluding remarks

We have developed a framework for studying the equilibrium of open fluid membranes endowed with a microstructure. We extended the results of [66] in the context of open surfaces which allow us to identify the equilibrium equations and related natural boundary conditions associated with minimising a general surface energy. We also discussed a range of essential boundary conditions.

We have shown that the tangential component of the shape is always satisfied whenever the other equilibrium equations are satisfied. As a result of this we considered only the normal increments to the normal component of the shape equation when considering the incremental problem.

We have derived the incremental equations for some straightforward cases, however the methods and lemmas and results we introduced can be applied to more complicated cases. We have covered the example of $w\left(q, \nabla_s q\right)$, where we have considered this case when the function w has a very simple form and have shown the stability of the shape and of q decouple. This example is not sufficient to show a coupling between the stability of the shape and the order parameters. Finally we have demonstrated the incremental equations for Canham-Helfrich-like energy and used this to determine stability of the solutions.

All results developed in this chapter will be used in the next chapter where numerical work is needed.

Chapter 4

Shape and stability of a nematic film suspended between two coaxial rings

4.1 Introduction

Our aim is to understand the interaction of geometry, material properties and temperature on the equilibrium configuration and stability of a film of liquid crystal suspended between two coaxial circular rings.

In order to perform calculations of the equilibrium configurations and the stability we need to parameterise the tensor $\mathbf{M}$. We do so by writing $\mathbf{M}$ in terms of an orthonormal basis of the tangent plane of the surface and two scalar order parameters. Then we derive the equilibrium equations for the two scalar order parameters, that involve the geometry of the surface. In our case, we derive the free energy density when two parameterisations of the tensor $\mathbf{M}$ are used, one using q_0 and q_m, the other using q and $\mathbf{n}$.

Our main results in this chapter are the derivation of the equilibrium equations and their numerical solutions for different dimensionless parameters, illustrating the effect of geometry and material parameters on the surface shape and nematic order. As a step towards studying the stability of such solutions we consider a simpler problem in which the geometry of the film is a fixed catenoid and study the effects of the intrinsic geometry on the isotropic-nematic transition. If our film was a simple soap solution then the minimum energy configuration of the film spanning two coaxial rings of equal radius is the classical catenoid. We solve the incremental equations numerically to find the most unstable mode at onset and perform a weakly nonlinear analysis to derive the amplitude in terms of a dimensionless parameter that measures distance from the transition temperature. We discuss the defects (melting points) that arise and prove that they have charge $-1/2$, arranged at different locations on the surface for different aspect ratios. We investigate the nonlinear solutions using a numerical method based on Jacobi relaxation.

4.2 Free energy functional

In this section we derive the expressions for the free energy in terms of a particular parameterisation of $\mathbf{Q}$. This has been done before in [54] and we present it here for completeness. This involves using the Landau-de Gennes potential (LdG) theory and parameterising the second order variance tensor $\mathbf{M}$ in terms of a particular parameterisation (see [54]). This is a one-constant approximation for simplicity but we could deal with a more general energy. The surface free energy consists of the elastic energy and the Landau-de Gennes potential, which can be formulated in terms of the scalar invariants and the surface gradient of the variance tensor $\mathbf{M}$. To the liquid crystal energy (the elastic and Landau-de Gennes terms) we also add a surface tension, a constant energy per unit area of the surface. A tensor theory for nematic liquid crystals, following the use of [68], gives, using a one-constant approximation for simplicity

$$W = \int_S \left(\gamma + \frac{1}{2}k\left|\nabla_s \mathbf{M}\right|^2 + w_{LdG}\right) dS, \tag{4.1}$$

where $w_{LdG} = \frac{a}{2}\operatorname{tr}(\mathbf{Q}^2) + \frac{c}{4}\operatorname{tr}(\mathbf{Q}^2)^2$, where $\mathbf{Q}$ is the traceless part of $\mathbf{M}$ and a depends on temperature and k and c are positive material constants.

4.2.1 Parameterisations of M using q_0 and q_m

We derive the appropriate surface in terms of q_0 and q_m and their gradients. The surface free energy also depends on the geometry of the surface coupled with the parameters q_0 and q_m and gradients of them. This gives us an energy density of the form $w\left(q_0, q_m, \nabla_s q_0, \nabla_s q_m, \boldsymbol{\nu}, \mathbf{L}\right)$.

Recall that the traceless part of the surface second-order variance tensor $\mathbf{M}$ is $\mathbf{Q}$, related by

$$\mathbf{M} = \mathbf{Q} + \frac{1}{2}\mathbf{P} \tag{4.2}$$

where $\mathbf{P} = \mathbf{I} - \boldsymbol{\nu} \otimes \boldsymbol{\nu}$ with $\boldsymbol{\nu}$ the outer unit normal to S. The tensor $\mathbf{M}$ represents the second moments of the statistical distribution of molecular unit vectors $\boldsymbol{l}$ on the surface S. Assuming that all the nematic molecules at a point on S are bound to lie on the local tangent plane, but are otherwise unconstrained, we have

$$\boldsymbol{l} \cdot \boldsymbol{\nu} = 0 \tag{4.3}$$

and so $\mathbf{M}\boldsymbol{\nu} = \mathbf{0}$ and since $\mathbf{P}\boldsymbol{\nu} = \mathbf{0}$ we have

$$\mathbf{Q}\boldsymbol{\nu} = \mathbf{0}. \tag{4.4}$$

The tensor $\mathbf{Q}$ is a symmetric, traceless second-rank tensor when $\mathbf{Q} = \mathbf{0}$ the distribution is isotropic *on the surface*. We want to parameterise $\mathbf{Q}$ using two scalar parameters q_0 and q_m. By introducing the orthonormal basis $(\mathbf{e}_1, \mathbf{e}_2)$ on S such that $\mathbf{e}_1 \times \mathbf{e}_2 = \boldsymbol{\nu}$ and $\mathbf{e}_1 \cdot \mathbf{e}_2 = 0$, the tensor $\mathbf{Q}$ can be represented as (following [54])

$$\mathbf{Q} = q_0 \left(\mathbf{e}_1 \otimes \mathbf{e}_1 - \mathbf{e}_2 \otimes \mathbf{e}_2\right) + q_m \left(\mathbf{e}_1 \otimes \mathbf{e}_2 + \mathbf{e}_2 \otimes \mathbf{e}_1\right). \tag{4.5}$$

The orthonormal basis for the tangent plane to the surface $\mathbf{e}_1$ and $\mathbf{e}_2$ vary as we move around the surface. At this point $\mathbf{e}_1$ and $\mathbf{e}_2$ are not chosen but then we will choose them to be principal directions of curvature. The parameters q_0 and q_m are two scalar order parameters and the tensor $\mathbf{Q}$ gives us information about how the molecules are ordered. In particular $q_0 = q_m = 0$ gives $\mathbf{Q} = \mathbf{0}$ and this corresponds to $\mathbf{M} = \frac{1}{2}\mathbf{P}$ which is the *isotropic* distribution in which there is no preferred orientation of the molecules on the surface. The eigenvalues of $\mathbf{Q}$ are

$$\lambda = \pm\sqrt{q_0^2 + q_m^2}. \tag{4.6}$$

We want to write the surface energy density $\frac{1}{2}k\left|\nabla_s \mathbf{M}\right|^2$ in terms of q_0, q_m, its derivatives, and H, K and other geometric quantities involving the geodesic curvature of lines of principal curvature on the surface. With $\mathbf{M} = \mathbf{Q} + \frac{1}{2}\mathbf{P}$, we calculate $|\nabla_s \mathbf{M}|^2 = M_{ij:k} M_{ij:k}$ (repeated indices indicate summation while the notation : denotes differentiation on the surface S) and we get

$$\left|\nabla_s \mathbf{M}\right|^2 = \left|\nabla_s \mathbf{Q}\right|^2 + \frac{1}{4}\left|\nabla_s \mathbf{P}\right|^2 + \nabla_s \mathbf{Q} \cdot \nabla_s \mathbf{P}. \tag{4.7}$$

We now calculate each of these terms in turn. The components of $\nabla_s \mathbf{P}$ are $\left(\nabla_s \mathbf{P}\right)_{ijk} = P_{ij:k}$ and the components of $\mathbf{P}$ are $P_{ij} = \delta_{ij} - \nu_i \nu_j$, so

$$\left(\nabla_s P\right)_{ijk} = P_{ij:k} = 0 - \nu_{i:k}\nu_j - \nu_i \nu_{j:k}, \tag{4.8}$$

and since $\mathbf{L} = -\nabla_s \boldsymbol{\nu}$, we write $\nabla_s \mathbf{P}$ in components as

$$\left(\nabla_s P\right)_{ijk} = L_{ik}\nu_j + \nu_i L_{jk}, \tag{4.9}$$

then, we can write

$$\begin{aligned}\left|\nabla_s \mathbf{P}\right|^2 &= \nabla_s \mathbf{P} \cdot \nabla_s \mathbf{P} = \left(\nabla_s P\right)_{ijk}\left(\nabla_s P\right)_{ijk} \\ &= \left(L_{ik}\nu_j + L_{jk}\nu_i\right)\left(L_{ik}\nu_j + L_{jk}\nu_i\right) = L_{ik}L_{ik} + L_{jk}L_{jk}\end{aligned}$$

so that

$$|\nabla_s \mathbf{P}|^2 = 2\,|\nabla_s \boldsymbol{\nu}|^2 = 2|\mathbf{L}|^2. \tag{4.10}$$

We can write (4.10) using the invariants of $\mathbf{L}$ (the mean and the Gauss curvature). One way to see this is to write $|\mathbf{L}|^2$ using the two principal curvatures c_1 and c_2 as follow,

$$\begin{aligned}\frac{1}{4}\,|\nabla_s \mathbf{P}|^2 = \frac{1}{2}\,|\mathbf{L}|^2 = \frac{1}{2}\left(c_1^2 + c_2^2\right) &= \frac{1}{2}\big((c_1+c_2)^2 - 2c_1c_2\big)\\ &= \frac{1}{2}\left(4\left[\frac{1}{2}\,(c_1+c_2)\right]^2 - 2\,(c_1c_2)\right),\end{aligned}$$

that is equivalent to,

$$\frac{1}{4}\,|\nabla_s \mathbf{P}|^2 = 2H^2 - K, \tag{4.11}$$

since $H = \frac{1}{2}\,(c_1 + c_2)$ and $K = c_1c_2$ (The mean and Gauss curvature, respectively). This means that even if the distribution is isotropic $\mathbf{Q} = \mathbf{0}$ there is still a bending energy contribution from the fact that the molecules are forced to align in the tangent plane on a curved surface, with no normal component. The term is similar to the Calman-Helfrich energy discussed in Chapter 3. For other terms in (4.7) we need $\nabla_s \mathbf{Q}$. We calculate $(\nabla_s \mathbf{Q}) \cdot (\nabla_s \mathbf{P})$. Since $\mathbf{Q}$ is symmetric, the components of $\nabla_s \mathbf{Q}$ satisfy

$$Q_{ij;k} = Q_{ji;k}, \tag{4.12}$$

also from (4.4), we have $Q_{ij}\nu_j = 0$ and $Q_{ij}\nu_i = 0$, then

$$Q_{ij;k}\nu_j + Q_{ij}\nu_{j;k} = 0, \quad Q_{ij;k}\nu_i + Q_{ij}\nu_{i;k} = 0, \tag{4.13}$$

by using (4.9) one can write

$$\begin{aligned}(\nabla_s Q)_{ijk}\,(\nabla_s P)_{ijk} = Q_{ij;k}P_{ij;k} &= Q_{ij;k}\,(L_{ik}\nu_j + L_{jk}\nu_i)\\ &= L_{ik}Q_{ij;k}\nu j + L_{jk}Q_{ij;k}\nu_i\\ &= 2L_{ik}Q_{ij;k}\nu_j \quad (\text{using } Q_{ij} = Q_{ji})\\ &= -2L_{ik}Q_{ij}\nu_{j;k} \quad (\text{using } (Q_{ij}\nu_j)_{;k} = 0).\end{aligned}$$

Therefore

$$(\nabla_s \mathbf{Q}) \cdot (\nabla_s \mathbf{P}) = 2\mathbf{Q} \cdot \mathbf{L}^2. \tag{4.14}$$

We can write (4.14) using the parameterisation of $\mathbf{Q}$ in terms of q_0 and q_1 and by taking $\mathbf{e}_1$ and $\mathbf{e}_2$ to be the principal directions of curvature. Consider $\mathbf{L}$ in terms of the principal curvatures and directions, $\mathbf{L} = c_1\,\mathbf{e}_1 \otimes \mathbf{e}_1 + c_2\,\mathbf{e}_2 \otimes \mathbf{e}_2$ where c_1 and c_2 are principal curvatures

and $\mathbf{e}_1$, $\mathbf{e}_2$ are the principal directions. Then $\mathbf{L}^2 = c_1^2\,\mathbf{e}_1 \otimes \mathbf{e}_1 + c_2^2\,\mathbf{e}_2 \otimes \mathbf{e}_2$ and so

$$\mathbf{Q}\cdot\mathbf{L}^2 = q_0\,c_1^2 - q_0\,c_2^2 = q_0\left(c_1^2 - c_2^2\right) = 4q_0\,\frac{1}{2}\left(c_1 - c_2\right)\cdot\frac{1}{2}\left(c_1 + c_2\right).$$

Which can be written as

$$\mathbf{Q}\cdot\mathbf{L}^2 = 4q_0 H\varsigma. \tag{4.15}$$

The quantity ς is the *asphericity* and measures the difference in the two principal curvatures where $\varsigma = (c_1 - c_2)/2$ (see §2.3.1).

Now we consider the final term in (4.7), square of surface gradient of $\mathbf{Q}$, $|\nabla_s\mathbf{Q}|^2$. To calculate $|\nabla_s\mathbf{Q}|^2$ we make use of the following lemma and corollary

Lemma 4.2.1. *If we have tensors* $\mathbf{S} = \lambda\,\mathbf{a}\otimes\mathbf{b}$ *and* $\mathbf{T} = \mu\,\mathbf{c}\otimes\mathbf{d}$*, with* $\mathbf{a},\mathbf{b},\mathbf{c},\mathbf{d}$ *all unit vectors then*

$$\begin{aligned}\nabla_s\mathbf{S}\cdot\nabla_s\mathbf{T} &= (\nabla_s\lambda)\cdot(\nabla_s\mu)\,(\mathbf{a}\cdot\mathbf{c})\,(\mathbf{b}\cdot\mathbf{d}) + \mu\,(\mathbf{b}\cdot\mathbf{d})\left[(\nabla_s\mathbf{c})^T\,\mathbf{a}\right]\cdot\nabla_s\lambda\\ &+ \mu\,(\mathbf{a}\cdot\mathbf{c})\left[(\nabla_s\mathbf{d})^T\,\mathbf{b}\right]\cdot\nabla_s\lambda + \lambda\,(\mathbf{b}\cdot\mathbf{d})\left[(\nabla_s\mathbf{a})^T\,\mathbf{c}\right]\cdot\nabla_s\mu + \lambda\mu\,(\mathbf{b}\cdot\mathbf{d})\,(\nabla_s\mathbf{a})\cdot(\nabla_s\mathbf{c})\\ &+ \lambda\mu\left[(\nabla_s\mathbf{a})^T\,\mathbf{c}\right]\cdot\left[(\nabla_s\mathbf{d})^T\,\mathbf{b}\right] + \lambda\,(\mathbf{a}\cdot\mathbf{c})\left[(\nabla_s\mathbf{b})^T\,\mathbf{d}\right]\cdot\nabla_s\mu + \lambda\mu\left[(\nabla_s\mathbf{c})^T\,\mathbf{a}\right]\cdot\left[(\nabla_s\mathbf{b})^T\,\mathbf{d}\right]\\ &+ \lambda\mu\,(\mathbf{a}\cdot\mathbf{c})\,(\nabla_s\mathbf{b})\cdot(\nabla_s\mathbf{d}).\end{aligned}$$

Proof. We write

$$\begin{aligned}\nabla_s\mathbf{S}\cdot\nabla_s\mathbf{T} &= \nabla_s\left(\lambda\,\mathbf{a}\otimes\mathbf{b}\right)\cdot\nabla_s\left(\mu\,\mathbf{c}\otimes\mathbf{d}\right) = \left(\lambda\,a_ib_j\right)_{;k}\left(\mu\,c_id_j\right)_{;k}\\ &= \left(\lambda_{;k}a_ib_j + \lambda a_{i;k}b_j + \lambda a_ib_{j;k}\right)\left(\mu_{;k}c_id_j + \mu c_{i;k}d_j + \mu c_id_{j;k}\right)\\ &= (\nabla_s\lambda)\cdot(\nabla_s\mu)\,(\mathbf{a}\cdot\mathbf{c})\,(\mathbf{b}\cdot\mathbf{d}) + \mu\,(\mathbf{b}\cdot\mathbf{d})\left[(\nabla_s\mathbf{c})^T\,\mathbf{a}\right]\cdot\nabla_s\lambda + \mu\,(\mathbf{a}\cdot\mathbf{c})\left[(\nabla_s\mathbf{d})^T\,\mathbf{b}\right]\cdot\nabla_s\lambda\\ &+ \lambda\,(\mathbf{b}\cdot\mathbf{d})\left[(\nabla_s\mathbf{a})^T\,\mathbf{c}\right]\cdot\nabla_s\mu + \lambda\mu\,(\mathbf{b}\cdot\mathbf{d})\,(\nabla_s\mathbf{a})\cdot(\nabla_s\mathbf{c}) + \lambda\mu\left[(\nabla_s\mathbf{a})^T\,\mathbf{c}\right]\cdot\left[(\nabla_s\mathbf{d})^T\,\mathbf{b}\right]\\ &+ \lambda\,(\mathbf{a}\cdot\mathbf{c})\left[(\nabla_s\mathbf{b})^T\,\mathbf{d}\right]\cdot\nabla_s\mu + \lambda\mu\left[(\nabla_s\mathbf{c})^T\,\mathbf{a}\right]\cdot\left[(\nabla_s\mathbf{b})^T\,\mathbf{d}\right] + \lambda\mu\,(\mathbf{a}\cdot\mathbf{c})\,(\nabla_s\mathbf{b})\cdot(\nabla_s\mathbf{d}).\end{aligned}$$

□

Corollary 4.2.1. *If we have a tensor* $\mathbf{S} = \lambda\,\mathbf{a}\otimes\mathbf{b}$*, with* $\mathbf{a},\mathbf{b}$ *are unit vectors and* $|\mathbf{a}|,|\mathbf{b}| = 1$ *then, we write*

$$|\nabla_s\mathbf{S}|^2 = |\nabla_s\lambda|^2 + \lambda^2\,|\nabla_s\mathbf{a}|^2 + \lambda^2\,|\nabla_s\mathbf{b}|^2. \tag{4.16}$$

In case if $\mathbf{a} = \mathbf{b}$*, then*

$$|\nabla_s\mathbf{S}|^2 = |\nabla_s\lambda|^2 + 2\lambda^2\,|\nabla_s\mathbf{a}|^2. \tag{4.17}$$

Proof. Write $|\nabla_s\mathbf{S}|^2 = S_{ij;k}S_{ij;k}$, then

$$S_{ij;k}S_{ij;k} = \left(\lambda\,a_i\,b_j\right)_{;k}\left(\lambda\,a_i\,b_j\right)_{;k}$$

$$= (\lambda_{;k}\, a_i\, b_j + \lambda\, a_{i;k}\, b_j + \lambda\, a_i\, b_{j;k}) \cdot (\lambda_{;k}\, a_i\, b_j + \lambda\, a_{i;k}\, b_j + \lambda\, a_i\, b_{j;k})$$

$$= |\nabla_s \lambda|^2 + \lambda^2 |\nabla_s \mathbf{a}|^2 + \lambda^2 |\nabla_s \mathbf{b}|^2 + \frac{1}{2}\nabla_s\left(\lambda^2\right) \cdot \nabla_s\left(|\mathbf{a}|^2\right) + \frac{1}{2}\nabla_s\left(\lambda^2\right) \cdot \nabla_s\left(|\mathbf{b}|^2\right) + \frac{1}{2}\lambda^2 \nabla_s\left(|\mathbf{a}|^2\right) \cdot \nabla_s\left(|\mathbf{b}|^2\right)$$

with $|\mathbf{a}| = 1$ and $|\mathbf{b}| = 1$, we obtain

$$|\nabla_s \mathbf{S}|^2 = |\nabla_s \lambda|^2 + \lambda^2 |\nabla_s \mathbf{a}|^2 + \lambda^2 |\nabla_s \mathbf{b}|^2 .$$

Now for $\mathbf{a} = \mathbf{b}$, we have

$$|\nabla_s \mathbf{S}|^2 = S_{ij;k} S_{ij;k} = (\lambda\, a_i\, a_j)_{;k} (\lambda\, a_i\, a_j)_{;k}$$

$$= (\lambda_{;k}\, a_i\, a_j + \lambda\, a_{i;k}\, a_j + \lambda\, a_i\, a_{j;k}) \cdot (\lambda_{;k}\, a_i\, a_j + \lambda\, a_{i;k}\, a_j + \lambda\, a_i\, a_{j;k})$$

$$= |\nabla_s \lambda|^2 + 2\lambda^2 |\nabla_s \mathbf{a}|^2 + \nabla_s\left(\lambda^2\right) \cdot \nabla_s\left(|\mathbf{a}|^2\right) + \frac{1}{2}\lambda^2 \nabla_s\left(|\mathbf{a}|^2\right) \cdot \nabla_s\left(|\mathbf{a}|^2\right)$$

again, with $|\mathbf{a}| = 1$, $|\nabla_s \mathbf{S}|^2 = |\nabla_s \lambda|^2 + 2\lambda^2 |\nabla_s \mathbf{a}|^2$. □

As discussed above, to compute $|\nabla_s \mathbf{Q}|^2$ we use (4.5) and choose $\mathbf{e}_1$ and $\mathbf{e}_2$ along the lines of principal curvatures of S, we also make use of Lemma 4.2.1 and Corollary 4.2.1. For this calculation we need to calculate the surface gradients of these principal directions $\mathbf{e}_1$ and $\mathbf{e}_2$. The details are given in [68] and are reproduced here for completeness

$$\nabla_s \mathbf{e}_1 = k_1\, \mathbf{e}_2 \otimes \mathbf{e}_1 - c_1\, \boldsymbol{\nu} \otimes \mathbf{e}_1 + k_1\, \mathbf{e}_2 \otimes \mathbf{e}_2, \tag{4.18}$$

$$\nabla_s \mathbf{e}_2 = -k_1\, \mathbf{e}_1 \otimes \mathbf{e}_1 - c_2\, \boldsymbol{\nu} \otimes \mathbf{e}_2 - k_2\, \mathbf{e}_1 \otimes \mathbf{e}_2, \tag{4.19}$$

where k_1, k_2 are the geodesic curvatures of the lines of principal curvatures while c_1, c_2 are the principal curvature of S. Since $\mathbf{e}_1$ and $\mathbf{e}_2$ are orthogonal unit vectors, then we have

$$(\nabla_s \mathbf{e}_1)^T\, \mathbf{e}_2 = -\,(\nabla_s \mathbf{e}_2)^T\, \mathbf{e}_1, \tag{4.20}$$

and we deduce that

$$\begin{aligned}
|\nabla_s \mathbf{Q}|^2 &= \left|\nabla_s\big(q_0\,(\mathbf{e}_1 \otimes \mathbf{e}_1 - \mathbf{e}_2 \otimes \mathbf{e}_2) + q_m\,(\mathbf{e}_1 \otimes \mathbf{e}_2 + \mathbf{e}_2 \otimes \mathbf{e}_1)\big)\right|^2 \\
&= |\nabla_s\,(q_0\, \mathbf{e}_1 \otimes \mathbf{e}_1)|^2 + |\nabla_s\,(q_0\, \mathbf{e}_2 \otimes \mathbf{e}_2)|^2 + |\nabla_s\,(q_m\, \mathbf{e}_1 \otimes \mathbf{e}_2)|^2 + |\nabla_s\,(q_m\, \mathbf{e}_2 \otimes \mathbf{e}_1)|^2 \\
&\quad - 2\,[\nabla_s q_0\,(\mathbf{e}_1 \otimes \mathbf{e}_1)] \cdot [\nabla_s q_0\,(\mathbf{e}_2 \otimes \mathbf{e}_2)] + 2\,[\nabla_s q_m\,(\mathbf{e}_1 \otimes \mathbf{e}_2)] \cdot [\nabla_s q_m\,(\mathbf{e}_2 \otimes \mathbf{e}_1)] \\
&\quad + 2\,[\nabla_s q_0\,(\mathbf{e}_1 \otimes \mathbf{e}_1)] \cdot [\nabla_s q_m\,(\mathbf{e}_1 \otimes \mathbf{e}_2)] + 2\,[\nabla_s q_0\,(\mathbf{e}_1 \otimes \mathbf{e}_1)] \cdot [\nabla_s q_m\,(\mathbf{e}_2 \otimes \mathbf{e}_1)] \\
&\quad - 2\,[\nabla_s q_0\,(\mathbf{e}_2 \otimes \mathbf{e}_2)] \cdot [\nabla_s q_m\,(\mathbf{e}_1 \otimes \mathbf{e}_2)] - 2\,[\nabla_s q_0\,(\mathbf{e}_2 \otimes \mathbf{e}_2)] \cdot [\nabla_s q_m\,(\mathbf{e}_2 \otimes \mathbf{e}_1)] .
\end{aligned} \tag{4.21}$$

We work to simplify $|\nabla_s \mathbf{Q}|^2$ and reduce the form of (4.21). Applying Lemma 4.2.1 and Corollary 4.2.1 for the first four terms in (4.21) gives

$$|\nabla_s (q_0\, \mathbf{e}_1 \otimes \mathbf{e}_1)|^2 = |\nabla_s q_0|^2 + 2\, q_0^2\, |\nabla_s \mathbf{e}_1|^2 \tag{4.22}$$

$$|\nabla_s (q_0\, \mathbf{e}_2 \otimes \mathbf{e}_2)|^2 = |\nabla_s q_0|^2 + 2\, q_0^2\, |\nabla_s \mathbf{e}_2|^2 \tag{4.23}$$

$$|\nabla_s (q_m\, \mathbf{e}_1 \otimes \mathbf{e}_2)|^2 = |\nabla_s q_m|^2 + q_m^2 \big(|\nabla_s \mathbf{e}_1|^2 + |\nabla_s \mathbf{e}_2|^2\big) \tag{4.24}$$

$$|\nabla_s (q_m\, \mathbf{e}_2 \otimes \mathbf{e}_1)|^2 = |\nabla_s q_m|^2 + q_m^2 \big(|\nabla_s \mathbf{e}_2|^2 + |\nabla_s \mathbf{e}_1|^2\big). \tag{4.25}$$

The remaining terms of (4.21) are simplified as follow: with the aid of (4.20) the fifth and sixth terms are simplified to be

$$-2\, [\nabla_s q_0\, (\mathbf{e}_1 \otimes \mathbf{e}_1)] \cdot [\nabla_s q_0\, (\mathbf{e}_2 \otimes \mathbf{e}_2)] = 2q_0^2 \left[(\nabla_s \mathbf{e}_1)^T\, \mathbf{e}_2\right] \cdot \left[(\nabla_s \mathbf{e}_2)^T\, \mathbf{e}_1\right] = -2q_0^2 \left(k_1^2 + k_2^2\right) \tag{4.26}$$

$$2\, [\nabla_s q_m\, (\mathbf{e}_1 \otimes \mathbf{e}_2)] \cdot [\nabla_s q_m\, (\mathbf{e}_2 \otimes \mathbf{e}_1)] = 2q_m^2 \left[\left|(\nabla_s \mathbf{e}_1)^T\, \mathbf{e}_2\right|^2 + \left|(\nabla_s \mathbf{e}_2)^T\, \mathbf{e}_1\right|^2\right] = 4q_m^2 \left(k_1^2 + k_2^2\right). \tag{4.27}$$

For the last four terms, using (4.20) we evaluate the scalar product and simplify, respectively as

$$\begin{aligned} 2\, [\nabla_s q_0\, (\mathbf{e}_1 \otimes \mathbf{e}_1)] \cdot [\nabla_s q_m\, (\mathbf{e}_1 \otimes \mathbf{e}_2)] &= 2\, q_m \left[(\nabla_s \mathbf{e}_2)^T\, \mathbf{e}_1\right] \cdot \nabla_s q_0 \\ &+ 2\, q_0\, q_m \left[(\nabla_s \mathbf{e}_1)^T\, \mathbf{e}_1\right] \cdot \left[(\nabla_s \mathbf{e}_2)^T\, \mathbf{e}_1\right] + 2\, q_0 \left[(\nabla_s \mathbf{e}_1)^T\, \mathbf{e}_2\right] \cdot \nabla_s q_m \\ &+ 2\, q_0\, q_m \left[(\nabla_s \mathbf{e}_1)^T\, \mathbf{e}_1\right] \cdot \left[(\nabla_s \mathbf{e}_1)^T\, \mathbf{e}_2\right] + 2\, q_0\, q_m\, (\nabla_s \mathbf{e}_1) \cdot (\nabla_s \mathbf{e}_2) \end{aligned} \tag{4.28}$$

$$\begin{aligned} 2\, [\nabla_s q_0\, (\mathbf{e}_1 \otimes \mathbf{e}_1)] \cdot [\nabla_s q_m\, (\mathbf{e}_2 \otimes \mathbf{e}_1)] &= 2\, q_m \left[(\nabla_s \mathbf{e}_2)^T\, \mathbf{e}_1\right] \cdot \nabla_s q_0 \\ &+ 2\, q_0 \left[(\nabla_s \mathbf{e}_1)^T\, \mathbf{e}_2\right] \cdot \nabla_s q_m + 2\, q_0\, q_m\, (\nabla_s \mathbf{e}_1) \cdot (\nabla_s \mathbf{e}_2) \\ &+ 2\, q_0\, q_m \left[(\nabla_s \mathbf{e}_1)^T\, \mathbf{e}_2\right] \cdot \left[(\nabla_s \mathbf{e}_1)^T\, \mathbf{e}_1\right] + 2\, q_0\, q_m \left[(\nabla_s \mathbf{e}_2)^T\, \mathbf{e}_1\right] \cdot \left[(\nabla_s \mathbf{e}_1)^T\, \mathbf{e}_1\right] \end{aligned} \tag{4.29}$$

$$\begin{aligned} -\, 2\, [\nabla_s q_0\, (\mathbf{e}_2 \otimes \mathbf{e}_2)] \cdot [\nabla_s q_m\, (\mathbf{e}_1 \otimes \mathbf{e}_2)] &= -2\, q_m \left[(\nabla_s \mathbf{e}_1)^T\, \mathbf{e}_2\right] \cdot \nabla_s q_0 \\ &- 2\, q_0 \left[(\nabla_s \mathbf{e}_2)^T\, \mathbf{e}_1\right] \cdot \nabla_s q_m - 2\, q_0\, q_m\, (\nabla_s \mathbf{e}_2) \cdot (\nabla_s \mathbf{e}_1) \\ &- 2\, q_0\, q_m \left[(\nabla_s \mathbf{e}_2)^T\, \mathbf{e}_1\right] \cdot \left[(\nabla_s \mathbf{e}_2)^T\, \mathbf{e}_2\right] - 2\, q_0\, q_m \left[(\nabla_s \mathbf{e}_1)^T\, \mathbf{e}_2\right] \cdot \left[(\nabla_s \mathbf{e}_2)^T\, \mathbf{e}_2\right] \end{aligned} \tag{4.30}$$

$$-2\left[\nabla_s q_0\left(\mathbf{e}_2\otimes\mathbf{e}_2\right)\right]\cdot\left[\nabla_s q_m\left(\mathbf{e}_2\otimes\mathbf{e}_1\right)\right]=-2\,q_m\left[\left(\nabla_s\mathbf{e}_1\right)^T\mathbf{e}_2\right]\cdot\nabla_s q_0$$
$$-2\,q_0\,q_m\left[\left(\nabla_s\mathbf{e}_2\right)^T\mathbf{e}_2\right]\cdot\left[\left(\nabla_s\mathbf{e}_1\right)^T\mathbf{e}_2\right]-2\,q_0\left[\left(\nabla_s\mathbf{e}_2\right)^T\mathbf{e}_1\right]\cdot\nabla_s q_m$$
$$-2\,q_0\,q_m\left[\left(\nabla_s\mathbf{e}_2\right)^T\mathbf{e}_2\right]\cdot\left[\left(\nabla_s\mathbf{e}_2\right)^T\mathbf{e}_1\right]-2\,q_0\,q_m\left(\nabla_s\mathbf{e}_2\right)\cdot\left(\nabla_s\mathbf{e}_1\right). \quad (4.31)$$

After simplifying the last four terms of (4.21), we add the relevant equations from (4.28)-(4.31) and so we get a reduced form

$$4q_m\nabla_s q_0\cdot\left[\left(\nabla_s\mathbf{e}_2\right)^T\mathbf{e}_1\right]-4q_0\nabla_s q_m\left[\left(\nabla_s\mathbf{e}_2\right)^T\mathbf{e}_1\right]+4q_m\nabla_s q_0\cdot\left[\left(\nabla_s\mathbf{e}_2\right)^T\mathbf{e}_1\right]$$
$$-4q_0\nabla_s q_m\cdot\left[\left(\nabla_s\mathbf{e}_2\right)^T\mathbf{e}_1\right]=4\left(q_m\nabla_s q_0-q_0\nabla_s q_m\right)\cdot\left(\nabla_s\mathbf{e}_2\right)^T\mathbf{e}_1. \quad (4.32)$$

To have the final form for $|\nabla_s\mathbf{Q}|^2$ we combine (4.22)-(4.27) with, (4.32)

$$|\nabla_s\mathbf{Q}|^2=2\left[|\nabla_s q_0|^2+|\nabla_s q_m|^2+\left(q_0^2+q_m^2\right)\left(4\left(k_1^2+k_2^2\right)+H^2-2K\right)\right]$$
$$+4\left(q_0\nabla_s q_m-q_m\nabla_s q_0\right)\cdot\left(k_1\mathbf{e}_1+k_2\mathbf{e}_2\right), \quad (4.33)$$

gathering equations (4.11), (4.15) and (4.33) show that (4.7) is equivalent to

$$|\nabla_s\mathbf{M}|^2=|\nabla_s\mathbf{Q}|^2+2\mathbf{Q}\cdot\mathbf{L}^2+\frac{1}{2}|\mathbf{L}|^2. \quad (4.34)$$

Now we are able to write the surface energy density in terms of q_0, q_m, its derivatives and H, K and other geometric quantities involving the geodesic curvature of lines of principal curvature on the surface,

$$\frac{1}{2}k\,|\nabla_s\mathbf{M}|^2=k\big[|\nabla_s q_0|^2+|\nabla_s q_m|^2+\left(q_0^2+q_m^2\right)\left(4\,|\boldsymbol{\omega}|^2+2\left(2H^2-K\right)\right)$$
$$+4\left(q_0\nabla_s q_m-q_m\nabla_s q_0\right)\cdot\boldsymbol{\omega}+\frac{1}{2}\left(2H^2-K\right)+4\,q_0H\zeta\big]. \quad (4.35)$$

given that $\boldsymbol{\omega}$ is the vector parameterising the spin connection on the surface where $\boldsymbol{\omega}=k_1\mathbf{e}_1+k_2\mathbf{e}_2$, $|\boldsymbol{\omega}|^2=k_1^2+k_2^2$ and k_i is the geodesic curvatures of the lines of principal curvature [14].

We consider the energy density supplemented by the internal Landau-de Gennes potential given in (2.85) plus a surface tension term that adds an energy cost γ per area,

then the total free energy is given as

$$W = \int_S \gamma + k\big[|\nabla_s q_0|^2 + |\nabla_s q_m|^2 + \left(q_0^2 + q_m^2\right)\left(4\,|\boldsymbol{\omega}|^2 + H^2 - 2K\right) + 4\left(q_0\nabla_s q_m - q_m\nabla_s q_0\right)\cdot\boldsymbol{\omega} + \frac{1}{4}\left(2H^2 - K\right) + 4\,q_0 H\zeta\big] + w_{LdG}\,dS. \quad (4.36)$$

When we parameterise $\mathbf{Q}$ using q_0 and q_m it is straightforward to show that

$$\mathbf{Q}^2 = \left(q_0^2 + q_m^2\right)\left(\mathbf{e}_1 \otimes \mathbf{e}_1 + \mathbf{e}_2 \otimes \mathbf{e}_2\right) = \left(q_0^2 + q_m^2\right)\mathbf{P} \quad (4.37)$$

and so

$$\operatorname{tr}\left(\mathbf{Q}^2\right) = 2\left(q_0^2 + q_m^2\right), \quad (4.38)$$

which can be used in the expression for w_{LdG},

$$w_{LdG} = a\left(q_0^2 + q_m^2\right) + c\left(q_0^2 + q_m^2\right)^2. \quad (4.39)$$

4.2.2 Parameterisations of M using q and n

An alternative and equivalent parameterisation of the variance tensor $\mathbf{M}$ is in terms of a two-dimensional degree of order q and a director $\mathbf{n}$. If $q = 0$ then the distribution is isotropic on the surface, if $q = 1$ then the distribution is perfect alignment along $\mathbf{n}$, if $q = -1$ then the distribution is perfect alignment along the direction $\mathbf{t} = \boldsymbol{\nu} \times \mathbf{n}$ (in other words perpendicular to the direction $\mathbf{n}$). We write the variance tensor $\mathbf{M}$ (all details are in §2.5) as,

$$\mathbf{M} = q\,\mathbf{n} \otimes \mathbf{n} + \frac{1}{2}\left(1 - q\right)\mathbf{P}, \quad (4.40)$$

where $|q| \leq 1$. In this parameterisation we have

$$\mathbf{Q} = q\left(\mathbf{n} \otimes \mathbf{n} - \mathbf{t} \otimes \mathbf{t}\right)/2, \quad (4.41)$$

and with $w_{LdG} = \frac{a}{4}q^2 + \frac{c}{8}q^4$ (see §2.5), the free-energy density is considered to be

$$w = \gamma + \frac{1}{2}k\,|\nabla_s \mathbf{M}|^2 + \frac{a}{4}q^2 + \frac{c}{8}q^4, \quad (4.42)$$

direct computations using Lemmas 4.2.1 and Corollary 4.2.1 give

$$|\nabla_s \mathbf{M}|^2 = \frac{1}{2}\,|\nabla_s q|^2 + 2q^2\,|\nabla_s \mathbf{n}|^2 + \frac{1}{2}\left(1 - q\right)^2|\mathbf{L}|^2 + 2q\left(1 - q\right)|\mathbf{L}\mathbf{n}|^2. \quad (4.43)$$

and the surface energy density (4.42) becomes

$$w = \gamma + \frac{1}{2}k\left[\frac{1}{2}\left|\nabla_s q\right|^2 + 2q^2\left|\nabla_s \mathbf{n}\right|^2 + \frac{1}{2}\left(1-q\right)^2\left|\mathbf{L}\right|^2 + 2q\left(1-q\right)\left|\mathbf{Ln}\right|^2\right] + \frac{a}{4}q^2 + \frac{c}{8}q^4. \quad (4.44)$$

The form (4.44) is useful when deriving the general equilibrium equations. A further useful step in parameterising $\mathbf{M}$ is to introduce the angle α between the direction $\mathbf{n}$ and one of the principal directions, say $\mathbf{e}_1$. Let us introduce

$$\mathbf{n} = \cos\alpha\,\mathbf{e}_1 + \sin\alpha\,\mathbf{e}_2 \quad (4.45)$$

$$\mathbf{t} = \boldsymbol{\nu}\times\mathbf{n} = -\sin\alpha\,\mathbf{e}_1 + \cos\alpha\,\mathbf{e}_2. \quad (4.46)$$

We see that in (4.44) we need $\nabla_s\mathbf{n}$ and so, using the definitions in (4.45)and (4.46), we find

$$\nabla_s\mathbf{n} = \mathbf{t}\otimes\nabla_s\alpha + \cos\alpha\nabla_s\mathbf{e}_1 + \sin\alpha\nabla_s\mathbf{e}_2 \quad (4.47)$$

$$\left|\nabla_s\mathbf{n}\right|^2 = \left|\nabla_s\alpha\right|^2 + \left|\boldsymbol{\omega}\right|^2 + \left|\mathbf{Ln}\right|^2 + 2\boldsymbol{\omega}\cdot\nabla_s\alpha \quad (4.48)$$

$$\nabla_s\mathbf{t} = -\mathbf{n}\otimes\nabla_s\alpha - \mathbf{n}\otimes\boldsymbol{\omega} + \boldsymbol{\nu}\otimes\mathbf{Lt}. \quad (4.49)$$

The energy density in (4.44) becomes

$$w = \gamma + \frac{1}{2}k\left[\frac{1}{2}\left|\nabla_s q\right|^2 + 2q^2\left(\left|\nabla_s\alpha\right|^2 + \left|\boldsymbol{\omega}\right|^2\right) + 4q^2\boldsymbol{\omega}\cdot\nabla_s\alpha + \frac{1}{2}\left(1+q^2\right)\left|\mathbf{L}\right|^2 + q\left(2\left|\mathbf{Ln}\right|^2 - \left|\mathbf{L}\right|^2\right)\right] + \frac{a}{4}q^2 + \frac{c}{8}q^4 \quad (4.50)$$

but we can write that

$$\left|\mathbf{Ln}\right|^2 = \left(\mathbf{Ln}\right)\cdot\left(\mathbf{Ln}\right) = \mathbf{n}\cdot\left(\mathbf{L}^T\mathbf{Ln}\right) = \mathbf{n}\cdot\left(\mathbf{L}^2\mathbf{n}\right) = 2Hc_n - K,$$

(using Cayley-Hamilton) where $c_n = \mathbf{n}\cdot\mathbf{Ln}$ denotes the normal curvature along $\mathbf{n}$ and

$$\left|\mathbf{L}\right|^2 = 4H^2 - 2K \quad (4.51)$$

with $\left|\mathbf{L}\right|^2 = c_1^2 + c_2^2$ and $\left|\mathbf{Ln}\right|^2 = \left[\mathbf{L}\left(\cos\alpha\mathbf{e}_1 + \sin\alpha\mathbf{e}_2\right)\right]^2 = c_1^2\cos^2\alpha + c_2^2\sin^2\alpha$. we get

$$2\left|\mathbf{Ln}\right|^2 - \left|\mathbf{L}\right|^2 = 2H\varsigma\cos 2\alpha. \quad (4.52)$$

This gives the surface energy in (4.50) as

$$w = \gamma + \frac{1}{2}k\left(\frac{1}{2}\left|\nabla_s q\right|^2 + 2q^2\left|\nabla_s \alpha\right|^2 + \frac{1}{2}q^2\left(4\left|\boldsymbol{\omega}\right|^2 + \left|\mathbf{L}\right|^2\right) + 4q^2\boldsymbol{\omega}\cdot\nabla_s\alpha + \frac{1}{2}\left|\mathbf{L}\right|^2 + 4qH\varsigma\cos 2\alpha\right) + \frac{a}{4}q^2 + \frac{c}{8}q^4. \quad (4.53)$$

4.2.3 Connection between the two parameterisations

We can derive the relationship between the two parameterisations. First note that, using both parameterisations yields,

$$\mathbf{Q} = q\left(\mathbf{n}\otimes\mathbf{n} - \frac{1}{2}\mathbf{P}\right) = q_0\left(\mathbf{e}_1\otimes\mathbf{e}_1 - \mathbf{e}_2\otimes\mathbf{e}_2\right) + q_m\left(\mathbf{e}_1\otimes\mathbf{e}_2 + \mathbf{e}_2\otimes\mathbf{e}_1\right), \quad (4.54)$$

and since $\mathbf{P} = \mathbf{n}\otimes\mathbf{n} + \mathbf{t}\otimes\mathbf{t}$ we can use the definitions (4.45) and (4.46) to show that

$$q_0 = \frac{q}{2}\cos 2\alpha, \quad q_m = \frac{q}{2}\sin 2\alpha. \quad (4.55)$$

From (4.55) we obtain

$$\nabla_s q_0 = \frac{1}{2}\cos 2\alpha\nabla_s q - \sin 2\alpha\, q\nabla_s\alpha$$
$$\nabla_s q_m = \frac{1}{2}\sin 2\alpha\nabla_s q + \cos 2\alpha\, q\nabla_s\alpha$$

then, we can deduce that

$$\left|\nabla_s q_0\right|^2 + \left|\nabla_s q_m\right|^2 = \frac{1}{4}\left|\nabla_s q\right|^2 + q^2\left|\nabla_s\alpha\right|^2 \quad (4.56)$$

and also

$$q_0\nabla_s q_m - q_m\nabla_s q_0 = \left(\frac{q}{2}\cos 2\alpha\right)\left(\frac{1}{2}\sin 2\alpha\nabla_s q + 2\cos 2\alpha\, q\nabla_s\alpha\right) - \left(\frac{q}{2}\sin 2\alpha\right)\left(\frac{1}{2}\cos 2\alpha\nabla_s q + 2\sin 2\alpha\, q\nabla_s\alpha\right) = \frac{1}{2}q^2\nabla_s\alpha. \quad (4.57)$$

4.3 General equilibrium equations

Now we have the two parameterisations we can find the equilibrium equations for a general surface. In order to find the equilibrium equations corresponding to minimisers of the energy (4.44) we follow the procedure discussed in Chapter 3 and in [66]. We need the following derivatives of the free energy density. It is easier to derive the general equilibrium equations when using the parameterisation of $\mathbf{Q}$ with $\mathbf{n}$ and q. The relevant derivatives

are

$$\boldsymbol{\Lambda} = \boldsymbol{\Lambda}_s = \frac{\partial w}{\partial \mathbf{L}} = k\left[\frac{1}{2}(1-q)^2\,\mathbf{L} + 2q\,(1-q)\,\mathbf{L}\mathbf{n}\otimes\mathbf{n}\right], \quad \mathbf{G} = \mathbf{G}_s = \frac{\partial w}{\partial \nabla_s \mathbf{n}} = 2kq^2\nabla_s\mathbf{n}, \tag{4.58}$$

$$\mathbf{g} = \mathbf{g}_s = \frac{\partial w}{\partial \mathbf{n}} = 2kq\,(1-q)\,\mathbf{L}^2\mathbf{n}, \quad \mathbf{b} = \mathbf{b}_s = \frac{\partial w}{\partial \nabla_s q} = \frac{1}{2}k\nabla_s q, \tag{4.59}$$

$$a = \frac{\partial w}{\partial q} = \frac{1}{2}k\left[4q\,|\nabla_s\mathbf{n}|^2 - (1-q)\,|\mathbf{L}|^2 + 2\,(1-2q)\,|\mathbf{L}\mathbf{n}|^2 + \frac{a}{2}q + \frac{c}{2}q^3\right], \tag{4.60}$$

and we note for completeness that $\boldsymbol{\beta} = \partial w/\partial \boldsymbol{\nu} = \mathbf{0}$. We need to consider,

$$\begin{aligned}\operatorname{div}_s \boldsymbol{\Lambda} = k\Bigg[&\frac{1}{2}(1-q)^2\operatorname{div}_s\mathbf{L} - (1-q)\,\mathbf{L}\nabla_s q \\ &+ 2\operatorname{div}_s\big[q\,(1-q)\,\mathbf{n}\big]\mathbf{L}\mathbf{n} + 2q\,(1-q)\,[\nabla_s\,(\mathbf{L}\mathbf{n})]\,\mathbf{n}\Bigg]\end{aligned} \tag{4.61}$$

as it is required for the expression of the stress tensor. Recall that, the stress tensor is $\boldsymbol{\sigma} = (\lambda + w)\,\mathbf{P} + \boldsymbol{\sigma}_E$ where λ is a Lagrange multiplier used to control local inextensibility. In our case $\lambda = 0$, then

$$\boldsymbol{\sigma} = \left(\gamma + \frac{k}{2}\,|\nabla_s\mathbf{M}|^2 + \frac{a}{4}q^2 + \frac{c}{8}q^4\right)\mathbf{P} + \boldsymbol{\sigma}_E, \tag{4.62}$$

we substitute (4.58) and (4.61) in the general form of $\boldsymbol{\sigma}_E$ that is given in (3.13),

$$\begin{aligned}\boldsymbol{\sigma}_E = &-\frac{k}{2}(1-q)^2\,\mathbf{L}^2 - 2kq\,(1-q)\,\mathbf{L}^2\mathbf{n}\otimes\mathbf{n} - 2kq^2\,(\nabla_s\mathbf{n})^T\,\nabla_s\mathbf{n} - \frac{k}{2}\nabla_s q\otimes\nabla_s q \\ &- \boldsymbol{\nu}\otimes\mathbf{P}\operatorname{div}_s\boldsymbol{\Lambda} - 2k\left[\operatorname{div}_s\left(q^2\mathbf{L}\mathbf{n}\right) + q^2\mathbf{L}\cdot\nabla_s\mathbf{n}\right]\boldsymbol{\nu}\otimes\mathbf{n}.\end{aligned} \tag{4.63}$$

We have seen that the normal component of the shape equation is the only component we need consider, $0 = \boldsymbol{\nu}\cdot\operatorname{div}_s\boldsymbol{\sigma} = \operatorname{div}_s\left(\boldsymbol{\sigma}^T\boldsymbol{\nu}\right) + \boldsymbol{\sigma}\cdot\mathbf{L}$. To calculate $\operatorname{div}_s\left(\boldsymbol{\sigma}^T\boldsymbol{\nu}\right)$, we find first

$$\begin{aligned}\boldsymbol{\sigma}^T\boldsymbol{\nu} = &-\frac{k}{2}(1-q)^2\,\mathbf{L}^2\boldsymbol{\nu} - 2kq\,(1-q)\left(\mathbf{n}\otimes\mathbf{L}^2\mathbf{n}\right)\boldsymbol{\nu} - 2kq^2\,(\nabla_s\mathbf{n})^T\,(\nabla_s\mathbf{n})\,\boldsymbol{\nu} - \frac{k}{2}\nabla_s q\otimes\nabla_s q\boldsymbol{\nu} \\ &- (\mathbf{P}\operatorname{div}_s\boldsymbol{\Lambda}\otimes\boldsymbol{\nu})\,\boldsymbol{\nu} - 2k\big(\operatorname{div}_s\left(q^2\mathbf{L}\mathbf{n}\right) + q^2\mathbf{L}\cdot\nabla_s\mathbf{n}\big)\,(\mathbf{n}\otimes\boldsymbol{\nu})\,\boldsymbol{\nu},\end{aligned}$$

This is can be simplified since $\mathbf{L}\boldsymbol{\nu} = 0$, so we get

$$\boldsymbol{\sigma}^T\boldsymbol{\nu} = -2kq\,(1-q)\left(\boldsymbol{\nu}\cdot\mathbf{L}^2\mathbf{n}\right)\mathbf{n} - \mathbf{P}\operatorname{div}_s\boldsymbol{\Lambda} - 2k\big(\operatorname{div}_s\left(q^2\mathbf{L}\mathbf{n}\right) + q^2\mathbf{L}\cdot\nabla_s\mathbf{n}\big)\mathbf{n}, \tag{4.64}$$

and then we obtain,

$$\operatorname{div}_s\left(\boldsymbol{\sigma}^T\boldsymbol{\nu}\right) = -\operatorname{div}_s\Big(\mathbf{P}\operatorname{div}_s\boldsymbol{\Lambda} + 2k\big(\operatorname{div}_s\left(q^2\mathbf{L}\mathbf{n}\right) + q^2\mathbf{L}\cdot\nabla_s\mathbf{n}\big)\mathbf{n}\Big). \tag{4.65}$$

Next, we find

$$\begin{aligned}\mathbf{L}\cdot\boldsymbol{\sigma} = \mathbf{L}\cdot\Big(w\mathbf{P} - \frac{k}{2}\left(1-q\right)^2\mathbf{L}^2 - 2kq\left(1-q\right)\mathbf{L}^2\mathbf{n}\otimes\mathbf{n} - 2kq^2\left(\nabla_s\mathbf{n}\right)^T\nabla_s\mathbf{n} - \frac{k}{2}\nabla_s q\otimes\nabla_s q \\ - \boldsymbol{\nu}\otimes\mathbf{P}\operatorname{div}_s\boldsymbol{\Lambda} - 2k\big[\operatorname{div}_s\left(q^2\mathbf{L}\mathbf{n}\right) + q^2\mathbf{L}\cdot\nabla_s\mathbf{n}\big]\boldsymbol{\nu}\otimes\mathbf{n}\Big).\end{aligned} \tag{4.66}$$

Using the identity $\mathbf{L}^2 = 2H\mathbf{L} - K\mathbf{P}$ (Cayley-Hamilton theorem) in addition to (4.65) and (4.66) the shape equation reads

$$\begin{aligned}&-\operatorname{div}_s\left\{\mathbf{P}\operatorname{div}_s\boldsymbol{\Lambda} + 2k\left[\operatorname{div}_s\left(q^2\mathbf{L}\mathbf{n}\right) + q^2\mathbf{L}\cdot\nabla_s\mathbf{n}\right]\mathbf{n}\right\} \\ &+2H\left[\gamma - k\left(1-q\right)^2\left(H^2-K\right) - kq\left(1-q\right)\left|\mathbf{L}\mathbf{n}\right|^2 + \frac{k}{4}\left|\nabla_s q\right|^2 + kq^2\left|\nabla_s\mathbf{n}\right|^2 + \frac{a}{4}q^2 + \frac{c}{8}q^4\right] \\ &+2kq\left(1-q\right)K\mathbf{L}\mathbf{n}\cdot\mathbf{n} - 2kq^2\left(\nabla_s\mathbf{n}\right)^T\left(\nabla_s\mathbf{n}\right)\cdot\mathbf{L} - \frac{k}{2}\nabla_s q\cdot\mathbf{L}\nabla_s q = 0.\end{aligned} \tag{4.67}$$

The equilibrium equation associated with $\mathbf{n}$ is (as detailed in chapter 3)

$$\left(\operatorname{div}_s\mathbf{G}_s - \mathbf{g}_s\right)\cdot\mathbf{t} = 0 \tag{4.68}$$

consider that (4.68) can be written as

$$\operatorname{div}_s\left(\mathbf{G}_s^T\mathbf{t}\right) - \mathbf{G}_s\cdot\nabla_s\mathbf{t} - \mathbf{g}_s\cdot\mathbf{t} = 0. \tag{4.69}$$

We need to get an equivalent form for (4.68) by substituting $\mathbf{G}_s^T$ and $\mathbf{g}_s$. We calculate $\mathbf{G}_s^T\mathbf{t}$, $\mathbf{G}_s\cdot\nabla_s\mathbf{t}$ and $\mathbf{g}_s\cdot\mathbf{t}$, respectively as follow

$$\mathbf{G}_s^T\mathbf{t} = 2kq^2\left(\nabla_s\mathbf{n}\right)^T\mathbf{t} = 2kq^2\left[\nabla_s\alpha + \boldsymbol{\omega}\right]. \tag{4.70}$$

For

$$\mathbf{G}_s\cdot\nabla_s\mathbf{t} = 2kq^2\nabla_s\mathbf{n}\cdot\nabla_s\mathbf{t} = 2kq^2\left(\mathbf{L}\mathbf{T}\right)\cdot\left(\mathbf{L}\mathbf{n}\right) = 2kq^2\mathbf{t}\cdot\left(\mathbf{L}^2\mathbf{n}\right) \tag{4.71}$$

and

$$\mathbf{g}_s\cdot\mathbf{t} = 2kq\left(1-q\right)\mathbf{t}\cdot\left(\mathbf{L}^2\mathbf{n}\right).$$

Therefore our equilibrium equation (4.68) becomes

$$\operatorname{div}_s\big(q^2\left(\nabla_s\alpha + \boldsymbol{\omega}\right)\big) - 2qH\tau_n = 0 \tag{4.72}$$

where $\tau_n = -\mathbf{Ln}\cdot\mathbf{t}$ is the *geodesic torsion*, of the flux line of $\mathbf{n}$.

The equilibrium equation related to the degree of orientation q is given as

$$\operatorname{div}_s(\mathbf{b}_s) - a = 0. \tag{4.73}$$

We substitute $\mathbf{b}_s$ and a that are provided by (4.58) in the equilibrium equation (4.73) to get an equivalent equilibrium equation for (4.73),

$$k\left[\Delta_s q - 4q\left|\nabla_s\mathbf{n}\right|^2 + (1-q)\left|\mathbf{L}\right|^2 - 2(1-2q)\left|\mathbf{Ln}\right|^2\right] - aq - cq^3 = 0. \tag{4.74}$$

On using $|\mathbf{L}|^2 = 4H^2 - 2K$ and $|\mathbf{Ln}|^2 = 2Hc_n - K$ the equilibrium equation in (4.74) becomes

$$k\left[\Delta_s q - 4q\left|\nabla_s\mathbf{n}\right|^2 - 2qK + 4qHc_n - 4(1-q)H\varsigma\cos 2\alpha\right] - aq - cq^3 = 0, \tag{4.75}$$

where

$$\left|\nabla_s\mathbf{n}\right|^2 = \left|\nabla_s\alpha\right|^2 + \left|\boldsymbol{\omega}\right|^2 + \left|\mathbf{Ln}\right|^2 + 2\boldsymbol{\omega}\cdot\nabla_s\alpha, \tag{4.76}$$

and ς is the local asphericity (see (2.40) in §2.3.1). Note that, the solution $q = 0$ only satisfies the equation for q if $H = 0$ or $\varsigma = 0$; that is a minimal surface or part of sphere.

4.3.1 Boundary conditions

Natural boundary conditions If the molecules of the nematic have a free rotation around the normal $\boldsymbol{\nu}$ at the boundary ($\mathbf{n}$ is not fixed), then the *natural boundary condition* is (see §3.1.2)

$$\mathbf{G}_s^T\mathbf{t}\cdot\mathbf{k} = 0, \tag{4.77}$$

by using the expression of $\mathbf{G}_s$ given in (4.70), our *natural boundary condition* becomes

$$2kq^2\left(\nabla_s\mathbf{n}\right)^T\mathbf{t}\cdot\mathbf{k} = 0 \tag{4.78}$$

(note that $q = 0$ satisfies this boundary condition). We can write (4.78) in terms of α, with the aid of (4.46) and (4.47) as

$$q^2\,\mathbf{k}\cdot(\nabla_s\alpha + \boldsymbol{\omega}) = 0. \tag{4.79}$$

If q is not fixed on the boundary then the *natural boundary condition* is

$$\mathbf{b}_s\cdot\mathbf{k} = 0, \tag{4.80}$$

which equivalent to (using the expression of $\mathbf{b}_s$ given in (4.58),

$$\frac{k}{2}\nabla_s q \cdot \mathbf{k} = 0. \tag{4.81}$$

Finally, we have the *natural boundary condition* related to the shape equation

$$\left[\mathbf{\Lambda}_s \mathbf{k} + \left(\mathbf{G}_s \mathbf{k} \cdot \boldsymbol{\nu}\right) \mathbf{n}\right] \cdot \mathbf{k} = 0. \tag{4.82}$$

On using the expressions given in (4.58) for $\mathbf{\Lambda}_s$ and $\mathbf{G}_s$ the *natural boundary conditions* in (4.82) becomes

$$\frac{1}{2}\left(1-q\right)^2 \left(\mathbf{k} \cdot \mathbf{L}\mathbf{k}\right) + 2q \left(\mathbf{L}\mathbf{n}\right) \cdot \mathbf{k} \left(\mathbf{n} \cdot \mathbf{k}\right) = 0. \tag{4.83}$$

Here note that $q = 0$ would demand that $(\mathbf{k} \cdot \mathbf{L}\mathbf{k} = 0)$ and the catenoid $(H = 0)$ does not satisfy the natural boundary condition for this problem.

We derived the equilibrium equations for general surfaces using $\mathbf{n}$ and α parameterisation. However the full problem for a general surface is very complicated and so we will consider a simpler situation in which we will restrict to a surface of revolution. We specialise to axisymmetric surfaces, which will allow us to explicitly calculate the spin connection, geodesic torsion of the lines of principal curvature, the mean and Gaussian curvatures and the directions of principal curvature and the geodesic curvatures of flux lines of the director. This restriction to axisymmetric surfaces may miss solutions and a more complete investigation will be necessary to determine whether there is a wider class of non-axisymmetric solutions with axisymmetric boundary.

4.4 Surfaces of revolution

To simplify our work we assuming that S is a surface of revolution, we represent S by a 2π-rotation about the $\mathbf{e}_z$ axis of the curve described on the (r, z) plane and positions on the surface are given by

$$\mathbf{x} = r\left(z\right)\mathbf{e}_r\left(\theta\right) + z\mathbf{e}_z, \quad \left(z \in \left[-h, h\right], \theta \in \left[0, 2\pi\right]\right) \tag{4.84}$$

where z is the coordinate along axis of the two coaxial circular rings of radius r placed at distance $2h$ apart and $z \in [-h, h]$, $z = 0$ is in the middle of the two rings and θ represents the coordinate goes around, $\theta \in [0, 2\pi]$. Two tangent directions on the surface are

$$\frac{\partial \mathbf{x}}{\partial z} = \mathbf{x}_z = r'\,\mathbf{e}_r + \mathbf{e}_z, \quad \frac{\partial \mathbf{x}}{\partial \theta} = \mathbf{x}_\theta = r\,\mathbf{e}_\theta, \tag{4.85}$$

and the boundary condition $r(\pm h) = R$. and the unit outward-pointing normal to the surface is

$$\boldsymbol{\nu} = \frac{\mathbf{x}_\theta \times \mathbf{x}_z}{|\mathbf{x}_\theta \times \mathbf{x}_z|} = \frac{\mathbf{e}_r - r'\mathbf{e}_z}{\sqrt{1+(r')^2}}. \tag{4.86}$$

The surface gradient of any scalar function, ϕ on S reads as

$$\nabla_s \phi = \frac{1}{1+(r')^2}\frac{\partial \phi}{\partial z}(r'\mathbf{e}_r + \mathbf{e}_z) + \frac{1}{r}\frac{\partial \phi}{\partial \theta}\mathbf{e}_\theta. \tag{4.87}$$

For an axisymmetric field, $\partial\phi/\partial\theta = 0$, then

$$\nabla_s \phi = \frac{(r'\mathbf{e}_r + \mathbf{e}_z)}{1+(r')^2}\frac{d\phi}{dz} \tag{4.88}$$

and

$$|\nabla_s \phi|^2 = \frac{1}{1+(r')^2}\left(\frac{d\phi}{dz}\right)^2. \tag{4.89}$$

The surface gradient of a vector field $\mathbf{a}$ is given as

$$\nabla_s \mathbf{a} = \frac{1}{1+(r')^2}\frac{\partial \mathbf{a}}{\partial z} \otimes (r'\mathbf{e}_r + \mathbf{e}_z) + \frac{1}{r}\frac{\partial \mathbf{a}}{\partial \theta} \otimes \mathbf{e}_\theta. \tag{4.90}$$

We use (4.90) to calculate the extrinsic curvature tensor $\mathbf{L}$,

$$\begin{aligned}
\mathbf{L} = -\nabla_s \boldsymbol{\nu} &= -\left[\frac{\partial}{\partial \theta}\left(\frac{\mathbf{e}_r - r'\mathbf{e}_z}{\sqrt{1+(r')^2}}\right) \otimes \frac{1}{r}\,\mathbf{e}_\theta + \frac{\partial}{\partial z}\left(\frac{\mathbf{e}_r - r'\mathbf{e}_z}{\sqrt{1+(r')^2}}\right) \otimes \frac{1}{(r')^2+1}\,(r'\,\mathbf{e}_r + \mathbf{e}_z)\right] \\
&= -\left[\frac{1}{r\sqrt{1+(r')^2}}\,\mathbf{e}_\theta \otimes \mathbf{e}_\theta + \left[\mathbf{e}_r\left(-\frac{1}{2}\frac{2r'r''}{\left(1+(r')^2\right)^{\frac{3}{2}}}\right)\frac{-r''}{\left(1+(r')^2\right)^{\frac{1}{2}}}\,\mathbf{e}_z\right.\right. \\
&\left.\left. + \frac{(r')^2\,r''}{\left(1+(r')^2\right)^{\frac{3}{2}}}\,\mathbf{e}_z\right] \otimes \frac{1}{(r')^2+1}\,(r'\mathbf{e}_r + \mathbf{e}_z)\right] \\
&= -\frac{1}{r}\frac{1}{\sqrt{1+(r')^2}}\,\mathbf{e}_\theta \otimes \mathbf{e}_\theta - \left[-\frac{r''}{\left(1+(r')^2\right)^{\frac{3}{2}}}\,\mathbf{e}_z - \frac{r'r''\mathbf{e}_r}{\left(1+(r')^2\right)^{\frac{3}{2}}}\right] \otimes \frac{1}{(r')^2+1}\,(r'\mathbf{e}_r + \mathbf{e}_z).
\end{aligned} \tag{4.91}$$

Let $\mathbf{t}_z$ be the unit vector pointing in the same direction as $\mathbf{x}_z$. Then $\mathbf{L}$ can be written in terms of $\mathbf{e}_\theta$ and $\mathbf{t}_z$ which form a basis of the tangent plane to the surface (the vectors change as we move around the surface but are always tangent to it).

$$\mathbf{L} = -\frac{1}{r}\frac{1}{\sqrt{1+(r')^2}}\,\mathbf{e}_\theta \otimes \mathbf{e}_\theta + \frac{r''}{\left(1+(r')^2\right)^{\frac{3}{2}}}\,\mathbf{t}_z \otimes \mathbf{t}_z. \tag{4.92}$$

As a result of (4.92), the principal curvatures c_1 and c_2 are

$$c_1 = -\frac{1}{r\left(1+(r')^2\right)^{\frac{1}{2}}}, \qquad c_2 = \frac{r''}{\left(1+(r')^2\right)^{\frac{3}{2}}}. \tag{4.93}$$

For future calculations we let $\mathbf{e}_1 = \mathbf{e}_\theta$ and $\mathbf{e}_2 = \mathbf{t}_z$, which are the principal directions. Now using (4.93), one easily find that, the mean and Gauss curvature and the asphericity are respectively

$$H = \frac{1}{2}(c_1 + c_2) = \frac{r\,r'' - (1+r'^2)}{2r\left(1+(r')^2\right)^{\frac{3}{2}}} \tag{4.94}$$

$$K = c_1\,c_2 = -\frac{r''}{r\left(1+(r')^2\right)^2} \tag{4.95}$$

$$\varsigma = \frac{1}{2}(c_1 - c_2) = -\frac{r\,r'' + (1+r'^2)}{2r\left(1+(r')^2\right)^{\frac{3}{2}}}. \tag{4.96}$$

Recall that the spin connection $\boldsymbol{\omega}$ is given by

$$\boldsymbol{\omega} = k_{g1}\mathbf{e}_1 + k_{g2}\mathbf{e}_2 = -\frac{r'}{r\sqrt{1+(r')^2}}\,\mathbf{e}_1 \tag{4.97}$$

where k_{g1} is the geodesic curvature of lines parallel to $\mathbf{e}_1$ (circling the surface) and k_{g2} is the geodesic curvature of the lines parallel to $\mathbf{e}_2$ (lines along the surface). Note that k_{g1} is calculated in the example in §2.3.3 and $k_{g2} = 0$ as lines along the surface are geodesics.

$$|\boldsymbol{\omega}|^2 = \frac{(r')^2}{r^2\left(1+(r')^2\right)}. \tag{4.98}$$

Also the surface Laplacian for an axisymmetric surface is given as

$$\Delta_s\phi = \frac{1}{r^2}\frac{\partial^2\phi}{\partial\theta^2} + \frac{1}{r\left(1+r'^2\right)^{1/2}}\frac{\partial}{\partial z}\left(\frac{r}{\left(1+r'^2\right)^{1/2}}\frac{\partial\phi}{\partial z}\right). \tag{4.99}$$

The surface gradients of the principal directions are given as follows

$$\nabla_s\mathbf{e}_1 = -\frac{r'}{r\sqrt{1+r'^2}}\,\mathbf{e}_2\otimes\mathbf{e}_1 - \frac{1}{r\sqrt{1+r'^2}+1}\,\boldsymbol{\nu}\otimes\mathbf{e}_1, \tag{4.100}$$

$$\nabla_s\mathbf{e}_2 = -\frac{r'}{r\sqrt{1+r'^2}}\,\mathbf{e}_1\otimes\mathbf{e}_1 + \frac{r''}{(1+r'^2)^{\frac{3}{2}}}\,\boldsymbol{\nu}\otimes\mathbf{e}_2. \tag{4.101}$$

The normal curvatures of the flux lines of $\mathbf{n}$ and $\mathbf{t}$ are

$$c_n = c_1\cos^2\alpha + c_2\sin^2\alpha, \quad c_t = c_1\sin^2\alpha + c_2\cos^2\alpha. \tag{4.102}$$

These quantities is expressed respectively as

$$c_n = \frac{r\,r''\sin^2\alpha - (1+r'^2)\cos^2\alpha}{r\,(1+r'^2)^{\frac{3}{2}}}, \tag{4.103}$$

$$c_t = \frac{r\,r''\cos^2\alpha - (1+r'^2)\sin^2\alpha}{r\,(1+r'^2)^{\frac{3}{2}}}. \tag{4.104}$$

The geodesic torsion of the flux lines of $\mathbf{n}$ is

$$\tau_n = (c_1 - c_2)\sin\alpha\cos\alpha \tag{4.105}$$

which can be written as

$$\tau_n = -\frac{r\,r''+r'^2+1}{r\,(1+r'^2)^{\frac{3}{2}}}\,\sin\alpha\cos\alpha. \tag{4.106}$$

Now we can write the surface energy when the surface is axisymmetric using the q_0, q_m parameterisation as

$$\begin{aligned} W = 2\pi\int_{-h}^{h}\Bigg(\gamma + k\Bigg[&\frac{1}{1+r'^2}\,q_0'^2 + \frac{1}{1+r'^2}\,q_m'^2 + \left(q_0^2+q_m^2\right)\left(\frac{4\,r'^2}{r^2\,(1+r'^2)} + \frac{(r\,r'')^2+(1+r'^2)}{r^2\,(1+r'^2)^3}\right) \\ &+ 4\left(q_0\,\frac{r'\mathbf{e}_r+\mathbf{e}_z}{1+r'^2}\,q_m' - q_m\,\frac{r'\mathbf{e}_r+\mathbf{e}_z}{1+r'^2}\,q_0'\right)\cdot\left(\frac{-r'}{r\sqrt{1+r'^2}}\mathbf{e}_1\right) + \frac{(r\,r'')^2+(1+r'^2)^2}{4r^2\,(1+r'^2)^3} \\ &- 4q_0\frac{(r\,r'')^2-(1+r'^2)^2}{4r^2\,(1+r'^2)^3}\Bigg] + a\left(q_0^2+q_m^2\right) + c\left(q_0^2+q_m^2\right)^2\Bigg)r\sqrt{1+(r')^2}\,dz, \end{aligned} \tag{4.107}$$

notice that $\mathbf{e}_1$ is the principle direction ($\mathbf{e}_\theta$ direction), $\mathbf{e}_\theta$ is perpendicular to both $\mathbf{e}_r$ and $\mathbf{e}_z$ then (4.107) becomes

$$\begin{aligned} W = 2\pi\int_{-h}^{h}\Bigg(\gamma + k\Bigg[&\frac{1}{1+r'^2}\,q_0'^2 + \frac{1}{1+r'^2}\,q_m'^2 + \left(q_0^2+q_m^2\right)\left(\frac{4\,r'^2}{r^2\,(1+r'^2)} + \frac{(r\,r'')^2+(1+r'^2)}{r^2\,(1+r'^2)^3}\right) \\ &+ \frac{(r\,r'')^2+(1+r'^2)^2}{4r^2\,(1+r'^2)^3} - 4q_0\frac{(r\,r'')^2-(1+r'^2)^2}{4r^2\,(1+r'^2)^3}\Bigg] + a\left(q_0^2+q_m^2\right) + c\left(q_0^2+q_m^2\right)^2\Bigg)r\sqrt{1+(r')^2}\,dz, \end{aligned} \tag{4.108}$$

4.5 Dimensionless axisymmetric case using q_0 and q_m

In this section we derive the equilibrium equations in Hamiltonian form for the parameterisation using q_0 and q_m and the appropriate boundary conditions. We transform the equilibrium equations to a set of first-order equations suitable for numerical simulation to find different axisymmetric solutions.

Using the dimensionless quantities:

$$r = R\rho\,,\ \zeta = \frac{z}{h}\,,\ \xi = \frac{h}{R}\,,\ \kappa = \frac{k}{2\gamma R^2}\,,\ A = \frac{a}{2\gamma}\,,\ C = \frac{c}{2\gamma}, \tag{4.109}$$

where R is the radius of rings, ξ is considered to be the aspect ratio, κ represents a measure of the ratio of surface energy to k, A is the dimensionless temperature and C is a positive material constant.

Using the scaling in (4.109) we can write the energy as

$$\begin{aligned} W = 2\pi\gamma R^2 \int_{-1}^{1} \Bigg(1 + \kappa \Bigg[& \frac{2}{(\xi^2+\rho'^2)} \left(q_0'^2 + q_m'^2\right) + 8\left(q_0^2+q_m^2\right) \frac{\rho'^2}{\rho^2\left(\xi^2+\rho'^2\right)} \\ & + \frac{1}{2}\left(1+4\left(q_0^2+q_m^2\right)\right) \frac{\xi^2\left(\rho^2\rho''^2 + \left(\xi^2+\rho'^2\right)^2\right)}{\rho^2\left(\xi^2+\rho'^2\right)^3} - \frac{2q_0\xi^2\left(\rho^2\rho''^2 - \left(\xi^2+\rho'^2\right)^2\right)}{\rho^2\left(\xi^2+\rho'^2\right)^3} \Bigg] \\ & + 2A\left(q_0^2+q_m^2\right) + 2C\left(q_0^2+q_m^2\right)^2 \Bigg) \rho\sqrt{\xi^2+\rho'^2}\, d\zeta. \end{aligned} \tag{4.110}$$

We use Hamilton's equations that help us to derive the dimensionless equilibrium equations ([25], [41], [110]). We need to introduce the following eight variables

$$q_1 = q_0\,,\quad p_0 = p_1 = \frac{\partial w}{\partial q_0'}, \qquad q_2 = q_m\,,\quad p_m = p_2 = \frac{\partial w}{\partial q_m'}, \tag{4.111}$$

$$q_3 = \rho\,,\quad p_3 = \frac{\partial w}{\partial \rho'} - \frac{d}{d\zeta}\left(\frac{\partial w}{\partial \rho''}\right), \tag{4.112}$$

the definition of p_3 is non-standard definition that applies to the derivation of Hamilton's equations, for more details see [84],

$$q_4 = \rho'\,,\quad p_4 = \frac{\partial w}{\partial \rho''}. \tag{4.113}$$

Now, we can easily find,

$$q_1' = \frac{p_0\sqrt{\xi^2+q_4^2}}{2\kappa q_3}, \tag{4.114}$$

$$q_2' = \frac{p_m\sqrt{\xi^2+q_4^2}}{2\kappa q_3}, \tag{4.115}$$

$$q_4' = \rho'' = \frac{p_4\left(\xi^2+q_4^2\right)^{\frac{5}{2}}}{\kappa\, q_3\, \xi^2\left[1+4\left(q_1^2+q_2^2\right)-4q_1\right]}\,. \tag{4.116}$$

The Hamiltonian is $\tilde{H} = p_0\, q_1' + p_m\, q_2' + p_3\, q_4 + p_4\, q_4' - w$, then

$$\tilde{H} = \frac{\left(\xi^2+q_4^2\right)^{\frac{1}{2}}}{8\kappa\, q_3}\left(p_0^2+p_m^2\right) + p_3\, q_4 + \frac{p_4^2\left(\xi^2+q_4^2\right)^{\frac{5}{2}}}{2\kappa\,\xi^2\, q_3\left[1+4\left(q_1^2+q_2^2\right)-4q_1\right]} - q_3\left(\xi^2+q_4^2\right)^{\frac{1}{2}} - \frac{8\kappa\left(q_1^2+q_2^2\right)q_4^2}{q_3\left(\xi^2+q_4^2\right)^{\frac{1}{2}}} - \frac{\kappa\,\xi^2\left[1+4\left(q_1^2+q_2^2\right)+4q_1\right]}{2\,q_3\left(\xi^2+q_4^2\right)^{\frac{1}{2}}} - 2A\, q_3\left(q_1^2+q_2^2\right)\left(\xi^2+q_4^2\right)^{\frac{1}{2}} - 2C\, q_3\left(q_1^2+q_2^2\right)^2\left(\xi^2+q_4^2\right)^{\frac{1}{2}}. \quad (4.117)$$

Now, we need to solve the following system of first order ODEs,

$$q_i' = \frac{\partial \tilde{H}}{\partial p_i}, \quad p_i' = -\frac{\partial \tilde{H}}{\partial q_i} \quad (i = 1,2,3,4), \quad (4.118)$$

we get the following for q_i'

$$q_1' = q_0' = \frac{\left(\xi^2+q_4^2\right)^{\frac{1}{2}} p_0}{4\kappa\, q_3}, \qquad q_2' = q_m' = \frac{\left(\xi^2+q_4^2\right)^{\frac{1}{2}} p_m}{4\kappa\, q_3}, \quad (4.119)$$

$$q_3' = q_4, \qquad q_4' = \frac{p_4\left(\xi^2+q_4^2\right)^{\frac{5}{2}}}{\kappa\xi^2\, q_3\left[1+4\left(q_1^2+q_2^2\right)-4q_1\right]}, \quad (4.120)$$

and for p_i' we have

$$p_1' = \frac{2p_4^2\left(\xi^2+q_4^2\right)^{\frac{5}{2}}(2q_1-1)}{\kappa\,\xi^2\, q_3\left[1+4\left(q_1^2+q_2^2\right)-4q_1\right]^2} + \frac{16q_1\, q_4^2\,\kappa}{q_3\left(\xi^2+q_4^2\right)^{\frac{1}{2}}} + \frac{2\,\kappa\,\xi^2\,(2q_1+1)}{q_3\left(\xi^2+q_4^2\right)^{\frac{1}{2}}} + 4A\, q_1\, q_3\left(\xi^2+q_4^2\right)^{\frac{1}{2}} + 8C\left(q_1^2+q_2^2\right) q_1\, q_3\left(\xi^2+q_4^2\right)^{\frac{1}{2}}, \quad (4.121)$$

$$p_2' = \frac{4p_4^2\left(\xi^2+q_4^2\right)^{\frac{5}{2}} q_2}{\kappa\,\xi^2\, q_3\left[1+4\left(q_1^2+q_2^2\right)-4q_1\right]^2} + \frac{16q_2\, q_4^2\,\kappa}{q_3\left(\xi^2+q_4^2\right)^{\frac{1}{2}}} + \frac{4\,\kappa\,\xi^2\, q_2}{q_3\left(\xi^2+q_4^2\right)^{\frac{1}{2}}} + 4A\, q_2\, q_3\left(\xi^2+q_4^2\right)^{\frac{1}{2}} + 8C\left(q_1^2+q_2^2\right) q_2\, q_3\left(\xi^2+q_4^2\right)^{\frac{1}{2}}, \quad (4.122)$$

$$p_3' = \frac{\left(\xi^2+q_4^2\right)^{\frac{1}{2}}\left(p_0^2+p_m^2\right)}{8\,\kappa\, q_3^2} + \frac{p_4^2\left(\xi^2+q_4^2\right)^{\frac{5}{2}}}{2\kappa\,\xi^2\, q_3^2\left[1+4\left(q_1^2+q_2^2\right)-4q_1\right]} + \left(\xi^2+q_4^2\right)^{\frac{1}{2}} - \frac{8\left(q_1^2+q_2^2\right)q_4^2\,\kappa}{q_3^2\left(\xi^2+q_4^2\right)^{\frac{1}{2}}} - \frac{\kappa\,\xi^2\left[1+4\left(q_1^2+q_2^2\right)+4q_1\right]}{2q_3^2\left(\xi^2+q_4^2\right)^{\frac{1}{2}}} + 2A\left(q_1^2+q_2^2\right)\left(\xi^2+q_4^2\right)^{\frac{1}{2}} + 2C\left(q_1^2+q_2^2\right)\left(\xi^2+q_4^2\right)^{\frac{1}{2}}, \quad (4.123)$$

$$p_4' = -\frac{q_4\,(p_0^2+p_m^2)}{8\,\kappa\,q_3\,(\xi^2+q_4^2)^{\frac{1}{2}}} - p_3 - \frac{5\,p_4^2\,q_4\,(\xi^2+q_4^2)^{\frac{3}{2}}}{2\kappa\,\xi^2\,q_3\,[1+4\,(q_1^2+q_2^2)-4q_1]} + \frac{q_3\,q_4}{(\xi^2+q_4^2)^{\frac{1}{2}}} + \frac{16\,(q_1^2+q_2^2)\,\kappa\,q_4}{q_3\,(\xi^2+q_4^2)^{\frac{1}{2}}} - \frac{8\,(q_1^2+q_2^2)\,\kappa\,q_4^3}{q_3\,(\xi^2+q_4^2)^{\frac{3}{2}}} - \frac{q_4\kappa\,\xi^2\,[1+4\,(q_1^2+q_2^2)+4q_1]}{2q_3\,(\xi^2+q_4^2)^{\frac{3}{2}}} + \frac{2A\,(q_1^2+q_2^2)\,q_3\,q_4}{(\xi^2+q_4^2)^{\frac{1}{2}}} + \frac{2C\,(q_1^2+q_2^2)^2\,q_3\,q_4}{(\xi^2+q_4^2)^{\frac{1}{2}}}. \quad (4.124)$$

The boundary conditions are a combination of essential and natural boundary. For the shape, one boundary condition is that the radius at the ends is fixed,

$$\rho = 1 \text{ at } \zeta = \pm 1, \quad (4.125)$$

(so $q_3 = 1$ at $\zeta = \pm 1$), and the other natural boundary conditions are

$$p_0 = 0 \text{ at } \zeta = \pm 1, \quad (4.126)$$

also we have

$$p_m = 0 \text{ at } \zeta = \pm 1. \quad (4.127)$$

The second, natural, boundary condition for the shape equation is

$$p_4 = 0 \text{ at } \zeta = \pm 1. \quad (4.128)$$

4.5.1 Numerical results for q_0 and q_m parameterisation

In this section we demonstrate and study solutions for different parameters. The following figures shows the numerical solutions for q_0, q_m and also numerical solutions for ρ for the axisymmetric equilibrium solutions for different values of the parameters (ξ, A, C, κ). We have used `bvp4c` to solve the equations with a mesh size of $N_z = 10000$ and an initial guess for the solution that is the wide catenoid solution, $q_m = 0$ and $q_0 = -\sqrt{-A/C}$ when $A < 0$ and $q_0 = 0$ when $A \geq 0$.

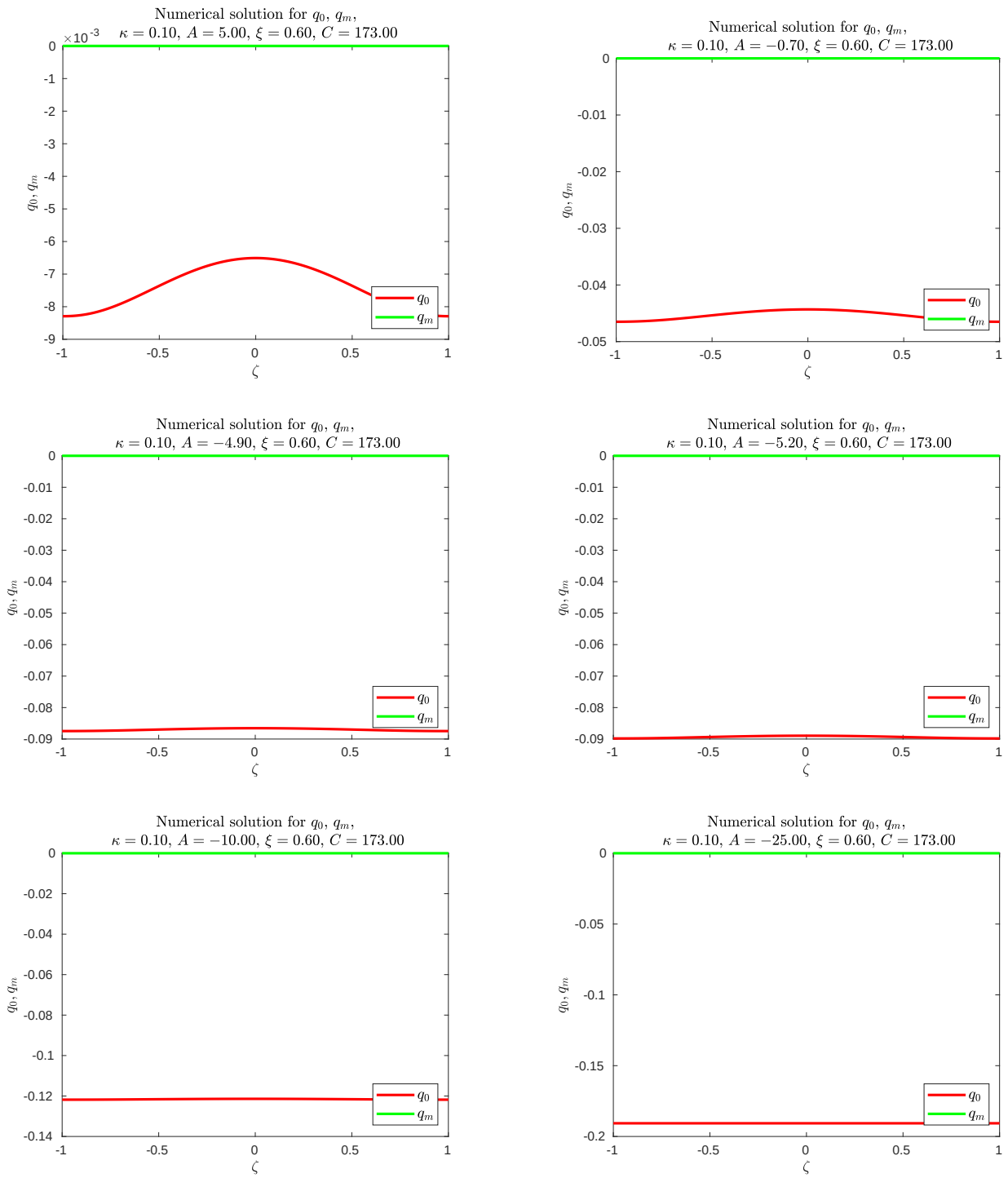


Figure 4.1: These figures shows solutions (with different y-axis scales) for q_0, q_m for different values of A, assuming the parameters κ, ξ, C have specific values. The red line corresponds to q_0 and the green one corresponds to q_m.

From figure 4.1 and depending on the value of A, we deduce that decreasing A increases the order and since the preferred direction appears to be along the meridians (from end to end) with $q_0 < 0$ and $q_m = 0$ then this means the surface would like to decrease the

energy cost of the surface by reducing its curvature, leading towards a cylindrical surface again ($q_m = 0$ and $q_0 < 0$ means preferred alignment along meridians (end to end)). This increases the surface area (when compared to the catenoid). Depending on our numerical work, we predict that as the parameter A gets large, the isotropic catenoid is recovered. Figure 4.2 shows numerical solutions for ρ as A decreases.

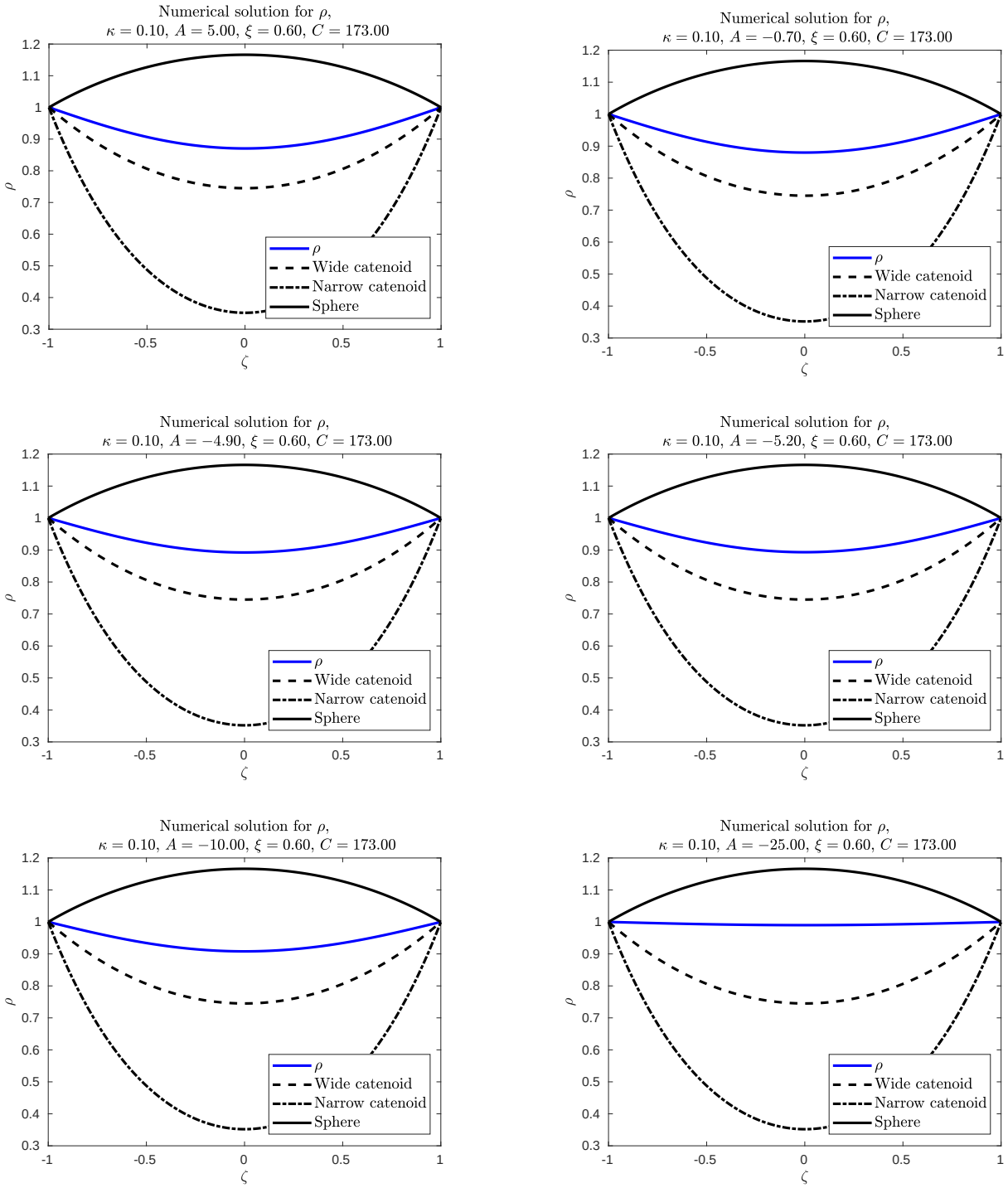


Figure 4.2: Numerical solutions for ρ for different values of the parameter A, assuming the parameters κ, ξ, C have a specific values. The blue solid line correspond to ρ, the black solid line corresponds to sphere, the dashed line corresponds to the wide catenoid and the dashed-doted line corresponds to the narrow catenoid.

Figures 4.3 and 4.4 show the branches and types of solutions as we vary ξ. In the soap film problem, as you move the rings apart the surface reduces its energy by contracting in the centre (lowering the surface area).

If the degree of order $\left(q = \sqrt{q_0^2 + q_m^2} = |q_0| \text{ when } q_m = 0\right)$ were to remain the same then, with a more curved surface the bending energy would increase, so we see a reduction in the degree of order near the centre. If A were more negative then we would also see competition from the Landau-de Gennes contribution.

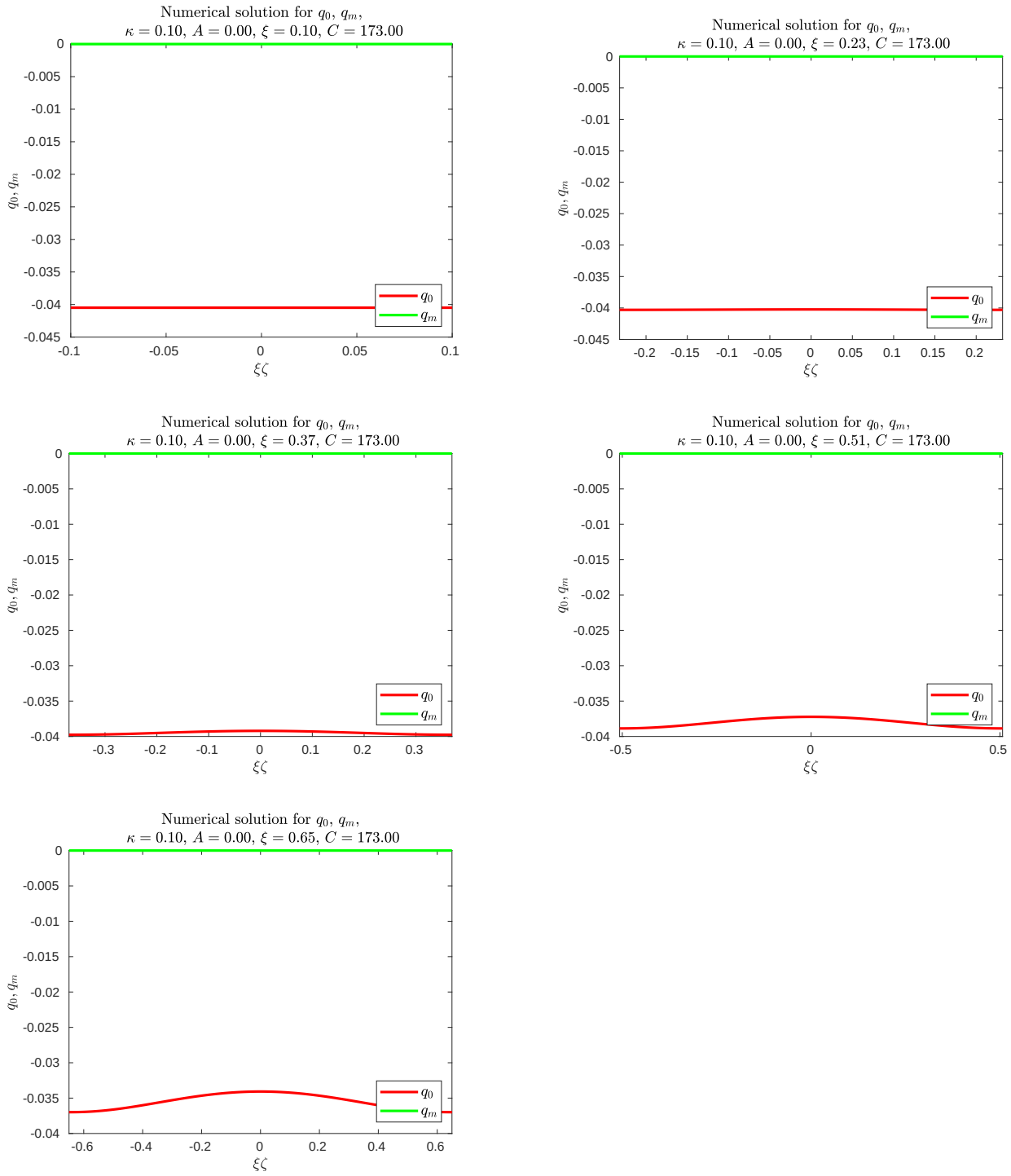


Figure 4.3: Numerical solutions for q_0, q_m for different values of ξ, assuming the parameters κ, A, C have specific values. The red line corresponds to q_0 and the green one corresponds to q_m.

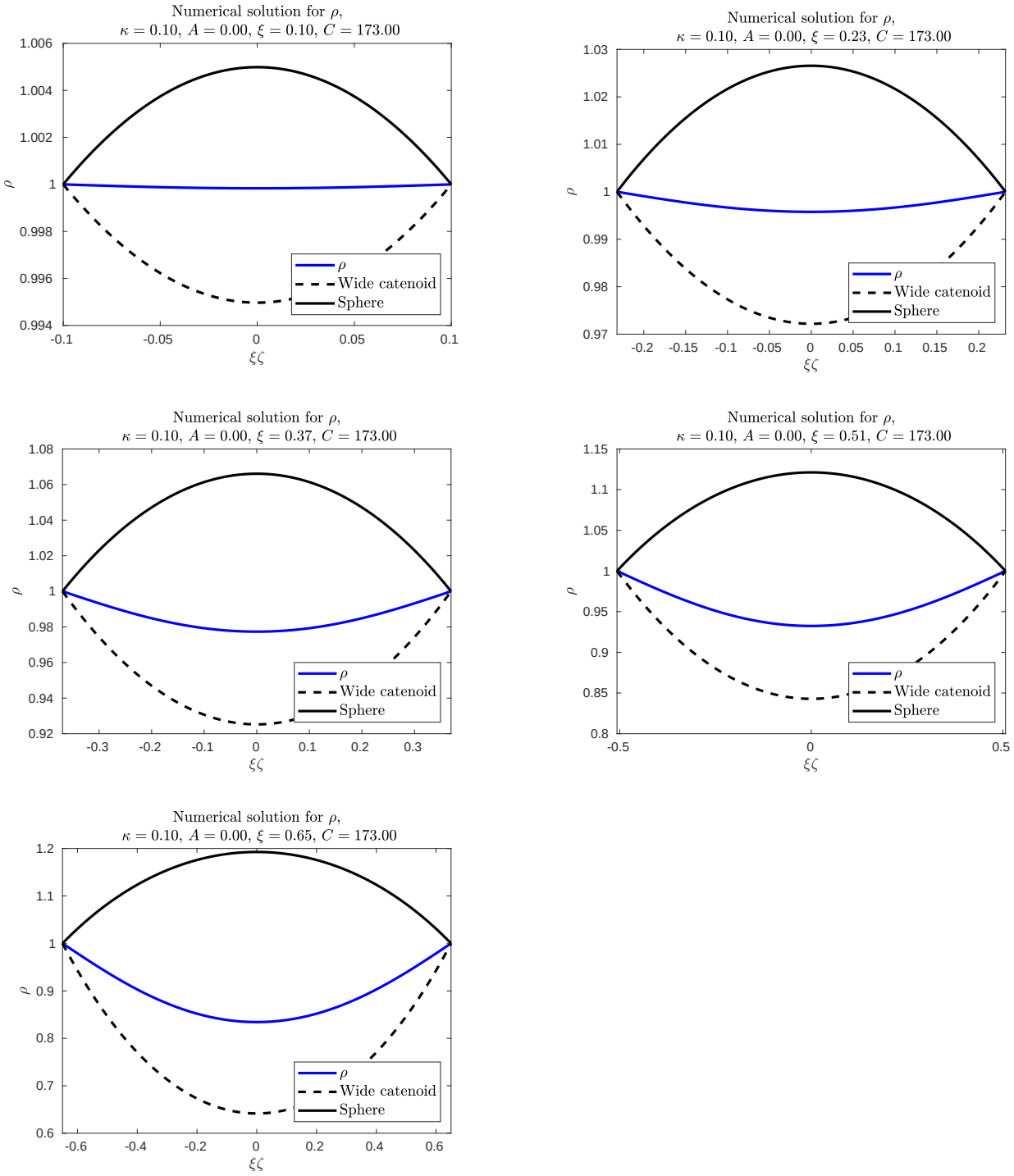
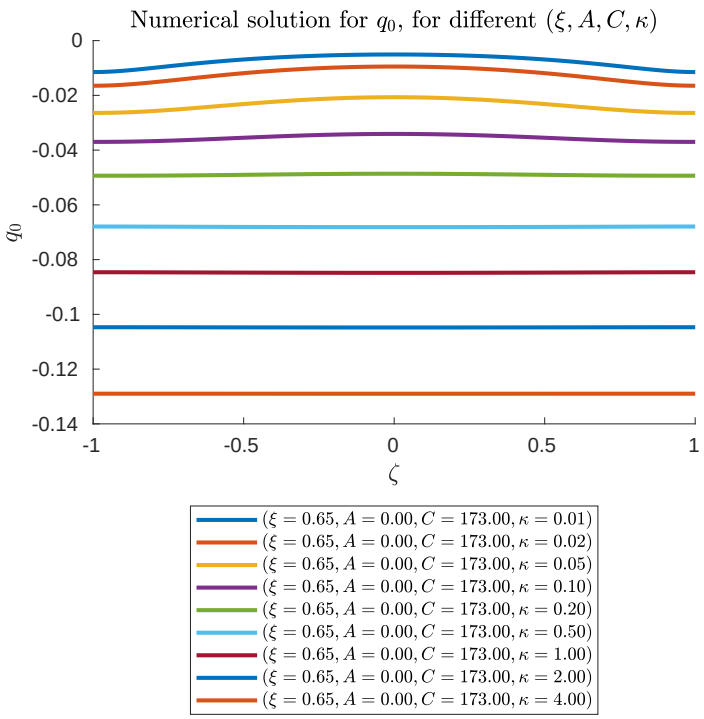


Figure 4.4: Numerical solutions for ρ for different values of the parameter ξ, assuming the parameters κ, A, C have a specific values. The blue solid line correspond to ρ, the black solid line corresponds to sphere, the dashed line corresponds to the wide catenoid.



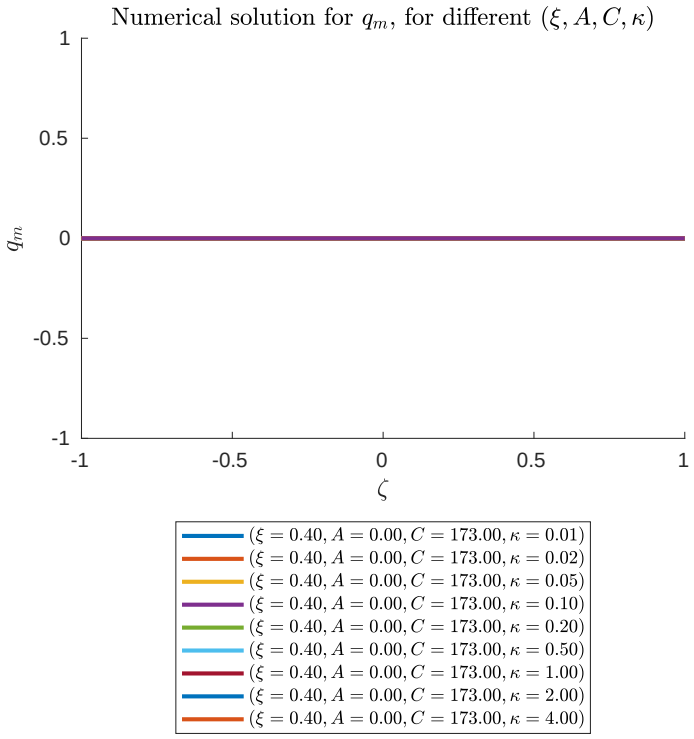


Figure 4.5: The first plot displays the numerical solutions for q_0 for different values of the parameter κ, assuming the parameters A, ξ, C are fixed. The second plot displays the numerical solution for q_m.

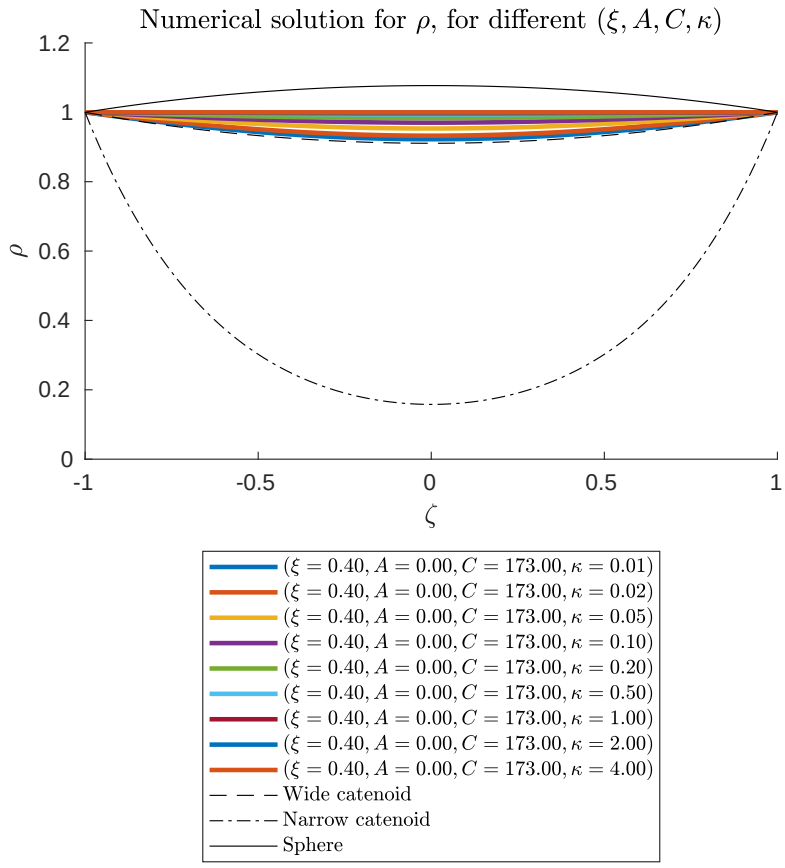
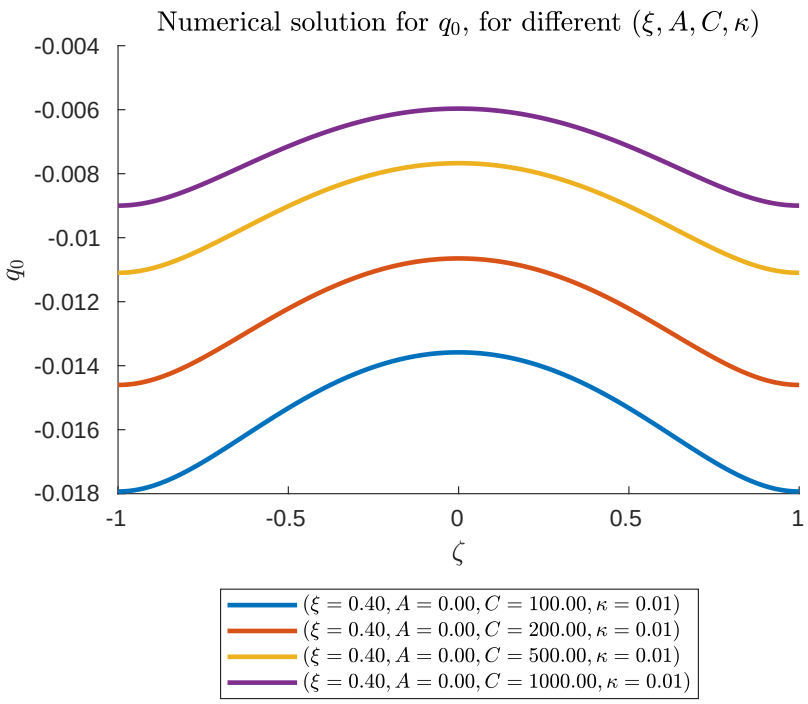


Figure 4.6: Numerical solutions for ρ for different values of the parameter κ, assuming the parameters A, ξ, C are the same in all the sets of parameters. The blue solid line correspond to ρ, the black solid line corresponds to sphere, the dashed line corresponds to the wide catenoid.

The main point we get from figures 4.5 and 4.6 is that increasing κ makes the equilibrium surface tend towards cylindrical. When compared to the catenoid, a cylindrical surface increases the surface area, but it decreases the bending energy (since the curvature reduces in both directions). Hence there is a balance between minimising surface area (as with small κ) and minimising bending energy (as with large κ).

Now we investigate the types of solutions for q_0, q_m and for ρ by varying the parameter C and specify a certain values for the parameters A, ξ, κ.



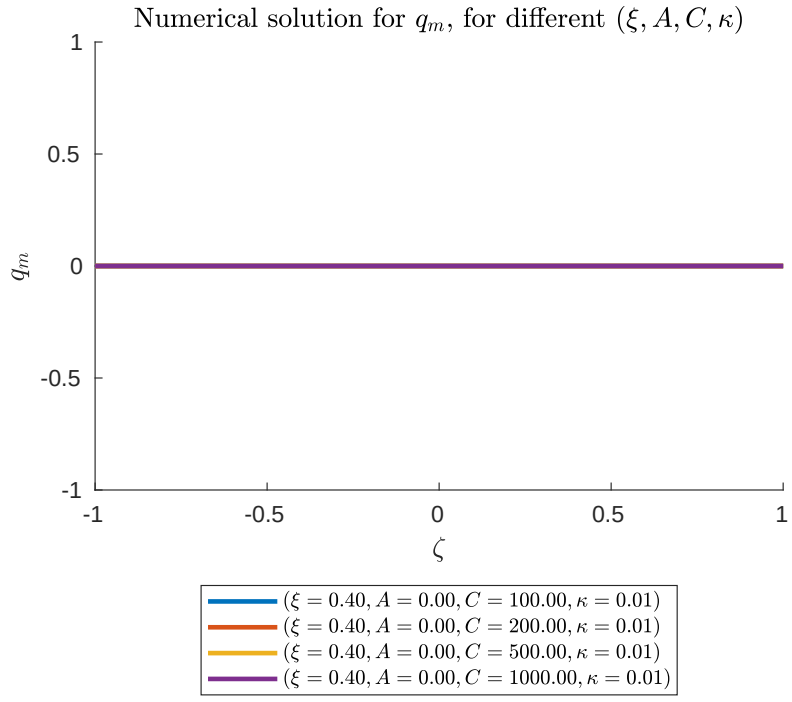


Figure 4.7: Numerical solutions for q_0 and q_m, respectively for different values of the parameter C, assuming the parameters A, ξ, κ are the same in all the sets of parameters.

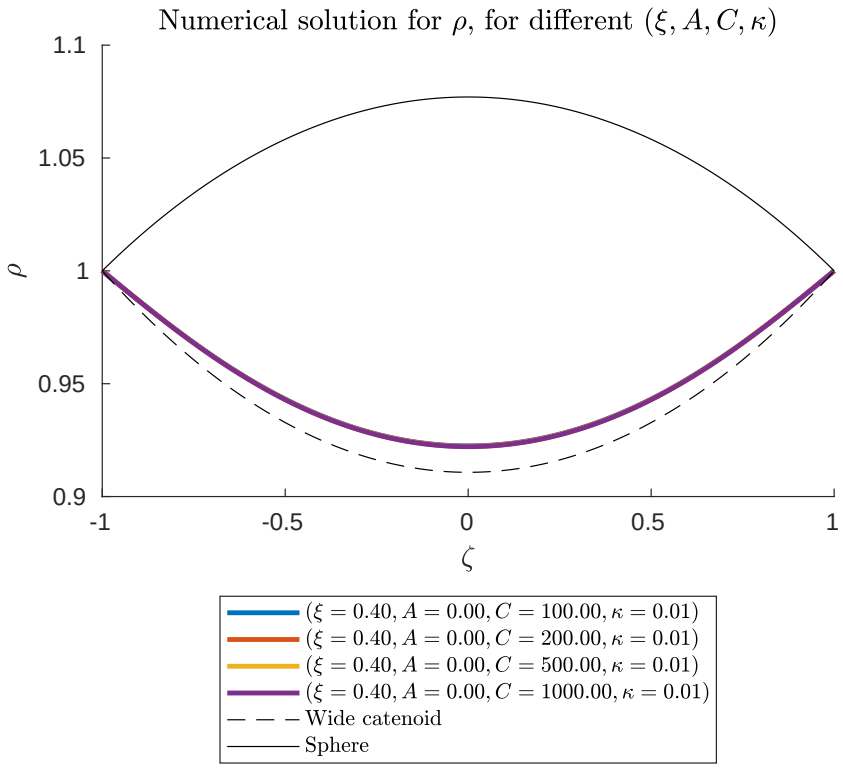


Figure 4.8: Numerical solutions for ρ for different values of the parameter C, assuming the parameters A, ξ, κ are the same in all the sets of parameters. The black solid line corresponds to sphere, the dashed line corresponds to the wide catenoid.

Notice that from the above figures 4.7 and 4.8, increasing C means that for fixed A the degree of order decreases and the effect is to move the shape of the surface towards the catenoidal shape (for small κ). We should also note that because we set the parameter $A = 0$, the parameter C does not have much influence on the shape.

One can notice that in all cases the boundary condition is $\rho'' = 0$ at the ends (not satisfied by the catenoid) and so for small κ there is a boundary later that matches the catenoid solution to the boundary condition at the ends.

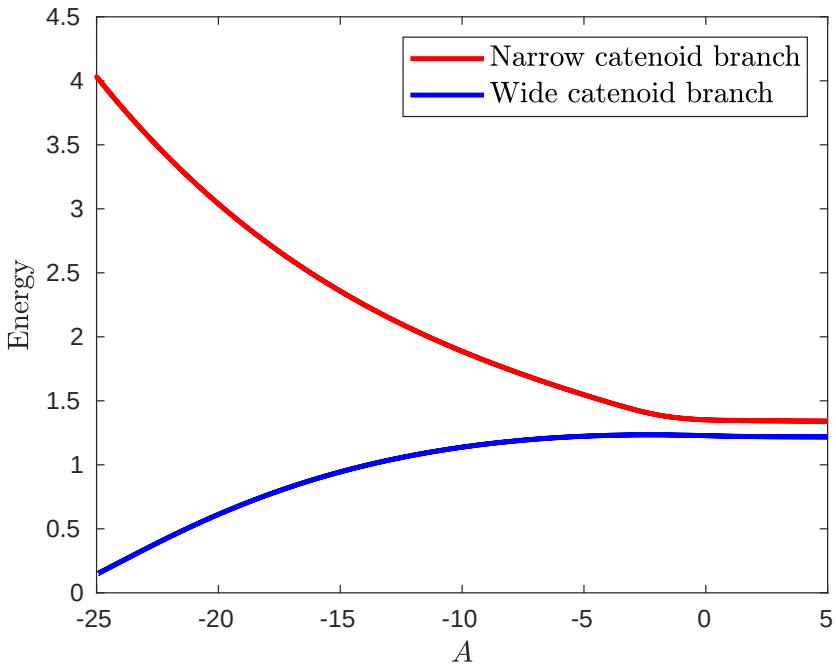


Figure 4.9: The energy as a function of A. The blue branch refers to the wide catenoid and the red brunch refers to the narrow catenoid.

4.6 Dimensionless axisymmetric case using q and n

We observe that in the figures preceding this section, where we use q_0, q_m, we notice that $q_0 < 0$ and $q_m = 0$, corresponds to $\alpha = \pi/2$, $q > 0$. In this section we derive the equilibrium equations in Hamiltonian form for the parameterisation using q and $\mathbf{n}$ and their relevant boundary conditions. Using the dimensionless quantities

$$\rho = R\varrho\,,\ z = h\zeta\,,\ \xi = \frac{h}{R}\,,\ \kappa = \frac{k}{2\gamma R^2}\,,\ A = \frac{a}{2\gamma}\,,\ C = \frac{c}{2\gamma}$$

and assuming axisymmetry we have the energy functional

$$W = 2\pi\gamma r^2 \left[\int_{-1}^{1} \tilde{w}\varrho\sqrt{\xi^2 + \varrho'^2}\, d\zeta\right]. \tag{4.129}$$

where the energy density is considered to be

$$\tilde{w} = 1 + \kappa\Bigg(\frac{1}{2}\frac{q'^2}{\xi^2+\varrho'^2} + \frac{2q^2}{\varrho^2\left(\xi^2+\varrho'^2\right)}\left(\varrho^2\alpha'^2+\varrho'^2\right) + \frac{q\xi^2}{\varrho^2\left(\xi^2+\varrho'^2\right)^3}\left(\left(\xi^2+\varrho'^2\right)^2-\varrho^2\varrho''^2\right)\cos 2\alpha + \frac{\left(1+q^2\right)\xi^2}{2\varrho^2\left(\xi^2+\varrho'^2\right)^3}\left(\left(\xi^2+\varrho'^2\right)^2+\varrho^2\varrho''^2\right)\Bigg) + \frac{A}{2}q^2+\frac{C}{4}q^4. \quad (4.130)$$

The Euler-Lagrange equations are

$$\frac{d^2}{d\zeta^2}\left(\frac{\partial w}{\partial \varrho''}\right) - \frac{d}{d\zeta}\left(\frac{\partial w}{\partial \varrho'}\right) + \frac{\partial w}{\partial \varrho} = 0 \quad (4.131)$$

$$\frac{d}{d\zeta}\left(\frac{\partial w}{\partial \alpha'}\right) - \frac{\partial w}{\partial \alpha} = 0 \quad (4.132)$$

$$\frac{d}{d\zeta}\left(\frac{\partial w}{\partial q'}\right) - \frac{\partial w}{\partial q} = 0 \quad (4.133)$$

4.6.1 Boundary conditions

For nematic films with boundary, the shape and director equations need appropriate boundary conditions. We find the natural boundary condition for α, q and ϱ where

$$w = \tilde{w}\varrho\left(\xi^2+\varrho'^2\right)^{\frac{1}{2}} = w\left(q, q', \alpha, \alpha', \varrho, \varrho', \varrho''\right) \quad (4.134)$$

where $\tilde{w}$ is given in (4.130). The *natural boundary condition* for α is

$$\frac{\partial w}{\partial \alpha'} = \frac{\partial}{\partial \alpha'}\left(\tilde{w}\varrho\sqrt{\xi^2+\varrho'^2}\right) = 0, \quad \text{at} \quad \zeta = \pm 1,$$

leads to the *natural boundary condition* (refers to (4.78))

$$q^2\alpha' = 0 \quad \text{at} \quad \zeta = \pm 1. \quad (4.135)$$

The *natural boundary condition* for q is,

$$\frac{\partial w}{\partial q'} = \frac{\partial}{\partial q'}\left(\tilde{w}\varrho\sqrt{\xi^2+\varrho'^2}\right) = 0, \quad \text{at} \quad \zeta = \pm 1,$$

that leads to

$$\varrho\sqrt{\xi^2+\varrho'^2}\,\frac{\kappa}{2}\frac{2q'}{\xi^2+\varrho^2} = 0, \quad \text{at} \quad \zeta = \pm 1, \quad (4.136)$$

Thus we get,

$$q' = 0 \quad \text{at} \quad \zeta = \pm 1. \quad (4.137)$$

The following two boundary conditions are required for the shape equation,

First we have the *essential boundary condition* where the boundary is fixed (rings with fixed radius),

$$\varrho = 1 \quad \text{at} \quad \zeta = \pm 1. \tag{4.138}$$

The natural boundary condition is

$$\frac{\partial}{\partial \varrho''}\left(w\varrho\sqrt{\xi^2+\varrho'^2}\right) = \varrho\sqrt{\xi^2+\varrho'^2}\,\frac{\partial w}{\partial \varrho''} = 0, \quad \text{at } \zeta = \pm 1. \tag{4.139}$$

Using the expression for the energy density this becomes

$$\begin{aligned}\frac{\partial}{\partial \varrho''}\left(w\varrho\sqrt{\xi^2+\varrho'^2}\right) &= \kappa\varrho\sqrt{\xi^2+\varrho^2}\left[\frac{-2q\xi^2\varrho''\cos 2\alpha}{\left(\xi^2+\varrho'^2\right)^3} + \frac{\left(1+q^2\right)\xi^2\varrho''}{\left(\xi^2+\varrho'^2\right)^3}\right] \\ &= \frac{\kappa\varrho\xi^2\varrho''}{\left(\xi^2+\varrho'^2\right)^{\frac{5}{2}}}\left(1+q^2-2q\cos 2\alpha\right)\end{aligned}$$

which simplifies to

$$\varrho''\left(1+q^2-2q\cos 2\alpha\right) = 0 \tag{4.140}$$

If $\alpha = 0, q = 1$ (Perfect order in circumferential direction). An alternative derivation of the boundary condition given in (4.140) is using the results of Chapter 3, the natural boundary condition for the shape equation

$$\left[\mathbf{\Lambda}_s\,\mathbf{k} + \left(\mathbf{G}_s\,\mathbf{k}\cdot\boldsymbol{\nu}\right)\mathbf{n}\right]\cdot\,\mathbf{k} = 0$$

Using the expressions

$$\mathbf{\Lambda}_s = \frac{1}{2}k\left(1-q\right)^2\mathbf{L} + 2q\left(1-q\right)\mathbf{Ln}\otimes\mathbf{n}\,, \qquad \mathbf{G}_s = 2kq^2\nabla_s\mathbf{n}$$

and with $\mathbf{G}_s\mathbf{k}\cdot\boldsymbol{\nu} = 2kq^2\left(\nabla_s\mathbf{n}^T\boldsymbol{\nu}\right)\cdot\mathbf{k} = 2kq^2\left(\mathbf{Ln}\right)\cdot\mathbf{k}$, we get the *natural boundary condition*,

$$\frac{1}{2}\left(1-q\right)^2\left(\mathbf{k}\cdot\mathbf{Lk}\right) + 2q\left(\mathbf{Ln}\right)\cdot\mathbf{k}\left(\mathbf{n}\cdot\mathbf{k}\right) = 0$$

which in terms of the axisymmetric variables and using that $\mathbf{k} = \pm\mathbf{e}_2$ at the ends, where $\mathbf{e}_2$ is parallel to the surface and perpendicular to tangent to curve, our *natural boundary condition* becomes

$$\left(\frac{1}{2}\left(1-q\right)^2 + 2q\sin^2\alpha\right)\frac{\varrho''}{\left(\xi^2+\varrho'^2\right)^{\frac{3}{2}}} = 0 \tag{4.141}$$

or

$$\left(1+q^2-2q\cos 2\alpha\right)\varrho'' = 0, \quad \text{at } \zeta = \pm 1. \tag{4.142}$$

If $q = 1$ and $\alpha = 0, \pi$ then ϱ'' could be anything, but if $q \neq 1$ and again $\alpha = 0, \pi$ then $\varrho'' = 0$. In the case that $q = 1$ and $\alpha \neq 0$ or π then $\varrho'' = 0$ (or $q = -1, \alpha = \frac{\pi}{2}$) perfect

alignment along end to end.

4.6.2 Derivation of the dimensionless equilibrium equations in Hamilton form

We use Hamilton's equation to derive the dimensionless equilibrium equations as an alternative to Lagrange's equations (4.131)-(4.133), which take the form of second order differential equation. The Hamiltonian equation we need to derive for our case is of the form,

$$\hat{H} = P_1 q' + P_2 \alpha' + P_3 \varrho' + P_4 \varrho'' - w. \tag{4.143}$$

Let us introduce the following eight variables,

$$Q_1 = q\,, \quad P_1 = \frac{\partial w}{\partial q'}, \qquad Q_2 = \alpha\,, \quad P_2 = \frac{\partial w}{\partial \alpha'}, \tag{4.144}$$

$$Q_3 = \varrho\,, \quad P_3 = \frac{\partial w}{\partial \varrho'} - \frac{d}{d\zeta}\left(\frac{\partial w}{\partial \varrho''}\right), \qquad Q_4 = \varrho'\,, \quad P_4 = \frac{\partial w}{\partial \varrho''}. \tag{4.145}$$

In order to obtain (4.143) we do the following calculations using the energy density given in (4.134), so we find

$$P_1 = \frac{\kappa\, q'}{\xi^2 + \varrho'^2}\, \varrho \sqrt{\xi^2 + \varrho'^2},$$

that gives

$$q' = \frac{P_1}{\kappa Q_3} \left(\xi^2 + Q_4^2\right)^{\frac{1}{2}}, \tag{4.146}$$

then we get

$$P_2 = \frac{4q^2 \alpha' \varrho \left(\xi^2 + \varrho'^2\right)^{\frac{1}{2}}}{\xi^2 + \varrho'^2},$$

so that

$$\alpha' = \frac{p_2}{4\, Q_1^2 Q_3 \kappa} \left(\xi^2 + \varrho'^2\right)^{\frac{1}{2}}, \tag{4.147}$$

and

$$P_4 = \frac{\varrho'' \kappa \xi^2}{\left(\xi^2 + \varrho^2\right)^3} \left(1 + q^2 - 2q \cos 2\alpha\right) \varrho \left(\xi^2 + \varrho'^2\right)^{\frac{1}{2}}$$

therefore

$$\varrho'' = \frac{P_4}{\kappa \xi^2 Q_3} \frac{\left(\xi^2 + Q_4^2\right)^{\frac{5}{2}}}{\left(1 + Q_1^2 - 2Q_1 \cos 2\, Q_2\right)}. \tag{4.148}$$

The Hamiltonian becomes

$$\hat{H} = Q_3 \left(Q_4^2 + \xi^2\right)^{\frac{1}{2}} \left(-1 - \frac{A}{2} Q_1^2 - \frac{C}{4} Q_1^4 + \frac{1}{2\kappa} \frac{p_1^2}{Q_3^2} + \frac{1}{8} \frac{p_2^2}{Q_1^2 Q_3^2 \kappa} - \frac{2\kappa Q_1^2 Q_4^2}{Q_3^2 \left(Q_4^2 + \xi^2\right)} \right.$$
$$\left. + \frac{p_4^2 \left(Q_4^2 + \xi^2\right)^2}{2\kappa \xi^2 Q_3^2 \left(1 + Q_1^2 - 2\, Q_1 \cos 2\, Q_2\right)} - \frac{\kappa \xi^2}{2 Q_3^2 \left(Q_4^2 + \xi^2\right)} \left(1 + Q_1^2 + 2\, Q_1 \cos 2 Q_2\right) \right) + p_3\, Q_4. \tag{4.149}$$

In other word, the function $\hat{H}$ is equal to the total energy of the system with no explicit dependence on the Q_i'.

In such a way, solving the boundary value problem (4.131)-(4.133) is equivalent to solving the following system of first order ODEs

$$Q_i' = \frac{\partial \hat{H}}{\partial P_i}, \quad P_i' = -\frac{\partial \hat{H}}{\partial Q_i} \quad (i = 1, 2, 3, 4)\,. \tag{4.150}$$

so that

$$Q_1' = \frac{P_1}{\kappa\, Q_3} \sqrt{Q_4^2 + \xi^2}, \qquad Q_2' = \frac{P_2}{4\kappa\, Q_1^2 Q_3} \sqrt{Q_4^2 + \xi^2}, \tag{4.151}$$

$$Q_3' = Q_4, \qquad Q_4' = \frac{P_4 \left(Q_4^2 + \xi^2\right)^{\frac{5}{2}}}{\kappa\, \xi^2\, Q_3 \left(1 - 2 Q_1 \cos 2 Q_2 + Q_1^2\right)} \tag{4.152}$$

and

$$P_1' = \frac{P_2^2 \left(\xi^2 + Q_4^2\right)^{\frac{1}{2}}}{4\kappa\, Q_3 Q_1^3} + \frac{P_4^2 \left(\xi^2 + Q_4^2\right)^{\frac{5}{2}}}{2\kappa\, \xi^2\, Q_3} \frac{\left(-2 \cos 2 Q_2 + 2 Q_1\right)}{\left(1 - 2 Q_1 \cos 2 Q_2 + Q_1^2\right)^2} + \frac{4\kappa Q_1 Q_4^2}{Q_3 \left(\xi^2 + Q_4^2\right)^{\frac{1}{2}}}$$
$$+ A\, Q_1\, Q_3 \left(\xi^2 + Q_4^2\right)^{\frac{1}{2}} + C Q_1^3 Q_3 \left(\xi^2 + Q_4^2\right)^{\frac{1}{2}} + \frac{\kappa\, \xi^2 \left(2 \cos 2 Q_2 + 2 Q_1\right)}{2 Q_3 \left(\xi^2 + Q_4^2\right)^{\frac{1}{2}}} \tag{4.153}$$

$$P_2' = \frac{2 P_4^2 \left(\xi^2 + Q_4^2\right)^{\frac{5}{2}} \left(Q_1 \sin 2 Q_2\right)}{\kappa\, \xi^2 Q_3 \left(1 - 2 Q_1 \cos 2 Q_2 + Q_1^2\right)^2} - \frac{2\kappa\, \xi^2 \left(Q_1 \sin 2 Q_2\right)}{Q_3 \left(\xi^2 + Q_4^2\right)^{\frac{1}{2}}} \tag{4.154}$$

$$P_3' = \frac{A}{2} Q_1^2 \left(\xi^2 + Q_4^2\right)^{\frac{1}{2}} + \frac{C}{4} Q_1^4 \left(\xi^2 + Q_4^2\right)^{\frac{1}{2}} + \left(\xi^2 + Q_4^2\right)^{\frac{1}{2}} + \frac{P_1^2 \left(\xi^2 + Q_4^2\right)^{\frac{1}{2}}}{2\kappa\, Q_3^2} + \frac{P_2^2 \left(\xi^2 + Q_4^2\right)^{\frac{1}{2}}}{8\kappa\, Q_1^2 Q_3^2}$$
$$+ \frac{P_4^2 \left(\xi^2 + Q_4^2\right)^{\frac{5}{2}}}{2\kappa\, \xi^2 Q_3^2 \left(1 - 2 Q_1 \cos 2 Q_2 + Q_1^2\right)} - \frac{2\kappa\, Q_1^2 Q_4^2}{Q_3^2 \left(\xi^2 + Q_4^2\right)^{\frac{1}{2}}} - \frac{\kappa\, \xi^2 \left(1 + 2 Q_1 \cos 2 Q_2 + Q_1^2\right)}{2 Q_3^2 \left(\xi^2 + Q_4^2\right)^{\frac{1}{2}}} \tag{4.155}$$

$$P_4' = -\frac{P_1^2 Q_4}{2\kappa\, Q_3\,(\xi^2+Q_4^2)^{\frac{1}{2}}} - \frac{P_2^2\, Q_4}{8\kappa\, Q_1^2 Q_3\,(\xi^2+Q_4^2)^{\frac{1}{2}}} - \frac{5P_4^2 Q_4\,(\xi^2+Q_4^2)^{\frac{3}{2}}}{2\kappa\,\xi^2 Q_3\,(1-2Q_1\cos 2Q_2+Q_1^2)} - \frac{\kappa\,\xi^2 Q_4\,(1+2Q_1\cos 2Q_2+Q_1^2)}{2Q_3\,(\xi^2+Q_4^2)^{\frac{3}{2}}} - P_3 + \frac{4\kappa\, Q_1^2 Q_4}{Q_3\,(\xi^2+Q_4^2)^{\frac{1}{2}}} - \frac{2\kappa\, Q_1^2\, Q_4^3}{Q_3\,(\xi^2+Q_4^2)^{\frac{3}{2}}} + \frac{Q_4\, Q_3\left(1+\frac{A}{2}Q_1^2+\frac{C}{4}Q_1^4\right)}{(\xi^2+Q_4^2)^{\frac{1}{2}}} \quad (4.156)$$

The boundary conditions are,

$$\varrho = 1 \text{ at } \zeta = \pm 1 \quad \text{so} \quad Q_3 = 1 \text{ at } \zeta = \pm 1. \quad (4.157)$$

Because of symmetry we have

$$\varrho' = 0 \text{ at } \zeta = 0 \quad \text{so} \quad Q_4 = 0 \text{ at } \zeta = 0. \quad (4.158)$$

Also we have

$$q' = 0 \text{ at } \zeta = \pm 1 \quad \text{so} \quad P_1 = 0 \text{ at } \zeta = \pm 1. \quad (4.159)$$

And

$$q^2\alpha' = 0 \text{ at } \zeta = 1 \quad \text{so} \quad P_2 = 0 \text{ at } \zeta = \pm 1. \quad (4.160)$$

Also because of symmetry we have

$$P_2 = 0 \text{ at } \zeta = 0, \quad (4.161)$$

and

$$P_3 = 0 \text{ at } \zeta = 0. \quad (4.162)$$

Also

$$P_4 = 0 \text{ at } \zeta = \pm 1. \quad (4.163)$$

In terms of the new variables $Q's$ and $P's$, the energy reads

$$W = 2\pi\gamma r^2 \int_{-1}^{1} \hat{w}\, d\zeta, \quad (4.164)$$

where

$$\hat{w} = \left(1 + \frac{p_1^2}{2\kappa Q_3^2} + \frac{p_2^2}{8\kappa Q_1^2 Q_3^2} + \frac{2\kappa Q_1^2 Q_4^2}{Q_3^2\,(Q_4^2+\xi^2)} + \frac{p_4^2\,(Q_4^2+\xi^2)^2}{2\kappa\,\xi^2\, Q_3^2\,(1+Q_1^2-2Q_1\cos 2Q_2)} + \frac{\kappa\,\xi^2\,(1+Q_1^2+2Q_1\cos 2Q_2)}{2Q_3^2\,(Q_4^2+\xi^2)} + \frac{A}{2}Q_1^2 + \frac{C}{4}Q_1^4\right) Q_3\sqrt{Q_4^2+\xi^2}. \quad (4.165)$$

Observations

The director equation for α is given by

$$\frac{d}{d\zeta}\left(\frac{\partial w}{\partial \alpha'}\right) - \frac{\partial w}{\partial \alpha} = 0 \tag{4.166}$$

$$\frac{d}{d\zeta}\left[\frac{4\kappa\, q^2 \alpha' \varrho}{(\xi^2+\varrho'^2)^{\frac{1}{2}}}\right] + \frac{2\kappa\, q\xi^2}{\varrho\,(\xi^2+\varrho'^2)^{\frac{5}{2}}}\left(\left(\xi^2+\varrho'^2\right)^2 - \varrho^2\varrho''^2\right)\sin 2\alpha = 0. \tag{4.167}$$

We note that (4.167) is automatically satisfied when $q = 0$. As discussed previously, the solution $q = 0$ is a solution of the equilibrium equation for q only when the surface has the property that $H = 0$ or $\varsigma = 0$. In our context of a film suspended between two coaxial rings this means either a catenoid or part of a sphere truncated at the two rings. However neither of these surfaces satisfies the boundary conditions for the shape equation, so we conclude that q cannot be zero everywhere for a solution of the equilibrium equations. We can however make more progress by observing that another solution of (4.167) is $\alpha = 0$ or $\alpha = \pi/2$. These solutions correspond to perfect alignment along the meridians ($\alpha = \pi/2$, along the surface between the rings) or circumferentially ($\alpha = 0$). We can use this observation to search for special solutions when $\alpha = 0$ or where $\alpha = \pi/2$, by substituting $Q_2 = 0$ or $Q_2 = \pi/2$ and $P_2 = 0$ in equations (4.151)-(4.156).

The following figures showing solution branches for the axisymmetric equilibrium solutions for $\alpha = 0$ and $\alpha = \pi/2$. We vary the parameter A for $\alpha = \pi/2$ and vary κ for $\alpha = 0$ and give a specific values for the other parameters ((ξ, C, κ) for $\alpha = \pi/2$ and (ξ, A, C) for $\alpha = 0$). This involves plotting the surface and the value of q and also the energy of solution branches. We should note that q positive for $\alpha = \pi/2$ is the same as q negative for $\alpha = 0$. If q is a solution for $\alpha = \pi/2$ then $-q$ is a solution for $\alpha = 0$. For the first set of parameters we need to prepare an initial guess for the solution. For the other parameters we will assume that the solution from using the previous set of parameters is a good guess for the solution for the next set of parameters. We vary only one of the parameters between the different sets of parameter values.

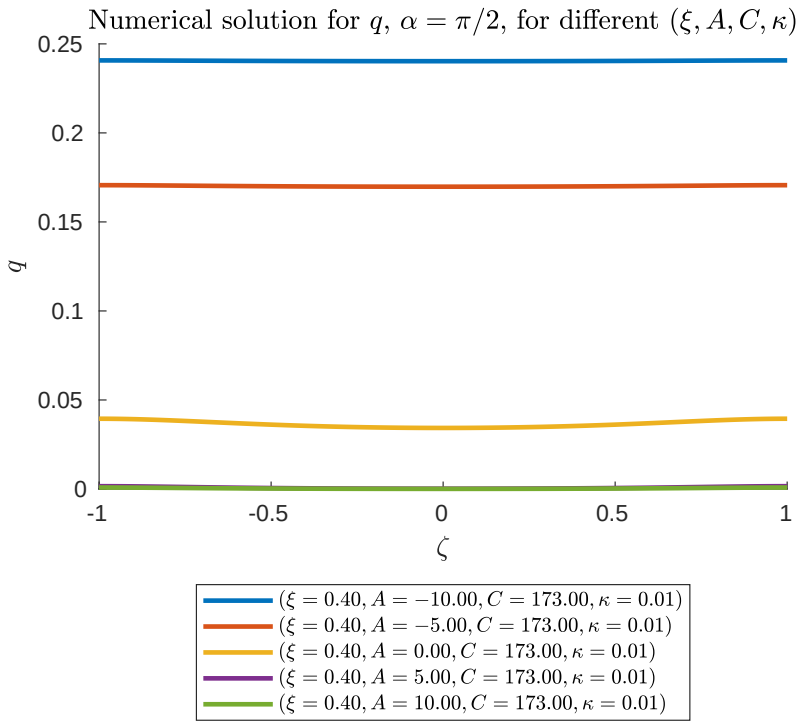


Figure 4.10: Types of solutions for q when $\alpha = \pi/2$ where we give specific values of the parameters (ξ, C, κ) and vary the parameter A.

It is clear that from figure 4.10 we have q is positive. The following figure 4.11 shows that as we increase the parameter A (get warmer) and starts to melt we get closer to the catenoid solution.

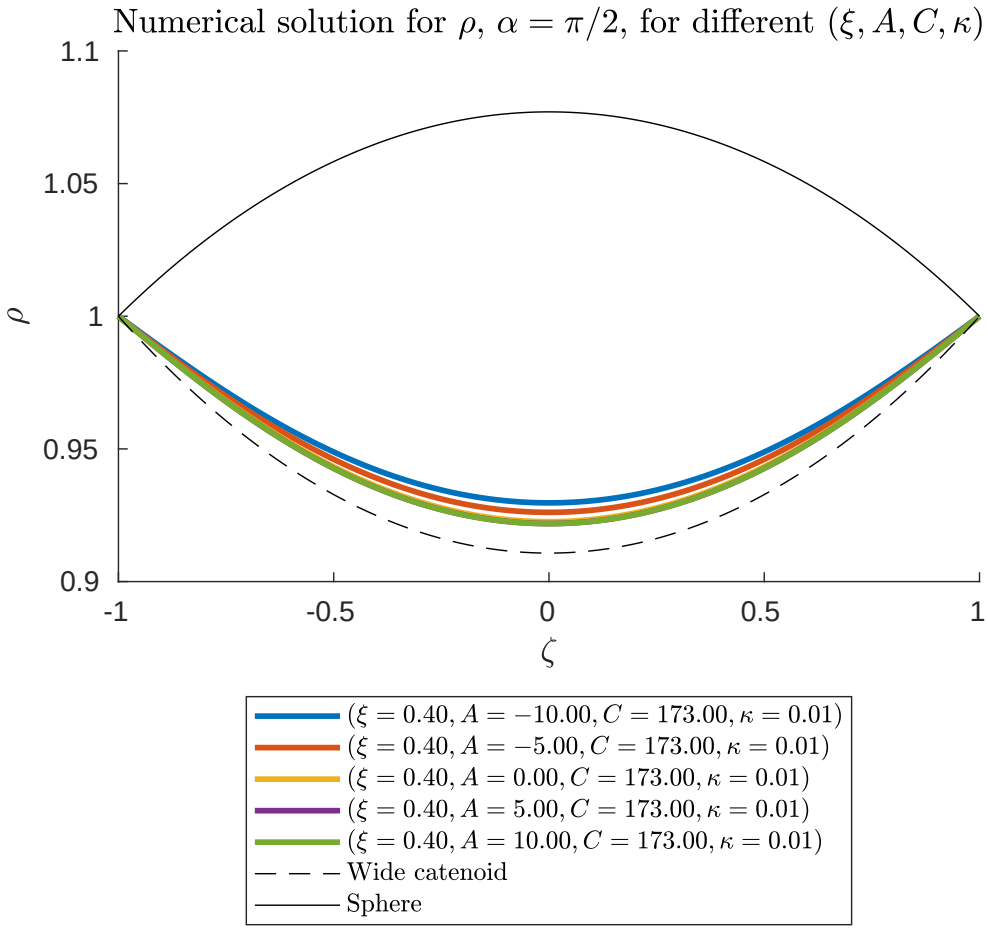


Figure 4.11: Types of solutions for ρ when $\alpha = \pi/2$ where we give specific values of the parameters (ξ, C, κ) and vary the parameter A.

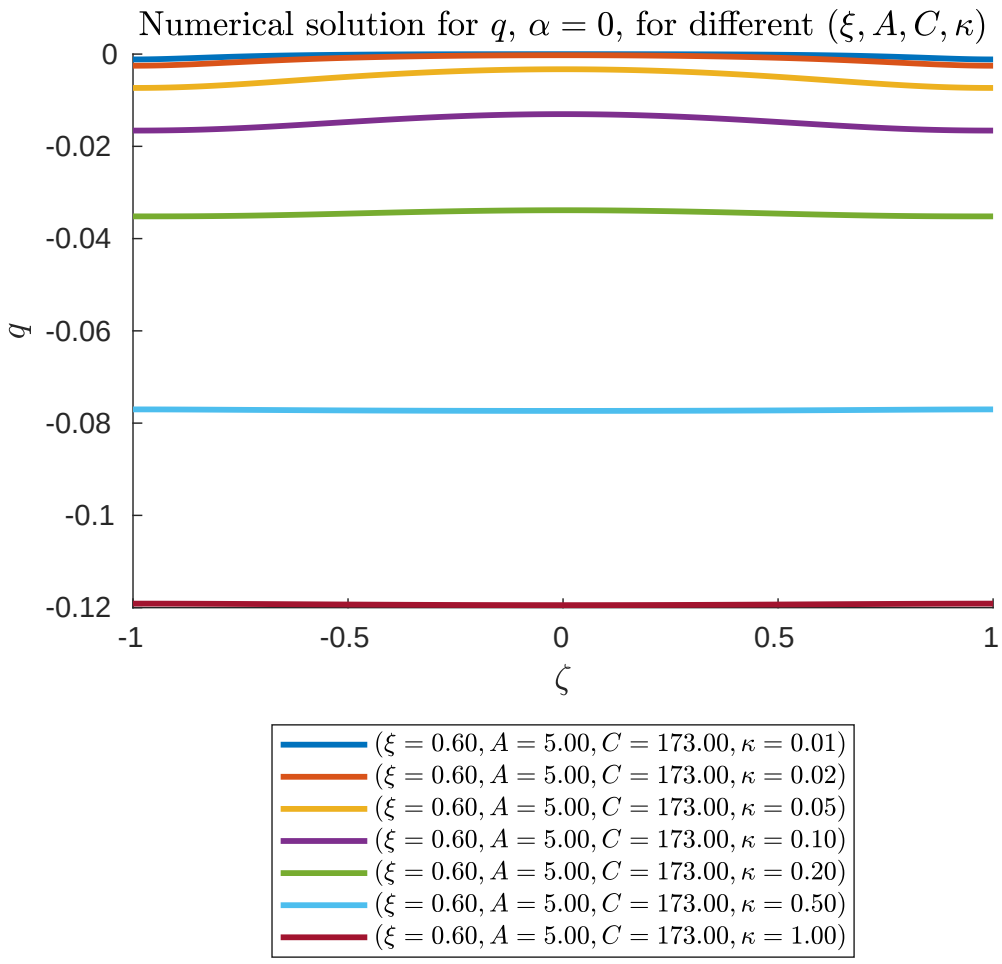


Figure 4.12: Types of solutions for q when $\alpha = 0$ where we give specific values of the parameters (ξ, A, C) and vary the parameter κ. So here, for a fixed temperature (fixed value of A) and increasing κ we use that $q < 0$ (with $\alpha = 0$), meaning alignment along the meridians, and for the trend in q (leads to greater orders as κ increases because $|q|$ increases).

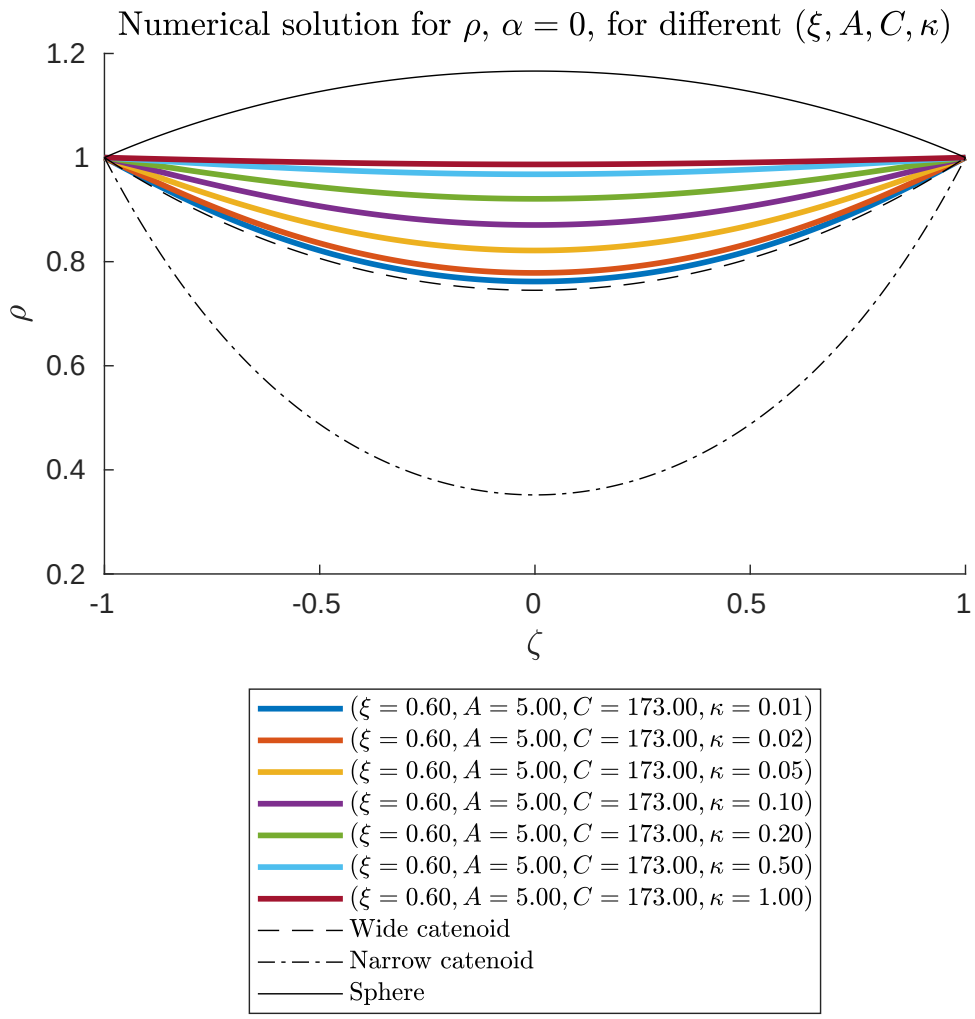


Figure 4.13: Types of solutions for ρ when $\alpha = 0$ where we give specific values of the parameters (ξ, A, C) and vary the parameter κ.

As you see from the Figure 4.12 we get q is negative with $\alpha = 0$ which means that all the molecules are aligned from end to end because $\alpha = 0$ is going around in $\mathbf{e}_\theta$ direction. As we vary κ, increasing κ the minimum energy solution has some molecules aligned for $A = 5$ and aligned from end to end (molecules are lying along the cylinder). For small κ, the molecules are bending (going down the surface and up in the other side) so in order to minimise the surface energy the molecules are not bend at all.

A special solution when $\varrho = 1$

We investigate a special solution when $\varrho = 1$, giving a relationship between A and Q that can be used to check the performance of our numerical work. In other words we are finding the special value of A where a cylinder is the solution.

We substitute $\varrho = 1$, $\alpha = 0$ and constant $q = Q$ into the equilibrium equations and ask what equations must be satisfied. The calculations are similar to §4.6.2. We substitute $Q_2 = 0$, $Q_1 = Q$ a constant, $Q_3 = 1$ and $Q_4 = 0$, $P_1 = 0$, $P_2 = 0$, $P_3 = 0$ and $P_4 = 0$. The differential equations are all automatically satisfied, except for the differential equations for P_1 and P_3. In order for the proposed solution to solve these equations we must have

$$A\,Q\;\xi + C\,Q^3\,\xi + \frac{\kappa\,\xi^2(Q+1)}{2\xi} = 0$$
$$\frac{A}{2}Q^2\xi + \frac{C}{4}Q^4\xi + \xi - \frac{\kappa\,\xi^2\,(Q+1)^2}{2\,\xi} = 0$$

This pair of equations can be simplified

$$A\,Q\; + C\,Q^3\; + \kappa(Q+1) = 0 \tag{4.168}$$
$$A\,Q^2 + \frac{C}{2}\,Q^4 + \;2 - \kappa\,(Q+1)^2 = 0 \tag{4.169}$$

To solve for Q, we multiply (4.168) by Q and subtract (4.169), getting

$$\frac{C}{2}\,Q^4 \;+\; \kappa\left(2Q^2{+}3Q+1\right) - 2 = 0 \tag{4.170}$$

Given C and κ we can solve this equation numerically and then calculate the value of A, recalling that Q should lie in the interval $[-1/2, 1/2]$.

Comparing to the numerical solution found previously, we give an example calculation when a cylinder is found. Figure 4.14 shows the values of $(A, \kappa, |Q|)$ for which a cylindrical solution exists.

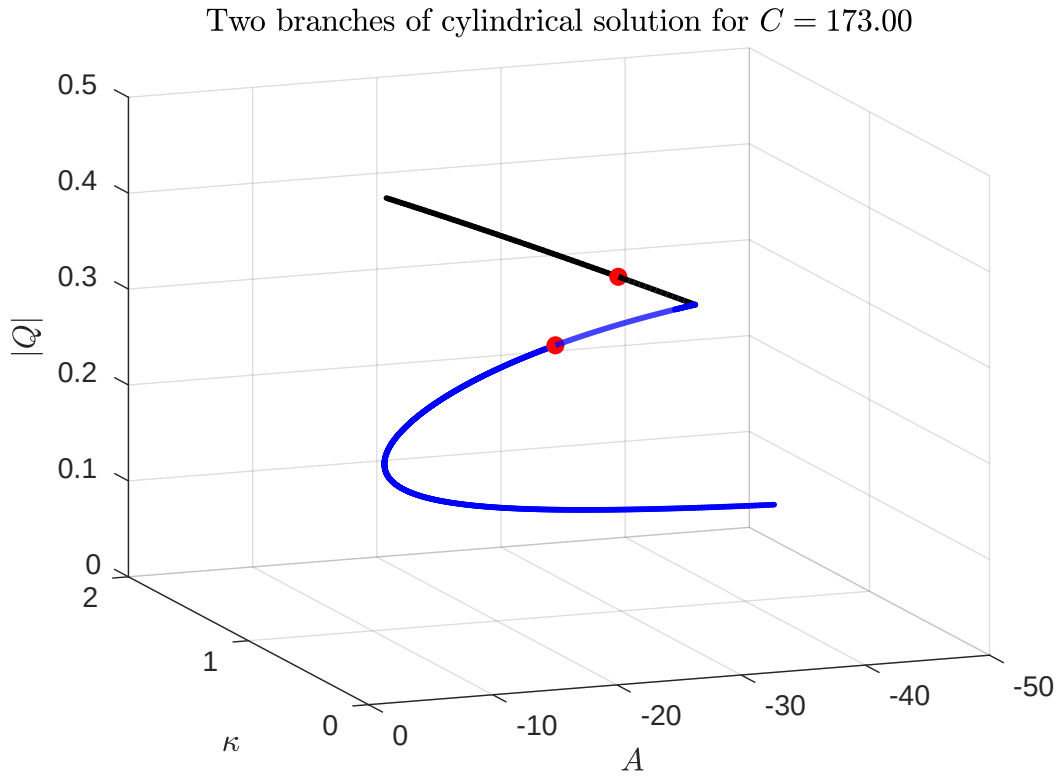


Figure 4.14: The cylindrical branches of solutions for fixed $C = 173$. The curves are two distinct branches of solution, one where $Q > 0$, $\alpha = 0$ (the black curve) and then other where $Q > 0$, $\alpha = \pi/2$ (the blue curve).

We compute numerically two solutions using q and α, one for $q < 0$ and the other one for $q > 0$. The first case when q is negative, we set $\kappa = 0.5087$, $A = -25.0279$ and $C = 173$. Note that, the value of ξ should not matter for a cylindrical solution but we can set it at $\xi = 0.6$, this gives the branch of solution that has $\alpha = \pi/2$ (along the cylinder) and $|Q| = 0.3864$ (or $\alpha = 0$ and $Q = -0.3864$). These values are predicted from the branches of the special solutions and confirmed by the numerical solution plots given in Figure 4.15.

The second case represents the solution for $q > 0$, we set $\kappa = 0.4992$, $A = -19.87$ and $C = 173$, this gives the branch with $\alpha = 0$ (aligned around) of cylindrical solution with $Q = 0.3209$. These values are predicted from the branches of the special solution and confirmed by the numerical solution plots given in Figure 4.16.

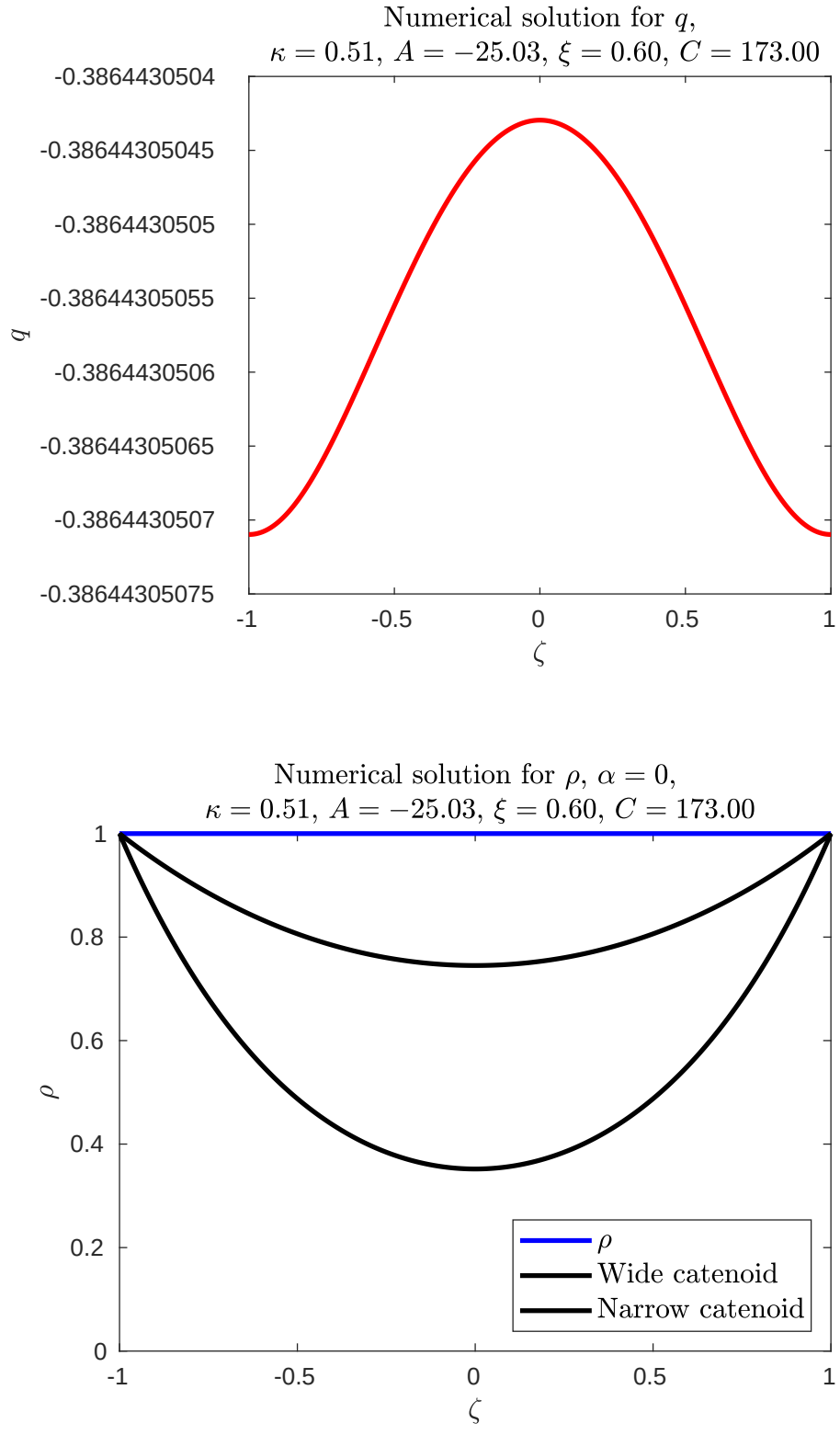


Figure 4.15: The first plot represents the numerical solution for q (when $q < 0$). The second plot represents the numerical solution for ρ when $\alpha = 0$, where we give specific values of the parameters (κ, A, ξ, C).

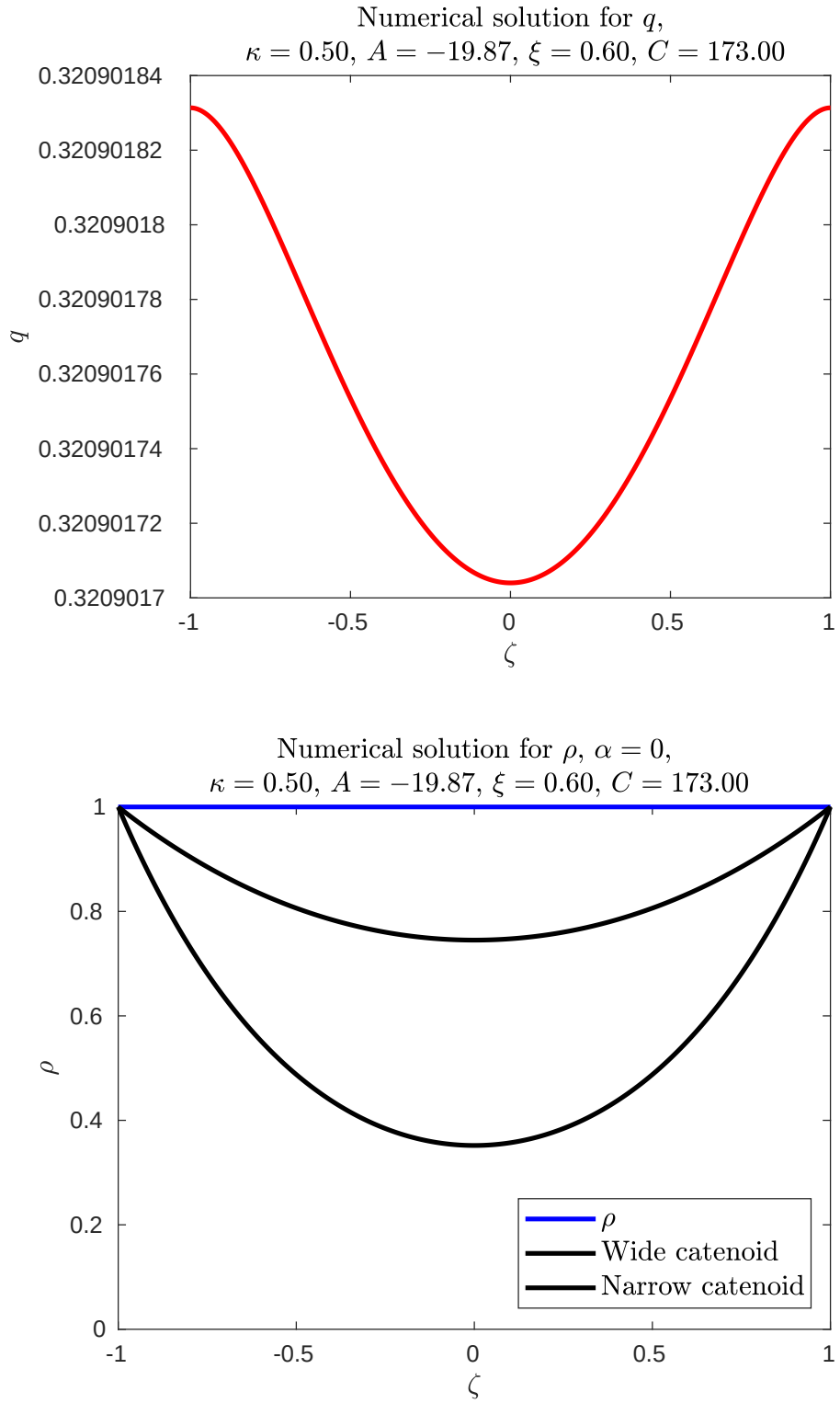


Figure 4.16: The first plot represents the numerical solution for q (when $q > 0$). The second plot represents the numerical solution for ρ when $\alpha = 0$, where we give specific values of the parameters (κ, A, ξ, C).

4.7 Stability of the isotropic distribution on the fixed geometry of the catenoid

In this section we consider the stability of the isotropic distribution by fixing the geometry (no shape equation or boundary condition for shape) of the catenoid ($H = 0$) and understand how q_0 and q_m are affected. We know that $q_0 = q_m = 0$ is a solution to the equilibrium equations in this case. Our interest here is stability and predicting the change of melting temperature. We calculate the change to the melting temperature as a function of the geometry of the film (the aspect ratio). Also we consider the structure of the solution at onset of nematic order and identify defects and their locations.

To derive the equilibrium equations for q_0 and q_m we consider the form of $\frac{1}{2}k\left|\nabla_s \mathbf{M}\right|^2$ given in (4.35), we obtain the surface energy density

$$\begin{aligned} w = \gamma + k\big[&\left|\nabla_s q_0\right|^2 + \left|\nabla_s q_m\right|^2 + \left(q_0^2 + q_m^2\right)\left(4\left|\boldsymbol{\omega}\right|^2 + 2\left(2H^2 - K\right)\right) \\ &+ 4\left(q_0\nabla_s q_m - q_m\nabla_s q_0\right)\cdot\boldsymbol{\omega} + \frac{1}{2}\left(2H^2 - K\right) + 4\,q_0 H\varsigma\big] + \frac{a}{2}\left(q_0^2 + q_m^2\right) + \frac{c}{2}\left(q_0^2 + q_m^2\right)^2. \end{aligned} \tag{4.171}$$

Let

$$a_0 = \frac{\partial w}{\partial q_0} \quad \text{and} \quad \mathbf{b}_0 = \frac{\partial w}{\partial \nabla_s q_0},$$

so that

$$a_0 = k\left[2q_0\left(4\left|\boldsymbol{\omega}\right|^2 + 2\left(2H^2 - K\right)\right) + 4\boldsymbol{\omega}\cdot\nabla_s q_m + 4H\varsigma\right] + aq_0 + cq_0\left(q_0^2 + q_m^2\right), \tag{4.172}$$

and

$$\mathbf{b}_0 = k\left[2\nabla_s q_0 - 4\boldsymbol{\omega}q_m\right]. \tag{4.173}$$

Similarly we let

$$a_m = \frac{\partial w}{\partial q_m} \quad \text{and} \quad \mathbf{b}_m = \frac{\partial w}{\partial \nabla_s q_m},$$

so that

$$a_m = k\left[2q_m\left(4\left|\boldsymbol{\omega}\right|^2 + 2\left(2H^2 - K\right)\right) + 4\boldsymbol{\omega}\cdot\nabla_s q_0 + 4H\zeta\right] + aq_m + cq_m\left(q_0^2 + q_m^2\right), \tag{4.174}$$

and

$$\mathbf{b}_m = k\left[2\nabla_s q_m + 4\boldsymbol{\omega}q_0\right]. \tag{4.175}$$

Note that $\mathbf{b}_{0s} = \mathbf{P}\mathbf{b}_0 = k\left(2\nabla_s q_0 - 4\boldsymbol{\omega}_s q_m\right)$ and $\mathbf{b}_{ms} = \mathbf{P}\mathbf{b}_m = k\left(2\nabla_s q_m + 4\boldsymbol{\omega}_s q_0\right)$ where

$\boldsymbol{\omega}_s = \boldsymbol{\omega}$ ($\boldsymbol{\omega}$ is tangential). We obtain the equilibrium equations

$$\operatorname{div}_s\left[\nabla_s q_0 - 2\boldsymbol{\omega}_s q_m\right] - q_0\left(4\left|\boldsymbol{\omega}\right|^2 + 2\left(2H^2 - K\right)\right) - 2\boldsymbol{\omega}\cdot\nabla_s q_m - 4H\varsigma - \frac{a}{2k}q_0 - \frac{c}{2k}q_0\left(q_0^2 + q_m^2\right) = 0 \quad (4.176)$$

$$\operatorname{div}_s\left[\nabla_s q_m + 2\boldsymbol{\omega}_s q_m\right] - q_m\left(4\left|\boldsymbol{\omega}\right|^2 + 2\left(2H^2 - K\right)\right) + 2\boldsymbol{\omega}\cdot\nabla_s q_0 - \frac{a}{2k}q_m - \frac{c}{2k}q_m\left(q_0^2 + q_m^2\right) = 0. \quad (4.177)$$

For the full problem we have two equilibrium equations and also the shape equation but since we freeze the geometry (fixed) we have only equations (4.176) and (4.177). The isotropic solution is when $q_0 = q_m = 0$ so from the equilibrium equation we deduce that the only solution if $H\varsigma = 0$ so either $H = 0$ (catenoid) or $\varsigma = 0$ (sphere or part of). Hence we fix geometry as a catenoid (minimal surface).

For the boundary conditions, recall that $\mathbf{k}$ is the outward unit normal to ∂S, $\mathbf{k}\cdot\mathbf{l} = 0$ ($\mathbf{l}$ is tangent to the boundary) on ∂S and in tangent plane $\mathbf{k}\cdot\boldsymbol{\nu} = 0$. Thus the *boundary conditions* are

$$\mathbf{k}\cdot\left[\nabla_s q_0 - 2\boldsymbol{\omega} q_m\right] = 0, \quad (4.178)$$

$$\mathbf{k}\cdot\left[\nabla_s q_m + 2\boldsymbol{\omega} q_0\right] = 0. \quad (4.179)$$

Note that $\boldsymbol{\omega}\cdot\mathbf{k} = 0$ in the case of axisymmetry of S, so $\mathbf{k}\cdot\nabla_s q_0 = 0$ and $\mathbf{k}\cdot\nabla_s q_m = 0$.

4.7.1 Incremental equations of the isotropic distribution

Having established that $q_0 = q_m = 0$ is a solution when the geometry is fixed ($H = 0$), we now consider stability. We derive the incremental equations and solve them numerically for the most unstable mode. We let ψ_0 and ψ_m be the increments of q_0 and q_m respectively. The incremental equations are

$$\operatorname{div}_s\left[\nabla_s\psi_0 - 2\boldsymbol{\omega}_s\psi_m\right] - \psi_0\left[4\left|\boldsymbol{\omega}\right|^2 + 2\left(2H^2 - K\right)\right] - 2\boldsymbol{\omega}\cdot\nabla_s\psi_m - \frac{a}{2k}\psi_0 = 0, \quad (4.180)$$

$$\operatorname{div}_s\left[\nabla_s\psi_m - 2\boldsymbol{\omega}_s\psi_0\right] - \psi_m\left[4\left|\boldsymbol{\omega}\right|^2 + 2\left(2H^2 - K\right)\right] - 2\boldsymbol{\omega}\cdot\nabla_s\psi_0 - \frac{a}{2k}\psi_m = 0. \quad (4.181)$$

The increment of

$$\delta\left[q_0\left(q_0^2 + q_m^2\right)\right] = \psi_0\left(q_0^2 + q_m^2\right) + 2q_0\left(q_0\psi_0 + q_m\psi_m\right) = \psi_0\left(3q_0^2 + q_m^2\right) + 2q_0\, q_m\psi_m,$$

but since we are interested in stability of the solution $q_0 = q_m = 0$ then this term is zero in the incremental equations and it is the same for the increment of $\delta\left[q_m\left(q_0^2 + q_m^2\right)\right]$. The

incremental boundary conditions are

$$\mathbf{k}\cdot[\nabla_s\psi_0 - 2\boldsymbol{\omega}\psi_m] = 0, \qquad \mathbf{k}\cdot[\nabla_s\psi_m + 2\boldsymbol{\omega}\psi_0] = 0, \tag{4.182}$$

(since $\mathbf{k}$ and $\boldsymbol{\omega}$ are fixed). We introduce the complex variable ψ so that $\psi = \psi_0 + i\psi_m$. A single complex incremental equation in terms of ψ represents both incremental equations (4.180) and (4.181) and reads

$$\mathrm{div}_s\left[\nabla_s\psi + i\,2\boldsymbol{\omega}\psi\right] - \psi\left[4\left|\boldsymbol{\omega}\right|^2 + 2\left(2H^2 - K\right)\right] - 2\,i\boldsymbol{\omega}\cdot\nabla_s\psi - \frac{a}{2k}\psi = 0. \tag{4.183}$$

and the boundary condition

$$\mathbf{k}\cdot[\nabla_s\psi + 2\,i\boldsymbol{\omega}\psi] = 0. \tag{4.184}$$

On this surface the catenoid has $\boldsymbol{\omega}\cdot\mathbf{k} = 0$ at the boundary as $\mathbf{k}$ is pointing in the $\mathbf{e}_\theta$ direction and $\boldsymbol{\omega} = \omega_\theta\mathbf{e}_\theta$ where $\boldsymbol{\omega}$ depends on z and goes in $\mathbf{e}_\theta$ direction. Also $\mathbf{k}\cdot\nabla_s\psi = 0$ at the boundary. Now we can rewrite (4.183) to be

$$\Delta_s\psi + 2\,i\left(\mathrm{div}_s\,\boldsymbol{\omega}_s\right)\psi + 4\,i\,\boldsymbol{\omega}_s\nabla_s\psi - \psi\left[4\left|\boldsymbol{\omega}\right|^2 + 2\left(2H^2 - K\right)\right] = \frac{a}{2k}\psi. \tag{4.185}$$

Define

$$L\left[\psi\right] = \mathrm{div}_s\left(\nabla_s\psi\right) + 2\,i\left(\mathrm{div}_s\,\boldsymbol{\omega}_s\right)\psi + 4\,i\,\boldsymbol{\omega}_s\nabla_s\psi - \psi\left[4\left|\boldsymbol{\omega}\right|^2 + 2\left(2H^2 - K\right)\right] \tag{4.186}$$

We need to write (4.185) as a linear operator $L\left[\psi\right] = \lambda\,\psi$. We now show that this operator is self-adjoint. Recall that the adjoint operator $L^\dagger$ is such that $\langle\phi, L\psi\rangle = \left\langle L^\dagger\phi, \psi\right\rangle$ for all ϕ, ψ,

$$\langle\phi,\psi\rangle = \int\int \phi^*\psi\,dz\,d\theta = \int_S \phi^*\psi\,dS.$$

If $L^\dagger = L$ then called self-adjoint and the eigenvalues are real. To show self-adjointness of L we need to find $\int_S \phi^*\,L\left[\psi\right]\,dS$ for $L\left[\psi\right]$ given in (4.186). For easier calculation we integrate each term separately,

$$\begin{aligned}\langle\phi, L\psi\rangle = \int_S \phi^*\ \mathrm{div}_s\left(\nabla_s\psi\right)\,dS &= \int_{\partial S}\phi^*\mathbf{k}\cdot\nabla_s\psi\,dl - \int_S \nabla_s\phi^*\cdot\nabla_s\psi\,dS \\ &= -\int_{\partial S}\psi\mathbf{k}\cdot\nabla_s\phi^*\,dl + \int_S \psi\,\mathrm{div}_s\left(\nabla_s\phi^*\right)\,dS.\end{aligned}$$

Note that $\mathbf{k}\cdot\nabla_s\psi = 0$ and $\psi\mathbf{k}\cdot\nabla_s\phi^* = 0$ (adjoint boundary condition). Next we have

$$\int_S \phi^*\left[-\psi\left(4\left|\boldsymbol{\omega}\right|^2 + 2\left(2H^2 - K\right)\right)\right] = \int_S \psi\left[-\phi\left(4\left|\boldsymbol{\omega}\right|^2 + 2\left(2H^2 - K\right)\right)\right]^*\,dS.$$

Then we consider

$$\int_S \phi^* \left(4\, i\, \boldsymbol{\omega}_s \nabla_s \psi\right)\, dS = -\int_S \left(4\, i\psi \left(\mathrm{div}_s\, \boldsymbol{\omega}_s\right) \phi^* + 4\, i\psi \boldsymbol{\omega}_s \cdot \nabla_s \phi^*\right) dS,$$

and the term $\int_S \phi^* \left(2\, i\, \mathrm{div}_s\, \boldsymbol{\omega}_s\right) \psi\, dS$ can be combined with the previous one. We end up with

$$\int_S (L\phi)^*\, \psi\, dS = \langle L\phi, \psi \rangle\,. \tag{4.187}$$

Thus $L = L^\dagger$ and $L\,[\psi]$ is self-adjoint and the eigenvalues are real. We want to reduce the problem to an eigenvalue problem, $L\psi = \frac{a}{2k}\psi$. In axisymmetric coordinates

$$L\,[\psi] = \frac{1}{r\left(1+r'^2\right)^{1/2}} \frac{\partial}{\partial z}\left(\frac{r}{\left(1+r'^2\right)^{1/2}} \frac{\partial \psi}{\partial z}\right) + \frac{1}{r^2}\frac{\partial^2 \psi}{\partial \theta^2} + 2\, i\, \frac{\omega_\theta}{r}\frac{\partial \psi}{\partial \theta} - \psi\left[4\left|\boldsymbol{\omega}\right|^2 + 2\left(2H^2 - K\right)\right] \tag{4.188}$$

where

$$\psi = \hat{\psi}\, e^{im\theta} \quad \text{and} \quad \frac{\partial \psi}{\partial \theta} = im\hat{\psi}\, e^{im\theta}, \tag{4.189}$$

and m is an integer, so that

$$\tilde{L}\left[\hat{\psi}\right] = \frac{1}{r\left(1+r'^2\right)^{1/2}} \frac{\partial}{\partial z}\left(\frac{r}{\left(1+r'^2\right)^{1/2}} \frac{\partial \hat{\psi}}{\partial z}\right) - \frac{m^2}{r^2}\hat{\psi} - \frac{2m\omega_\theta}{r}\hat{\psi} - \hat{\psi}\left[4\left|\boldsymbol{\omega}\right|^2 + 2\left(2H^2 - K\right)\right] \tag{4.190}$$

where

$$\frac{\partial \hat{\psi}}{\partial z} = 0 \quad \text{at the ends.} \tag{4.191}$$

Remember that $\boldsymbol{\omega} = \omega\, \mathbf{e}_\theta$ and with the spin connection given in (4.97), $\omega_\theta = \frac{-r'}{r(1+r'^2)^{1/2}}$, solve when are no trivial solutions to $\tilde{L}\hat{\psi} = a\hat{\psi}$. Let R_m be the minimum radius of the catenoid surface and $\rho = h/R_m$ be dimensionless reciprocal minimum radius. We scale radius with the minimum and scale z with h,

$$r\,(z) = R_m\, \cosh\left(\rho\, \zeta\right), \qquad r'\,(z) = \frac{1}{h} R_m\, \rho\, \sinh\left(\rho\, \zeta\right) \tag{4.192}$$

where $\zeta = z/h$. Now, we can write (4.190) as

$$\begin{aligned} \frac{1}{R_m\, \cosh^2\left(\rho\, z\right)} \frac{R_m}{h^2}\frac{\partial^2 \hat{\psi}}{\partial \zeta^2} - \frac{m^2}{R_m^2\, \cosh^2\left(\rho\, \zeta\right)}\hat{\psi} - \frac{2m}{R_m\, \cosh\left(\rho\, \zeta\right)}\left(-\frac{\sinh\left(\rho\zeta\right)}{R_m\, \cosh^2\left(\rho\, z\right)}\right)\hat{\psi} \\ - \left(4\,\frac{1}{R_m^2}\,\frac{\sinh^2(\rho\,\zeta)}{\cosh^4\left(\rho\,\zeta\right)} + 2\left(\frac{\rho}{h}\,\frac{\cosh\left(\rho\,\zeta\right)}{R_m\, \cosh^5\left(\rho\,\zeta\right)}\right)\right)\hat{\psi} = \frac{a}{2k}\,\hat{\psi}. \end{aligned} \tag{4.193}$$

Multiply by R_m^2, we get

$$\frac{1}{\rho^2}\frac{1}{\cosh^2(\rho\,\zeta)}\frac{\partial^2\hat{\psi}}{\partial\zeta^2}-\frac{m^2}{\cosh^2(\rho\,\zeta)}\hat{\psi}+2m\frac{\sinh(\rho\zeta)}{\cosh^3(\rho\,\zeta)}\hat{\psi}-\left(\frac{4\sinh^2(\rho\,\zeta)+2}{\cosh^4(\rho\,\zeta)}\right)\hat{\psi}=a2k\,R_m^2\,\hat{\psi}, \tag{4.194}$$

and multiply by ρ^2 we have

$$\frac{1}{\cosh^2(\rho\,\zeta)}\frac{d^2\hat{\psi}}{d\zeta^2}-\frac{m^2}{\cosh^2(\rho\,\zeta)}\hat{\psi}+2m\frac{\sinh(\rho\zeta)}{\cosh^3(\rho\,\zeta)}\hat{\psi}-\left(\frac{4\sinh^2(\rho\,\zeta)+2}{\cosh^4(\rho\,\zeta)}\right)\hat{\psi}=a\,R_m^2\,\rho^2\,\hat{\psi}=\left(\frac{ah^2}{2k}\right)\hat{\psi}. \tag{4.195}$$

We define $\bar{a}=ah^2/2k$. We need to discretise (4.195) to find the onset of order.

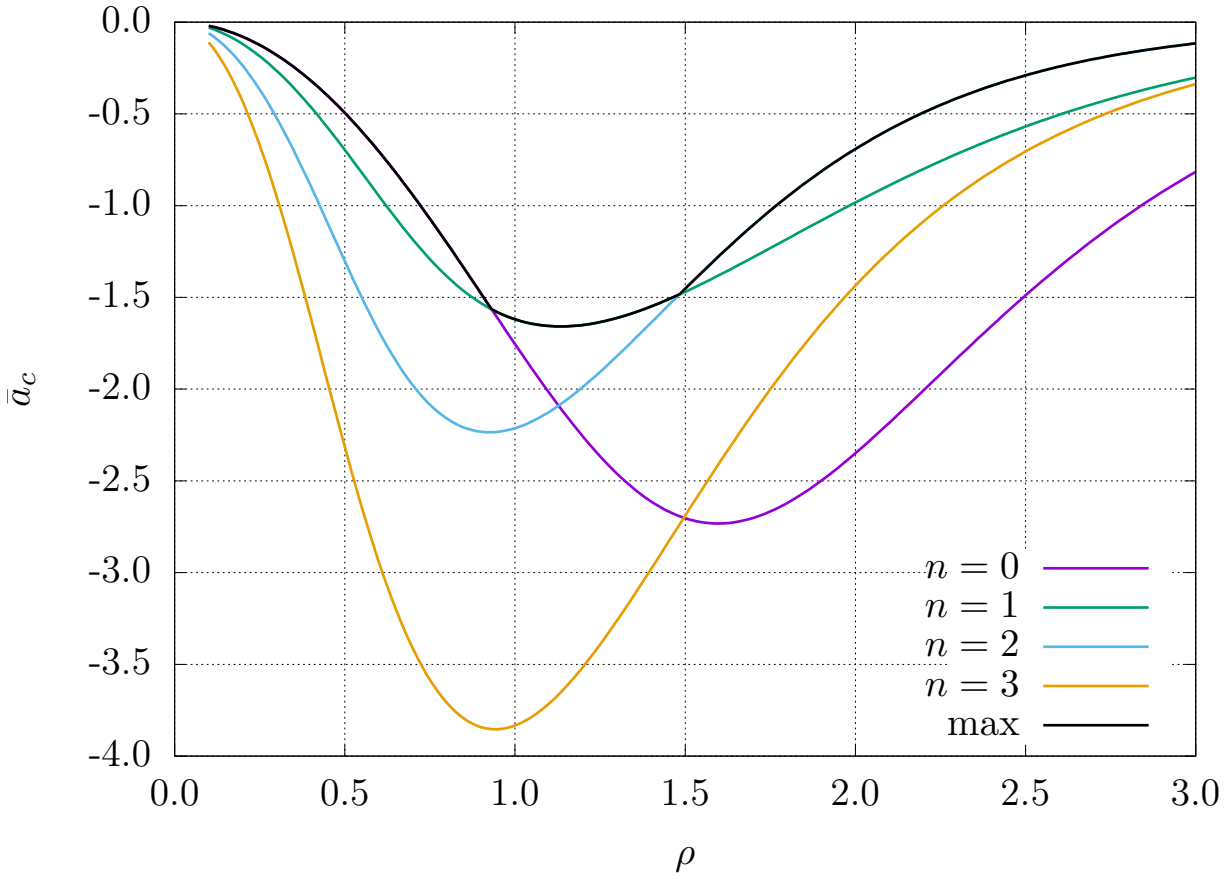


Figure 4.17: Plot of the critical value $\bar{a}_{c,n}$ against ρ for different mode numbers. The critical value of ρ is $\rho_c \approx 1.1996$. The wide catenoid is for $\rho < \rho_c$ and the narrow one is for for $\rho > \rho_c$.

Figure 4.17 shows that, depending on the aspect ratio of the catenoid (and whether the catenoid is narrow or wide) different mode numbers are unstable. In particular depending on the aspect ratio the isotropic distribution is unstable to perturbations with $n = 0$, $n = 1$ or $n = 2$. Having studied the linear stability we can now investigate the amplitude near onset by performing Lyapunov-Schmidt reduction (a weakly nonlinear analysis). Next section will provide more explanation and details about that.

Note that, in our investigation and in the range of ρ we considered, $n \geq 3$ is never the maximum.

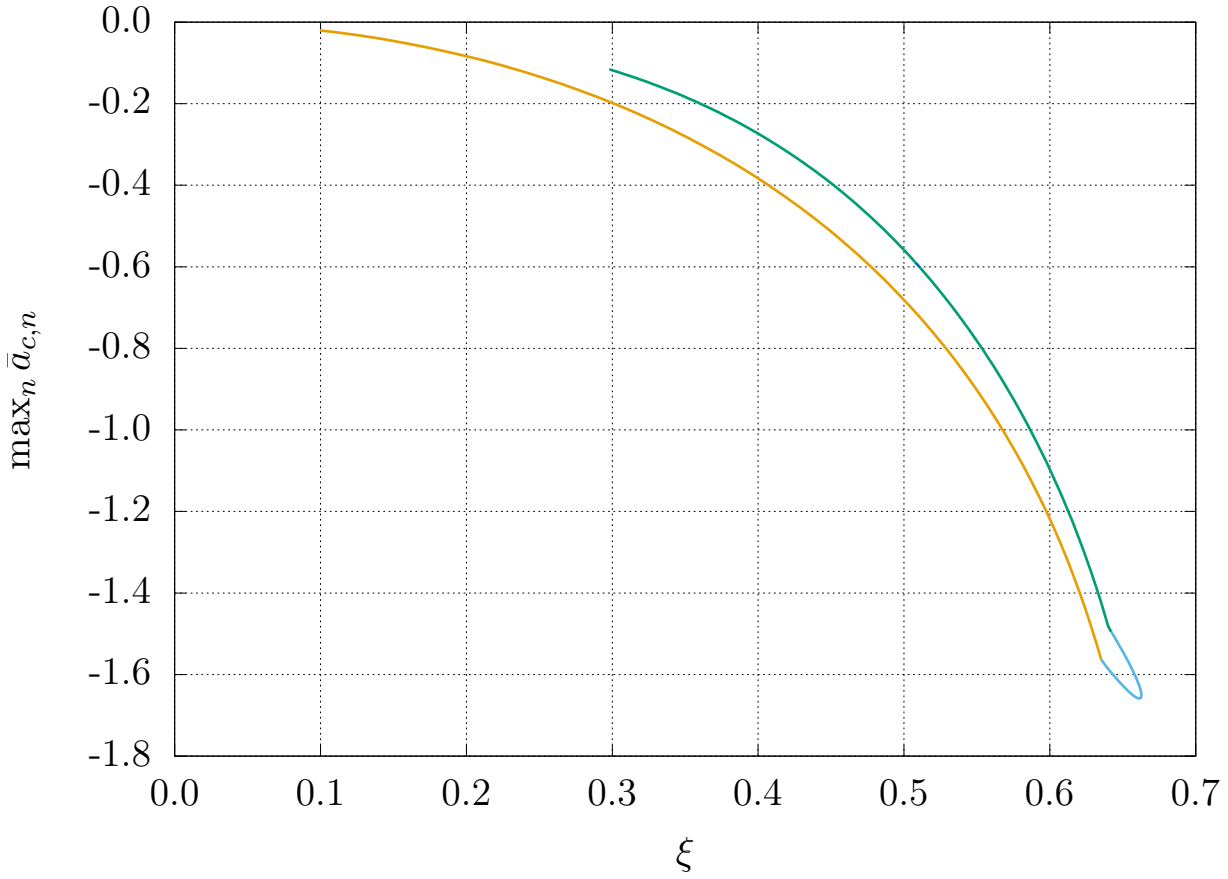


Figure 4.18: Plot of $\max_n \bar{a}_{c,n}$ against the aspect ratio ξ. Critical value of $\xi = \xi_c \approx 0.6627..$ and taking in the account that $\xi = \rho/\cosh\rho$, then wide catenoid is for $\xi < \xi_c$ and the narrow one is for for $\xi > \xi_c$. The narrow catenoid is the upper branch (the green one) and the wide catenoid is the lower branch (the yellow one) and the transition between the two modes is denoted by the blue colour.

In Figure 4.18, at the transition points between (yellow-blue) and (green-blue) branches there is a point where multiple modes are unstable. We have not analysed what the pattern looks like when the two modes become unstable at the same point.

4.8 Weakly non-linear analysis

On using the Lyapunov-Schmidt reduction ([45], [83]) we study the structure of the non-linear solution at the onset of order. For values of ρ for which $n = 0$ is the most unstable mode, our problem can be written

$$Lq = \bar{a}q + \bar{c}q\,|q|^2\,, \tag{4.196}$$

where also

$$LQ = \bar{a}_c\,Q, \tag{4.197}$$

and $Q(z)$ is the axisymmetric eigenfunction (corresponding to $n = 0$). Note that we take the combination of (4.176) $+i\times$ (4.177) to obtain (4.196) where $q = q_0 + i\,q_m$. . When $n \neq 0$ we will introduce eigenfunctions Q_+ and Q_- that correspond to the eigenfunctions for n and $-n$ respectively so that $L\left(Q_+e^{in\theta}\right) = \bar{a}_cQ_+e^{in\theta}$ and $L\left(Q_-e^{-in\theta}\right) = \bar{a}_cQ_-e^{-in\theta}$. The operator L is a linear operator where $q'(z) = 0$ at $z = \pm 1$ and, as we have shown, L is self-adjoint $\left(L = L^\dagger\right)$ with real eigenvalues and the eigenfunctions are orthogonal with respect to the following inner product

$$\langle\psi, \phi\rangle = \int_0^{2\pi}\int_{-1}^{1} c^2\psi^*\phi\,dz\,d\theta. \tag{4.198}$$

where $c = \cosh\rho z$.

The self-adjoint operator L is

$$Lq = \frac{1}{c^2}\left(\rho^2\,q_{\theta\theta} + q_{zz}\right) - 4\rho^2\,i\,\frac{s}{c^3}q_\theta - \rho^2\frac{2+4s^2}{c^4}q, \tag{4.199}$$

where ρ is the dimensionless reciprocal minimum radius, $c = \cosh\rho z$ and $s = \sinh\rho z$. The idea of Lyapunov-Schmidt reduction is to write the solution to the nonlinear problem when $\bar{a}$ is near the critical value $\bar{a}_c$ as some multiple of the eigenfunction Q plus some correction. This sometimes called a weakly nonlinear analysis. If a is very large then the only solution to our problem given in (4.196) is $q = 0$. Bifurcation is determined by whether there is a non-trivial solution to $Lq = \bar{a}q$, $q'(z) = 0$ at $z = \pm 1$. To find non-trivial solutions, we let $\bar{a} = \bar{a}_c + \epsilon^2\mu$ for some small parameter ϵ and $\mu = \pm 1$, then the formal expansion of q is written as

$$q = \epsilon AQ(z) + \epsilon^2 q_1 + \epsilon^3 q_2 + \ldots \tag{4.200}$$

where A is the unknown complex amplitude and q_1 and q_2 are in the orthogonal complement of the span of $\{Q(z)\}$. Now substitute (4.200) into (4.196), then compare at

different orders of ϵ. At order ϵ we have

$$LQ = \bar{a}_c Q \tag{4.201}$$

which is satisfied automatically by choice of Q. . At order ϵ^2 we have

$$Lq_1 = \bar{a}_c q_1 \tag{4.202}$$

since $q_n \in N^\perp$, $(L - \bar{a}_c \mathbf{I})\, q_n = 0$ implies that $q_n = 0$. At order ϵ^3 we have

$$Lq_2 = \bar{a}_c\, q_2 + AQ\mu + \bar{c}A\,|A|^2\, Q\,|Q|^2\,. \tag{4.203}$$

Since the operator is self-adjoint we have

$$\langle Q, L\phi\rangle = \langle LQ, \phi\rangle = \bar{a}_c\,\langle Q, \phi\rangle\,, \tag{4.204}$$

for any ϕ and so the equation (4.203) leads to

$$0 = A\mu\,\langle Q, Q\rangle + \bar{c}A\,|A|^2\,\left\langle Q, Q\,|Q|^2\right\rangle \tag{4.205}$$

and so the amplitude equation becomes

$$A\left(Q_2\mu + \bar{c}Q_4\,|A|^2\right) = 0, \tag{4.206}$$

where

$$Q_2 = \int_{-1}^{2} c^2\,|Q|^2\,dz, \quad Q_4 = \int_{-1}^{1} c^2\,|Q|^4\,dz. \tag{4.207}$$

If $\mu > 0$ then the only solution to the amplitude equation is $A = 0$. If $\mu < 0$ then solutions are $|A| = 0$ and

$$|A| = \sqrt{-\frac{Q_2\mu}{Q_4\bar{c}}}. \tag{4.208}$$

Then the solution near the critical when $\mu < 0$ is

$$q = \sqrt{\frac{a_c - \bar{a}}{\bar{c}}}\left(\sqrt{\frac{Q_2}{Q_4}}Q\right)e^{i\alpha}, \tag{4.209}$$

where α is an arbitrary real number and the function $Q\sqrt{Q_2/Q_4}$ is invariant under changes of choice of amplitude of Q.

4.8.1 Non-axisymmetric case

Suppose $L\left(Q_+\mathbf{e}^{in\theta}\right) = a_c\, Q_+\mathbf{e}^{in\theta}$ and $L\left(Q_-\mathbf{e}^{-in\theta}\right) = a_c\, Q_-\mathbf{e}^{-in\theta}$ and $\bar{a} = a_c + \epsilon^2\mu$ where $\mu = \pm 1$ and $n \neq 0$, we write

$$q = \epsilon\left[\left(A\, Q_+\mathbf{e}^{in\theta} + B\, Q_-\mathbf{e}^{-in\theta}\right) + \epsilon q_1 + \epsilon^2 q_2\right] \tag{4.210}$$

At order ϵ^3 (expanding in powers of ϵ)

$$\begin{aligned} L\, q_2 = a_c\, q_2 + \mu\left[A\, Q_+\mathbf{e}^{in\theta} + B\, Q_-\mathbf{e}^{-in\theta}\right] \\ + \left(A\, Q_+\mathbf{e}^{in\theta} + B\, Q_-\mathbf{e}^{-in\theta}\right)^2\left(\bar{A}\, Q_+\mathbf{e}^{-in\theta} + \bar{B}\, Q_-\mathbf{e}^{in\theta}\right). \end{aligned}$$

Take $\left\langle Q_+\mathbf{e}^{in\theta}, \mu\, q_0 + \bar{c}\, q_0\left|q_0\right|^2\right\rangle$ then

$$\mu\, A\left\langle Q_+, Q_+\right\rangle + A\,\left|A\right|^2\left\langle Q_+^3, Q_+\right\rangle + 2A\left|B\right|^2\left\langle Q_+\, Q_-^2, Q_+\right\rangle = 0 \tag{4.211}$$

and take $\left\langle Q_-\mathbf{e}^{-in\theta}, \mu\, q_0 + \bar{c}\, q_0\left|q_0\right|^2\right\rangle$ then

$$\mu\, B\left\langle Q_-, Q_-\right\rangle + B\,\left|B\right|^2\left\langle Q_-^3, Q_-\right\rangle + 2B\left|A\right|^2\left\langle Q_+^2\, Q_-, Q_-\right\rangle = 0 \tag{4.212}$$

so the amplitude equations are

$$\mu\, A\, Q_2 + A\left(\left|A\right|^2 Q_4 + 2\left|B\right|^2 Q_{2,2}\right) = 0, \tag{4.213}$$

$$\mu\, B\, Q_2 + B\left(\left|B\right|^2 Q_4 + 2\left|A\right|^2 Q_{2,2}\right) = 0. \tag{4.214}$$

One solution is $|A| = |B|$ and if $\mu < 0$ then

$$\left|A\right|^2\left(Q_4 + 2Q_{2,2}\right) = -\mu\, Q_2, \tag{4.215}$$

so that

$$\left|A\right| = \sqrt{\frac{-\mu\, Q_2}{Q_4 + 2Q_{2,2}}}, \tag{4.216}$$

where

$$Q_2 = \left\langle Q_+, Q_+\right\rangle = \left\langle Q_-, Q_-\right\rangle, \qquad Q_4 = \left\langle Q_+^2, Q_+^2\right\rangle = \left\langle Q_-^2, Q_-^2\right\rangle,$$
$$Q_{2,2} = \left\langle Q_-^2, Q_+^2\right\rangle = \left\langle Q_+^2, Q_-^2\right\rangle.$$

We can find the energy in terms of Q, where

$$E[q] = -\frac{1}{2}\langle q, L\,q\rangle + \int_0^{2\pi}\int_{-1}^{1} c^2\left(\frac{\bar{a}}{2}|q|^2 + \frac{\bar{c}}{2}|q|^4\right) dz\,d\theta,$$
$$\int_0^{2\pi}\int_{-1}^{1} c^2\left(\frac{\bar{a}-a_c}{2}|q|^2 + \frac{\bar{c}}{4}|q|^4\right) dz\,d\theta \tag{4.217}$$

$$|q|^2 = |A|^2|Q_+|^2 + |B|^2|Q_-|^2 + AQ_+\bar{B}\bar{Q}e^{2in\theta} + \bar{A}\bar{Q}_+B\,Q_-e^{-2in\theta}, \tag{4.218}$$

$$|q|^4 = |A|^4|Q_+|^4 + |B|^4|Q_-|^4 + 2|A|^2|B|^2|Q_+|^2|Q_-|^2 + AQ_+\bar{B}\bar{Q}e^{2in\theta} + \bar{A}\bar{Q}_+B\,Q_-e^{-2in\theta}. \tag{4.219}$$

we integrate to 0 and get the energy

$$\left(\frac{\bar{a}-a_c}{2}\right)\left(|A|^2+|B|^2\right)Q_2 + \frac{\bar{c}}{4}\left[|A|^4Q_4 + |B|^4Q_4 + 2|A|^2|B|^2Q_{2,2}\right], \tag{4.220}$$

If $|B| = 0$ then we have

$$\left(\frac{\bar{a}-a_c}{2}\right)Q_2 \cdot \left(\frac{a_c-\bar{a}}{\bar{c}}\right)\frac{Q_2}{Q_4} + \frac{\bar{c}}{4}\frac{(a_c-\bar{a})^2}{\bar{c}^2}\frac{Q_2^2}{Q_4^2}Q_4 = -\frac{1}{4}\frac{Q_2^2}{Q_4}\frac{(a_c-\bar{a})^2}{\bar{c}} \tag{4.221}$$

which is same for $|A| = 0$.

If $|A| = |B|$ then

$$-\frac{1}{2}\frac{(a_c-\bar{a})^2}{\bar{c}}\frac{2Q_2^2}{Q_4+2Q_{2,2}} + \frac{\bar{c}\,(a_c-\bar{a})^2}{4}\frac{2Q_2^2\,(Q_4+Q_{2,2})}{\bar{c}^2\,(Q_4+2Q_{2,2})^2}$$
$$= -\frac{(a_c-\bar{a})^2\,Q_2^2}{4\bar{c}\,(Q_4+2Q_{2,2})^2}\left[2Q_4+6Q_{2,2}\right]. \tag{4.222}$$

Since there is more than one solution to the amplitude equations we can use these expressions for the energies of each solution to predict which branch we expect to see.

However, numerically we have calculated that for $\rho = 2$ and $n = 2$ the quantities $E_{a0} = Q_2^2/(4\,Q_4) \approx 0.1298$ and $E_{ab} = Q_2^2\,(2\,Q4 + 6\,Q_{2,2})\,/\,(4(Q_4+2\,Q_{2,2})^2) \approx 0.2595$. Similarly for $n = 1$ and $\rho = 1.25$, $E_{a0} = 0.1987$ and $E_{ab} = 0.3878$. In both cases $E_{ab} > E_{a0}$ and so the branch with $|A| = |B|$ has lower energy.

4.8.2 Defects

One of the most important and significant patterns associated with nematic liquid crystals are defects structures. Defects are widely used in the area of physics and technological applications [20], [52], [38], [104]. There are many mathematical literature have studied

liquid crystal defects such as [1], [7], [17], [47], [58], [71], [82], [86], [104].

Defects play an essential role of determining the structure and dynamics of liquid crystals. They are also used to recognise phases of many liquid crystals [53], [104]. When polarised light is passed through a liquid crystal sample, defects are observed as sudden, localised variations in the intensity and/or polarisation of the light [38]. On the other hand, deformation of the shells or external fields might cause a change in defect position [69]. Point defects in the liquid crystals are points where the director $\mathbf{n}$ can not be determined [23], [38], [51]. Because of the Poincare-Hopf Theorem, nematics present defects on any closed surface with genus different than one [60], [62], [73]. The situation for open surfaces is different and the allowed total charge of defects depends on what happens at the boundary.

In this section we investigate defects within the Landau-de Gennes theory where defects are defined as melting points, i.e isolated points where q vanishes.

We consider the structure of the solution at onset of nematic order and identify defects and their locations. At onset we have from Lyapunov-Schmidt reduction, $n \neq 0$

$$q = A\, e^{in\theta}\, Q_n(z) + B\, e^{-in\theta}\, Q_n(-z) \tag{4.223}$$

where A, B are real and Lyapunov-Schmidt gives $|A| = |B|$. Without loss of generality let $A = |A|\, e^{i\alpha}$ and $B = |A|\, e^{i\beta}$ so that $|A| = |B|$ and

$$\begin{aligned} q &= |A| \left[e^{i(\alpha+n\theta)} Q_n(z) + e^{-i(n\theta-\beta)} Q_n(-z) \right] \\ &= |A|\, e^{i((\alpha+\beta)/2)} \left[e^{i(\alpha/2-\beta/2+n\theta)} Q_n(z) + e^{-i(\alpha/2-\beta/2+n\theta)} Q_n(-z) \right]. \end{aligned} \tag{4.224}$$

We can see that by adjusting the origin for θ we can simplify this expression, and set $\alpha = \beta$ and since invariance of equation under $q \to q\, e^{i\alpha}$. This means if q is a solution then so is $q\, e^{i\alpha}$ for any α. Which implies also without loss of generality we can set $\alpha = 0$

$$q = A \left[e^{in\theta}\, Q_n(z) + e^{-in\theta}\, Q_n(-z) \right] \tag{4.225}$$

where A is real.

There are defects (melting points) where $q = 0$ so

$$[Q_n(z) + Q_n(-z)] \cos n\theta = 0, \tag{4.226}$$

$$[Q_n(z) - Q_n(-z)] \sin n\theta = 0, \tag{4.227}$$

Considering (4.227) that is clearly solved when $z = 0$, and then, provided $Q_n(-z) \neq 0$. For (4.226), is solved when $n\theta = \frac{\pi}{2} + k\pi$ where $k = 0, 1, \ldots, 2n-1$ and $\theta_k = \frac{1}{n}\left(\frac{\pi}{2} + k\pi\right)$, $k = 0, 1, \ldots, 2n-1$ (we have at least $2n$ defects).

The charge of defect describes the qualitative behaviour of the order parameter in the neighbourhood of the defect [86]. The charge of a defect is defined by the formula (for more details see [50], [105])

$$f = \frac{1}{2\pi}\oint_c \frac{\partial \alpha}{\partial s}\, ds = \frac{1}{4\pi}\oint_c \frac{q_0\left(\partial q_m/\partial s\right) - q_m\left(\partial q_0/\partial s\right)}{q_0^2 + q_m^2}\, ds, \tag{4.228}$$

Now let C be a contour that goes anti-clockwise around the defect (note that we can take any contour) and

$$\mathbf{Q} = \begin{bmatrix} q_0 & q_m \\ q_m & -q_0 \end{bmatrix} = \left(\mathbf{e}_1 \otimes \mathbf{e}_1 - \mathbf{e}_2 \otimes \mathbf{e}_2\right) q_0 + \left(\mathbf{e}_1 \otimes \mathbf{e}_2 + \mathbf{e}_2 \otimes \mathbf{e}_1\right) q_m, \tag{4.229}$$

where $\mathbf{e}_1$ is in the $\mathbf{e}_\theta$ direction and $\mathbf{e}_2$ is in the $\mathbf{t}$ direction. For the location of the defect, expand about

$$\theta = \theta_k + \varepsilon \cos t \tag{4.230}$$

$$z = 0 + \varepsilon \sin t. \tag{4.231}$$

Near the defect we have

$$q_0 = \left.\frac{\partial q_0}{\partial z}\right|_{(0,\theta_k)} (\varepsilon \sin t) + \left.\frac{\partial q_0}{\partial \theta}\right|_{(0,\theta_k)} (\varepsilon \cos t)\,, \tag{4.232}$$

$$q_m = \left.\frac{\partial q_m}{\partial z}\right|_{(0,\theta_k)} (\varepsilon \sin t) + \left.\frac{\partial q_m}{\partial \theta}\right|_{(0,\theta_k)} (\varepsilon \cos t)\,, \tag{4.233}$$

where

$$\left.\frac{\partial q_0}{\partial z}\right|_{(0,\theta_k)} = A\big(Q_n'(0) - Q_n'(0)\big)\cos(n\theta_k) = 0, \tag{4.234}$$

$$\begin{aligned}\left.\frac{\partial q_0}{\partial \theta}\right|_{(0,\theta_k)} &= A\big(Q_n(0) + Q_n(0)\big)(-n)\sin(n\theta_k) = -2An\,\theta_n(0)\sin\left(\frac{\pi}{2} + \pi k\right), \\ &= -2An\,\theta_n(0)(-1)^k = 0,\end{aligned} \tag{4.235}$$

$$\left.\frac{\partial q_m}{\partial \theta}\right|_{(0,\theta_k)} = 0, \qquad \left.\frac{\partial q_m}{\partial z}\right|_{(0,\theta_k)} = 2A\,Q_n'(0)(-1)^k\,. \tag{4.236}$$

so on the contour, to leading order,

$$q_0 \approx -2An\,Q_n(0)(-1)^k\,\varepsilon\cos t, \tag{4.237}$$

$$q_m \approx 2A\,Q_n'(0)(-1)^k\,\varepsilon\sin t. \tag{4.238}$$

Note that $2A(-1)^k$ does not affect the charge of defects, using our calculations above we

can write charge of defects given in (4.228) as

$$\begin{aligned} f &= -\frac{1}{4\pi}\int_0^{2\pi} \frac{n\,Q_n(0)\;Q_n'(0)}{n^2\,Q_n(0)^2\,\cos^2 t + Q_n'(0)^2\,\sin^2 t}\,dt \\ &= -\frac{1}{4\pi}\,2\pi\frac{n\,Q_n(0)\;Q_n'(0)}{n\,|Q_n(0)|\,|Q_n'(0)|} = -\frac{1}{2}\mathrm{sign}\left[Q_n(0)\;Q_n'(0)\right], \end{aligned} \tag{4.239}$$

if $Q_n(0) > 0$ and $Q_n'(0) > 0$ then $f = -\frac{1}{2}$.

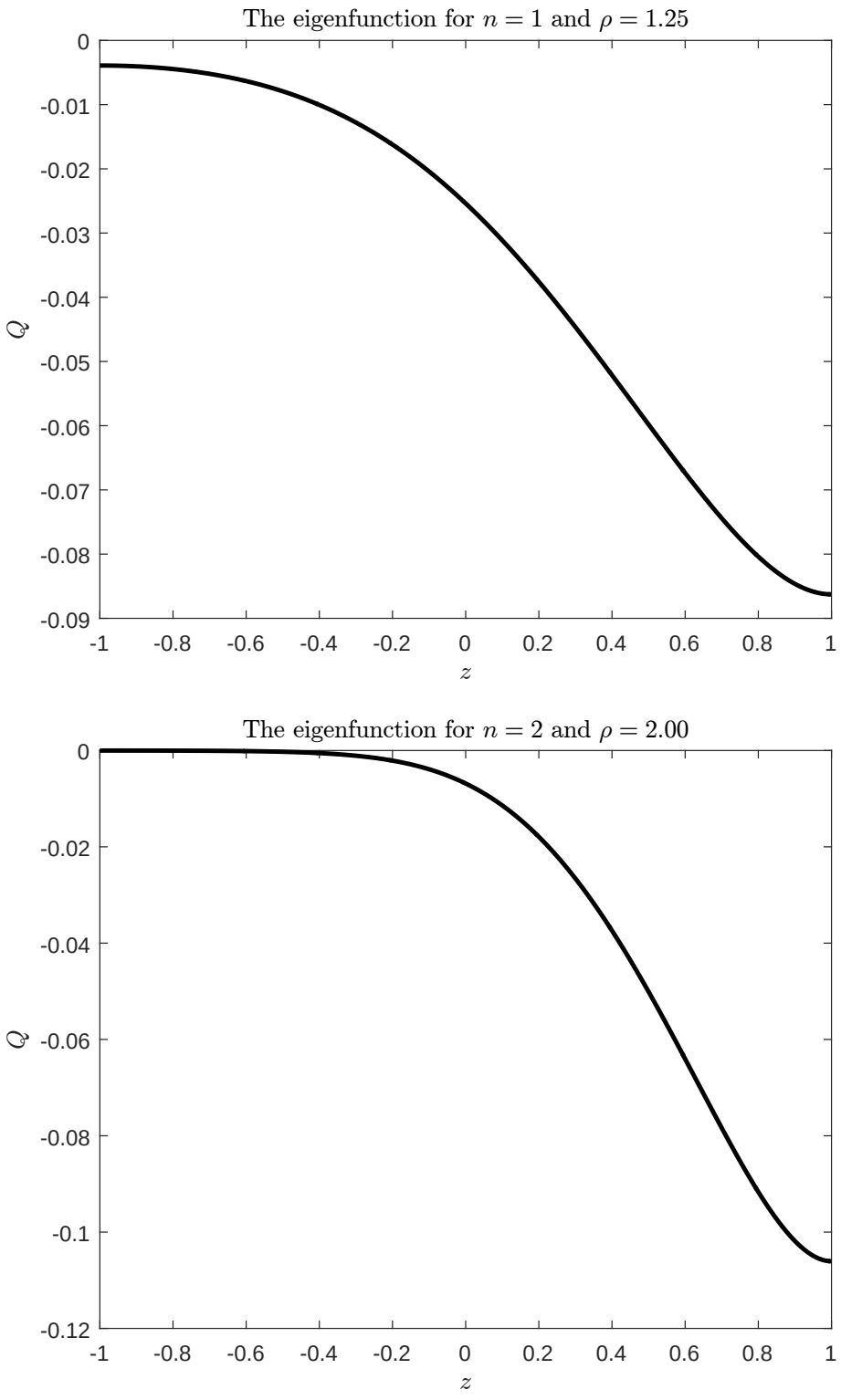


Figure 4.19: The first figure shows an eigenfunction for $n = 1$ and $\rho = 1.25$ and the second one shows an eigenfunction for $n = 2$ and $\rho = 2$.

Figure 4.20 shows that at $z = 0$, the sign of eigenfunctions $Q\,Q'$ is positive and so the charges we calculate at the end of this section (see (4.239)) are confirmed to be $m = -1/2$.

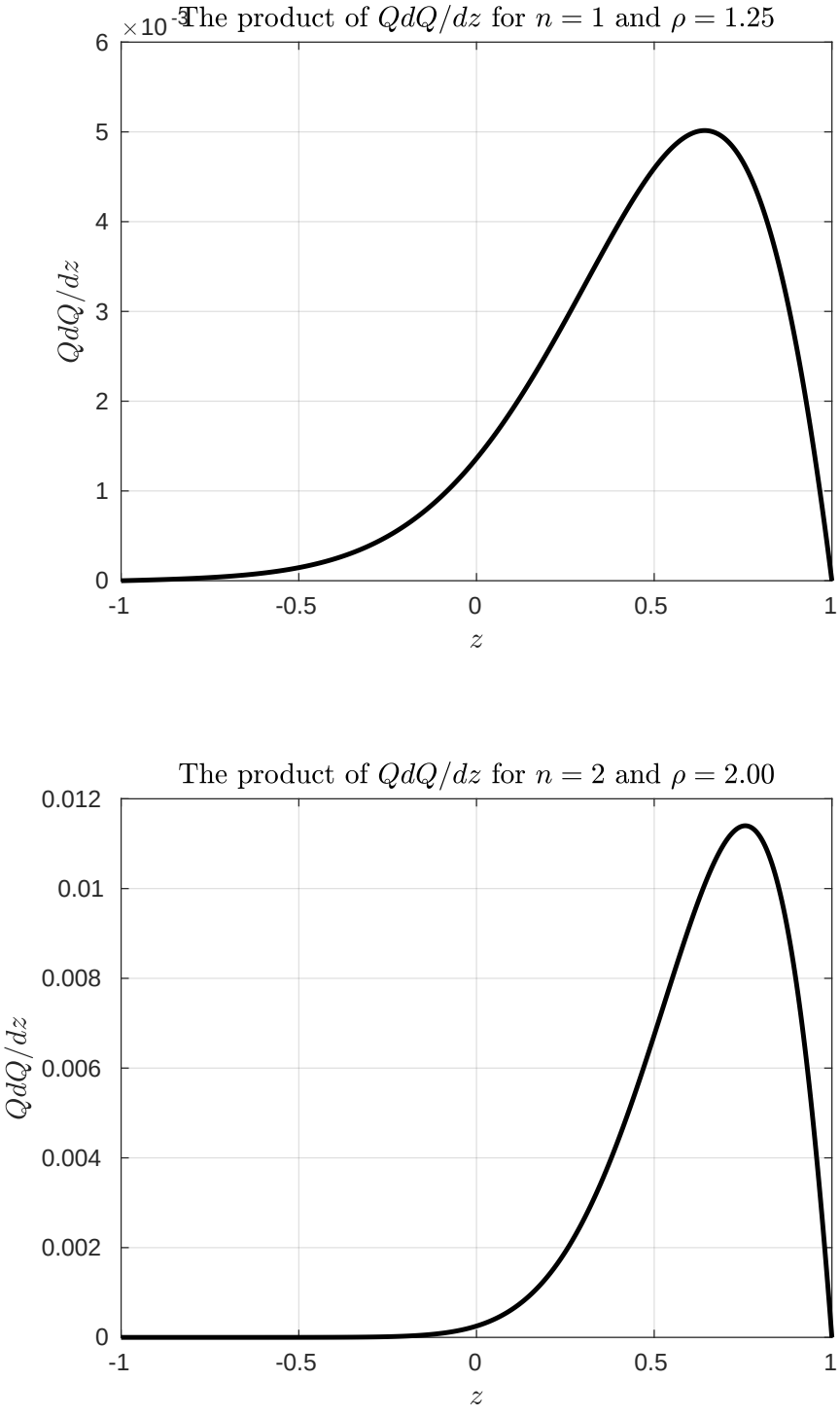


Figure 4.20: The product of $Q\,Q'$, the first one for $n = 1$ and $\rho = 1.25$ and the second one for $n = 2$ and $\rho = 2$.

Now we focus on the numerical methods involved in studying nonlinear solutions. The Jacobi iteration is the simplest of the iterative methods.

4.9 Jacobi iteration

One way to solve a *linear* system of equations is by Jacobi iteration. Given

$$Ax = b \tag{4.240}$$

where $x \in \mathbb{R}^n$ and $b \in \mathbb{R}^n$ and A an $n \times n$ matrix, we decompose A into its diagonal and off diagonal parts. We assume that the diagonal entries of A are all non-zero, so that the diagonal part D is invertible. Then

$$A = D + (A - D) \tag{4.241}$$

and

$$\begin{aligned} Ax &= b \\ Dx + (A - D)\, x &= b \\ Dx &= b - (A - D)\, x \\ x &= D^{-1}b - D^{-1}\,(A - D)\, x \\ x &= D^{-1}b + Gx \end{aligned}$$

which can be turned into an iterative method

$$x_{k+1} = D^{-1}b + Gx_k \tag{4.242}$$

which is called *Jacobi* iteration. This converges to the solution we want provided the eigenvalues of G are all less than 1 in modulus. The maximum modulus of the eigenvalues is called the spectral radius $\rho(G)$ and it can be shown that $\rho(G)$ is less than a certain matrix norm of G, in turn this can be shown to mean that if A is strictly diagonally dominant,

$$|A_{ii}| > \sum_{j \neq i} |A_{ij}|, \quad \forall i, \tag{4.243}$$

then $\rho(G) < 1$ and so the iterative method converges.

4.10 Application to nonlinear equation

Our nonlinear equation that obtained from (4.196) and (4.199) is

$$\frac{1}{c^2}\left(\rho^2 q_{\theta\theta} + q_{zz}\right) - 4\rho^2\, i\, \frac{s}{c^3} q_\theta - \frac{2+4s^2}{c^4}\rho^2 q - \bar{a}q - \bar{c}q\,|q|^2 = 0, \tag{4.244}$$

Recall that $c = \cosh \rho z$ and $s = \sinh \rho z$. The equation is solved on $(z, \theta) \in [-1, 1] \times [0, 2\pi)$ with periodic boundary conditions in θ and $q_z = 0$ at $z = \pm 1$.

4.10.1 Discretisation

Now we want to discretise (4.244). Let $z_j = -1 + h_z j$ where $h_z = 2/N$ and let $\theta_k = h_\theta k$ where $h_\theta = 2\pi/M$. Let $q_{j,k}$ be an approximation to the solution of the PDE at (z_j, θ_k). Periodicity demands $q_{j,k} = q_{j,k+M}$ for all j and k, the boundary condition $q_z = 0$ at the ends demands that $q_{-1,k} = q_{1,k}$. Discrete operators that approximate the derivatives are

$$\begin{aligned} D_\theta\,[q]_{j,k} &= \frac{q_{j,k+1} - q_{j,k-1}}{2h_\theta} \\ D_{\theta\theta}\,[q]_{j,k} &= \frac{q_{j,k+1} + q_{j,k-1} - 2q_{j,k}}{h_\theta^2} \\ D_{zz}\,[q]_{j,k} &= \frac{q_{j-1,k} + q_{j-1,k} - 2q_{j,k}}{h_z^2}. \end{aligned}$$

We can now discretise the PDE, using the notation $c_j = \cosh \rho z_j$, $s_j = \sinh \rho z_j$,

$$\begin{aligned} &\frac{1}{c_j^2}\left(\rho^2 D_{\theta\theta}\,[q]_{j,k} + D_{zz}\,[q]_{j,k}\right) \\ &\qquad - 4\rho^2 i \frac{s_j}{c_j^3} D_\theta\,[q]_{j,k} - \frac{2+4s_j^2}{c_j^4}\rho^2 q_{j,k} - \bar{a}q_{j,k} - \bar{c}q_{j,k}|q_{j,k}|^2 = 0. \end{aligned} \tag{4.245}$$

The idea is to solve (4.245) for $q_{j,k}$, $j = 0, \ldots, N$ and $k = 0, \ldots, M-1$. This is challenging because the equations are nonlinear, but we can design an iterative method inspired by Jacobi iteration (see §4.9). For example, rearranging the equation

$$\begin{aligned} &\rho^2 \frac{(q_{j,k+1} + q_{j,k-1})}{h_\theta^2} + \frac{(q_{j+1,k} + q_{j-1,k})}{h_z^2} - 4\rho^2 i \frac{s_j}{c_j} \frac{(q_{j,k+1} - q_{j,k-1})}{2h_\theta} - \bar{a}c_j^2 q_{j,k} \\ &\qquad = \left[2\left(\frac{\rho^2}{h_\theta^2} + \frac{1}{h_z^2}\right) + \rho^2 \frac{2+4s_j^2}{c_j^2} + \bar{c}c_j^2 |q_{j,k}|^2\right] q_{j,k} \end{aligned} \tag{4.246}$$

and this can be turned into an iterative method as follows

$$\left[2\left(\frac{\rho^2}{h_\theta^2}+\frac{1}{h_z^2}\right)+\rho^2\frac{2+4s_j^2}{c_j^2}+\bar{c}c_j^2|q_{j,k}^n|^2\right]q_{j,k}^{n+1}=$$
$$\rho^2\frac{\left(q_{j,k+1}^n+q_{j,k-1}^n\right)}{h_\theta^2}+\frac{\left(q_{j+1,k}^n+q_{j-1,k}^n\right)}{h_z^2}-4\rho^2\imath\frac{s_j}{c_j}\frac{\left(q_{j,k+1}^n-q_{j,k-1}^n\right)}{2h_\theta}-\bar{a}c_j^2q_{j,k}^n. \quad (4.247)$$

We have not proved convergence of this numerical method but numerical experiments show that it is capable of capturing nonlinear solutions.

4.11 Nonlinear solutions

In this section we illustrate the solutions of the nonlinear equations obtained by our iterative method described in §4.10. The following figures show the defect structure for different values of the parameters. We start the iterative method with a random initial field for q (made of random superpositions of different modes). We investigate the solutions for a certain values of ρ and $\bar{a}$ such that we have a bifurcation of non-zero axisymmetric solution.

Above a certain value of $\bar{a}$ we expect $q = 0$ is the only solution and below a certain value of $\bar{a}$ which depends on ρ we get different non-zero solutions. The figures show that the predicted pattern appears when $\bar{a}$ is below the critical value predicted for that ρ. We can show that if $\bar{a}$ is below the critical value given in the curves of Figure 4.17, the onset of order is either no defect, 2 defects or 4 defects solutions (see §4.8.2). Whereas for very large and negative values $\bar{a}$ we have obtained numerically solutions for $1, 3$ or might be 6 defect solutions.

Note that the choice of initial condition for the iterative method can lead to different solutions of the equilibrium equations that correspond to local minima of the energy. Our numerical investigations suggest this is particularly the case when $\bar{a}$ is far beneath the critical where we have found numerical solutions with 1, 3 and sometimes 6 defects, arranged off-centre of the catenoid.

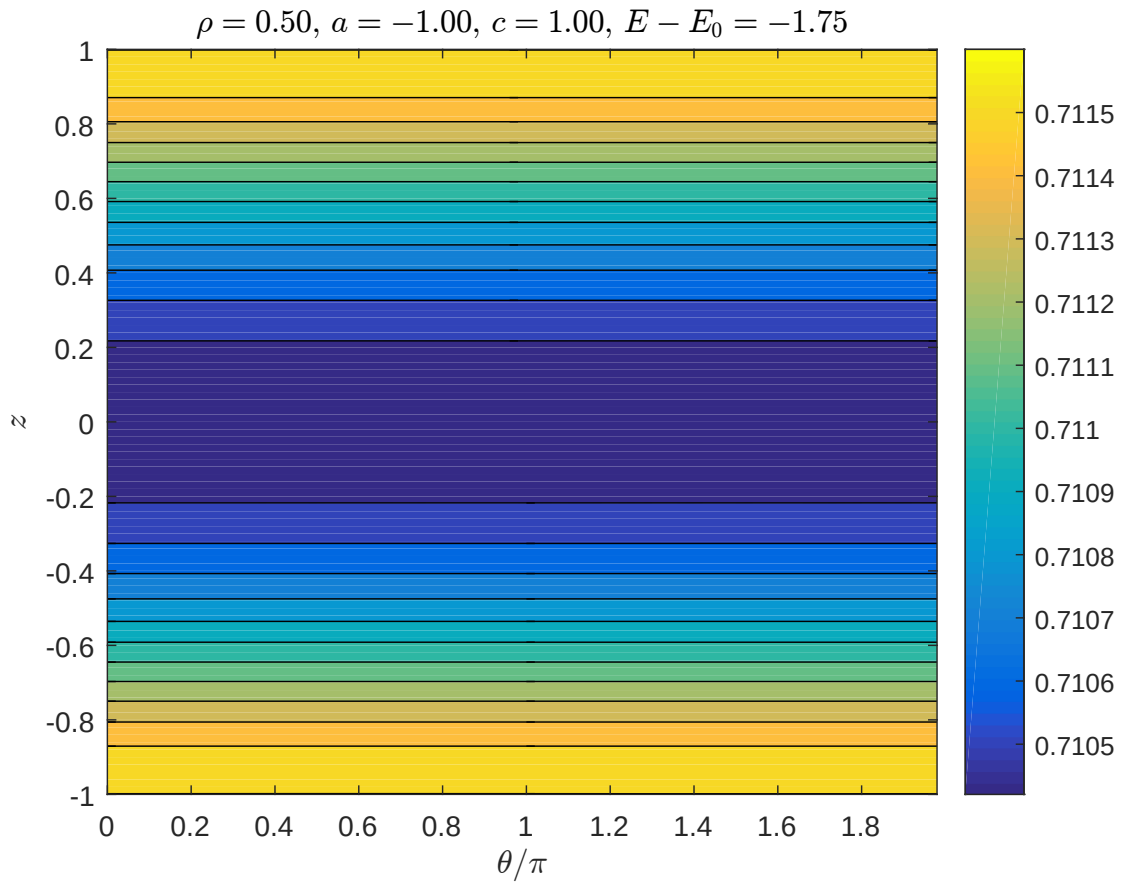


Figure 4.21: Plot of $|q|$ for $\rho = 0.5$ and $\bar{a} = -1$ we get an axisymmetric solution, with no defects. This agrees with the results in Figure 4.17.

Figure 4.22 and Figure 4.23 show 2-defect solutions for a certain ρ and $\bar{a}$. We calculate the charge of the defects, numerically by doing a rectangular contour integral (the contour is shown in black).

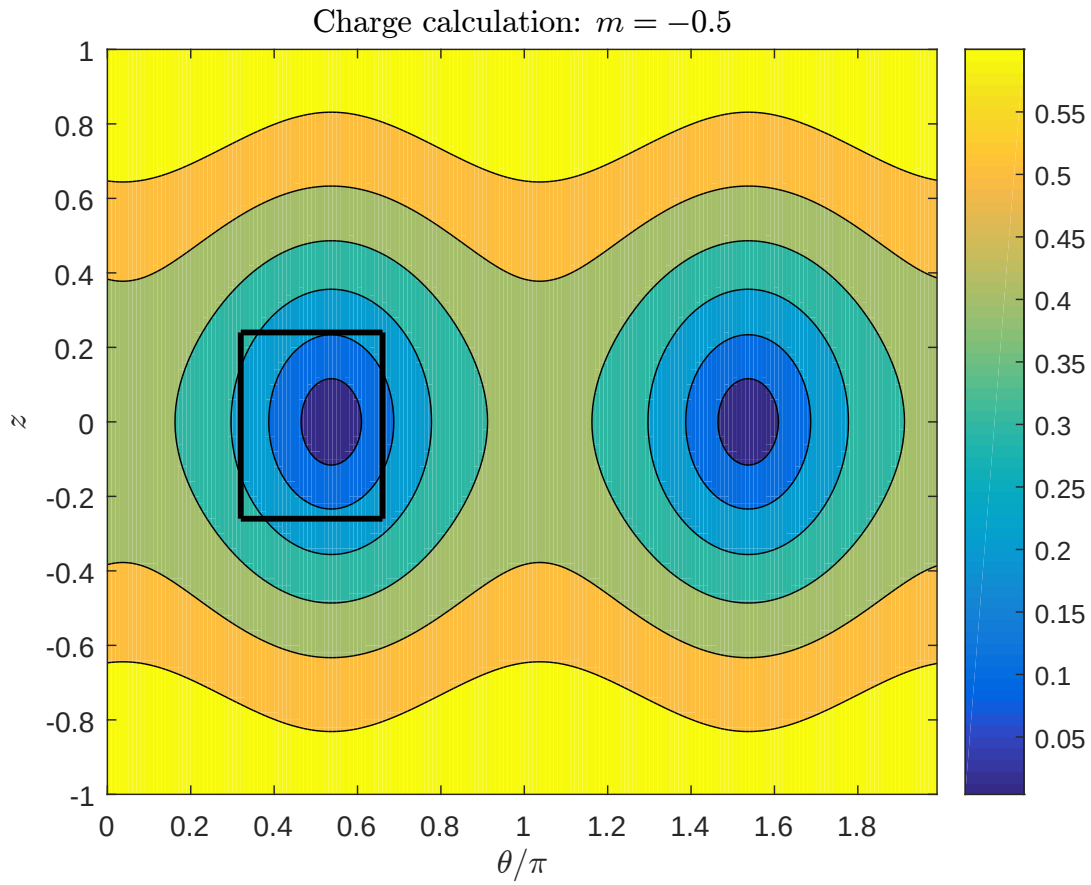


Figure 4.22: Plot of $|q|$ for $\rho = 1.2$ and $\bar{a} = -2$ give a two defect solution with the charge of defects calculated numerically as -0.5 (which agrees our prediction based on the linear stability calculation Figure 4.17).

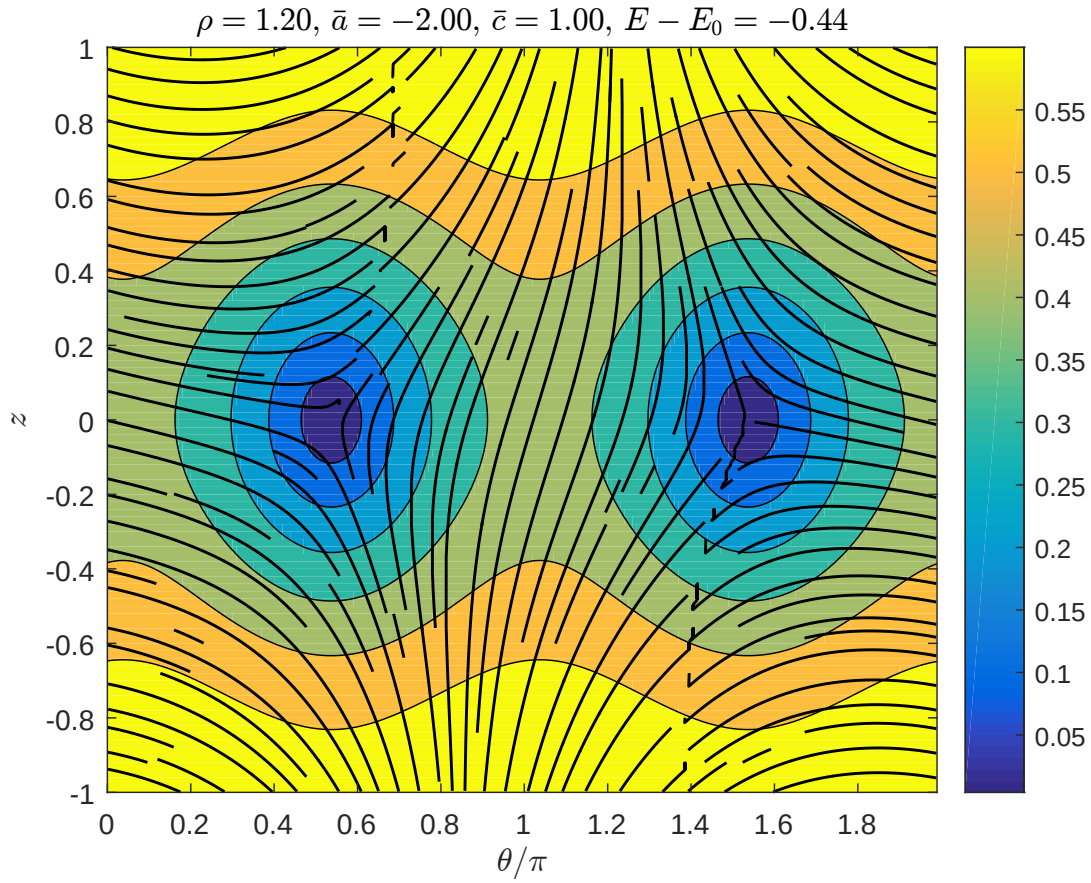


Figure 4.23: The patterns of the field-lines for 2 defects solutions .

At each point x, given q_0, q_m we can calculate Q and therefore the eigenvectors of Q. We choose the eigenvector with maximum eigenvalue and this gives a direction at x. We do this at the discretised locations and then have an approximate line-field, the lines constructed are parallel to this line field (streamlines).

The black curved lines in Figure 4.23 represent the field-lines for 2 defects solutions, that lines are parallel to the director everywhere. The pattern of the field-lines also predict that the charge of defects $m = -1/2$, consistent with our contour integrals

In Figure 4.24, we generate numerical solution that have 3 defects and these are not predicted by the linear stability but seem to be solutions of the nonlinear equations. These kind of defects (1 or 3 defects) appears for large value of $\bar{a}$.

We have investigated nonlinear solutions numerically and our simulations agree with the linear stability calculation. One observation here is that the location of the defects is not at $z = 0$ (slightly away from the middle) that is called "spontaneous symmetry breaking" in the z direction. This is interesting and unexpected and worth exploring it in future work.

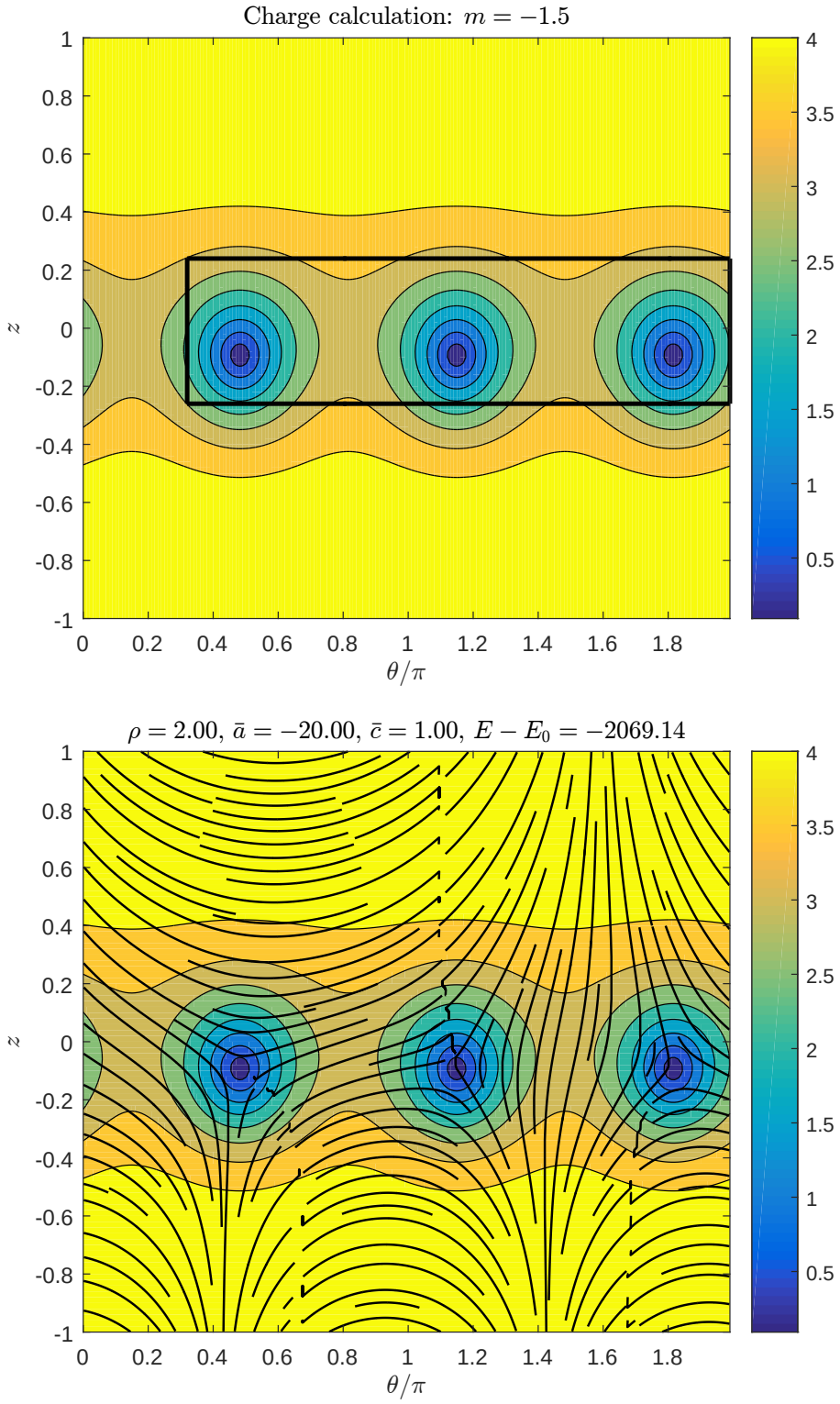


Figure 4.24: Plot of $|q|$ for $\rho = 2$ and $\bar{a} = -20$ make three defect solutions, all defects appears are $-1/2$, where we calculate the charge by doing a rectangular contour integral around the defect. The second part of Figure 4.24 shows the patterns of the field-lines (black curves) for 3 defects solutions.

Also we can generate 4-defect solutions and calculate the charge of defect as you see in Figure 4.25.

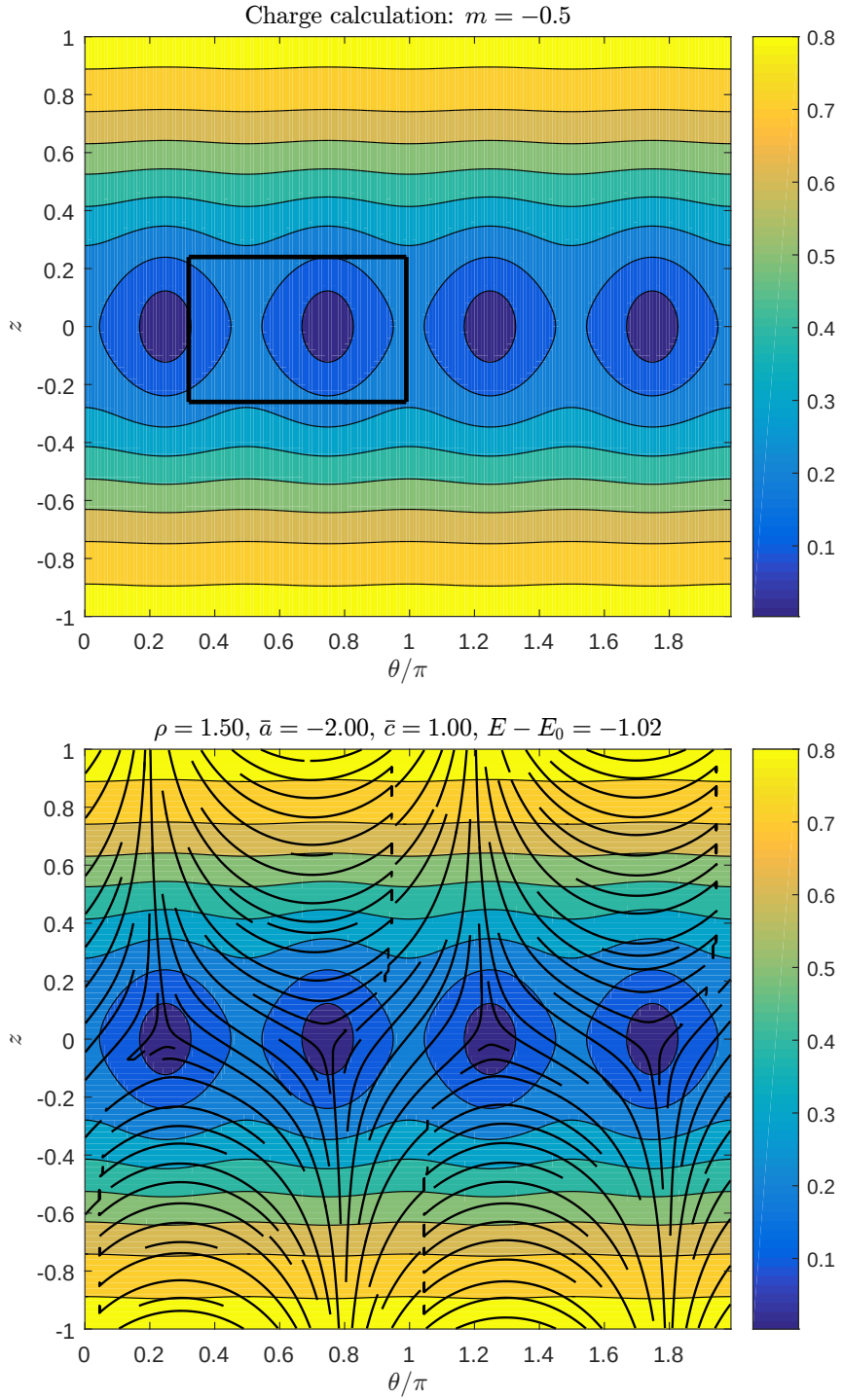


Figure 4.25: The values of $\rho = 1.5$ and $\bar{a} = -2$, generate 4 defects solutions with the charge $m = -1/2$ for each defects that is calculated by doing a contour integral around the defect. In the second part of Figure 4.25 we have obtained the field-lines (black curves). This agrees with the results in Figure 4.17.

In this section we have demonstrated nonlinear non-axisymmetric solutions to the equations for q_0 and q_m on the fixed catenoidal surface. We have shown that our predictions from linear stability and Lyapunov-Schmidt reduction agree with our numerical results. We have also found numerical results in which we have an odd number of defects. Future work could consider how n defects arrange themselves on the catenoidal surface.

4.12 Concluding remarks

The main results of chapter 4 are the derivation of the equilibrium equations and their numerical solution for different dimensionless parameters. We have considered equilibrium equations for general surfaces using the $\mathbf{n}$ and α parameterisation which is very complicated and so we have considered simpler situations in which we have worked for axisymmetric solutions to the full equations and derived all the quantities that we need to describe axisymmetric solutions. Also we have simplified the energy using an axisymmetric assumption for both parameterisations (are detailed in §4.2.1 and §4.2.2) and have derived the dimensionless equilibrium equations in Hamiltonian form. We have solved the equilibrium equations numerically to obtain different axisymmetric solutions and show the effects of different parameters (aspect ratio, ratio of surface energy to k, the temperature, the value of c).

Another contribution is the stability. We have implemented the discretisation of the incremental problem and found the eigenvalues to test the stability. We have not solved the full stability problem, but we have studied a reduced problem in which the geometry of the catenoid is fixed. We have studied the linear stability and shown that the isotropic distribution is unstable to different modes depending on the geometry of the catenoid. Also we use Lyapunov-Schmidt reduction (weakly nonlinear analysis) to study the nonlinear solutions. We have discussed the defects (melting points) that arise and have shown that they are $m = -1/2$ defects, arranged at different locations on the surface. We have shown the defect structure for different values of the parameters and compared our expressions for the energy with those predicted from the weakly nonlinear analysis.

Chapter 5

Conclusions

We conclude this thesis with an overview of the results presented in the previous chapters. We also highlight our contribution made to the existing literature and indicate possible future directions.

We began the thesis by giving the necessary mathematical background and introductory materials that are concerned with the behaviour of liquid crystal films and shells in different geometries.

We have extended the results of [66] to the equilibrium of open surfaces and developed a framework to consider the stability of solutions by using the incremental equations. In order to do this we have established that the tangential component of the equation derived from considering variations to the shape of the surface is automatically satisfied whenever the other equilibrium equations are satisfied. We also derived the natural boundary conditions for a general surface energy. This allowed us to concentrate on normal increments to the shape equation and other equilibrium equations. We illustrated the approach by applying it to two simple cases, the soap film spanning two coaxial rings and a film whose energy is a constant plus a Canham-Helfrich contribution. We examined the stability numerically.

Using the results above, we have extended the results of [70] (who used the Frank energy) by studying a thin film of nematic liquid crystal spanning two coaxial rings, using the Q-tensor approach. In particular we derived the appropriate surface free energy involving LdG theory and parameterise the second order variance tensor $\mathbf{M}$. We found the equilibrium equations and boundary conditions for two parameterisation of $\mathbf{M}$ (q_0, q_m and q, α) and transformed the equilibrium equations to a set of first-order equations (Hamilton's equations) suitable for numerical simulation to find different axisymmetric solutions. The corresponding equilibrium equations and their numerical solutions are for different dimensionless parameters (ξ, A, C, κ) and we illustrated the effect of geometry and material parameters on the surface shape and nematic order.

We also studied the stability of the isotropic state for a film on a fixed catenoidal

surface ($H = 0$). In this case $q_0 = q_m = 0$ is the solution to the equilibrium equations. We calculated the change in melting temperature as a result of the curvature of the surface. We also investigated the amplitude near onset using a weakly nonlinear analysis (Lyapunov-Schmidt reduction). We have predicted the structure of the solutions at onset of nematic order and shown that defects occur. We proved that defects have charge $-1/2$, arranged at different locations on the surface for different aspect ratios. Using Jacobi iteration we showed numerical solutions of the nonlinear equations and the defect structure for different values of the parameters. Our work has proved that the predicted pattern appears when $\bar{a}$ is below the critical value predicted for that ρ and the onset of order is either no defect, 2 defects or 4 defects solutions.

The location and behaviour of defects depends on the boundary conditions and further work is required to understand this. It is worth saying here that whether we could observe such patterns physically would depend on whether a stable film of liquid crystal could be produced. In such an experiment we could adjust the aspect ratio and the temperature to see if the predicted patterns of defects could be generated.

5.1 Future work directions

In this section we list the recommendations and possible future directions to extend this work.

1. One of the most important direction and extension of this work would be to study the full stability problem for the surface considered in Chapter 4 (of the shape of the surface as well as the nematic order). We need to be clear that there are possibly other branches of solutions that could exist ([70], [71], [72]) which they look at solutions where $\alpha = 0$ for example, and also the narrow catenoid and that exploring the full 4-dimensional parameter space.

2. Another extension is to consider different boundary conditions (for the fixed catenoid) and the study the effects these have on the structure at onset, for example strong anchoring.

3. Also we can work to consider other surfaces, for example surfaces with both positive and negative Gauss curvature, since our results predict negatively charged defects on the negative Gauss curvature surface that is the catenoid and other works predict positive charge defects on the sphere (positive Gauss curvature) [53], [54].

4. There are possibly other branches of solutions (related to our problem) that could exist when studying the axisymmetric solutions in chapter 4 there may be other equilibrium branches (both axisymmetric or non-axisymmetric) to explore.

5. We can study the influence of external fields such as magnetic field on the nematic film and working on the applications to thin films of magnetic material.

Appendix A

Details of proofs

Given that $\mathbf{L} = -\nabla_s \boldsymbol{\nu} = -\left(-c_{1s}\,\mathbf{e}_1 \otimes \mathbf{e}_1 - c_{2s}\,\mathbf{e}_2 \otimes \mathbf{e}_2\right)$, then

$$\operatorname{tr}(\mathbf{L}) = 2H\,, \tag{A.1}$$

and

$$\operatorname{tr}\left(\mathbf{L}^2\right) = 4\left(H^2 - \frac{1}{2}K\right). \tag{A.2}$$

Proof. Since $\mathbf{L} = -\nabla_s \boldsymbol{\nu} = -\left(-c_{1s}\,\mathbf{e}_1 \otimes \mathbf{e}_1 - c_{2s}\,\mathbf{e}_2 \otimes \mathbf{e}_2\right)$,then

$$\begin{aligned}\operatorname{tr}(\mathbf{L}) &= c_{1s}\,\mathbf{e}_1 \cdot \mathbf{e}_1 + c_{2s}\,\mathbf{e}_2 \cdot \mathbf{e}_2 \\ &= c_{1s} + c_{2s} = 2H.\end{aligned}$$

and

$$\begin{aligned}\operatorname{tr}\left(\mathbf{L}^2\right) &= \operatorname{tr}\left(c_{1s}^2\,\mathbf{e}_1 \otimes \mathbf{e}_1 + c_{2s}^2\,\mathbf{e}_2 \otimes \mathbf{e}_2\right) \\ &= c_{1s}^2 + c_{2s}^2 = \left(c_{1s} + c_{2s}\right)^2 - 2c_{1s}\,c_{2s} \\ &= (2H)^2 - 2K = 4\left(H^2 - \frac{1}{2}K\right).\end{aligned}$$

□

Given two vectors $\mathbf{a}$ and $\mathbf{b}$,we define the tensor product of the given vectors as $\mathbf{a} \otimes \mathbf{b}$ such that $(\mathbf{a} \otimes \mathbf{b})\,\mathbf{v} = (\mathbf{b} \cdot \mathbf{v})\,\mathbf{a}$ and depending on this definition we have the following:

$$(\mathbf{a} \otimes \mathbf{b})\,(\mathbf{v} + \mathbf{w}) = (\mathbf{a} \otimes \mathbf{b})\,\mathbf{v} + (\mathbf{a} \otimes \mathbf{b})\,\mathbf{w}. \tag{A.3}$$

Proof.

$$\begin{aligned}(\mathbf{a}\otimes\mathbf{b})(\mathbf{v}+\mathbf{w}) &= [\mathbf{b}\cdot(\mathbf{v}+\mathbf{w})]\,\mathbf{a}\\ &= [\mathbf{b}\cdot\mathbf{v}+\mathbf{b}\cdot\mathbf{w}]\,\mathbf{a}\\ &(\mathbf{b}\cdot\mathbf{v})\,\mathbf{a}+(\mathbf{b}\cdot\mathbf{w})\,\mathbf{a}\\ &= (\mathbf{a}\otimes\mathbf{b})\,\mathbf{v}+(\mathbf{a}\otimes\mathbf{b})\,\mathbf{w}.\end{aligned}$$

□

and for any scalar λ, we have

$$(\mathbf{a}\otimes\mathbf{b})(\lambda\mathbf{v}) = \lambda\,(\mathbf{a}\otimes\mathbf{b})\,\mathbf{v}. \tag{A.4}$$

Proof.

$$\begin{aligned}(\mathbf{a}\otimes\mathbf{b})(\lambda\mathbf{v}) &= [\mathbf{b}\cdot(\lambda\mathbf{v})]\,\mathbf{a}\\ &= [\lambda\,\mathbf{b}\cdot\mathbf{v}]\,\mathbf{a} = \lambda\,[(\mathbf{b}\cdot\mathbf{v})\,\mathbf{a}]\\ &= \lambda\,(\mathbf{a}\otimes\mathbf{b})\,\mathbf{v}.\end{aligned}$$

□

$$\operatorname{div}_s\mathbf{P} = 2\,H\,\boldsymbol{\nu}. \tag{A.5}$$

Proof. Note that,

$$\operatorname{div}_s\left(\mathbf{P}^T\mathbf{a}\right) = \mathbf{a}\cdot(\operatorname{div}_s\mathbf{P})$$

where $\mathbf{a}$ is a constant vector, and $\mathbf{P}^T = [\mathbf{I}-(\boldsymbol{\nu}\otimes\boldsymbol{\nu})]\,\mathbf{a} = \mathbf{a} - \boldsymbol{\nu}\,(\boldsymbol{\nu}\cdot\mathbf{a})$. Then

$$\begin{aligned}\operatorname{div}_s\big(\mathbf{a}-\boldsymbol{\nu}\,(\boldsymbol{\nu}\cdot\mathbf{a})\big) &= -\,(\operatorname{div}_s\boldsymbol{\nu})\,\boldsymbol{\nu}\cdot\mathbf{a}-\boldsymbol{\nu}\cdot\nabla_s\,(\boldsymbol{\nu}\cdot\mathbf{a})\\ &= -2H\boldsymbol{\nu}\cdot\mathbf{a}-\boldsymbol{\nu}\cdot[\mathbf{a}\cdot\nabla_s\boldsymbol{\nu}]\\ &= -2H\boldsymbol{\nu}\cdot\mathbf{a}-\left(\nabla_s\boldsymbol{\nu}^T\boldsymbol{\nu}\right)\cdot\mathbf{a}\\ &= 2H\boldsymbol{\nu}\cdot\mathbf{a} = \mathbf{a}\cdot\operatorname{div}_s\mathbf{P}.\end{aligned}$$

□

$$\operatorname{div}_s(\mathbf{L}\mathbf{P}) = 2\big(\nabla_s H\;+\;\left(2H^2-K\right)\boldsymbol{\nu}\big) \tag{A.6}$$

Proof. We can write

$$\begin{aligned}\operatorname{div}_s(\mathbf{LP}) &= \operatorname{div}_s\big(\mathbf{L}(1-\boldsymbol{\nu}\otimes\boldsymbol{\nu})\big)\\ &= \operatorname{div}_s(\mathbf{L}) - \operatorname{div}_s(\mathbf{L}\boldsymbol{\nu}\otimes\boldsymbol{\nu}), \text{ but } (\mathbf{L}\cdot\boldsymbol{\nu}=0)\\ &= 2\big(\nabla_s H + \big(2H^2-K\big)\boldsymbol{\nu}\big).\end{aligned}$$

□

$$\operatorname{div}_s(\mathbf{LP})\cdot\boldsymbol{\nu} = 2\left(K+4H^2\right) \tag{A.7}$$

Proof. Using the identity in (2.55)

$$\begin{aligned}\operatorname{div}_s(\mathbf{LP})\cdot\boldsymbol{\nu} &= \operatorname{div}_s\big((\mathbf{LP})^T\boldsymbol{\nu}\big) - (\mathbf{LP})\cdot\nabla_s\boldsymbol{\nu}\\ &= (\mathbf{LP})\cdot\mathbf{L} = \mathbf{L}^2\cdot\mathbf{P}\\ &= 2\left(K+4H^2\right).\end{aligned}$$

□

$$\boldsymbol{\beta}\cdot\delta\boldsymbol{\nu} = -(\boldsymbol{\nu}\otimes\mathbf{P}\boldsymbol{\beta})\cdot\nabla_s\mathbf{u}. \tag{A.8}$$

Proof. We have introduced $\boldsymbol{\beta} = \frac{\partial w}{\partial \boldsymbol{\nu}}$, then

$$\begin{aligned}\frac{\partial w}{\partial\boldsymbol{\nu}}\cdot\delta\boldsymbol{\nu} &= \boldsymbol{\beta}\cdot\left(-(\nabla_s\mathbf{u})^T\boldsymbol{\nu}\right)\\ &= \boldsymbol{\beta}\cdot\left(-\mathbf{P}^T\nabla\mathbf{u}^T\boldsymbol{\nu}\right)\\ &= -(\mathbf{P}\boldsymbol{\beta})\cdot\left((\nabla_s\mathbf{u})^T\boldsymbol{\nu}\right)\\ &= -\boldsymbol{\nu}\cdot\left((\nabla_s\mathbf{u})\mathbf{P}\boldsymbol{\beta}\right)\\ &= -(\boldsymbol{\nu}\otimes\mathbf{P}\boldsymbol{\beta})\cdot\nabla_s\mathbf{u}.\end{aligned}$$

□

$$\mathbf{g}\cdot\delta\mathbf{n} = \mathbf{g}\cdot\boldsymbol{\tau}\delta\theta + \mathbf{g}\cdot\boldsymbol{\nu}(\boldsymbol{\nu}\otimes\mathbf{n})\cdot\nabla_s\mathbf{u}. \tag{A.9}$$

Proof. we have set $\mathbf{g} = \frac{\partial w}{\partial\mathbf{n}}$, then,

$$\begin{aligned}\frac{\partial w}{\partial\mathbf{n}}\cdot\delta\mathbf{n} &= \mathbf{g}\cdot\left(\boldsymbol{\tau}\delta\theta + (\boldsymbol{\nu}\cdot\nabla_s\mathbf{u}\,\mathbf{n})\boldsymbol{\nu}\right)\\ &= \mathbf{g}\cdot\boldsymbol{\tau}\,\delta\theta + \mathbf{g}\cdot\boldsymbol{\nu}(\boldsymbol{\nu}\otimes\mathbf{n})\cdot\nabla_s\mathbf{u}.\end{aligned}$$

□

For the term $\mathbf{\Lambda} = \frac{\partial w}{\partial \mathbf{L}}$,

$$\mathbf{\Lambda} \cdot \delta\mathbf{L} = \mathbf{\Lambda} \cdot \left(\mathbf{L}\left(\nabla_s \mathbf{u}\right)^T \boldsymbol{\nu} \otimes \boldsymbol{\nu}\right) - \mathbf{\Lambda} \cdot \left(\mathbf{L}\nabla_s \mathbf{u}\right) - \boldsymbol{\nu} \cdot \nabla_{\mathbf{u}} \operatorname{div}_s \mathbf{\Lambda}. \tag{A.10}$$

Proof. By taking into the account the definition of $\mathbf{L}$,

$$\delta\mathbf{L} = \mathbf{L}\left(\nabla \mathbf{u}_s\right)^T \boldsymbol{\nu} \otimes \boldsymbol{\nu} + \nabla_s \left[\left(\nabla_s \mathbf{u}\right)^T \boldsymbol{\nu}\right] - \mathbf{L}\left(\nabla_s \mathbf{u}\right).$$

then,

$$\mathbf{\Lambda} \cdot \delta\mathbf{L} = \mathbf{\Lambda} \cdot \left[\mathbf{L}\left(\nabla \mathbf{u}_s\right)^T \boldsymbol{\nu} \otimes \boldsymbol{\nu} + \nabla_s\left(\left(\nabla_s \mathbf{u}\right)^T \boldsymbol{\nu}\right) - \mathbf{L}\left(\nabla_s \mathbf{u}\right)\right]$$

where,

$$\begin{aligned}
\mathbf{\Lambda} \cdot \nabla_s\left(\left(\nabla_s \mathbf{u}\right)^T \boldsymbol{\nu}\right) &= \operatorname{div}_s\left(\mathbf{\Lambda}^T \left(\nabla_s \mathbf{u}\right)^T \boldsymbol{\nu}\right) - \left(\operatorname{div}_s \mathbf{\Lambda}\right) \cdot \left(\nabla_s \mathbf{u}\right)^T \boldsymbol{\nu} \\
&= \operatorname{div}_s\left(\mathbf{\Lambda}^T \left(\nabla_s \mathbf{u}\right)^T \boldsymbol{\nu}\right) - \boldsymbol{\nu} \cdot \left(\nabla_s \mathbf{u}\right) \operatorname{div}_s \mathbf{\Lambda} \\
&= \operatorname{div}_s\left(\left(\nabla_s \mathbf{u} \mathbf{\Lambda}_s\right)^T \boldsymbol{\nu}\right) - \boldsymbol{\nu} \cdot \nabla_s \mathbf{u} \operatorname{div}_s \mathbf{\Lambda}.
\end{aligned}$$

and,

$$\mathbf{\Lambda} \cdot \left(\mathbf{\Lambda} \nabla_s \mathbf{u}\right) = \left(\mathbf{L}^T \mathbf{\Lambda}\right) \cdot \nabla_s \mathbf{u},$$

whereas $\mathbf{L}^T = \mathbf{L}$ and $\mathbf{L}\mathbf{\Lambda} = \mathbf{L}\mathbf{\Lambda}_s$. Now we consider $\mathbf{\Lambda} \cdot \left(\mathbf{L}\left(\nabla_s \mathbf{u}\right)^T \boldsymbol{\nu} \otimes \boldsymbol{\nu}\right)$,

$$\begin{aligned}
\mathbf{\Lambda} \cdot \left(\mathbf{L}\left(\nabla_s \mathbf{u}\right)^T \boldsymbol{\nu} \otimes \boldsymbol{\nu}\right) &= \left(\mathbf{L}^T \mathbf{\Lambda}\right) \cdot \left(\nabla_s \mathbf{u}^T \boldsymbol{\nu} \otimes \boldsymbol{\nu}\right) \\
&= \left(\mathbf{L}^T \mathbf{\Lambda}\right)^T \cdot \left(\boldsymbol{\nu} \otimes \boldsymbol{\nu} \nabla_s \mathbf{u}\right) \\
&= \left(\left(\boldsymbol{\nu} \otimes \boldsymbol{\nu}\right)^T \mathbf{\Lambda}^T \mathbf{L}\right) \cdot \nabla_s \mathbf{u} \\
= \boldsymbol{\nu} \otimes \boldsymbol{\nu}\, \mathbf{\Lambda}^T \mathbf{L} \cdot \nabla_s \mathbf{u} &= \left[\boldsymbol{\nu} \otimes \left(\mathbf{L}^T \mathbf{\Lambda} \boldsymbol{\nu}\right)\right] \cdot \nabla_s \mathbf{u}.
\end{aligned}$$

□

$$\operatorname{div}_s \mathbf{r} = 2. \tag{A.11}$$

Proof. Recalling that $\operatorname{div}_s \mathbf{F} = (\nabla \mathbf{F}) \cdot \mathbf{P}$. Also $(\nabla \mathbf{r})^T = \mathbf{I}$ and $\nabla \mathbf{r} = \mathbf{I}$.Then,

$$\begin{aligned}
\operatorname{div}_s \mathbf{r} &= \mathbf{I} \cdot \mathbf{P} \\
&= \operatorname{tr}\left(\mathbf{I}\,\mathbf{P}\right) = \operatorname{tr}\left(\mathbf{P}\right) \\
&= \operatorname{tr}\left(\mathbf{I} - \boldsymbol{\nu} \otimes \boldsymbol{\nu}\right) \\
&= 3 - \boldsymbol{\nu} \cdot \boldsymbol{\nu} \\
&= 3 - 1 = 2.
\end{aligned}$$

□

$$\mathbf{P}^2 = \mathbf{P}. \tag{A.12}$$

Proof. We have $\mathbf{P} = \mathbf{I} - \boldsymbol{\nu} \otimes \boldsymbol{\nu}$,then

$$\begin{aligned}\mathbf{P}^2 &= (\mathbf{I} - \boldsymbol{\nu} \otimes \boldsymbol{\nu})(\mathbf{I} - \boldsymbol{\nu} \otimes \boldsymbol{\nu}) \\ &= \mathbf{I} - \boldsymbol{\nu} \otimes \boldsymbol{\nu} - \boldsymbol{\nu} \otimes \boldsymbol{\nu} + (\boldsymbol{\nu} \otimes \boldsymbol{\nu})(\boldsymbol{\nu} \otimes \boldsymbol{\nu}) \\ &= \mathbf{I} - 2\boldsymbol{\nu} \otimes \boldsymbol{\nu} + \boldsymbol{\nu}(\boldsymbol{\nu} \cdot \boldsymbol{\nu}) \otimes \boldsymbol{\nu} \\ &= \mathbf{I} - \boldsymbol{\nu} \otimes \boldsymbol{\nu} = \mathbf{P}.\end{aligned}$$

□

$$\operatorname{div}_s(S\mathbf{P}) = \operatorname{div}_s(S). \tag{A.13}$$

Proof.

$$\operatorname{div}_s(S\mathbf{P}) = \operatorname{div}_s(S) - \operatorname{div}_s(S\,\boldsymbol{\nu} \otimes \boldsymbol{\nu})$$

so if S is tangential then $S\boldsymbol{\nu} = 0$ and $\operatorname{div}_s(S\mathbf{P}) = \operatorname{div}_s(S)$. □

If $\mathbf{b} = \frac{\delta w}{\delta \nabla_s q}$ and $\mathbf{b} \cdot \boldsymbol{\nu} = 0$, then

$$\operatorname{div}_s \mathbf{b}_s = \operatorname{div}_s \mathbf{b}. \tag{A.14}$$

Proof.

$$\begin{aligned}\operatorname{div}_s \mathbf{b}_s = \operatorname{div}_s(\mathbf{P}\mathbf{b}) &= (P_{ij}\, b_j)_{,k}\, P_{ki} \\ &= P_{ij,k}\, b_j\, P_{ki} + P_{ij}\, b_{j,k}\, P_{ki} \\ &= \operatorname{div}_s \mathbf{b} + b_j\,(L_{ii}\nu_j + L_{ji}\nu_i) \\ &= \operatorname{div}_s \mathbf{b} + (\mathbf{b} \cdot \boldsymbol{\nu})(\mathbf{L} \cdot \mathbf{P}) + \mathbf{b} \cdot (\mathbf{L}\boldsymbol{\nu}) \\ \operatorname{div}_s \mathbf{b}_s &= \operatorname{div}_s \mathbf{b} + (\mathbf{b} \cdot \boldsymbol{\nu})(\mathbf{L} \cdot \mathbf{P}).\end{aligned}$$

If $\mathbf{b} \cdot \boldsymbol{\nu} = 0$ then $\operatorname{div}_s \mathbf{b}_s = \operatorname{div}_s \mathbf{b}$. □

$$\mathbf{P} \operatorname{div}_s \boldsymbol{\sigma} = \operatorname{div}_s(\mathbf{P}\boldsymbol{\sigma}) - \mathbf{L}\boldsymbol{\sigma}^T\boldsymbol{\nu} - (\mathbf{L} \cdot \boldsymbol{\sigma})\,\boldsymbol{\nu} \tag{A.15}$$

Proof.

$$\begin{aligned}\mathbf{P} \operatorname{div}_s \boldsymbol{\sigma} &= P_{ij}\sigma_{jk;k} \\ &= (P_{ij}\sigma_{jk})_{;k} - P_{ij;k}\sigma_{jk}\end{aligned}$$

where,

$$\begin{aligned} P_{ij;k} &= \left(\delta_{ij} - \nu_i\nu_j\right)_{;k} \\ &= -\nu_{i;k}\nu_j - \nu_i\nu_{j;k} = L_{ik}\nu_j + L_{jk}\nu_i \end{aligned}$$

and

$$\begin{aligned} P_{ij;k}\sigma_{jk} &= L_{ik}\nu_j\sigma_{jk} + L_{jk}\nu_i\sigma_{jk} \\ &= \mathbf{L}\boldsymbol{\sigma}^T\boldsymbol{\nu} + \left(\mathbf{L}\cdot\boldsymbol{\sigma}\right)\boldsymbol{\nu}. \end{aligned}$$

Therefore,

$$\mathbf{P}\,\mathrm{div}_s\,\boldsymbol{\sigma} = \mathrm{div}_s\left(\mathbf{P}\boldsymbol{\sigma}\right) - \mathbf{L}\boldsymbol{\sigma}^T\boldsymbol{\nu} - \left(\mathbf{L}\cdot\boldsymbol{\sigma}\right)\boldsymbol{\nu}.$$

□

Appendix B

Code used to produce results

B.1 Solution of axisymmetric equations

The code below is used in chapter 4 to calculate solutions to the axisymmetric the shape and solutions for q_0 and q_m. The code in appendix B.1 was written in collaboration with my supervisor, Dr. Steven Roper.

Listing B.1: Initial guess for the solution when using q_0 and q_m

```
function pq0 = pqinit_q0qm(x,A,pars)

% This function initialises the guess for the solution of
   ↪ the
% equilibrium equations

    if(pars.a<0)
        q0=sqrt(-pars.a/pars.c); % The initial guess for
           ↪ q0
        qm=0;
    else
        q0=0;
        qm=0;
    end

O=ones(size(x));

pq0 =[q0*O;
      qm*O;
      pars.xi*cosh(A*x)/A;
```

```
19        pars.xi*sinh(A*x);
20        0*0;
21        0*0;
22        (pars.xi^2*(8*pars.c*(q0.^2+qm.^2).^2 + 4*pars.a*(
            ↪ q0.^2+qm.^2) + 2).*cosh(A*x).^4+ 16*A^2*cosh(A
            ↪ *x).^2*pars.k.*(q0.^2+qm.^2)+16*A^2*pars.k*(q0
            ↪ .^2+qm.^2)).*sinh(A*x).*(pars.xi^2*cosh(A*x)
            ↪ .^2).^(-0.5)./cosh(A*x).^3/A/2;
23        (4*(q0.^2+qm.^2)+1)*pars.k./cosh(A*x).^2.*(pars.xi
            ↪ ^2*cosh(A*x).^2).^(-0.5);];
24  end
```

Listing B.2: The axisymmetric equations.

```
1   function out=bvfun_q0qm(x,y,pars)
2
3   % The vector y contains (in the Hamilton notation)
4
5   q1=y(1);
6   q2=y(2);
7   q3=y(3);
8   q4=y(4);
9
10  p0=y(5);
11  pm=y(6);
12  p3=y(7);
13  p4=y(8);
14
15  % Extract the parameters from the structure pars
16
17  xi=pars.xi;
18  k=pars.k;
19  a=pars.a;
20  c=pars.c;
21
22  % Useful factor
23
24  s=sqrt(q4.^2+xi^2);
25
```

```
26 % The equations
27
28 out=[p0*s/4./k./q3; % q1'
29      pm*s/4./k./q3; % q2'
30      q4; % q3'
31      p4*s^5/k/xi^2/q3/(1.+4.*(q1^2+q2^2)-4*q1); % q4'
32      -(-2*p4^2*s^5*(2*q1-1)/k/xi^2/q3/(1.+4.*(q1^2+q2^2)
           ↪ -4.*q1)^2-16*k*q1*q4^2/q3/s-2*k*xi^2*(2*q1+1)/
           ↪ q3/s-(4*a+16*c*(q1^2+q2^2))*q1*q3*s); % p1'
33        -(-2*p4^2*s^5*(2*q2+0)/k/xi^2/q3/(1.+4.*(q1^2+q2
             ↪ ^2)-4.*q1)^2-16*k*q2*q4^2/q3/s-2*k*xi^2*(2*q2
             ↪ +0)/q3/s-(4*a+16*c*(q1^2+q2^2))*q2*q3*s); %
             ↪ p2'
34        -(-(p0^2+pm^2)*s/8./k/q3^2-p4^2*s^5/2./k/xi^2/q3
             ↪ ^2/(1.+4.*(q1^2+q2^2)-4*q1)+k*xi^2*(1.+4.*(q1
             ↪ ^2+q2^2)+4*q1)/2./q3^2/s+8.*k*q4^2*(q1^2+q2
             ↪ ^2)/q3^2/s-s*(1+2.*a*(q1^2+q2^2)+4.*c*(q1^2+
             ↪ q2^2)^2)); % p3'
35        -((p0^2+pm^2)*q4/8/k/q3/s+5.*p4^2*s^3*q4/2/k/xi^2/
             ↪ q3/(1.+4.*(q1^2+q2^2)-4.*q1)+k*xi^2*q4
             ↪ *(1.+4.*(q1^2+q2^2)+4*q1)/2/q3/s^3+p3-16*k*(
             ↪ q1^2+q2^2)*q4/q3/s+8.*k*(q1^2+q2^2)*q4^3/q3/s
             ↪ ^3-q3*q4*(1+2.*a*(q1^2+q2^2)+4.*c*(q1^2+q2^2)
             ↪ ^2)/s);]; %p4'
36
37 end
```

Listing B.3: The boundary conditions.

```
1  function [out]=bvbc_q_0q_m(ya,yb,pars)
2
3  % Boundary conditions for the full problem (q1,q2,rho)
4
5  % Extract the parameters from pars
6
7  xi=pars.xi;
8  k=pars.k;
9
10 % Obtain the left and right end-point values of the
```

```
   ↪ hamilton variables

q0a=ya(1);p0a=ya(5);
qma=ya(2);pma=ya(6);
q3a=ya(3);p3a=ya(7);
q4a=ya(4);p4a=ya(8);

q0b=yb(1);p0b=yb(5);
qmb=yb(2);pmb=yb(6);
q3b=yb(3);p3b=yb(7);
q4b=yb(4);p4b=yb(8);

qa=2*sqrt(q0a.^2+qma.^2);
qb=2*sqrt(q0b.^2+qmb.^2);

out=[q3a-1.;
     q3b-1;
     p0a;
     p0b;
     pma;
     pmb;
     p4a;
     p4b;
%    qma;
%    qmb;
%    2*(qa*p4a*(q4a^2+xi^2)^(5/2)/(k*xi^2*(1+4*(q0a^2+qma
   ↪ ^2)-4*q0a))-(1-qa)*(q4a^2+xi^2)^2);
%    2*(qb*p4b*(q4b^2+xi^2)^(5/2)/(k*xi^2*(1+4*(q0b^2+qmb
   ↪ ^2)-4*q0b))-(1-qb)*(q4b^2+xi^2)^2);
];

end
```

Listing B.4: Code to follow branches of solutions.

```
%% Intro

% In this script we find solutions for given sets of
   ↪ parameters
```

```
4  % The code expects to have a variable called set_of_pars
     ↪ which is an array of structures containing pars
5  % set_of_pars could have for example different parameters
     ↪  where we vary only one of the parameters between
     ↪ the different sets of parameter values
6
7  %% Set up
8
9  % Here we define an initial guess for the very first
     ↪ value of 'a'
10 % The initial grid
11 Nz=10000
12 z=linspace(-1,1,Nz+1);
13 n=length(z);
14
15 % Get the number of parameter values
16 Np=length(set_of_pars);
17
18 % For the first set of parameters we need to prepare an
     ↪ initial guess for the solution. For the other
     ↪ parameters we will assume that the solution from
     ↪ using the previous set of parameters is a good guess
     ↪  for the solution for the next set of parameters
19
20 % Use the first set of parameters
21 pars=set_of_pars(1);
22
23 % If narrow is false then use the wide catenoid as the
     ↪ initial guess, if it is true then use the narrow
     ↪ catenoid
24 narrow=false;
25
26 % Find the parameter A that controls the shape of the
     ↪ wide catenoid
27 Aw=pars.xi;
28 for i=1:1000;
29     Aw=pars.xi*cosh(Aw);
30 end
```

```
31
32 % Find the parameter An that controls the shape of the
   ↪ narrow catenoid
33 An=1.;
34 for i=1:1000;
35     An=acosh(An/pars.xi);
36 end
37
38 % Here we set which type of solution we are looking for,
   ↪ if narrow is true we have the narrow catenoid as the
   ↪  initial guess for the shape, if narrow is false
   ↪ then we use the wide catenoid as the initial guess
   ↪ for the shape
39
40 if(narrow)
41     A=An;
42 else
43     A=Aw;
44 end
45
46 % Initialise the solution with constant q, constant alpha
   ↪  and the
47 % catenoidal shape
48
49 solinit=bvpinit(z,@(x)pqinit_q0qm(x,A,pars));
50
51 %% Get an initial guess before entering the loop
52
53 sol=bvp4c(@(x,y)bvfun_q0qm(x,y,pars),@(x,y)bvbc_q0qm(x,y,
   ↪ pars),solinit);
54 solinit=sol;
55
56
57 %% Loop
58
59 % Now we loop over the different values of 'a',
   ↪ calculating a solution in
60 % each case. We need to use solution obtained from the
```

```
   ↪ previous value of
% 'a' as the initial guess for the next solution

for p=1:Np

    pars=set_of_pars(p);

    E_cat=pars.xi^2/A+0.5*pars.xi^2*sinh(2*A)/A^2+2*pars.
       ↪ k*tanh(A);

    % Solve by collocation
    sol=bvp4c(@(x,y)bvfun_q0qm(x,y,pars),@(x,y)bvbc_q0qm(
       ↪ x,y,pars),solinit);

    % Mean curvature
    %    H=0.5*(rho.*rhopp-(rhop.^2+pars.xi^2))./(rho.*(
       ↪ pars.xi^2+rhop.^2).^(3/2));

    % The energy
    E(p)=calc_energy_q0qm(sol,pars);

    % Store the solution
    SOL{p}=sol;

    % Give an update
    disp(sprintf('Parameter set %d : The energy of the
       ↪ solution, relative to the catenoid solution is %
       ↪ f',p,E(p)-E_cat))

    % Make the initial solution for the next step in the
       ↪ loop the
    % solution obtained in the current step
    solinit=sol;

end

%% To make the figures, we plot q and rho for the
   ↪ different values of the parameters on the same
```

```
    ↪ figure
```

B.2 Solution of nonlinear equations

The code in appendix B.2 was written and checked in collaboration with my supervisor, Dr. Steven Roper. I have performed the calculations needed to produce the equations and checked the code against these, I have also modified the parameters to explore different solutions and used the charge calculation function to compute the charges of any defects.

Listing B.5: The code to solve the nonlinear equations using a nonlinear relaxation method

```
1  %% Solve the nonlinear equations using Jacobi iteration
2
3  %% Set parameters
4
5  % Geometrical parameter
6  rho=1.2;
7
8  % Temperature and material parameters
9  abar=-2.0;
10 cbar=1.0; % Note that the equation can be rescaled so
     ↪ that cbar=1
11
12 % Declare the number of sub-intervals in theta, controls
     ↪ the discetisation in the theta direction
13 Nth=200;
14
15 % Discretisation of th
16 th=linspace(0,2*pi,Nth+1);
17 dth=(2*pi/Nth);
18
19 % Declare the number of sub-intervals in z, controls the
     ↪ discretisation in the z direction
20 Nz=100;
21
22 % Discretisation of z
23 z=linspace(-1,1,Nz+1);
24 dz=2/Nz;
```

```
25
26 % Calcualte the mesh
27 [Z,TH]=meshgrid(z,th(1:end-1));
28
29 % Useful quantities
30 c=cosh(rho*Z);
31 s=sinh(rho*Z);
32 t=tanh(rho*Z);
33
34 %% Declare the solution matrix and the initial guess for
   ↪ solution
35
36 % This is a zero initial guess
37 q=zeros(size(Z));
38
39 % Different random initial guesses, made up of different
   ↪ modes, to try to obtain different solutions
40 amp=0.01;
41
42 % Totally random
43 q=amp*(2.*rand(size(Z))-1);
44
45 %
46 %q=amp*(rand(1)+rand(1)*exp(i*rand(1)*2*pi)*cos(TH)+rand
   ↪ (1)*exp(i*rand(1)*2*pi)*cos(2*TH)+rand(1)*exp(i*rand
   ↪ (1)*2*pi)*cos(TH)+cos(4*TH)+1*rand(1)*exp(i*rand(1)
   ↪ *2*pi)*cos(8*TH).*cos(pi*Z));
47
48 %q=q+amp*(exp(i*rand(1)*2*pi)*cos(3*TH+3*pi*Z).*exp
   ↪ (-2.*(1.+Z))+exp(i*rand(1)*2*pi)*cos(3*TH-2*pi*Z).*
   ↪ exp(-2.*(1.-Z)));
49
50 %q=q+amp*(exp(i*rand(1)*2*pi)*cos(6*TH+3*pi*Z).*exp
   ↪ (-2.*(1.+Z))+exp(i*rand(1)*2*pi)*cos(6*TH-3*pi*Z).*
   ↪ exp(-2.*(1.-Z)));
51
52 %q=amp*(exp(-2.*(1+Z)+i*3*TH)+exp(-(1-Z)-i*3*TH))+amp*
   ↪ rand(1)*exp(2*pi*i*rand(1))*(exp(-(1+Z)+i*TH)+exp
```

```
   ↪ (-2.*(1-Z)-i*TH));
53
54 %q=amp*(cos(2*TH+2*pi*Z).*exp(-2.*(1+Z)))*exp(i*rand(1)
   ↪ *2*pi);
55
56 %q=q+0.5*exp(i*2*pi*rand(1))*cos(TH.*exp(-abs(Z)));
57
58 %q=amp*cos(6*TH).*(1+cos(2*pi*Z))+rand(size(q))*amp*amp;
59
60 %q=sqrt(-abar/cbar)*place_defect([-0.25,pi/3;0.25,pi
   ↪ ;-0.25,5*pi/3],Z,TH,0.1);
61
62 %% Start the iterations
63
64 % Number of iterations in the inner iteration
65 Nit=Nz*Nth;
66
67 disp(sprintf('Each outer iteration has %d inner
   ↪ iterations',Nit));
68
69 Nouterit=25;
70
71 %Initially set Eq=0
72 Eq=0;
73
74 for outerit=1:Nouterit,
75
76     disp(sprintf('Doing outer iteration number: %d/%d',
       ↪ outerit,Nouterit));
77
78     % Plot intermediate results (during the iterative
       ↪ method)
79     contourf(TH'/pi,Z',abs(q'));colorbar
80     xlabel('$\theta/\pi$','Interpreter','latex');
81     ylabel('$z$','Interpreter','latex');
82     title(sprintf('$\\rho=%5.2f $, $a=%5.2f $, $c=%5.2f $
       ↪ , $E-E_0=%5.2f $',rho,abar,cbar,Eq),'Interpreter
       ↪ ','latex','FontSize',12);
```

```
83
84      drawnow;
85
86      for it=1:Nit,
87
88          [d2qdz2,d2qdth2,dqdz,dqdth]=derivs_offdiag(q);
89          d2qdz2=d2qdz2/dz^2;dqdz=dqdz/dz;
90          d2qdth2=d2qdth2/dth^2;dqdth=dqdth/dth;
91
92          q=(rho^2*d2qdth2+d2qdz2-4*rho^2*i*s.*dqdth./c-
               ↪ abar*q.*c.^2)./(rho^2*(2.+4*s.^2)./c.^2+cbar
               ↪ *abs(q).^2.*c.^2+2.*(rho^2/dth^2+1./dz^2));
93
94      end
95
96      % Calculate the energy density
97      [d2qdz2,d2qdth2,dqdz,dqdth]=derivs(q);
98      dqdz=dqdz/dz;
99      dqdth=dqdth/dth;
100     d2qdz2=d2qdz2/dz^2;
101     d2qdth2=d2qdth2/dth^2;
102
103     % w0 is the energy density when q=0 and so consists
           ↪ just of elastic contribution due to curvature of
           ↪  the catenoid surface
104     w0=rho^2./(2.*c.^4);
105
106     % wq is the part of the energy density that has
           ↪ dependance on q
107     wq=0.5*((rho^2*abs(dqdth).^2+abs(dqdz).^2)./c.^2+4.*
           ↪ rho^2*t.*imag(q.*conj(dqdth))./c.^2+rho^2*(2+4*s
           ↪ .^2).*abs(q).^2./c.^4)+0.5*abar*abs(q).^2+0.25*
           ↪ cbar*abs(q).^4;
108
109     % The total energy
110     w=w0+wq;
111
112     % Calculate the energy, note the energy is real
```

```
113
114     E0=trapz(z,sum(w0.*c.^2))*dth/rho;
115     Eq=trapz(z,sum(wq.*c.^2))*dth/rho;
116
117     % The energy can be manipulated and if q solves the
          ↪ nonlinear equation then the energy is just -(
          ↪ cbar/4)*\int_S |q|^4,dS
118
119     Eqq=-0.25*cbar*trapz(z,sum(c.^2.*abs(q).^4))*dth/rho;
120
121     % Calculate the residual (whether we solve equation,
          ↪ this should be zero, to within machine precision
          ↪ )
122
123     residual=(d2qdth2*rho^2+d2qdz2)./c.^2-4*rho^2*i*s.*
          ↪ dqdth./c.^3-rho^2*(2.+4*s.^2).*q./c.^4-abar*q-
          ↪ cbar*q.*abs(q).^2;
124
125     rnorm2=trapz(z,sum(abs(residual).^2.*c.^2))*dth/rho;
126     rnorm=sqrt(rnorm2);
127
128     qnorm2=trapz(z,sum(abs(q).^2.*c.^2))*dth/rho;
129     qnorm=sqrt(qnorm2);
130
131     % Display the energy and residual
132
133     disp(sprintf('Energies: Eq = %f, Eqq = %f, rnorm = %e
          ↪ , relnorm = %e',Eq,Eqq,rnorm,rnorm/qnorm));
134
135 end
136
137 % Plot final result
138 contourf(TH'/pi,Z',abs(q'));colorbar
139 xlabel('$\theta/\pi$','Interpreter','latex');
140 ylabel('$z$','Interpreter','latex');
141 title(sprintf('$\\rho=%5.2f $, $a=%5.2f $, $c=%5.2f $, $E
      ↪ -E_0=%5.2f $',rho,abar,cbar,Eq),'Interpreter','latex
      ↪ ','FontSize',12);
```

```
142
143 % Send a message that the code has finished
144 disp('The specified number of outer iterations has been
    ↪ completed. Now use other functions to plot the
    ↪ results');
```

Listing B.6: Finite difference approximation to derivatives

```
1  function [D2z,D2th,Dz,Dth]=derivs(q);
2
3      %% Finite difference combinations
4
5      [N,M]=size(q);
6
7      q_extended=[q(:,2),q,q(:,M-1)];
8
9      D2z=[q_extended(:,1:M)+q_extended(:,3:M+2)-2.*
           ↪ q_extended(:,2:M+1)];
10     Dz=0.5*[q_extended(:,3:M+2)-q_extended(:,1:M)];
11     D2th=circshift(q,1)+circshift(q,-1)-2*q;
12     Dth=0.5*(circshift(q,-1)-circshift(q,1));
13
14 end
```

```
1  function [D2z,D2th,Dz,Dth]=derivs_offdiag(q);
2
3      %% Finite difference combinations, off-diagonal terms
           ↪  only
4
5      [N,M]=size(q);
6
7      q_extended=[q(:,2),q,q(:,M-1)];
8
9      D2z=[q_extended(:,1:M)+q_extended(:,3:M+2)];
10     Dz=0.5*[q_extended(:,3:M+2)-q_extended(:,1:M)];
11     D2th=circshift(q,1)+circshift(q,-1);
12     Dth=0.5*(circshift(q,-1)-circshift(q,1));
13
14 end
```

Listing B.7: Code to calculate the charge of the defects by performing a counter integral

```
function out=find_charge(q,Z,TH,ZRANGE,THRANGE,plt)
% Usage
%
% out=find_charge2(q,Z,TH,ZRANGE,THRANGE,plt)
% Where Z and TH are an NtxNz+1 arrays
% q is an NtxNz+1 array containing the solution
% ZRANGE is a 1x2 array containing the range of z of the rectangular contour
% THRANGE is a 1x2 array containing the range of theta of the rectanglar contour
% plt is a boolean (true/false) indicating whether a plot should be generated and saved

    [n,m]=size(q);
    dth=2.*pi/n;
    dz=2./(m-1);

    % Obtain the derivatives, we only need the first derivatives
    [~,~,dqdz,dqdth]=derivs(q);
    dqdz=dqdz/dz;
    dqdth=dqdth/dth;

    % Obtain the real and imaginary parts of q and the derivatives of q
    q1=real(q);
    q2=imag(q);

    dq1dz=real(dqdz);
    dq2dz=imag(dqdz);

    dq1dth=real(dqdth);
    dq2dth=imag(dqdth);

    % Obtain the Q=sqrt(q1^2+q2^2)
    Q2=abs(q).^2;

```

```
33      % Obtain indices of the corners
34      zs=max(round(m*0.5*(ZRANGE(1)+1)),1);
35      ze=max(round(m*0.5*(ZRANGE(2)+1)),1);
36
37      ts=max(round(n*THRANGE(1)/(2*pi)),1);
38      te=max(round(n*THRANGE(2)/(2*pi)),1);
39
40      % Calculate the line integrals
41      line1=(q1(ts:te,zs).*dq2dth(ts:te,zs)-q2(ts:te,zs).*
           ↪ dq1dth(ts:te,zs))./Q2(ts:te,zs);
42      line2=(q1(te,zs:ze).*dq2dz(te,zs:ze)-q2(te,zs:ze).*
           ↪ dq1dz(te,zs:ze))./Q2(te,zs:ze);
43      line3=(q1(ts:te,ze).*dq2dth(ts:te,ze)-q2(ts:te,ze).*
           ↪ dq1dth(ts:te,ze))./Q2(ts:te,ze);
44      line4=(q1(ts,zs:ze).*dq2dz(ts,zs:ze)-q2(ts,zs:ze).*
           ↪ dq1dz(ts,zs:ze))./Q2(ts,zs:ze);
45
46      %   sum(line1)*dth
47      l1=simps(TH(ts:te,zs),line1);
48      %   sum(line2)*dz
49      l2=simps(Z(te,zs:ze),line2);
50      %   sum(line3)*dth
51      l3=simps(TH(ts:te,ze),line3);
52      %   sum(line4)*dz
53      l4=simps(Z(ts,zs:ze),line4);
54
55      %    disp(sprintf('Line integrals: %f %f %f %f',l1,l2
           ↪ ,l3,l4));
56      %    out=trapz(TH(ts:te,zs),line1)+trapz(Z(te,zs:ze),
           ↪ line2)-trapz(TH(ts:te,ze),line3)-trapz(Z(ts,zs:
           ↪ ze),line4);
57
58      out=l1+l2-l3-l4;
59      %   out=dth*sum(line1)+dz*sum(line2)-dth*sum(line3)-
           ↪ dz*sum(line4)
60
61      out=out/(4.*pi);
62
```

```
63
64      % Plot the contour so we can identiy where it runs on
            ↪  the plot of q
65      if(plt)
66          figure;
67          % Contour plot of the order q (q=0 are melting
                ↪ points)
68          contourf(TH/pi,Z,abs(q));
69          colormap parula;
70          colorbar
71          xlabel('$\theta/\pi$','Interpreter','latex','
                ↪ FontSize',12);
72          ylabel('$z$','Interpreter','latex','FontSize',12)
                ↪ ;
73          title(sprintf('Charge calculation: $m=%2.1f $',
                ↪ out),'Interpreter','latex','FontSize',12);
74
75          hold on
76          plot(TH(ts:te,zs)/pi,Z(ts:te,zs),'k','LineWidth'
                ↪ ,2);
77          plot(TH(te,zs:ze)/pi,Z(te,zs:ze),'k','LineWidth'
                ↪ ,2);
78          plot(TH(ts:te,ze)/pi,Z(ts:te,ze),'k','LineWidth'
                ↪ ,2);
79          plot(TH(ts,zs:ze)/pi,Z(ts,zs:ze),'k','LineWidth'
                ↪ ,2);
80          hold off
81
82          filename=sprintf('Charge_calculation_%s_.pdf',
                ↪ datestr(now,'mm-dd-yyyy-HH-MM'))
83
84          savepdf('./',filename);
85      end
86
87
88  end
```

Bibliography

[1] M. V. A. Segatti, M. Snarski. Equilibrium configurations of nematic liquid crystals on a torus. *Physical Review E*, page 90(1):012501, 2014.

[2] M. B. Amar, P. de Silva, N. Limodin, A. Langlois, and M. Brazovskaia. Stability and vibrations of catenoid-shaped smectic films. *The European Physical Journal B*, 1998.

[3] A. Ambrosetti and G. Prodi. *A Primer of Nonlinear Analysis*. Cambridge University Press, 1995.

[4] J. B. and L. W. Creating evenly-spaced streamlines of arbitrary density. In *Visualization in Scientific Computing '97: Proceedings of the Eurographics Workshop*, pages 43–55, April 1997.

[5] C. Bar. *Elementary Differential Geometry*. Cambridge University Press, 2010.

[6] P. Biscari and P. Cesana. Ordering effects in electric splay freedericksz transitions. *Continuum Mechanics and Thermodynamics*, 19(5):285–298, Oct. 2007. doi: 10.1007/s00161-007-0055-8.

[7] P. Biscari and E. Virga. Local stability of biaxial nematic phases between two cylinders. *Int. J. Non-Linear Mechanics*, 1997.

[8] P. Biscari, S. M. Canevese, and G. Napoli. Impermeability effects in three-dimensional vesicles. *Journal of Physics*, 2004.

[9] P. Biscari, Terentjev, and E. M. Nematic membranes: Shape instabilities of closed achiral vesicles. *Physical Review E*, 73(5):051706, May 2006. doi: 10.1103/PhysRevE.73.051706.

[10] F. Bisi, E. G. Virga, J. Gartland, Eugene C., G. De Matteis, A. M. Sonnet, and G. E. Durand. Universal mean-field phase diagram for biaxial nematics obtained from a minimax principle. *Physical Review E*, 73(5):051709, May 2006. doi: 10.1103/PhysRevE.73.051709.

[11] F. Bisi, A. M. Sonnet, and E. G. Virga. Steric effects in a mean-field model for polar nematic liquid crystals. *Physical Review E*, 82(4):041709, Oct. 2010. doi: 10.1103/PhysRevE.82.041709.

[12] G. A. Bliss. *Calculus Of Variations*. The Mathematical Association Of America, 1925.

[13] G. A. Bliss. The calculus of variations for multiple integrals. *Taylor & Francis, Ltd. On behalf of the Mathematical Association of America*, 1942.

[14] M. J. Bowick and L. Giomi. Two dimensional matter: Order, curvature and defects. *Advances in Physics Preprint*, 2009.

[15] G. H. Brown. Properties and applications of liquid crystals. *Journal of Electronic Materials*, 1973.

[16] F. F. C. On the theory of liquid crystals. *Discussions of the Faraday Society*, 25: 19–28, 1958. doi: 10.1039/df9582500019.

[17] G. Canevari. Biaxiality in the asymptptic analysis of a 2-d landau-de gennes model for liquid crystals. *arXiv:*, 2013.

[18] P. B. Canham. The minmum energy of bending as a possible explanation of the biconcave shape of the human red blood cell. *Journal of Theoretical Biology*, 1970.

[19] R. Capovilla and J. Guven. Stresses in lipid membranes. *Journal of Physics*, 2002.

[20] P. M. Chaikin and T. C. Lubensky. *Principle of condensed matter physics*. Cambridge University Press, 1995.

[21] S. Chandrasekhar. *Liquid Crystals*. Cambridge University Press, 1992.

[22] S. Chandrasekhar and N. V. M. adhusudana. Liquid crystals. *Annu. Rev. Mater. Sci*, 1980.

[23] S. Chandrasekhar and G. S. Ranganath. The structure and energetics of defects in liquid crystals. *Advanced in Physics*, 1986.

[24] B. G. Chen and R. D. Kamien. Nematic films and radially anisotropic delaunay surfaces. *Eur. Phys. J*, 2009.

[25] J. C. Clegg. *Calculus Of Variations*. Interscience Publishers INC, 1968.

[26] W. H. De Jeu. *In Liquid Crystals Solid State Physics Supplement*. L. Liebert, 1978.

[27] G. De Matteis, A. M. Sonnet, and E. G. Virga. Landau theory for biaxial nematic liquid crystals with two order parameter tensors. *Continuum Mechanics and Thermodynamics*, 20(6):347–374, Dec. 2008. doi: 10.1007/s00161-008-0086-9.

[28] H. J. Deuling and W. Helfrich. The curvature elasticity of fluid membranes. *J. Phys*, 1976.

[29] S. Dhakal, F. J. Solis, and M. O. de la Cruz. Nematic liquid crystals on spherical surfaces: Control of defect configurations by temperature, density, and rod shape. *Physical Review E*, 86(1):011709, July 2012. doi: 10.1103/PhysRevE.86.011709.

[30] M. P. DoCarmo. *Differential Geometry of Curves and Surfaces*. Prentice-Hall, 1976.

[31] J. L. Ericksen. Anisotropic fluids, arch.rational mech. *Anal*, 1960.

[32] J. L. Ericksen. Liquid crystals with variables degree of orientation. *Springer-Verlag*, 1991.

[33] A. Fernandez-Nieves, V. Vitelli, A. S. Utada, D. R. Link, and M. Marquez. Novel defect structures in nematic liquid crystal shells. *Physical Review Letters*, 2007.

[34] A. Fernandez-Nieves, V. Vitelli, A. S. Utada, D. R. Link, M. Marquez, D. R. Nelson, and D. A. Weitz. Novel defect structures in nematic liquid crystal shells. *Phys. Rev*, 2007.

[35] R. Fosdick and H. Tang. Surface transport in continuum mechanics. *SAGE Publications*, 2009.

[36] J.-B. Fournier. On the stress and torque tensors in fluid membranes. *Soft Matter*, 2007.

[37] J. R. Frank and M. Kardar. Defects in nematic membranes can buckle into pseudospheres. *Phys. Rev. Anal*, 2008.

[38] G. D. Fratta, J. Robbins, V. Slastikov, and A. Zarnescu. Profiles of point defect in two dimensions in landau-de gennes theory. *cite arXiv:1403.2566vl*, 2014.

[39] G. D. Fratta, J. M. Robbins, and V. Slasikov. Half-integer point defects in the q-tensor theory of nematic liquid crystals. *Journal of Nonlinear Science*, 2015.

[40] N. G. and V. L. Effective free energies for cholesteric shells. *The Royal Society of Chemistry*, 9:8378–8387, July 2013.

[41] I. M. Gelfand and S. V. Fomin. *Calculus Of Variations*. Dover Publications, INC., 2000.

[42] P. G. D. Gennes and J. Prost. *The Physics of liquid crystal.* Oxford Science Publications Publications, 1993.

[43] M. E. Gurtin and A. I. Murdoch. A continuum theory of elastic material surfaces. *Arch. Rational Mech. Anal*, 1975.

[44] W. Helfrich. Elastic properties of lipid bilayers: Theory and possiple experiments. *Z. Naturforsch*, 1973.

[45] E. J. Hinch. *Perturbation Methods.* Cambridge University Press, 1991.

[46] S. Hyde, B. W. Ninham, and S. Lidin. *The Language of Shape. The Role of Curvature in condensed Matter: Physics, Chemistry and Biology.* Elsevier, 1997.

[47] R. Ignat, L. Nguyen, V. Slastikov, and A. Zarnescu. Stability of the vortex defect in landau-de gennes theory of nematic liquid crystals. *C. R. Acad. Sci. Paris*, 2013.

[48] J. T. Jenkins. Equation of mechanical equilibrium of a model membrane. *SIAM J. Appl. Math*, 1977.

[49] B. Jerome. Surface effects and anchoring in liquid crystals. *Reports on Progress in Physics*, 1991.

[50] M. Kleman. defect densities in directional media, mainly liquid crystals. *The Philosophical Magazine: A Journal of Theoretical Experimental and Applied Physics*, 1973.

[51] M. Kleman and O. D. Laverntovich. Topological point defects in nematic liquid crystals. *Philosophical Magazine*, 2006.

[52] M. Kleman and O. D. Lavrentovich. *Soft Matter Physics: An introduction.* Springer, 2003.

[53] S. Kralj, E. G. Virga, and S. Zumer. Biaxial torus around nematic point defects. *Phys. Rev. E*, 1999.

[54] S. Kralj, R. Rosso, and E. G. Virga. Curvature control of valence on nematic shells. *Soft Matter*, 7(2):670–683, 2011. doi: 10.1039/c0sm00378f.

[55] Q.-H. Liu, Z. Haijun, J. X. Liu, and Z. C. Ou-Yang. Spheres and prolate and oblate ellipsoids from analytical solution of the spontaneous-curvature fluid membrane model. *Phys. Rev*, 1999.

[56] L. Longa, D. Monselesan, and H. R. Trebin. An extension of the landau-ginzburg-de gennes theory for liquid crystals. *Taylor and Francis*, 1987.

[57] T. Lopez-Leon, V. Koning, K. B. S. Devaiah, V. Vitelli, and A. Fernandez-Nieves. Frustrated nematic order in spherical geometries. *Nature Physics*, 7(5):391–394, May 2011. doi: 10.1038/NPHYS1920.

[58] T. Lopez-Leon, V. Koning, K. B. S. Devaiah, V. Vitelli, and A. Fernandez-Nieves. Frustrated nematic order in spherical geometries. *Nature Physics*, 2011.

[59] T. C. Lubensky and F. C. MacKintosh. Theory of ripple phases of lipid bilayers. *Phys. Rev. Lett*, 2009.

[60] T. C. Lubensky and J. Prost. Orientational order and vesicle shape. *J. Phys II*, 1992.

[61] G. R. Luckhurst. *The Landau-De Gennes Theory of Liquid Crystals*. Springer, Dordrecht, 1985.

[62] F. C. MacKintosh and T. C. Lubensky. Orientational order, topology and vesicle shapes. *Phys. Rev. Lett*, 1991.

[63] L. V. Mirantsev, A. M. Sonnet, and E. G. Virga. Geodesic defect anchoring on nematic shells. *Physical Review E*, 86(2):020703, Aug. 2012. doi: 10.1103/PhysRevE.86.020703.

[64] Mori, Hiroyuki, Gartland, E. C., Kelly, J. R., and P. J. Bos. Multidimensional director modeling using the **q** tensor representation in a liquid crystal cell and its application to the π cell with patterned electrodes. *Japanese Journal of Applied Physics*, 1999.

[65] M. M. Muller, M. Deserno, and J. Guven. Interface-mediated interactions between particles: a geometrical approach. *Phys. Rev*, 2005.

[66] G. Napoli and L. Vergori. Equilibrium of nematic vesicles. *Journal of Physics A-mathematical and Theoretical*, 43(44):445207, Nov 2010. doi: 10.1088/1751-8113/43/44/445207.

[67] G. Napoli and L. Vergori. Extrinsic curvature effects on nematic shells. *Physical Review Letters*, 108(20):207803, May 2012. doi: 10.1103/PhysRevLett.108.207803.

[68] G. Napoli and L. Vergori. Surface free energies for nematic shells. *Physical Review E*, 85(6):061701, June 2012. doi: 10.1103/PhysRevE.85.061701.

[69] G. Napoli and L. Vergori. Curvature-induced ordering in cylindrical nematic shells. *International Journal of Non-linear Mechanics*, 49:66–71, Mar. 2013. doi: 10.1016/j.ijnonlinmec.2012.09.007.

[70] G. Napoli and L. Vergori. Influence of the extrinsic curvature on two-dimensional nematic films. *Physical Review E*, 2018.

[71] G. Napoli, O. V. Pylypovskyi, D. D. Sheka, and L. Vergori. Lifted textures in nematic shells. *arXiv:2102.13497v1*, 2021.

[72] G. Napoli, O. V. Pylypovskyi, D. D. Sheka, and L. Vergori. Supplementary information: Lifted textures in nematic shells. *arXiv:2102.13497v1*, 2021.

[73] D. R. Nelson. Order, frustration and defects in liquids and glasses. *Physical Review B*, 1983.

[74] D. R. Nelson. Toward a tetravalent chemistry of colloids. *Nano Letters*, 2(10): 1125–1129, Oct. 2002. doi: 10.1021/nl0202096.

[75] P. Nelson and T. Powers. Rigid chiral membranes. *Phys. Rev. Lett*, 1992.

[76] M. Nestler, I. Nitschke, H. Lowen, and A. Voigt. Properties of surface landau-de gennes q-tensor theory models. *Soft Matter*, 2020.

[77] R. W. Ogden. *Non-Linear Elastic Deformations*. Dover Publications, INC, 1997.

[78] L. S. Ornstein and W. Kast. New arguments for the swarm theory of liquid crystals. *Transactions of the Faraday Society*, 1933.

[79] C. W. Oseen. The theory of liquid crystals. *Trans. Faraday Soc*, 1933.

[80] C. W. Oseen. Liquid crystals materials and liquid crystal displays. *Annu. Rev. Mater. Sci*, 1997.

[81] Z. C. Ou-Yang, J.-X. Liu, and Y.-Z. Xie. Geometric methods in the elastic theory of membranes in liquid crystals phases. *Advanced Series on Theoretical Physical Science*, 1999.

[82] J. Park and D. Phillips. Analysis of nematic liquid crystals with disclination lines. *Arch. Ration. Mech. Anal*, 2012.

[83] R. H. Rand and D. Armbruster. Perturbation methods, bifurcation theory and computer algebra. *Springer*, 1988.

[84] M. S. Rashid and S. S. Khalil. Hamiltonian description of higher order lagrangians. *International Journal of Modern Physics A*, 1996.

[85] R. Rosso. Curvature effects in vesicle-particle interactions. *The Royal Society*, 2003.

[86] R. Rosso, E. G. Virga, and S. Kralj. Parallel transport and defects on nematic shells. *Continuum Mech. Thermodyn*, 2012.

[87] M. Schadt. Topics in physical chemistry. *Springer*, 1994.

[88] M. Schadt. Liquid crystal materials and liquid crystal displays. *Annual Review Inc*, 27:305–379, 1997.

[89] M. Schadt and W. Helfrich. Voltage dependent optical activity of a twisted nematic liquid crystal. *Applied Physics Letters*, 1971.

[90] A. Segatti, M. Snarski, and M. Veneroni. Analysis of a variational model for nematic shells. *Mathematical Models & Methods In Applied Sciences*, 26(10):1865–1918, Sept. 2016. doi: 10.1142/S0218202516500470.

[91] R. H. SELF, C. P. PLEASE, and T. J. SLUCKIN. Deformation of nematic liquid crystals in an electric field. *Euro. Jnl of Applied Mathematics*, 2002.

[92] A. Sengupta. *Topological Microfluidics*. Springer International Publishing Switzerland, 2013.

[93] D. D. Sheka, O. V. Pylypovskyi, P. Landeros, Y. Gaididei, A. Kakay, and D. Makarov. Micromagnetic theory of curvilinear ferromagnetic shells. *arXiv:1904,02641*, 2019.

[94] J. V. Slinger. Nematic order on a deformable vesicle: theory and simulation. *Soft Matter*, 2013.

[95] A. M. Sonnet and E. G. Virga. Steric effects in dispersion forces interactions. *Physical Review E*, 77(3):031704, Mar. 2008. doi: 10.1103/PhysRevE.77.031704.

[96] A. M. Sonnet and E. G. Virga. Flow and reorientation in the dynamics of nematic defects. *Liquid Crystals*, 36(10-11):PII 913277950, 2009. doi: 10.1080/02678290903034480.

[97] A. M. Sonnet and E. G. Virga. Reorientational dynamics of conjugated nematic point defects. *Liquid Crystals*, 37(6-7):PII 923875366, 2010. doi: 10.1080/02678292.2010.481905.

[98] A. M. Sonnet and E. G. Virga. Dissipative ordered fluids: Theories for liquid crystals. *Dissipative Ordered Fluids: Theories For Liquid Crystals*, pages 1–313, 2012.

[99] A. M. Sonnet and E. G. Virga. Bistable curvature potential at hyperbolic points of nematic shells. *Soft Matter*, 13(38):6792–6802, Oct. 2017. doi: 10.1039/c7sm01216k.

[100] J. Stasiek, M. Jewartowski, and T. Kowalewski. The use of liquid crystal thermography in selected technical and medical applications – recent development. *Journal of Crystallization Process and Technology*, 2014.

[101] D. J. Steigmann. Fluid films with curvature elasticity. *Arch. Ration. Mech. Anal*, 1999.

[102] R. Streubel. Magnetism in curved geometries. *Journal of Physics D: Applied Physics*, 2016.

[103] F. Szoka, Jr, and D. Papahadjopoulos. Comparative properties and methods of preparation of lipid vesicles. *Annual Review of Biophysics and Bioengineering*, 1980.

[104] X. Tang and J. V. Selinger. Orientation of topological defects in 2d nematic liquid crystals. *Soft Matter*, 2017.

[105] H. R. Trebin. The topology of non-uniform media in condensed matter physics. *Adv. Phys*, 1982.

[106] C. Tschierske and D. J. Photinos. Biaxial nematics phases. *Journal of Material Chemistry*, 2010.

[107] C. Z. Tu and U. Seifert. Concise theory of chiral lipid membranes. *Phys. Rev*, 2007.

[108] Z. C. Tu and Z. C. Ou-Yang. Geometric theory on the elasticity of bio-membranes. *Journal of Physics A General Physics*, 2004.

[109] S. U., B. K., and L. R. Shape transformations of vesicles: phase diagram for spontaneous curvature and bilayer coupling models. *Phys. Rev*, 1991.

[110] E. G. Virga. *Vartional Theories for Liquid Crystal*. Chapman & Hall, 1994.

[111] V. Vitelli and D. R. Nelson. Nematic textures in spherical shells. *Physical Review E*, 74(2):021711, Aug. 2006. doi: 10.1103/PhysRevE.74.021711.

[112] X. Xing, H. Shin, M. J. Bowick, Z. Yao, L. Jia, and M. H. Li. Morphology of nematic and smectic vesicles. *PNAS*, 2012.

[113] O. Y. Zhong-can and W. Helfrich. Bending energy of vesicle membranes - general expressions for the 1st, 2nd, and 3rd variation of the shape energy and applications to spheres and cylinders. *Physical Review A*, 39(10):5280–5288, May 1989. doi: 10.1103/PhysRevA.39.5280.

[114] H. Zocher. The effect of a magnetic field on the nematic state. *Transactions of the Faraday Society*, 1933.